On the polynomial swallowtail and cusp singularities of stochastic Burgers equation.

Reynolds, Christopher

On the Polynomial Swallowtail and Cusp Singularities of Stochastic Burgers Equation

Thesis submitted to the University of Wales Swansea
by

Christopher Reynolds
chris@penbre.co.uk

in candidature for the degree of
Doctor of Philosophy

Department of Mathematics
University of Wales Swansea
Singleton Park
Swansea SA2 8PP
United Kingdom

2002

Declaration

This work has not previously been accepted in substance for any degree and is not being concurrently submitted in candidature for any degree.

Signed .. .. (candidate)

Date ..27th Sept 2002..

Statement 1

This thesis is the result of my own investigations, except where otherwise stated. Other sources are acknowledged by explicit references. A bibliography is appended.

Signed .. . (candidate)

Date ..27th Sept 2002..

Statement 2

I herby give consent for my thesis, if accepted, to be available for photocopying and for inter-library loan, and for the title and summary to be made available to outside organisations.

Signed . .. (candidate)

Date ..27th Sept 2002..

Contents

Abstract

This thesis is concerned with singularities of the stochastic heat and Burgers equations. We study the classification of caustics (shockwaves) for Burgers equation and the level surfaces of the corresponding heat equation. Particular attention is paid to two examples of a two dimensional caustic, namely the semicubical parabolic cusp and the polynomial swallowtail. These examples, whose names have been adopted in recognition of Thom's list of seven elementary catastrophes, may be viewed as special cases of the larger class of initial functions $S_0(\boldsymbol{x}_0) = f(x_0) + g(x_0)y_0$ where f and g are polynomials in x_0.

The thesis is structured as follows:

Chapter 1 introduces many of the concepts required throughout the thesis. In particular the stochastic heat and Burgers equations are introduced and the notion of shockwaves discussed.

In Chapter 2 we restrict ourselves to the deterministic free case and set about deriving a polynomial initial condition that produces a swallowtail type caustic. This is considered for both the two and three dimensional cases.

In Chapter 3 the examples of the cusp and polynomial swallowtail are considered under the presence of white noise. The stochastic heat kernel is derived by a direct approach and used to obtain explicit formulae for the stochastic caustic and corresponding level surfaces.

Chapter 4 is dedicated to the study of hot and cool parts of the caustic. Building upon the work of Truman, Davies and Zhao we develop a new method for determining whether one side of the caustic is hot or cool and show, that under a certain type of noise, only the deterministic case need be considered.

In Chapter 5 we consider touching points of the pre-curves and show how this leads to the concept of turbulent times in the stochastic case. We derive a stochastic process whose zeros are the turbulent times for a particular class of examples and study the properties of this process.

In Chapter 6 we repeat much of our earlier analysis in the presence of a harmonic oscillator potential.

Acknowledgements

First and foremost I would like to thank Prof. Aubrey Truman, my supervisor, for his many suggestions, constant support and encouragement during this research. I am also thankful to Dr. Ian Davies for his assistance with LaTeX and *Mathematica*. In addition Prof. David Williams was helpful with aspects of the probability and responsible for introducing me to Strassen's law of the iterated logarithm and the work of Kalvis Jansons. Indeed all the staff and secretaries at the mathematics department should be thanked for creating such a pleasant working environment.

I am also grateful to the Engineering and Physical Sciences Research Council (EPSRC) for providing all the financial support during the first three years of my postgraduate studies.

Finally, I wish to thank the following: Scott, Shaun and Simon (the 3 S's) for their office humour and banter; Brett (for offering to proof read this thesis); and most of all Liz (for putting up with me during the last three and a half years).

University of Wales, Swansea
September 2002

Christopher Reynolds

Chapter 1

Preliminaries

This chapter is intended as a primer for many of the concepts that will be required throughout this thesis. The material presented in this chapter is standard and we will only touch upon some very broad subjects of mathematics. We begin by providing an elementary account of Lagrangian and Hamiltonian mechanics. This is followed by discussions on Hydrodynamics, Catastrophe Theory and stochastic heat and Burgers equations. The chapter concludes with a consideration of caustics (shockwaves) of Burgers equation and the corresponding level surfaces for the heat equation. We claim no originality here apart from the style of presentation.

1.1 Lagrangian and Hamiltonian Mechanics

In this section we discuss two useful reformulations of classical (Newtonian) mechanics. We begin with Lagrangian mechanics, first demonstrated by Lagrange in 1788, which essentially uses potential and kinetic energies as the fundamental concepts rather than the physics of forces used in Newtonian mechanics. Throughout this section we carefully follow the work in [2] and [22]. Other references found to be useful include [47] and [50].

1.1.1 Euler-Lagrange Equations

We consider a system whose instantaneous configuration can be described by n generalised coordinates $q_1, q_2, \ldots, q_n$. Taking the q's as n coordinates we form a hyperspace called *configuration space*. As time progresses, the state of the system changes and this is represented by the system point moving along a path in configuration space. We further assume that the system is *holonomic*, namely a system in which the q's may be varied independently without violating the constraints.

Consider the functional

$$A[q] := \int_0^t \mathcal{L}[q(s), \dot{q}(s), s] \, \mathrm{d}s \ ,$$

where $q_s = q(s)$, $s \in [0,t]$, is a curve in configuration space. Assuming $\mathcal{L}[q(s), \dot{q}(s), s] \in C^{2,2,1}(\mathbb{R}^n \times \mathbb{R}^n \times \mathbb{R}^+)$ we have the following result.

Lemma 1.1.1. *If the path $q_s = q(s)$, $s \in [0,t]$, has fixed end points $q(0) = \alpha$ and $q(t) = \beta$ then for sufficiently well behaved $h(s)$ we have*

$$\left.\frac{d}{d\varepsilon}\right|_{\varepsilon=0} A[q+\varepsilon h] = \int_0^t \left[\frac{\partial \mathcal{L}}{\partial q} - \frac{d}{ds}\left(\frac{\partial \mathcal{L}}{\partial \dot{q}}\right)\right] h(s)\,\mathrm{d}s \ . \tag{1.1.1}$$

Proof. Let $h(s) \in C_0^\infty[0,t]$ with $h(0) = h(t) = 0$. Then the variation of A yields

$$\begin{aligned}\delta A[q] &= A[q+\varepsilon h] - A[q] \\ &= \int_0^t \Big(\mathcal{L}[q+\varepsilon h, \dot{q}+\varepsilon \dot{h}, s] - \mathcal{L}[q,\dot{q},s]\Big)\,\mathrm{d}s \\ &= \int_0^t \left(\frac{\partial \mathcal{L}}{\partial q}\varepsilon h + \frac{\partial \mathcal{L}}{\partial \dot{q}}\varepsilon \dot{h}\right)\mathrm{d}s + \mathrm{O}(\varepsilon^2) \ .\end{aligned}$$

Thus it follows from integration by parts and $h(0) = h(t) = 0$ that

$$\begin{aligned}\delta A[q] &= \int_0^t \left(\frac{\partial \mathcal{L}}{\partial q}\varepsilon h - \varepsilon h \frac{d}{ds}\left(\frac{\partial \mathcal{L}}{\partial \dot{q}}\right)\right)\mathrm{d}s + \left[\varepsilon h \frac{\partial \mathcal{L}}{\partial \dot{q}}\right]_0^t + \mathrm{O}(\varepsilon^2) \\ &= \int_0^t \left(\frac{\partial \mathcal{L}}{\partial q} - \frac{d}{ds}\left(\frac{\partial \mathcal{L}}{\partial \dot{q}}\right)\right)\varepsilon h(s)\,\mathrm{d}s + \mathrm{O}(\varepsilon^2) \ .\end{aligned}$$

Equation (1.1.1) follows from the definition of the directional derivative. □

Corollary 1.1.2. *If $q_s = q(s)$ has fixed end points $q(0) = \alpha$ and $q(t) = \beta$ then a necessary condition for q_s to be an extremiser is*

$$\frac{d}{ds}\left(\frac{\partial \mathcal{L}}{\partial \dot{q}_s}\right) - \frac{\partial \mathcal{L}}{\partial q_s} = 0 \ , \tag{1.1.2}$$

for $s \in [0,t]$.

Proof. For an extremal, $\left.\frac{d}{d\varepsilon}\right|_{\varepsilon=0} A[q+\varepsilon h] = 0$, so that by Equation (1.1.1)

$$\int_0^t \left[\frac{\partial \mathcal{L}}{\partial q} - \frac{d}{ds}\left(\frac{\partial \mathcal{L}}{\partial \dot{q}}\right)\right] h(s)\,\mathrm{d}s = 0 \ ,$$

for all smooth functions $h(s)$ with $h(0) = h(t) = 0$. If $h(s)$ is continuous, or even infinitely differentiable, then the desired result follows from the continuity of $\frac{\partial \mathcal{L}}{\partial q} - \frac{d}{ds}\frac{\partial \mathcal{L}}{\partial \dot{q}}$. □

This result may be easily generalised to n-dimensions. We refer to Equations (1.1.2) as the *Euler-Lagrange equations* for the functional $A[q]$. The following straightforward corollary highlights the relationship with trajectories of a mechanical system.

Corollary 1.1.3. *The trajectories of the mechanical system, in cartesian coordinates $\boldsymbol{q}$,*

$$\frac{d}{dt}(m\dot{q}_i) + \frac{\partial V}{\partial q_i}(\boldsymbol{q}) = 0 \ , \tag{1.1.3}$$

coincide with extremals of $A[q]$ where $\mathcal{L} = T - V$ is the difference between kinetic and potential energy.

Proof. Using $T = \frac{m}{2}\sum_{i=1}^n \dot{q}_i^2$ and $V = V(\boldsymbol{q})$ in the definition of $\mathcal{L}$, it is easily shown that Equation (1.1.3) is equivalent to the Euler Lagrange equations. □

In a mechanical system we call $\mathcal{L} = T - V$ the *Lagrangian* and $A[\gamma]$ the *action functional.*

1.1.2 The Hamilton Equations of Motion

Hamiltonian mechanics was discovered in 1834 by Sir William Hamilton (1805–1865). Like Lagrangian mechanics it is a reformulation of classical mechanics. The Lagrangian formulation may be thought of as a description of mechanics in terms of the generalised coordinates and velocities, with time as a parameter. Hamilton considered a formulation in which the independent variables are the generalised coordinates and generalised momenta

$$p_i = \frac{\partial \mathfrak{L}}{\partial \dot{q}_i}(\boldsymbol{q}, \dot{\boldsymbol{q}}, t) \; .$$

The change in basis from $(\boldsymbol{q}, \dot{\boldsymbol{q}}, t)$ to $(\boldsymbol{q}, \boldsymbol{p}, t)$ is accomplished by means of a Legendre transformation with respect to $\dot{\boldsymbol{q}}$ on $\mathfrak{L}$. This leads to the following result.

Theorem 1.1.4. *The system of Lagrange's equations is equivalent to the solution of* $2n$ *first order equations*

$$\dot{\boldsymbol{p}} = -\frac{\partial H}{\partial \boldsymbol{q}} \qquad \text{and} \qquad \dot{\boldsymbol{q}} = \frac{\partial H}{\partial \boldsymbol{p}} \; , \tag{1.1.4}$$

where $H(\boldsymbol{q}, \boldsymbol{p}, t) = p_\sigma q_\sigma - \mathfrak{L}(\boldsymbol{q}, \dot{\boldsymbol{q}}, t)$.

Proof. The Legendre transformation of $\mathfrak{L}(\boldsymbol{q}, \dot{\boldsymbol{q}}, t)$ with respect to $\dot{\boldsymbol{q}}$ is the function

$$H(\boldsymbol{q}, \boldsymbol{p}, t) = \sup_{\dot{\boldsymbol{q}}}\{\boldsymbol{p}\dot{\boldsymbol{q}} - \mathfrak{L}(\boldsymbol{q}, \dot{\boldsymbol{q}}, t)\} \; .$$

This yields

$$H(\boldsymbol{q}, \boldsymbol{p}, t) = \boldsymbol{p}\dot{\boldsymbol{q}} - \mathfrak{L}(\boldsymbol{q}, \dot{\boldsymbol{q}}, t) \; ,$$

where $\dot{\boldsymbol{q}}$ is expressed in terms of $\boldsymbol{p}$ by means of $\boldsymbol{p} = \frac{\partial \mathfrak{L}}{\partial \dot{\boldsymbol{q}}}(\boldsymbol{q}, \dot{\boldsymbol{q}}, t)$. Using this we observe that

$$\begin{aligned} \delta H &= \delta(p_\sigma \dot{q}_\sigma - \mathfrak{L}(\boldsymbol{q}, \dot{\boldsymbol{q}}, t)) \\ &= \delta p_\sigma \dot{q}_\sigma - \frac{\partial \mathfrak{L}}{\partial q_\sigma}\delta q_\sigma - \frac{\partial \mathfrak{L}}{\partial t}\delta t \; . \end{aligned}$$

However by Lagrange

$$\frac{\partial \mathfrak{L}}{\partial q_\sigma} = \frac{d}{dt}\left(\frac{\partial \mathfrak{L}}{\partial \dot{q}_\sigma}\right) = \dot{p}_\sigma \; ,$$

so that

$$\delta H = \delta p_\sigma \dot{q}_\sigma - \dot{p}_\sigma \delta q_\sigma - \frac{\partial \mathfrak{L}}{\partial t}\delta t \; .$$

This yields the $2n$ equations in Equation (1.1.4) and $\frac{\partial H}{\partial t} = -\frac{\partial \mathfrak{L}}{\partial t}$. The converse is proved in a similar way. □

Remark 1.1.1.

i). The function H is called the *Hamiltonian* and Equations (1.1.4) are the *canonical equations of Hamilton.* The $2n$ dimensional space with coordinates $p_1, \ldots, p_n, q_1, \ldots, q_n$ is called *phase space.*

ii). We obtained Lagrange's equations by means of a variational principle. A modified variational principle may be used to obtain Hamilton's equations of motion directly, details of which may be found in [22].

Corollary 1.1.5. *In a mechanical (conservative holonomic) system in which T is a homogeneous quadratic functions of the $\dot{q}$'s, the Hamiltonian H is the total energy $H = T + V$.*

Proof. T is a homogeneous quadratic function of the $\dot{\boldsymbol{q}}$'s and so satisfies Euler's equation,

$$2T = \frac{\partial T}{\partial \dot{q}_\sigma}\dot{q}_\sigma = \frac{\partial \mathfrak{L}}{\partial \dot{q}_\sigma}\dot{q}_\sigma = p_\sigma \dot{q}_\sigma \ .$$

Thus

$$H = p_\sigma \dot{q}_\sigma - \mathfrak{L} = 2T - (T - V) = T + V \ .$$

□

1.1.3 Hamilton-Jacobi Theory

Here we consider the action as a function of coordinates and time as defined below.

Definition 1.1.1. The action function $A[\boldsymbol{q}_0, \boldsymbol{q}, t]$ is the integral

$$A[\boldsymbol{q}_0, \boldsymbol{q}, t] = \int_\gamma \mathfrak{L}\, \mathrm{d}s \ , \tag{1.1.5}$$

along the extremal γ connecting the points (q_0, t_0) and (q, t).

Theorem 1.1.6. *The differential of the action function (for a fixed initial point) is equal to*

$$\mathrm{d}A = \boldsymbol{p}\,\mathrm{d}\boldsymbol{q} - H\,\mathrm{d}t \ ,$$

where $\boldsymbol{p} = \frac{\partial \mathfrak{L}}{\partial \dot{q}}$ and $H = p_\sigma \dot{q}_\sigma - \mathfrak{L}$ are defined with the help of the terminal velocity $\dot{\boldsymbol{q}}$ of the trajectory.

Proof. See [2]. □

By Theorem 1.1.6 we see that $\frac{\partial A}{\partial t} = -H(\boldsymbol{p}, \boldsymbol{q}, t)$ and $\boldsymbol{p} = \frac{\partial A}{\partial \boldsymbol{q}}$. Thus the action function satisfies the equation

$$\frac{\partial A}{\partial t} + H\left(\frac{\partial A}{\partial \boldsymbol{q}}, \boldsymbol{q}, t\right) = 0 \ . \tag{1.1.6}$$

Equation (1.1.6) is called the *Hamilton-Jacobi equation*, solutions of which are customarily denoted by $\mathcal{S}$, known as *Hamilton's principal function.* The preceding theorem may be extended to show that the action function with initial condition S_0, namely

$$\mathcal{A} = A[\boldsymbol{q}_0, \boldsymbol{q}, t] + S_0(\boldsymbol{q}_0) \ ,$$

is a solution of the Cauchy problem

$$\frac{\partial \mathcal{S}}{\partial t} + H\left(\frac{\partial \mathcal{S}}{\partial \boldsymbol{q}}, \boldsymbol{q}, t\right) = 0 \ , \qquad \mathcal{S}(\boldsymbol{q}, t_0) = S_0(\boldsymbol{q}) \ .$$

Remark 1.1.2.

i). The Hamilton-Jacobi equation may also be obtained by finding a canonical transformation leading to a new Hamiltonian function $\tilde{H}$ which is identically zero.

ii). In a conservative system where $\mathcal{L}(\boldsymbol{q},\dot{\boldsymbol{q}}) = \frac{m}{2}\dot{\boldsymbol{q}}^2 - V(\boldsymbol{q})$ and $H(\boldsymbol{q},\boldsymbol{p}) = \frac{1}{2m}|\boldsymbol{p}|^2 + V(\boldsymbol{q})$, Equation (1.1.6) is simply

$$\frac{1}{2m}|\nabla\mathcal{S}|^2 + V(\boldsymbol{q}) + \frac{\partial\mathcal{S}}{\partial t} = 0 \ .$$

1.2 Hydrodynamics

Consider a region D filled with a fluid which is assumed to be continuous so that it contains no holes. A fluid in motion which exerts a tangential stress on a surface with which it is in contact is said to be *viscous*. If the fluid has no tangential reaction with any surface of contact then it is said to be *perfect* or *inviscid*.

1.2.1 The Continuity Equation

Let $\boldsymbol{u}(\boldsymbol{x},t)$ denote the velocity of a particle of fluid moving through $\boldsymbol{x}$ at time t, so that $\boldsymbol{u}$ defines a spatial velocity field of the fluid. If W is a fixed subregion of D and $\rho(\boldsymbol{x},t)$ is a well defined mass density for each t, then the mass of fluid in W at time t is given by

$$m(W,t) = \int_W \rho(\boldsymbol{x},t)\,\mathrm{d}V \ .$$

Assuming $\boldsymbol{u}$, ρ and the boundary ∂W are smooth we see

$$\begin{aligned} \text{Rate of change of mass in } W &= \frac{d}{dt}m(W,t) \\ &= \int_W \frac{\partial\rho}{\partial t}(\boldsymbol{x},t)\,\mathrm{d}V \ . \end{aligned}$$

But the principle of conservation of mass states that this must be equal to the rate at which fluid is entering W, namely

$$\frac{d}{dt}m(W,t) = -\int_{\partial W} \rho\,\boldsymbol{u}.\boldsymbol{n}\,\mathrm{d}A \ ,$$

where $\boldsymbol{n}$ is the unit outward normal defined at points of ∂W. Thus by the divergence theorem

$$\int_W \left[\frac{\partial\rho}{\partial t} + \mathrm{div}(\rho\,\boldsymbol{u})\right]\,\mathrm{d}V = 0 \ ,$$

for any arbitrary chosen volume W. Hence the integrand itself must vanish giving

$$\frac{\partial \rho}{\partial t} + \mathrm{div}(\rho \boldsymbol{u}) = 0 \ , \tag{1.2.1}$$

which is the differential form of the *conservation of mass* or the *continuity equation.*

1.2.2 Convected Derivative

Suppose that an element α is in position $\boldsymbol{x}$ at the instant of time t, then at $t + \delta t$ the element α will be in position $\boldsymbol{x} + \boldsymbol{u}(\boldsymbol{x}, t)\delta t$. Let $f(\boldsymbol{x}, t)$ be the Eulerian representation of any physical variable associated with the element α that is in position $\boldsymbol{x}$ at time t. Then the time rate of change of $f(\boldsymbol{x}, t)$ for this element is

$$\lim_{\delta t \to 0} \frac{f(\boldsymbol{x} + \boldsymbol{u}\delta t, t + \delta t) - f(\boldsymbol{x}, t)}{\delta t} \ ,$$

which for $\boldsymbol{x} = (x_1, x_2, \ldots, x_n)$ and $\boldsymbol{u} = (u_1, u_2, \ldots, u_n)$ yields

$$\begin{aligned} \text{Rate of change of } f &= \sum_{i=1}^{n} \frac{\partial f}{\partial x_i} u_i + \frac{\partial f}{\partial t} \\ &= \frac{\partial f}{\partial t} + (\boldsymbol{u} \, . \nabla) f \ . \end{aligned}$$

The operator $\frac{D}{Dt} := \frac{\partial}{\partial t} + (\mathbf{u} \, . \nabla)$ is known as the *material* or *convected* derivative. It takes into account the fact that the fluid is moving and that the positions of fluid particles change with time. More precisely the term $\frac{\partial}{\partial t}$ represents the rate of change with respect to time at a fixed point in space, whilst $(\mathbf{u} \, . \nabla)$ gives the rate of change at a particular time due to the change in the position of the particle. In particular the fluid acceleration is given by

$$\frac{D\boldsymbol{u}}{Dt} = \frac{\partial \boldsymbol{u}}{\partial t} + \boldsymbol{u} \, . \nabla \boldsymbol{u} \ .$$

Remark 1.2.1. Note that we have made explicit use of standard cartesian coordinates in space. Care must be employed when other systems are used.

Full introductions to the subject of Hydrodynamics and much more beside may be found in [55] and [13].

1.3 Catastrophe Theory

In this section we provide a brief introduction to Catastrophe Theory, the study of singularities. We carefully follow the work in [11] and [45]. More detailed expositions of the subject may be found in [48] and [1].

In what follows any critical points considered are assumed to be at the origin.

1.3.1 Morse Functions

Consider a function $f(\boldsymbol{x}_0)$, for $\boldsymbol{x}_0 \in \mathbb{R}^n$. A point $\boldsymbol{x}_0 = 0$ is a critical point of f if $\nabla|_{\boldsymbol{x}_0=0} f(\boldsymbol{x}_0) = 0$. Any critical point of f is called a *singularity.*

Definition 1.3.1. If at the critical point $\mathrm{Det}\,[f''(\boldsymbol{x}_0)] \neq 0$ then the critical point is said to be *non-degenerate.* Otherwise it is classified as *degenerate.*

Near a non-degenerate critical point of f its local geometry looks like a saddle. The saddle will curve downwards in r directions and upwards in $(n-r)$, where the integer r is called the *index* of the critical point.

A smooth function having only non-degenerate critical points is called a *structurally stable* or *Morse* function. For such functions we have the following lemma due to Morse (1930).

Lemma 1.3.1 (Morse's Lemma). *If $\boldsymbol{x}_0 \in \mathbb{R}^n$ is a non-degenerate critical point of a function $f : \mathbb{R}^n \to \mathbb{R}$, then there are neighbourhoods U of $\boldsymbol{x}_0 \in \mathbb{R}^n$ and V of $0 \in \mathbb{R}^n$ and a diffeomorphism $H : U \to V$ with the property that*

$$f \circ H^{-1}(\boldsymbol{x}) = f(\boldsymbol{x}_0) - \frac{1}{2}\sum_{i=1}^{r} x_i^2 + \frac{1}{2}\sum_{i=r+1}^{n} x_i^2 \ ,$$

where r is the index of f at $\boldsymbol{x}_0$.

Proof. Following [23] we note that after a translation and a linear change of coordinates, we may assume $\boldsymbol{x}_0 = 0$ and that

$$f = \frac{1}{2}\left(-x_1^2 - \cdots - x_r^2 + x_{r+1}^2 + \cdots + x_n^2\right) + \mathrm{O}\left(|\boldsymbol{x}|^3\right) \ , \tag{1.3.1}$$

for $\boldsymbol{x} \to 0$. Observe that using the chain rule we have

$$\begin{aligned} f(\boldsymbol{x}) &= \int_0^1 (1-t)\frac{d^2}{dt^2}(f(t\boldsymbol{x}))\,\mathrm{d}t \\ &= \int_0^1 (1-t)\sum_{k=1}^{n}\sum_{j=1}^{n}\frac{\partial^2 f}{\partial x_j \partial x_k}(t\boldsymbol{x})x_j x_k\,\mathrm{d}t \\ &= \frac{1}{2}\sum_{k=1}^{n}\sum_{j=1}^{n} q_{j,k}(\boldsymbol{x})x_j x_k = \frac{1}{2}\langle \boldsymbol{x}, Q(\boldsymbol{x})\boldsymbol{x}\rangle \ , \end{aligned}$$

where $Q(\boldsymbol{x}) = (q_{j,k}(\boldsymbol{x}))$ and $q_{j,k}(\boldsymbol{x}) = 2\int_0^1 (1-t)\frac{\partial^2 f}{\partial x_j \partial x_k}(t\boldsymbol{x})\,\mathrm{d}t$. Thus

$$\begin{aligned} q_{j,k}(0) &= \frac{\partial^2 f}{\partial x_j \partial x_k}(0) \\ &= \begin{cases} -1 & \text{if } j = k \leq r \ , \\ 1 & \text{if } j = k > r \ , \\ 0 & \text{otherwise,} \end{cases} \end{aligned}$$

and

$$Q(0) = \begin{pmatrix} -1 & & & & & \\ & \ddots & & & 0 & \\ & & -1 & & & \\ & & & 1 & & \\ & 0 & & & \ddots & \\ & & & & & 1 \end{pmatrix},$$

which is the matrix representing the Hessian $f''(0)$ with respect to the basis $\frac{\partial}{\partial x_1}\Big|_0, \ldots, \frac{\partial}{\partial x_n}\Big|_0$. We wish to obtain H of the form $H(\boldsymbol{x}) = A(\boldsymbol{x})\boldsymbol{x}$ where the matrix $A(\boldsymbol{x})$ depends smoothly on $\boldsymbol{x}$ and satisfies $A(0) = I$. Thus $A(\boldsymbol{x})$ should satisfy $\langle \boldsymbol{x}, Q(\boldsymbol{x})\boldsymbol{x}\rangle = \langle A(\boldsymbol{x})\boldsymbol{x}, Q(0)A(\boldsymbol{x})\boldsymbol{x}\rangle$, i.e. Quadratic part of $f \circ H(\boldsymbol{x}) = f(\boldsymbol{x})$, and so it suffices to have $Q(\boldsymbol{x}) = A^T(\boldsymbol{x})Q(0)A(\boldsymbol{x})$.

Let $\mathrm{Mat}(n)$ denote the space of all real $n \times n$ matrices and $\mathrm{Sym}(n) \subset \mathrm{Mat}(n)$ be the space of symmetric real matrices. Consider the map

$$\mathcal{F} : \mathrm{Mat}(n) \ni A \mapsto A^T Q(0) A \in \mathrm{Sym}(n) .$$

The differential at the point $A = I$ is

$$\mathrm{d}\mathcal{F} : \mathrm{Mat}(n) \ni \delta A \mapsto (\delta A)^T Q(0) + Q(0)\,(\delta A) \in \mathrm{Sym}(n) .$$

Now $\mathrm{d}\mathcal{F}$ is onto and by the implicit function theorem, $\mathcal{F}$ has a local smooth right inverse $\mathcal{G}$, mapping a neighbourhood of 0 in $\mathrm{Sym}(n)$ into a neighbourhood of 0 in $\mathrm{Mat}(n)$. We then get A with the required properties by taking $A(\boldsymbol{x}) = \mathcal{G}(Q(\boldsymbol{x}))$. The map $H(\boldsymbol{x}) = A(\boldsymbol{x})\boldsymbol{x}$ is then a diffeomorphism from a neighbourhood of 0 onto a neighbourhood of 0, since $\mathrm{d}H(0) = A(0) = I$. □

An alternative proof of the Morse Lemma may be found in [37].

1.3.2 Universal Unfoldings

Consider an m-parameter family of functions, for instance a polynomial in x with m coefficients which may be varied (Eg. $f(x) = x^4 + ux^2 + vx$ is a 2-parameter family). Allowing the parameters to vary continuously they form an m-dimensional coordinate space in which any function is represented by a point. Consider a function f_P corresponding to the point P. If for any point Q sufficiently close to P, f_Q has the same form as f_P then f_P is a *structurally stable* function of the family. The complement of the set of structurally stable functions is called the *bifurcation set.*

A family of functions is said to be *structurally stable* if the small perturbation leaves the qualitative nature as a family unchanged. Namely, whatever forms individual members of the family have must occur in both the original and perturbed family.

If a function f has a degenerate critical point, then a family which separates out this degeneracy is called an *unfolding.* Moreover if this unfolding is stable it is called *versal.*

Definition 1.3.2. A *universal unfolding* of a function f is the versal unfolding that contains the minimum number of parameters.

Example 1.3.1. Consider the structurally unstable function $f(x) = x^4$. Both $\tilde{V}(x) = x^4 + ux^3 + vx^2 + wx + t$ and $V(x) = x^4 + ux^2 + vx$ are versal unfoldings, but $V(x)$ is a universal unfolding.

Essentially if we have a structurally unstable function then we ask about the minimal number of independent terms that need to be added to the non-Morse function to make it Morse. This quantity is called the *co-dimension* and coincides with the *n-fold* degeneracy, i.e. the number of terms beyond the second derivative we have to go to before we can identify the type of critical point we have.

1.3.3 The Thom Classification Theorem

We begin by discussing the so-called "Splitting Lemma". If the Hessian $f''(\boldsymbol{x}_0)$ has rank $n - r$ for some $r > 0$ then there exists a coordinate transformation such that we may write

$$f = p(x_1, \dots, x_r) + \sum_{i=r+1}^{n} e_i x_i^2 \,,$$

where the constants e_i are equal to ± 1 and p is a function of order 3 or higher. Thus the structural instability is confined to the essential variables $x_1, x_2, \dots, x_r$.

The number r is called the *co-rank* of the Hessian and is a measurement of the degree to which the second order terms in a Taylor series are independent of each other. Geometrically it represents the number of coordinate directions in which f is flat near the critical point.

Let us now state the pivotal result first proposed by René Thom.

Theorem 1.3.2 (Thom's Classification Theorem). *Up to multiplication by a constant and addition of a non-degenerate quadratic form, every non-Morse function of codimension less than or equal to* 4 *is smoothly equivalent near the origin to one of the seven forms shown in the table.*

Co-rank / Codimension	*Function*	*Universal Unfolding*	*Name*
1/1	x^3	$x^3 + ux$	*Fold*
1/2	x^4	$x^4 + ux^2 + vx$	*Cusp*
1/3	x^5	$x^5 + ux^3 + vx^2 + wx$	*Swallowtail*
1/4	x^6	$x^6 + ux^4 + vx^3 + wx^2 + tx$	*Butterfly*
2/3	$x^3 - 3xy^2$	$x^3 - 3xy^2 + u(x^2 + y^2) + vx + wy$	*Elliptic Umbilic*
2/3	$x^3 + y^3$	$x^3 + y^3 + uxy + vx + wy$	*Hyperbolic Umbilic*
2/4	$x^2y + y^4$	$x^2y + y^4 + ux^2 + vy^2 + wx + ty$	*Parabolic Umbilic*

Remark 1.3.1. The classification stops after functions of codimension 4 because if it gets much larger the classification is no longer finite.

1.3.4 Bifurcation Set

To conclude this section we discuss how one proceeds to examine the geometry of the seven elementary catastrophes of Thom. If $V(x)$ is the universal unfolding then the equilibrium surface is determined by $\nabla_x V(x) = 0$. Moreover the singularity set S is defined to be those points at which $\nabla_x V(x) = 0$ and $\mathrm{Det}\,[V''(x)] = 0$.

We obtain the *bifurcation set* B by projecting S down into the control space C. This amounts to eliminating x from

$$\nabla_x V(x) = 0 \qquad \text{and} \qquad \mathrm{Det}\,[V''(x)] = 0\ .$$

The geometry of the bifurcation set explains the names chosen for the elementary catastrophes. See Chapter 2 for an example of the Swallowtail bifurcation set.

1.4 Asymptotics and Integration

1.4.1 Laplace's Method for Integrals

In this section we follow the work in [7]. We are concerned with integrals over real intervals which may depend on a parameter μ^{-2}. Our interest lies in the asymptotic behaviour of the integral as $\mu \to 0$. Note that we may extend the interval to the whole line $(-\infty, \infty)$ by defining the integrand to be zero outside the original interval.

Consider the integral

$$I = \int\limits_{\mathbb{R}} \exp\left\{-\frac{1}{\mu^2}\mathcal{A}(x_0)\right\} \mathrm{d}x_0\ ,$$

where $\mathcal{A} \in C^2(\mathbb{R})$ and is assumed to have an absolute minimum at $x_0 = 0$. Without loss of generality we assume $\mathcal{A}(0) = 0$. Moreover we insist $\mathcal{A}(x_0) > 0$ for $x_0 \neq 0$ and that there exist b, $c > 0$ such that

$$\mathcal{A}(x_0) \geq b \quad \text{if} \quad |x_0| \geq c\ .$$

Furthermore, we require that I converges for sufficiently small μ and for simplicity we assume it converges for $\mu = 1$. Finally we assume $\mathcal{A}''(0) > 0$.

The essence of Laplace's idea is that the integrand decays exponentially fast if x_0 is away from the minimum of $\mathcal{A}$, hence it is sufficient to look at the integral over a small neighbourhood of $x_0 = 0$ where we approximate $\mathcal{A}(x_0) \approx \mathcal{A}''(0)\frac{x_0^2}{2}$. More formally we have:

Lemma 1.4.1 (Laplace's Lemma). *If $\mathcal{A}''(0) > 0$ then as $\mu \to 0$ we have*

$$I \sim \left(2\pi\mu^2\right)^{\frac{1}{2}} \left(\mathcal{A}''(0)\right)^{-\frac{1}{2}}\ , \tag{1.4.1}$$

to leading order. Moreover if $\mathcal{A}(0) \neq 0$ then

$$I \sim \left(2\pi\mu^2\right)^{\frac{1}{2}} \left(\mathcal{A}''(0)\right)^{-\frac{1}{2}} e^{-\frac{1}{\mu^2}\mathcal{A}(0)}\ . \tag{1.4.2}$$

Proof. It follows from our assumptions that for each $\delta > 0$ there exists $\eta(\delta) > 0$ such that $\mathcal{A}(x_0) \geq \eta(\delta)$ for $|x_0| \geq \delta$. Then for $\mu^2 < 1$

$$\int\limits_{|x_0|\geq\delta} \exp\left\{-\frac{1}{\mu^2}\mathcal{A}(x_0)\right\} \mathrm{d}x_0 = \int\limits_{|x_0|\geq\delta} \exp\{-\mathcal{A}(x_0)\}\exp\left\{\left(1-\frac{1}{\mu^2}\right)\mathcal{A}(x_0)\right\} \mathrm{d}x_0$$
$$\leq \exp\left\{\left(1-\frac{1}{\mu^2}\right)\eta(\delta)\right\}\int\limits_{\mathbb{R}} \exp\{-\mathcal{A}(x_0)\} \mathrm{d}x_0 . \qquad (1.4.3)$$

For any $\varepsilon \in \left(0, \frac{\mathcal{A}''(0)}{3}\right)$ we can obtain $\delta(\varepsilon) > 0$ such that

$$\left|\mathcal{A}(x_0) - \frac{1}{2}x_0^2\mathcal{A}''(0)\right| \leq \varepsilon x_0^2 ,$$

for $|x_0| \leq \delta$. This is due to the fact that if $\phi(x_0) := \mathcal{A}(x_0) - \frac{1}{2}x_0^2\mathcal{A}''(0)$, then $\phi(0) = \phi'(0) = \phi''(0) = 0$. Hence $\frac{1}{x_0}(\phi'(x_0) - \phi'(0)) \to 0$ as $x_0 \to 0$ so that $\phi'(x_0) = \mathrm{o}(x_0)$. By the Mean Value Theorem, $\phi(x_0) - \phi(0) = x_0\phi'(\theta x_0)$ for some $0 < \theta < 1$, so that $\phi(x_0) = x_0\,\mathrm{o}(\theta x_0) = \mathrm{o}(x_0^2)$. It follows that

$$-\frac{x_0^2}{2\mu^2}(\mathcal{A}''(0) + 2\varepsilon) \leq -\frac{1}{\mu^2}\mathcal{A}(x_0) \leq -\frac{x_0^2}{2\mu^2}(\mathcal{A}''(0) - 2\varepsilon) ,$$

so that

$$\int_{-\delta}^{\delta} e^{-\frac{x_0^2}{2\mu^2}(\mathcal{A}''(0)+2\varepsilon)} \mathrm{d}x_0 \leq \int_{-\delta}^{\delta} e^{-\frac{1}{\mu^2}\mathcal{A}(x_0)} \mathrm{d}x_0 \leq \int_{-\delta}^{\delta} e^{-\frac{x_0^2}{2\mu^2}(\mathcal{A}''(0)-2\varepsilon)} \mathrm{d}x_0 .$$

Each of the above integrals differs from the corresponding $\int_{-\infty}^{\infty}$ integral by $\mathrm{O}\left(e^{-\frac{\alpha}{\mu^2}}\right)$ where $\alpha = \alpha(\delta) > 0$. In the case of the middle integral this is obtained by using Equation (1.4.3). Hence for $\mu^2 < 1$

$$\int_{-\infty}^{\infty} \exp\left\{-\frac{1}{\mu^2}\mathcal{A}(x_0)\right\} \mathrm{d}x_0 \leq \int_{-\infty}^{\infty} \exp\left\{-\frac{x_0^2}{2\mu^2}(\mathcal{A}''(0) - 2\varepsilon)\right\} \mathrm{d}x_0 + \mathrm{O}\left(e^{-\frac{\alpha}{\mu^2}}\right)$$
$$= \left(2\pi\mu^2\right)^{\frac{1}{2}}(\mathcal{A}''(0) - 2\varepsilon)^{-\frac{1}{2}} + \mathrm{O}\left(e^{-\frac{\alpha}{\mu^2}}\right)$$
$$\leq \left(2\pi\mu^2\right)^{\frac{1}{2}}(\mathcal{A}''(0) - 2\varepsilon)^{-\frac{1}{2}} .$$

A similar lower bound may be found, and since ε is arbitrary we obtain Equation (1.4.1). □

Corollary 1.4.2. *Consider $T_0(x_0) \in C_0^\infty(\mathbb{R})$, $\mathcal{A}(x_0) \in C^2(\mathbb{R})$ where $\mathcal{A}(x_0)$ attains a unique minimum at $\tilde{x}_0 \in$ int supp T_0. Then to leading order, if $\mathcal{A}''(x_0) > 0$,*

$$\int\limits_{\mathbb{R}} T_0(x_0)\exp\left\{-\frac{1}{\mu^2}\mathcal{A}(x_0)\right\} \mathrm{d}x_0 \sim \left(2\pi\mu^2\right)^{\frac{1}{2}}\left[\mathcal{A}''(\tilde{x}_0)\right]^{-\frac{1}{2}} T_0(\tilde{x}_0)\exp\left\{-\frac{1}{\mu^2}\mathcal{A}(\tilde{x}_0)\right\} .$$

Let us briefly discuss the n-dimensional case where

$$I = \int_{\mathbb{R}^n} T_0(\boldsymbol{x}_0) \exp\left\{-\frac{1}{\mu^2}\mathcal{A}(\boldsymbol{x}_0)\right\} \mathrm{d}\boldsymbol{x}_0 \ .$$

It may be shown that

$$I \sim \int_{\mathbb{R}^n} T_0(\boldsymbol{x}_0) \exp\left\{-\frac{1}{\mu^2}\left(\mathcal{A}(\tilde{\boldsymbol{x}}_0) + \frac{1}{2}\left(\boldsymbol{x}_0 - \tilde{\boldsymbol{x}}_0\right)^T \mathcal{A}''(\tilde{\boldsymbol{x}}_0)\left(\boldsymbol{x}_0 - \tilde{\boldsymbol{x}}_0\right)\right)\right\} \mathrm{d}\boldsymbol{x}_0 \ ,$$

where $\mathcal{A}''(\tilde{\boldsymbol{x}}_0)$ is the Hessian of $\mathcal{A}$ at the critical point $\tilde{\boldsymbol{x}}_0$. Since $\mathcal{A}''$ is real symmetric we can find an orthogonal matrix B such that $\mathcal{A}''(\tilde{\boldsymbol{x}}_0) = B^T \Lambda B$ where Λ is the diagonal matrix with eigenvalues λ_i of $\mathcal{A}''(\tilde{\boldsymbol{x}}_0)$. Thus

$$\begin{aligned}(\boldsymbol{x}_0 - \tilde{\boldsymbol{x}}_0)^T \mathcal{A}''(\tilde{\boldsymbol{x}}_0)(\boldsymbol{x} - \tilde{\boldsymbol{x}}_0) &= (\boldsymbol{x}_0 - \tilde{\boldsymbol{x}}_0)^T B^T \Lambda B(\boldsymbol{x} - \tilde{\boldsymbol{x}}_0) \\ &= (\boldsymbol{\zeta} - \tilde{\boldsymbol{\zeta}})^T \Lambda (\boldsymbol{\zeta} - \tilde{\boldsymbol{\zeta}}) \ \text{ where } \boldsymbol{\zeta} = B\boldsymbol{x}_0 \\ &= \sum \lambda_i (\zeta_i - \tilde{\zeta}_i)^2 \ .\end{aligned}$$

Hence

$$I \sim \exp\left\{-\frac{1}{\mu^2}\mathcal{A}(\tilde{\boldsymbol{x}}_0)\right\} \int_{\mathbb{R}^n} T_0\left(B^T\boldsymbol{\zeta}\right) \exp\left\{-\frac{1}{2\mu^2}\sum_i \lambda_i(\zeta_i - \tilde{\zeta}_i)^2\right\} \mathrm{d}\boldsymbol{\zeta} \ .$$

If we set $\boldsymbol{\xi} = \frac{\boldsymbol{\zeta} - \tilde{\boldsymbol{\zeta}}}{\mu}$ so that $\boldsymbol{\zeta} = \tilde{\boldsymbol{\zeta}} + \mu\boldsymbol{\xi}$ and $B^T\boldsymbol{\zeta} = \tilde{\boldsymbol{x}}_0 + B^T\mu\boldsymbol{\xi}$, then assuming all the λ_i's are positive for convergence purposes we obtain

$$\begin{aligned}I &\sim \exp\left(-\frac{1}{\mu^2}\mathcal{A}(\tilde{\boldsymbol{x}}_0)\right) \int_{\mathbb{R}^n} T_0(\tilde{\boldsymbol{x}}_0 + B^T\mu\boldsymbol{\xi}) \exp\left\{-\frac{1}{2}\sum_i \lambda_i \xi_i^2\right\} \mu^n \,\mathrm{d}\boldsymbol{\xi} \\ &\sim \mu^n \exp\left(-\frac{1}{\mu^2}\mathcal{A}(\tilde{\boldsymbol{x}}_0)\right) T_0(\tilde{\boldsymbol{x}}_0) \prod_i \int_{\mathbb{R}} \exp\left(-\frac{\lambda_i}{2}\xi_i^2\right) \mathrm{d}\xi_i \\ &= (2\pi\mu^2)^{-\frac{n}{2}} \exp\left(-\frac{1}{\mu^2}\mathcal{A}(\tilde{\boldsymbol{x}}_0)\right) T_0(\tilde{\boldsymbol{x}}_0) \left[\prod_i \lambda_i\right]^{-\frac{1}{2}} \ .\end{aligned}$$

Hence

$$I \sim (2\pi\mu^2)^{-\frac{n}{2}} \left[\mathrm{Det}\left(\mathcal{A}''(\tilde{\boldsymbol{x}}_0)\right)\right]^{-\frac{1}{2}} T_0(\tilde{\boldsymbol{x}}_0) \exp\left(-\frac{1}{\mu^2}\mathcal{A}(\tilde{\boldsymbol{x}}_0)\right) \ .$$

1.4.2 The Method of Stationary Phase

The work in this section is based on material in Chapter 2 of [35] and the paper [19]. We consider the integral

$$I(\mu) = \int_{\Omega} T_0(x_0) \exp\left\{-\frac{i}{\mu^2}\mathcal{A}(x_0)\right\} \mathrm{d}x_0 \ ,$$

where $\Omega \subset \mathbb{R}^n$ is a bounded domain, $T_0 \in C_0^\infty(\Omega)$, $\mathcal{A}(x_0) \in C^\infty(\Omega)$, and $\mathcal{A}$ is real valued. Our interest lies in the asymptotic behaviour of $I(\mu)$ as $\mu \to 0$. Physicists usually refer to $T_0(x_0)$ as the *amplitude* and $\mu^{-2}\mathcal{A}$ as the *phase* of the expression under the integral sign. We shall simply refer to $\mathcal{A}$ as the *phase* function.

If $\mathcal{A}(x_0)$ has no critical points in Ω, namely $\nabla\mathcal{A} \neq 0$ for all $x_0 \in \Omega$, then it may be shown that $I(\mu) = \mathrm{O}(\mu^\infty)$ as $\mu \to 0$. Intuitively $e^{-\frac{i}{\mu^2}\mathcal{A}}$ oscillates rapidly whilst $T_0(x_0)$ changes slowly so that the integrand cancels out due to oscillation. When $\mathcal{A}(x_0)$ has critical points in Ω, the principal contribution to $I(\mu)$ as $\mu \to 0$ corresponds to the critical points, in the neighbourhoods of which the exponential $e^{-\frac{i}{\mu^2}\mathcal{A}}$ ceases to oscillate rapidly. We suppose that the critical points of $\mathcal{A}$ are isolated, in which case it is sufficient to consider the situation where $\mathcal{A}$ has one isolated critical point in Ω.

For the one dimensional case ($n = 1$) we have the following result.

Theorem 1.4.3. *Let $T_0 \in C_0^\infty[a,b]$, $\mathcal{A} \in C^\infty[a,b]$ and let $\mathcal{A}$ be real valued. Consider the integral*

$$I(\mu) = \int_a^b T_0(x_0) \exp\left\{-\frac{i}{\mu^2}\mathcal{A}(x_0)\right\} \mathrm{d}x_0 \ ,$$

where we assume that there exists $\tilde{x}_0 \in [a,b]$ such that $\mathcal{A}'(\tilde{x}_0) = 0$, $\mathcal{A}''(\tilde{x}_0) \neq 0$ and $\mathcal{A}'(x_0) \neq 0$ for $x_0 \neq \tilde{x}_0$. Then as $\mu \to 0$ we have $I(\mu) = \mathrm{O}(\mu)$, or more precisely to leading order

$$I(\mu) \sim \left(\frac{2\pi\mu^2}{|\mathcal{A}''(\tilde{x}_0)|}\right)^{\frac{1}{2}} T_0(\tilde{x}_0) \exp\left\{-\frac{i}{\mu^2}\mathcal{A}(\tilde{x}_0) - \frac{i\pi}{4}\operatorname{sgn}\mathcal{A}''(\tilde{x}_0)\right\} \ .$$

Proof. See [19]. □

Let us now direct our attention to the multi-dimensional case. If the critical points of $\mathcal{A}$ are non-degenerate ($\mathrm{Det}[\mathcal{A}''] \neq 0$) then it is possible to reduce the analysis of $I(\mu)$ to the one-dimensional case as follows:

i). By Morse (Lemma 1.3.1) we are able, in a neighbourhood of a non-degenerate critical point $\tilde{\boldsymbol{x}}_0$, to transform $\mathcal{A}(\boldsymbol{x}_0)$ to a sum of squares.

ii). Successively apply the one dimensional phase method (Theorem 1.4.3) to each of the variables in the sum of squares.

These two steps result in the following theorem.

Theorem 1.4.4. *Let $\Omega \subset \mathbb{R}^n$ be a bounded domain, $T_0 \in C_0^\infty(\Omega)$, $\mathcal{A} \in C^\infty(\Omega)$ and let $\mathcal{A}$ be real valued. Suppose that $\mathcal{A}$ has exactly one non-degenerate critical point $\tilde{\boldsymbol{x}}_0$ in Ω. Then as $\mu \to 0$ we have to leading order*

$$I(\mu) \sim \left(2\pi\mu^2\right)^{\frac{n}{2}} T_0(\tilde{\boldsymbol{x}}_0) \left|\mathrm{Det}\left[\mathcal{A}''(\tilde{\boldsymbol{x}}_0)\right]\right|^{-\frac{1}{2}} \exp\left\{-\frac{i}{\mu^2}\mathcal{A}(\tilde{\boldsymbol{x}}_0) - \frac{i\pi}{4}\operatorname{sgn}\mathcal{A}''(\tilde{\boldsymbol{x}}_0)\right\}$$

where

$\mathcal{A}''$ is the Hessian of $\mathcal{A}$,

$\operatorname{sgn}\mathcal{A}'' = \nu_+ - \nu_-$,

ν_+ and ν_- are the respective numbers of positive and negative eigenvalues of the real symmetric matrix $\mathcal{A}''$.

Remark 1.4.1. If the phase function $\mathcal{A}(\boldsymbol{x}_0)$ has a degenerate critical point then $I(\mu)$ decreases more slowly. In fact as $\mu \to 0$,

$$I(\mu) \sim C\mu^{2\beta} \ln^{\gamma} \mu^2 + \dots ,$$

where the index β is smaller than the usual n. The indices β and γ can, in many cases, be found from the Newton boundary of the phase function, see [3] for details.

1.5 Itô and Stratonovich Calculus

1.5.1 The Wiener Process

Definition 1.5.1. A real valued stochastic process $\{W_t : t \geq 0\}$ is a *standard Wiener process* if it has the properties:

i). $W_0(\omega) = 0$, $\forall\omega$;

ii). the map $t \mapsto W_t(\omega)$ is a continuous function of $t \geq 0$ for all ω;

iii). for every $t, h \geq 0$, $W_{t+h} - W_t$ is independent of $\{W_u : 0 \leq u \leq t\}$, and has a Gaussian distribution with mean 0 and variance h.

For any finite sequence of times $0 < t_1 < \cdots < t_n$ and Borel sets $A_1, \dots, A_n \subset \mathbb{R}$,

$$\mathbb{P}\{W(t_1) \in A_1, \dots, W(t_n) \in A_n\} = \int_{A_1} \cdots \int_{A_n} p_{t_1}(0, x_1) p_{t_2-t_1}(x_1, x_2) \dots p_{t_n-t_{n-1}}(x_{n-1}, x_n)\, \mathrm{d}x_1 \dots \mathrm{d}x_n ,$$

where

$$p_t(x, y) := (2\pi t)^{-\frac{1}{2}} \exp\left[-\frac{(x-y)^2}{2t}\right] ,$$

is the Brownian transition density.

The foundations of the Wiener process were laid down by Wiener in 1923 as a mathematical description of Brownian motion, the erratic motion of a grain of pollen on a water surface due to continual bombardment by water molecules. We adopt the term Wiener process rather than Brownian motion in order to distinguish between the mathematical and physical processes.

1.5.2 Itô Calculus

Much work has been done in the study of stochastic integrals by the mathematicians Itô and McKean, see for instance Mckean's book [36]. An introduction to Itô stochastic calculus may be found in [39], [8], [51] and [24], amongst others. Here we briefly describe how one defines the Itô integral and consider the main result of stochastic calculus - the celebrated Itô's formula.

Consider a Wiener process $W = \{W_s : s \geq 0\}$ on the probability space $\{\Omega, \mathfrak{F}, \mathbb{P}\}$. If $\mathfrak{F}_t$ is the sigma algebra generated by $W_t(\omega)$, then we define the class of functions H_2 as follows.

Definition 1.5.2. Let $H_2[0,t]$ be the class of functions $f(t,\omega) : [0,\infty) \times \Omega \to \mathbb{R}$ such that

i). $(t,\omega) \to f(t,\omega)$ is $\mathcal{B}[0,\infty) \times \mathfrak{F}$-measurable,

ii). $f(t,\omega)$ is non-anticipating, that is $\omega \to f(t,\omega)$ is $\mathfrak{F}_t$-measurable for each $t \geq 0$,

iii). $\mathbb{E}\left[\int_0^t f(s,\omega)^2 \, \mathrm{d}s\right] < \infty$.

A function $\phi(s,\omega) \in H_2[0,t]$ is said to be a *simple non-anticipating* function if

$$\phi(s,\omega) = \sum_j \phi(s_j,\omega) \mathcal{X}_{[s_j,s_{j+1})}(s) \ ,$$

where the fact that $\phi \in H_2[0,t]$ implies $\phi(s_j,\omega)$ must be $\mathfrak{F}_{s_j}$ measurable. For such functions we define almost surely

$$\int_0^t \phi(s,\omega) \, \mathrm{d}W_s := \sum_j \phi(s_j,\omega)[W_{s_{j+1}} - W_{s_j}](\omega) \ ,$$

where

$$s_j = s_j^{(m)} = \begin{cases} j.2^{-m} & \text{if } 0 \leq j.2^{-m} \leq t \\ 0 & \text{if } j.2^{-m} < 0 \\ t & \text{if } j.2^{-m} > t \end{cases} .$$

This leads to the following definition of the Itô integral.

Definition 1.5.3. For any $f \in H_2[0,t]$ there exists a sequence $\{\phi_n\}$ of simple non-anticipating functions such that

$$\mathbb{E}\left[\int_0^t (f(s,\omega) - \phi_n(s,\omega))^2 \, \mathrm{d}s\right] \to 0 \ ,$$

as $n \to \infty$. The Itô integral of f is defined by

$$\int_0^t f(s,\omega) \, \mathrm{d}W_s(\omega) := \lim_{n\to\infty} \int_0^t \phi_n(s,\omega) \, \mathrm{d}W_s(\omega) \ ,$$

where the limit is in $L^2(\mathbb{P})$ and is independent of the sequence $\{\phi_n\}$.

Remark 1.5.1. It may be shown that there exists a t-continuous version of the integral and so we shall assume that $\int_0^t f(s,\omega)\,\mathrm{d}W_s(\omega)$ means a t-continuous version.

It is possible to define the Itô integral for a larger class of functions $f \in H[0,t]$ where condition (iii) of Definition 1.5.2 is replaced by

iii') $\mathbb{P}\left[\int_0^t f(s,\omega)^2\,\mathrm{d}s < \infty\right] = 1$ for all $t \geq 0$.

However whilst $\int_0^t f(s,\omega)\,\mathrm{d}W_s(\omega)$ is a martingale for $f \in H_2[0,t]$ it is only in general a local martingale for $f \in H[0,t]$, see [32].

The main result of Itô stochastic calculus is Itô's formula which we now state for the one dimensional case.

Theorem 1.5.1 (Itô's Formula). *A stochastic process X_t of the form*

$$X_t = X_0 + \int_0^t u(s,\omega)\,\mathrm{d}s + \int_0^t v(s,\omega)\,\mathrm{d}W_s\ ,$$

where $v, \sqrt{|u|} \in H_2[0,t]$ is called an Itô process. *If $Y_t = g(t,X_t)$ where $g(t,x) \in C^{(1,2)}$ then Y_t is also an Itô process and*

$$\mathrm{d}Y_t = \frac{\partial g}{\partial t}(t,X_t)\,\mathrm{d}t + \frac{\partial g}{\partial x}(t,X_t)\,\mathrm{d}X_t + \frac{1}{2}\frac{\partial^2 g}{\partial x^2}(t,X_t)(\,\mathrm{d}X_t)^2\ ,$$

where $(\,\mathrm{d}X_t)^2$ is evaluated by means of the McKean multiplication table

$\times$	$\mathrm{d}W_t$	$\mathrm{d}t$
$\mathrm{d}W_t$	$\mathrm{d}t$	0
$\mathrm{d}t$	0	0

.

1.5.3 The Stratonovich Calculus

Itô's formulation of the stochastic integral $\int_0^t f(s,\omega)\,\mathrm{d}W_s$ is not the only one which may be used. Stratonovich proposed an integral in which the integrand is essentially evaluated at the mid point $\frac{1}{2}(s_j^{(n)} + s_{j+1}^{(n)})$ of each partition $[s_j^{(n)}, s_{j+1}^{(n)}]$. The major advantage of the Stratonovich stochastic integral is that it obeys the usual transformation rules of calculus.

Following [43] and [33] we state the following relationship between Itô and Stratonovich integrals, which we adopt as our definition for the Stratonovich integral.

Definition 1.5.4. For Itô processes X_t and Y_t, the Stratonovich integral $S = \int Y \circ \partial X$ is defined by

$$S_t = \int_0^t Y \circ \partial X := \int_0^t Y\,\mathrm{d}X + \frac{1}{2}\int_0^t \mathrm{d}X_s\,\mathrm{d}Y_s\ , \qquad (1.5.1)$$

which in differential form is just

$$Y_t \circ \partial X_t = Y_t\,\mathrm{d}X_t + \frac{1}{2}\mathrm{d}X_t\,\mathrm{d}Y_t\ .$$

In order to distinguish between the two types of differential we use d to denote the Itô differential and ∂ to denote the Stratonovich differential. Thus (1.5.1) may be written as

$$\partial S_t = Y_t \circ \partial X_t \ ,$$

or

$$\mathrm{d}S_t = Y_t \,\mathrm{d}X_t + \frac{1}{2}\,\mathrm{d}X_t \,\mathrm{d}Y_t \ .$$

Observe that if $\frac{1}{2}\int_0^t \mathrm{d}X_s \,\mathrm{d}Y_s = 0$ then we have

$$\int_0^t Y \circ \partial X = \int_0^t Y \,\mathrm{d}X \ ,$$

so that the Itô and Stratonovich integrals coincide.

All the information we require to handle Stratonovich integrals is contained in the following theorem.

Theorem 1.5.2. *The Stratonovich calculus obeys the same rules as the Newton-Leibnitz calculus in the following sense. If X and Y are as before and $f \in \mathcal{C}^3$, then*

$$X_tY_t - X_0Y_0 = \int_0^t X_s \circ \partial Y_s + \int_0^t Y_s \circ \partial X_s \ , \tag{1.5.2}$$

$$f(X_t) - f(X_0) = \int_0^t f'(X_s) \circ \partial X_s \ . \tag{1.5.3}$$

Proof. Equation (1.5.2) is obtained by applying Itô's rule for a product and the definition of the Stratonovich integral, this yields

$$\begin{aligned} d(X_tY_t) &= X_t dY_t + Y_t dX_t + dX_t dY_t \\ &= X_t dY_t + \frac{1}{2} dX_t dY_t + Y dX_t + \frac{1}{2} dY_t dX_t \\ &= X_t \circ \partial Y_t + Y_t \circ \partial X_t \ . \end{aligned}$$

To prove Equation (1.5.3) we observe that for $f \in \mathcal{C}^3$ we have

$$d(f(X_t)) = f'(X_t)dX_t + \frac{1}{2}f''(X_t)(dX_t)^2 \tag{1.5.4}$$

$$d(f'(X_t)) = f''(X_t)dX_t + \frac{1}{2}f'''(X_t)(dX_t)^2 \tag{1.5.5}$$

but from (1.5.5) we obtain

$$d(f'(X_t))dX_t = f''(X_t)(dX_t)^2 \ ,$$

so that

$$\begin{aligned} f'(X_t) \circ \partial X_t &= f'(X_t)dX_t + \frac{1}{2} d\left(f'(X_t)\right) dX_t \\ &= f'(X_t)dX_t + \frac{1}{2}f''(X_t)(dX_t)^2 \\ &= d(f(X_t)) \ . \end{aligned}$$

□

Observe that Equations (1.5.2) and (1.5.3) may be written in differential form as

$$\partial(X_tY_t) = X_t \circ \partial Y_t + Y_t \circ \partial X_t \ ,$$

and

$$\partial f(X_t) = f'(X_t) \circ \partial X_t \ .$$

1.6 Burgers and Heat Equation

The viscous Burgers equation is a nonlinear partial differential equation of second order, namely

$$\frac{\partial v^\mu}{\partial t} + (v^\mu.\nabla)v^\mu = \frac{\mu^2}{2}\Delta v^\mu \ , \qquad (1.6.1)$$

with initial velocity $v^\mu(x,0) = \nabla S_0(x)$. From our earlier work on hydrodynamics we recognise that Burgers equation simply represents a fluid moving under the force $\frac{\mu^2}{2}\Delta v^\mu$. It may be considered as a simplified form of the Navier-Stokes equation and is used in fluid dynamics and engineering as a simplified model for turbulence, boundary layer behaviour, shock wave formation and mass transport. The equation has even been used in the study of the formation of large clusters in the universe, see [46]. Burgers first introduced the equation as a simple model of hydrodynamic turbulence for compressible fluids, where the parameter μ^2 describes the viscosity of the fluid, and the solution $v^\mu(x,t)$ represents the velocity field of a fluid particle located at x at time t.

Applying the logarithmic Hopf-Cole transformation $v^\mu = -\mu^2\nabla \ln u^\mu$, see [26], leads to the well known heat equation

$$\frac{\partial u^\mu}{\partial t} = \frac{\mu^2}{2}\Delta u^\mu \ , \qquad (1.6.2)$$

with $u^\mu(x,0) = \exp\left(-\frac{S_0(x)}{\mu^2}\right)$, where $u(x,t)$ is the temperature, t is time and $\frac{2}{\mu^2}$ is a constant known as *thermal diffusivity* which describes the rate at which heat is conducted through a medium.

1.6.1 Basic Solution

Following [9], we take

$$u^\mu(x,t) = \frac{1}{\sqrt{2\pi t\mu^2}}\int_{-\infty}^{\infty} F(x_0)\exp\left[-\frac{(x-x_0)^2}{2\mu^2 t}\right] \mathrm{d}x_0 \ ,$$

as a general solution of Equation (1.6.2), for an infinite domain and $t > 0$, where initially $F(x_0)$ is an arbitrary function with $F \in C_0^\infty(\mathbb{R})$ to ensure convergence of the integral.

Setting $x_0 = x + z\sqrt{t}$ and letting $t \searrow 0$, we obtain

$$\begin{aligned} u^\mu(x,t) &= \left(2\pi\mu^2\right)^{-\frac{1}{2}} \int_{-\infty}^{\infty} \exp\left[-\frac{z^2}{2\mu^2}\right] F(x+z\sqrt{t})\,\mathrm{d}z \\ &\to (2\pi\mu^2)^{-\frac{1}{2}} F(x) \int_{-\infty}^{\infty} \exp\left[-\frac{z^2}{2\mu^2}\right] \mathrm{d}z \\ &= F(x)\ , \end{aligned}$$

by dominated convergence. Hence

$$\begin{aligned} F(x) &= u^\mu(x,0) \\ &= \exp\left\{-\frac{1}{\mu^2}\int_0^x v^\mu(\eta,0)\,\mathrm{d}\eta\right\}\ , \end{aligned}$$

so that

$$u^\mu(x,t) = \frac{1}{\sqrt{2\pi t\mu^2}} \int_{-\infty}^{\infty} \exp\left[-\frac{1}{\mu^2}\left\{\frac{(x-x_0)^2}{2t} + S_0(x_0)\right\}\right] \mathrm{d}x_0\ .$$

We actually consider

$$\tilde{u}^\mu(x,t) = \frac{1}{\sqrt{2\pi t\mu^2}} \int_{-\infty}^{\infty} T_0(x_0) \exp\left[-\frac{1}{\mu^2}\left\{\frac{(x-x_0)^2}{2t} + S_0(x_0)\right\}\right] \mathrm{d}x_0\ , \qquad (1.6.3)$$

where $T_0(x_0) \in C_0^\infty(\mathbb{R})$. The above will satisfy

$$\frac{\partial \tilde{u}^\mu}{\partial t} = \frac{\mu^2}{2}\Delta\tilde{u}^\mu\ ,$$

with $\tilde{u}^\mu(x,0) = T_0(x)\exp\left(-\frac{S_0(x)}{\mu^2}\right)$. However, since we are interested in solutions $v^0(x,t) = \lim_{\mu\to 0} v^\mu(x,t)$ of the inviscid Burgers equation, we will eventually be able to set $T_0 \equiv 1$ because

$$\begin{aligned} \tilde{v}^\mu(x,0) &= -\mu^2\nabla \ln \tilde{u}^\mu(x,0) \\ &= -\mu^2\nabla\left[\ln T_0(x) - \frac{S_0(x)}{\mu^2}\right] \\ &= v^\mu(x,0) + \mathrm{O}(\mu^2)\ . \end{aligned}$$

Thus from here on we drop the use of tilde.

1.6.2 The Inviscid Limit and Shockwaves

Here we choose values of x and $t > 0$ and allow the viscosity to tend to zero. As stated in [5]: "Roughly, when the viscosity tends to 0, the dynamics of the system of particles corresponds to completely inelastic shocks, in the sense that if two (clumps of) particles collide at a given time, then they form a larger clump of particles in such a way that mass and momentum are preserved."

From our work on Laplace and the integral in Equation (1.6.3) we have

$$-\mu^2 \ln u^\mu(x,t) \to \inf_{x_0} \mathcal{A}(x_0,x,t) =: \mathcal{S}(x,t) \ ,$$

where

$$\mathcal{A}(x_0,x,t) := \frac{(x-x_0)^2}{2t} + S_0(x_0) \ .$$

Hence as $\mu \to 0$, $v^\mu(x,t) \to v^0(x,t)$ where

$$\begin{aligned} v^0(x,t) &\sim \nabla_x \mathcal{S}(x,t) \\ &= \frac{x - x_0(x,t)}{t} \ . \end{aligned}$$

The last equality follows from the fact that if ∇S_0 has no discontinuities then the minimum condition for $\mathcal{A}(\xi)$ implies $\left.\frac{\partial \mathcal{A}}{\partial x_0}\right|_{x_0 = x_0(x,t)} = 0$. Hence, observing $\frac{x - x_0(x,t)}{t} = \nabla S_0(x_0(x,t))$, the asymptotic solution v^0 is

$$v^0(x,t) = \nabla S_0(x_0(x,t)) \ , \qquad x = x_0(x,t) + t\nabla S_0(x_0(x,t)) \ . \tag{1.6.4}$$

This is the solution formula of the inviscid Burgers equation

$$\frac{\partial v}{\partial t} + (v.\nabla)v = 0 \ ,$$

with initial data $S_0(x_0)$ obtained via the method of characteristics.

Remark 1.6.1.

i). We have used $\mathcal{S}(x,t)$ to denote the infimum of $\mathcal{A}(x_0,x,t)$ because it satisfies the Hamilton-Jacobi function, and hence is a Hamilton principal function.

ii). Considering $x = x_0 + t\nabla S_0(x_0)$ we observe that, in some regions, one point x corresponds to several different points x_0^i, $(i = 1, 2, \ldots, n)$. However even though all points x_0^i are critical points of $\mathcal{A}(x_0,x,t)$, only one (say $x_0 = x_0^1$) is the infimum of $\mathcal{A}(x_0,x,t)$: $\mathcal{A}(x_0^1,x,t) < \mathcal{A}(x_0^i,x,t)$ for $i = 2, \ldots, n$. See Chapter 4 for further discussion on this.

The fact that solutions of Equation (1.6.4) are not always uniquely determined leads to the concept of shockwaves for Burgers fluid. Considering the function $\mathcal{S}(x,t) = \inf_{x_0} \mathcal{A}(x_0,x,t)$ we will show that shock waves occur when the infimum of $\mathcal{A}$ is attained at more than one point.

Observe that the minimum function $\mathcal{S}(x,t)$ may be described geometrically as follows. We plot the (negative) initial data curve $-S_0(\xi)$ and the parabola $z = \frac{(x_0 - x)^2}{2t} + C$, where the constant C is initially large enough so that the parabola is above the initial data curve.

The minimum condition requires that $\frac{\partial z}{\partial x_0} = -\frac{\partial S_0}{\partial x_0}$, namely $\frac{\partial \mathcal{A}}{\partial x_0} = 0$, which is satisfied when the tangents of $z(x_0)$ and $-S_0(x_0)$ are parallel. We push down the parabola (decrease C) until it first touches the initial data curve. The height of the parabola at this point gives $-\mathcal{S}(x,t)$.

For t small the parabola will be thin and so the point of contact between the parabola and initial data curve will be unique, see Figure 1.1. In this case the point of contact depends smoothly on x.

For larger t the parabola widens and for certain x there will be more than one point of contact, see Figure 1.1. As soon as double contacts between the parabola and initial data curve have appeared this leads to the development of shockwaves in $v^0(x,t)$ considered as a function of x.

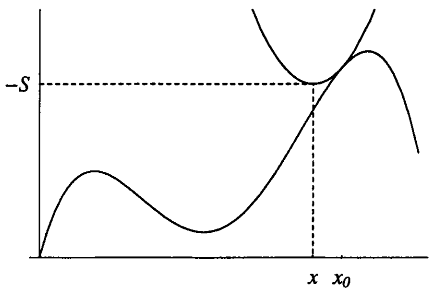

Figure 1.1: Example when x is non-singular

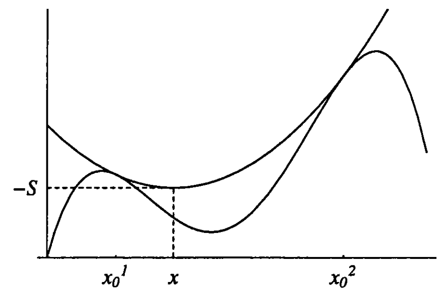

Figure 1.2: Example when x is singular

Remark 1.6.2. For very large t the parabola becomes increasingly wide so that it can only touch $-S_0(x_0)$ in the vicinity of the smallest minima of $S_0(x_0)$. Moreover, because the parabola flattens out, the value of $S(x,t)$ will approach the smallest minima of $S_0(x_0)$.

Example 1.6.1. Consider the inviscid Burgers equation

$$\frac{\partial v}{\partial t} + v\frac{\partial v}{\partial x} = 0 \ , \tag{1.6.5}$$

where

$$v(x,0) = \begin{cases} 1 & x \leq 0 \\ 1-x & 0 < x < 1 \\ 0 & x \leq 1 \end{cases} .$$

The characteristic equations are $\frac{dt}{dr} = 1$ and $\frac{dx}{dr} = v$ so that Equation (1.6.5) may be written $\frac{dv}{dr} = 0$. According to the method of characteristics

$$v(x,t) = v(x_0, 0) = F(x_0) \ ,$$

where the characteristics are

$$x = vt + x_0 \ .$$

The characteristics are shown in Figure 1.3, where we observe that points (x,t) below D lie on just one characteristic.

We have

i). For $x \leq t < 1$, $F(x_0) = v(x_0, 0) = 1$ so that $v(x,t) = 1$,

ii). For $x \geq 1 > t$, $F(x_0) = v(x_0, 0) = 0$ so that $v(x,t) = 0$,

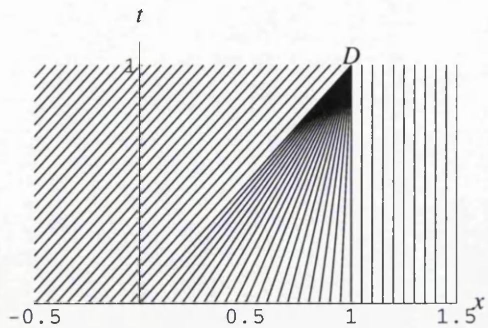

Figure 1.3: Characteristics for the Inviscid Burgers Equation

iii). For $t < 1$, $t < x < 1$, $F(x_0) = 1 - x_0$ so that $v(x,t) = 1 - (x - vt)$ and we obtain $v(x,t) = \frac{1-x}{1-t}$.

The appearance of the shockwave in $v = v(x,t)$ can be clearly seen in Figure 1.4.

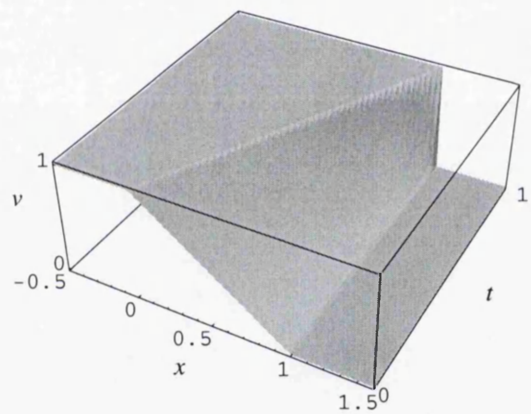

Figure 1.4: Shockwave for the Inviscid Burgers Equation

We refer to the time $t = 1$ as the *caustic time* and call the point D the *caustic* (focus). The region for $x \in [0,1]$ corresponds to the *pre-caustic* with the minimiser $x_0(x,t)$ jumping from 0 to 1 at $t = 1$ and $x = 1$. More shall be said on this in the next section.

1.7 Stochastic Burgers and Heat Equation

Consider the stochastic partial differential equation

$$du(x,t) = \frac{\mu^2}{2}\frac{\partial^2 u}{\partial x^2}(x,t)\,dt + \frac{1}{\mu^2}V(x)u(x,t)\,dt + \frac{\varepsilon}{\mu^2}k(x,t)u(x,t)\,dW_t + R(x)u(x,t)\,dt\ , \tag{1.7.1}$$

where $V, k \in C^2$, W_t is a one dimensional Wiener process on the probability space $\{\Omega, \mathfrak{F}, \mathbb{P}\}$ and $R(x)$ is a function to be defined shortly. Applying Itô's formula to $S_t =$

$-\mu^2 \ln u$ yields

$$\mathrm{d}S_t = -\frac{\mu^4}{2u}\frac{\partial^2 u}{\partial x^2}\,\mathrm{d}t - V(x)\,\mathrm{d}t - \varepsilon k(x,t)\,\mathrm{d}W_t - \mu^2 R(x)\,\mathrm{d}t + \frac{\varepsilon^2}{2\mu^2}k(x,t)^2\,\mathrm{d}t\ .$$

Hence setting $R(x) := \frac{\varepsilon^2}{2\mu^4}k(x,t)^2$ reduces the above to

$$\mathrm{d}S_t = -\frac{\mu^4}{2u}\frac{\partial^2 u}{\partial x^2}\,\mathrm{d}t - V(x)\,\mathrm{d}t - \varepsilon k(x,t)\,\mathrm{d}W_t\ ,$$

or

$$\mathrm{d}S_t + \frac{1}{2}\left|\nabla S\right|^2\,\mathrm{d}t + V(x)\,\mathrm{d}t + \varepsilon k(x,t)\,\mathrm{d}W_t = \frac{\mu^2}{2}\Delta S\,\mathrm{d}t\ . \tag{1.7.2}$$

Equation (1.7.2) arises in the study of stochastic optimisation and may naturally be called the *stochastic Hamilton-Jacobi-Bellman* equation. If we now let $v = \nabla S$, then we obtain the stochastic viscous Burgers equation

$$\mathrm{d}v = \frac{\mu^2}{2}\Delta v\,\mathrm{d}t - (v.\nabla)v\,\mathrm{d}t - \nabla V(x)\,\mathrm{d}t - \varepsilon\nabla k(x,t)\,\mathrm{d}W_t\ , \tag{1.7.3}$$

describing a fluid whose particles are subject to a force $(-\nabla V(x) - \varepsilon\nabla k(x,t)\dot{W}_t)$.

Observe that inserting our choice of $R(x)$ into the original stochastic partial differential equation (1.7.1) yields

$$\mathrm{d}u = \frac{\mu^2}{2}\Delta u\,\mathrm{d}t + \frac{1}{\mu^2}V(x)u\,\mathrm{d}t + \frac{\varepsilon}{\mu^2}k(x,t)u\,\mathrm{d}W_t + \frac{\varepsilon^2}{2\mu^4}k(x,t)^2 u\,\mathrm{d}t\ . \tag{1.7.4}$$

But

$$\begin{aligned}\varepsilon k(x,t)u \circ \partial W_t &= \varepsilon k(x,t)u\,\mathrm{d}W_t + \frac{\varepsilon}{2}\mathrm{d}(k(x,t)u)\,\mathrm{d}W_t \\ &= \varepsilon k(x,t)u\,\mathrm{d}W_t + \frac{\varepsilon^2}{2\mu^2}k(x,t)^2 u\,\mathrm{d}t\ ,\end{aligned}$$

so that Equation (1.7.4) may be written in Stratonovich form as

$$\mathrm{d}u = \frac{\mu^2}{2}\Delta u\,\mathrm{d}t + \frac{1}{\mu^2}V(x)u\,\mathrm{d}t + \frac{\varepsilon}{\mu^2}k(x,t)u \circ \partial W_t\ .$$

This is the corresponding Stratonovich type heat equation. Summarising the above we have the following proposition.

Proposition 1.7.1. *The stochastic viscous Burgers equation for velocity field* $v^\mu = v^\mu(x,t)$, $x \in \mathbb{R}^d$, $t > 0$

$$\frac{\partial v^\mu}{\partial t} + (v^\mu.\nabla)v^\mu = \frac{\mu^2}{2}\Delta v^\mu - \nabla V(x) - \varepsilon\nabla k(x,t)\dot{W}_t\ ,$$

with initial velocity $v^\mu(x,0) = \nabla S_0(x)$, *is related to the corresponding Stratonovich type heat equation*

$$\frac{\partial u^\mu}{\partial t} = \frac{\mu^2}{2}\Delta u^\mu + \frac{1}{\mu^2}V(x)u^\mu + \frac{\varepsilon}{\mu^2}k(x,t)u^\mu \circ \dot{W}_t\ ,$$

with $u^\mu(x,0) = \exp\left(-\frac{1}{\mu^2}S_0(x)\right)$, *by means of the logarithmic Hopf-Cole transformation* $v^\mu = -\mu^2\nabla \ln u^\mu$.

We are interested in the advent of shockwaves (caustics) in v^0 where $v^0(x,t) = \lim_{\mu\to 0} v^\mu(x,t)$. Defining the stochastic action as

$$A[X(0),x,t] = \inf_{\substack{X(s)\\ X(t)=x}} \left\{ \int_0^t \left(\frac{1}{2}\dot{X}^2(s) - V(X(s)) \right) \mathrm{d}s - \varepsilon \int_0^t k(X(s),s)\,\mathrm{d}W_s \right\} ,$$

and

$$\mathcal{A}[X(0),x,t] = A[X(0),x,t] + S_0(X(0)) ,$$

we expect that,

$$-\mu^2 \ln u^\mu(x,t) \to \inf_{X(0)} \mathcal{A}[X(0),x,t] =: \mathcal{S}(x,t) ,$$

for almost all ω as $\mu \to 0$, see [21]. Now $\mathcal{S}(x,t)$ is a solution of the stochastic Hamilton Jacobi equation

$$\mathrm{d}S_t + \frac{|\nabla S|^2}{2}\,\mathrm{d}t + V(x)\,\mathrm{d}t + \varepsilon k(x,t)\,\mathrm{d}W_t = 0 \quad , \quad S(x,0) = S_0(x) ,$$

so that $\mathcal{S}(x,t)$ is Hamilton's principal function for a stochastic mechanical path.

As $\mu \to 0$, u^μ will switch from being exponentially large to exponentially small across the level surface

$$\mathcal{S}(x,t) = 0 ,$$

which is called the *wavefront.*

Observing that necessary conditions for the extremiser are

$$\mathrm{d}\dot{X}(s) + \nabla V(X(s))\,\mathrm{d}s + \varepsilon \nabla k(X(s),s)\,\mathrm{d}W_s = 0 , \qquad \dot{X}(0) = \nabla S_0(X(0)) ,$$

we define the random map $\Phi_s : \mathbb{R}^d \to \mathbb{R}^d$ by

$$\mathrm{d}_s\dot{\Phi}_s = -\nabla V(\Phi_s)\,\mathrm{d}s - \varepsilon \nabla k(\Phi_s,s)\,\mathrm{d}W_s ,$$

with $\Phi_0 = I$ and $\dot{\Phi}_0 = \nabla S_0$, so that $X(s) = \Phi_s \Phi_t^{-1} x$ where we accept $x_0(x,t) = \Phi_t^{-1}(x)$ is not necessarily unique.

It is expected that non-uniqueness of $x_0(x,t)$ will be associated with the appearance of discontinuities in $v^0(x,t)$ and $u^0(x,t)$. This can arise if infinitely many paths $X(s)$ focus in a set of zero volume centred at x,

$$\mathrm{Det}\left(\frac{\partial X(t)}{\partial x_0} \right) = 0 ,$$

giving the pre-caustic $\Phi_t^{-1} C_t$, or eliminating x_0 by using $x = \Phi_t x_0$ we obtain the caustic C_t

$$\mathrm{Det}\left(\frac{\partial X(t)}{\partial x_0} \right)\Bigg|_{x_0 = \Phi_t^{-1} x} = 0 .$$

Up to the caustic time $x_0(x,t)$ is unique and

$$v^0(x,t) = \dot{\Phi}_t \Phi_t^{-1} x = \nabla \mathcal{S}(x,t) , \tag{1.7.5}$$

is a well defined formal solution of Burgers equation with $\mu = 0$. Moreover, for polynomial S_0, $x_0(x,t)$ will usually have finite multiplicity after the caustic time, so that as long as the minimising $\tilde{x}_0(x,t)$ is unique, Equation (1.7.5) may still be assumed true if we take the part of the level surface of $\mathcal{S}(x,t)$ corresponding to $\tilde{x}_0(x,t)$. More detailed information regarding the behaviour of v^0 on the caustic is given in [18].

For a non-degenerate critical point, when the multiplicity of $x_0(x,t)$ is finite so that $\Phi_t^{-1}\{x\} = \{x_0^1(x,t), x_0^2(x,t), \ldots, x_0^n(x,t)\}$, it may be deduced that

$$u^\mu(x,t) \sim \sum_{i=1}^{n} \theta_i \exp\left\{-\frac{S_i(x,t)}{\mu^2}\right\} , \tag{1.7.6}$$

where $S_i(x,t) = \mathcal{A}(x_0^i(x,t), x, t)$ for $i = 1, 2, \ldots, n$ and θ_i is an asymptotic series in μ^2 whose detailed structure may be found in [54].

The *zero level surface* of Hamilton's principal function is given by

$$H_t = \{x : S_i(x,t) = 0, \text{ for some i}\} ,$$

where $i = 1, 2, \ldots, n$. We denote the corresponding *pre-zero level surface* by $\Phi_t^{-1}H_t$. Clearly the dominant term in Equation (1.7.6) comes from the minimising $x_0^i(x,t)$ so that

$$\mathcal{S}(x,t) = \min_{i=1,2,\ldots,n} S_i(x,t) .$$

Thus H_t includes the wavefront where u^0 switches smoothly from being exponentially large to exponentially small. We shall say more regarding the wavefront and discontinuities in $u^0(x,t)$ in Chapter 4.

Chapter 2

Polynomial Swallowtail

In this chapter we study a specific singularity of the free Burgers equation, namely the swallowtail. At the outset we consider Burgers equation in two dimensions and establish an initial polynomial condition $S_0(\boldsymbol{x}_0)$ that gives rise to a two dimensional shockwave possessing the geometric structure of a swallowtail. This is then extended to an initial polynomial condition that gives rise to a three dimensional swallowtail. We refer to these non-generic swallowtails brought about by polynomial initial conditions as *polynomial swallowtails*. Explicit expressions for the pre-caustic, pre-level surface and corresponding image curves of the polynomial swallowtail are obtained for the free case. Moreover we discuss the relationship between intersections of the pre-curves and cusped meeting points of the image curves. We conclude the chapter by obtaining explicit equations for the lines of intersection of the shockwave and level surface in the free case.

2.1 Introduction

According to Thom's famous list of seven elementary catastrophes, see [1], [11], [45] and [48], the three dimensional generic swallowtail has universal unfolding

$$\mathcal{V} = x_0^5 + ux_0^3 + vx_0^2 + wx_0 \ .$$

The singularity set consists of those points at which both $\nabla_{x_0}\mathcal{V} = 0$ and $\text{Det}\left\{\frac{\partial^2\mathcal{V}}{\partial x_0^2}\right\} = 0$ are satisfied. Projecting this singularity set onto uvw-space produces the bifurcation set shown in Figure 2.1 and the origin of the name "swallowtail" becomes evident. In order to obtain a swallowtail shockwave for Burgers equation in two dimensions we can take the initial condition $S_0 = x_0^5 + |x_0|^{\frac{3}{2}}y_0$. Similarly in the three dimensional case we have $S_0 = x_0^5 + |x_0|^{1+c}y_0 + |x_0|^c z_0$ for $\frac{1}{2} < c < 1$, see [14]. An interesting question is whether we can determine a polynomial initial condition that gives rise to a shockwave for Burgers equation possessing the geometrical properties of a swallowtail. We shall refer to this as a *polynomial swallowtail*.

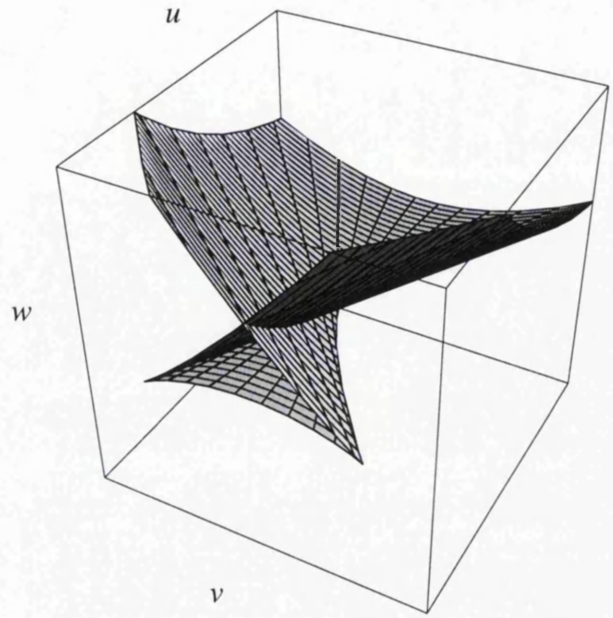

Figure 2.1: Bifurcation set of the swallowtail

Our interest lies in the viscous Burgers equation

$$\frac{\partial v^\mu}{\partial t}(\boldsymbol{x},t) + (v^\mu \cdot \nabla)\, v^\mu = \frac{\mu^2}{2}\Delta v^\mu - \nabla V(\boldsymbol{x}) \ ,$$

with initial velocity $v^\mu(\boldsymbol{x},0) = \nabla S_0(\boldsymbol{x})$ where μ^2 denotes the co-efficient of viscosity. Let us begin by considering the classical action for the initial momentum $\nabla S_0(\boldsymbol{x})$,

$$\mathcal{A}(\boldsymbol{x}_0,\boldsymbol{x},t) = A(\boldsymbol{x}_0,\boldsymbol{x},t) + S_0(\boldsymbol{x_0}) \ ,$$

where in the deterministic case

$$A(\boldsymbol{x}_0,\boldsymbol{x},t) = \inf_{\substack{X(s)\\ X(t)=x}} \frac{1}{2}\int_0^t \dot{X}^2(s)\,\mathrm{d}s - \int_0^t V\left(X(s)\right)\,\mathrm{d}s \ .$$

This is the action for the classical mechanical paths starting from x_0 and getting to x at time t under some deterministic external potential $V(x)$.

Following the treatment in [14] and [15], we assume $\mathcal{A} \in C^2$ so that the classical mechanical flow is determined by the equation

$$\nabla_{\boldsymbol{x}_0}\mathcal{A}(\boldsymbol{x}_0,\boldsymbol{x},t) = 0 \ . \tag{2.1.1}$$

From this we obtain

$$\boldsymbol{x} = \Phi_t \boldsymbol{x}_0 \qquad \text{and} \qquad \tilde{\boldsymbol{x}}_0(\boldsymbol{x},t) = \Phi_t^{-1}\boldsymbol{x} \ ,$$

where because of the possible non-uniqueness of $\boldsymbol{x}_0$ we use the notation $\tilde{\boldsymbol{x}}_0$ to indicate that we are considering the minimiser of $\mathcal{A}(\boldsymbol{x}_0,\boldsymbol{x},t)$. The non-uniqueness is discussed further in Chapter 4.

Using this notation we see that the level surface condition becomes

$$\mathcal{A}(\boldsymbol{x_0}, \boldsymbol{x}, t) = c \qquad \text{and} \qquad \nabla_{\boldsymbol{x_0}} \mathcal{A}(\boldsymbol{x_0}, \boldsymbol{x}, t) = 0 \ , \tag{2.1.2}$$

where the pre-level surface $\Phi_t^{-1} H_t$ is obtained by eliminating $\boldsymbol{x}$ and the level surface H_t by eliminating $\boldsymbol{x_0}$.

Moreover recalling from our work on Laplace's method that the residual expression in the integrand for the solution of the heat equation is given by

$$C \exp \left\{ -\frac{1}{2\mu^2} (\boldsymbol{x} - \tilde{\boldsymbol{x}}_0(\boldsymbol{x}, t))^T \mathcal{A}''_{\boldsymbol{x_0}}(\tilde{\boldsymbol{x}}_0, \boldsymbol{x}, t)(\boldsymbol{x} - \tilde{\boldsymbol{x}}_0(\boldsymbol{x}, t)) \right\} \ ,$$

we see that the caustic condition is simply

$$\nabla_{\boldsymbol{x_0}} \mathcal{A}(\boldsymbol{x_0}, \boldsymbol{x}, t) = 0 \qquad \text{and} \qquad \text{Det}\left(\mathcal{A}''_{\boldsymbol{x_0}}(\boldsymbol{x_0}, \boldsymbol{x}, t)\right) = 0 \ , \tag{2.1.3}$$

where the pre-caustic $\Phi_t^{-1} C_t$ is obtained by eliminating $\boldsymbol{x}$ and the caustic C_t by eliminating $\boldsymbol{x_0}$.

2.2 Geometrical Results of Davies, Truman and Zhao

Throughout this chapter we are concerned with the free Burgers equation, namely the case when $V(x) \equiv 0$. It is an immediate consequence of Equations (2.1.2) and (2.1.3) that the pre-level surface is described by the Eikonal equation

$$\frac{t}{2} \left| \nabla_{\boldsymbol{x_0}} S_0(\boldsymbol{x_0}) \right|^2 + S_0(\boldsymbol{x_0}) = c \ , \tag{2.2.1}$$

whilst the pre-caustic is given by

$$\text{Det}\left(I + t S_0''(\boldsymbol{x_0})\right) = 0 \ , \tag{2.2.2}$$

where $S_0''(\boldsymbol{x_0})$ is the Hessian matrix of $S_0(\boldsymbol{x_0})$.

In this section we provide an account of the work done in [15] on the geometrical relationship between level surfaces of the heat equation and shock waves of Burgers equation. We only consider the two dimensional case and refer the interested reader to [15] for details of the three dimensional case.

Let us begin with a brief discussion of singular points, in which we carefully follow [25]. Suppose the Cartesian equation of a curve of degree n arranged in ascending powers of x and y is

$$0 = b_0 x + b_1 y + c_0 x^2 + 2c_1 xy + c_2 y^2 + d_0 x^3 + 3d_1 x^2 y + 3d_2 xy^2 + d_3 y^3 + e_0 x^4 + \cdots \ .$$

If we assume b_0 and b_1 are zero then our curve meets $y = mx$ where

$$0 = x^2(c_0 + 2c_1 m + c_2 m^2) + x^3(d_0 + 3d_1 m + 3d_2 m^2 + d_3 m^3) + x^4(e_0 + \cdots) + \cdots \ .$$

Observe that at least two roots of this equation are zero for any value of m. Since every line through the origin (except the tangents) meets the curve in two points coinciding with O we call the origin a *double point*. The tangents at O are defined to be those lines meeting the curve at three points coinciding with O. It may be easily shown that the tangents at O are

$$c_0 x^2 + 2c_1 xy + c_2 y^2 = 0 \ .$$

Definition 2.2.1. Consider a curve with a double point at the origin O. The origin is called

i). a *crunode* (or *node*) if the tangents are real so that the curve has two real branches passing through O,

ii). an *acnode* (or *isolated point*) if the tangents are unreal, in which case O is a real point of the curve with no neighbouring point,

iii). a *cusp* if the tangents are coincident.

The term *node* is regularly used to mean any double point that is not a cusp. Note that the concept of a double point and the corresponding tangents may be extended as follows.

Proposition 2.2.1. *If the terms of lowest degree in the Cartesian equation of a curve are of degree k, then O is called a* **multiple point of order k** *(a k-ple point). Any line through O meets the curve in k points coinciding with O except the k tangents at O obtained by equating to zero the terms of lowest degree, which meet the curve in (at least) $k+1$ points coinciding with O.*

The following proposition provides a condition for a double point and moreover a way of classifying the type of double point.

Proposition 2.2.2. *If $(\tilde{x}, \tilde{y})$ is a double point on the curve $f(x, y) = 0$ then*

$$f(\tilde{x}, \tilde{y}) = \frac{\partial f}{\partial x}(\tilde{x}, \tilde{y}) = \frac{\partial f}{\partial y}(\tilde{x}, \tilde{y}) = 0 \ .$$

Moreover if $f''_{(x,y)}(\tilde{x}, \tilde{y})$ is the Hessian of f at $(\tilde{x}, \tilde{y})$ then the double point is

i). a crunode if $\mathrm{Det}\left[f''_{(x,y)}(\tilde{x}, \tilde{y})\right] < 0$,

ii). an acnode if $\mathrm{Det}\left[f''_{(x,y)}(\tilde{x}, \tilde{y})\right] > 0$,

iii). a cusp if $\mathrm{Det}\left[f''_{(x,y)}(\tilde{x}, \tilde{y})\right] = 0$.

(Similarly if $(\tilde{x}, \tilde{y})$ is a k-ple point, all the partial derivatives of f with respect to x and y up to order $k-1$ inclusive must vanish.)

Proof. If we consider a curve with Cartesian equation $f(x, y) = 0$, then transferring the origin to a point $(\tilde{x}, \tilde{y})$ on the curve so that $f(x + \tilde{x}, y + \tilde{y}) = 0$ yields

$$0 = f(\tilde{x}, \tilde{y}) + x\frac{\partial f}{\partial x}(\tilde{x}, \tilde{y}) + y\frac{\partial f}{\partial y}(\tilde{x}, \tilde{y}) + \frac{1}{2}\left(x^2\frac{\partial^2 f}{\partial x^2}(\tilde{x}, \tilde{y}) + 2xy\frac{\partial^2 f}{\partial x \partial y}(\tilde{x}, \tilde{y}) + y^2\frac{\partial^2 f}{\partial y^2}(\tilde{x}, \tilde{y})\right) + \cdots \ .$$

Observe that if the new origin is a double point then

$$f(\tilde{x}, \tilde{y}) = \frac{\partial f}{\partial x}(\tilde{x}, \tilde{y}) = \frac{\partial f}{\partial y}(\tilde{x}, \tilde{y}) = 0 \ ,$$

and the tangents at the new origin are

$$x^2\frac{\partial^2 f}{\partial x^2}(\tilde{x},\tilde{y}) + 2xy\frac{\partial^2 f}{\partial x \partial y}(\tilde{x},\tilde{y}) + y^2\frac{\partial^2 f}{\partial y^2}(\tilde{x},\tilde{y}) = 0 \ .$$

□

The previous proposition eludes to a relationship between cusped points of the level surface and the caustic curve. This will now be made clear.

Remark 2.2.1. In [15] the term *node* is used for any singular point with two or more different directions of the tangent plane. We reserve the use of the term for a non-cusped *double* point.

Definition 2.2.2. Consider a curve $x = x(s)$ parameterised by s. We say that $x(s)$ has a *generalised cusp* at $s = \tilde{s}$ if

$$\left.\frac{dx(s)}{ds}\right|_{s=\tilde{s}} = 0 \ . \tag{2.2.3}$$

Recall that $\boldsymbol{x} = \Phi_t \boldsymbol{x}_0 = \boldsymbol{x}_0 + t\nabla S_0(\boldsymbol{x}_0)$ and observe that the derivative map $D\Phi_t(x_0)$ is defined by

$$\begin{aligned} x + \delta x &= \Phi_t(x_0 + \delta x_0) \\ &= \Phi_t(x_0) + D\Phi_t(x_0)\delta x_0 + \mathrm{O}(\delta x_0^2) \ . \end{aligned}$$

Note that since $\Phi_t x_0 = x$ we have $\delta x = D\Phi_t(x_0)\delta x_0 + \mathrm{O}(\delta x_0^2)$ so that to second order $D\Phi_t(x_0)$ is a linear map from tangent space T_{x_0} to tangent space T_x. Trivially for our Φ_t we see that $D\Phi_t(x_0) : T_{x_0} \to T_x$ is given by $D\Phi_t(x_0) = (I + tS_0''(x_0))$ and it follows that

$$\begin{aligned} \nabla_{\boldsymbol{x}_0}\left\{\frac{t}{2}\left|\nabla_{\boldsymbol{x}_0} S_0(\boldsymbol{x}_0)\right|^2 + S_0(\boldsymbol{x}_0)\right\} &= \left(I + tS_0''(\boldsymbol{x}_0)\right)\nabla S_0(\boldsymbol{x}_0) \\ &= D\Phi_t(\boldsymbol{x}_0)\nabla S_0(\boldsymbol{x}_0) \ . \end{aligned} \tag{2.2.4}$$

Lemma 2.2.3. *Assume that the pre-level surface meets the pre-caustic at the point* $\boldsymbol{x}_0$*, where the vector* $n(\boldsymbol{x}_0) = \left(I + tS_0''(\boldsymbol{x}_0)\right)\nabla S_0(\boldsymbol{x}_0)$ *is such that* $\|n(\boldsymbol{x}_0)\| \neq 0$ *and* $\dim\left(\mathrm{Ker}\left(I + tS_0''(\boldsymbol{x}_0)\right)\right) = 1$. *Then the tangent plane to the pre-level surface* $T_{\boldsymbol{x}_0}$ *is spanned by* $\mathrm{Ker}\left(I + tS_0''(\boldsymbol{x}_0)\right)$.

Proof. It follows for Equation (2.2.4) that where the pre-level surface meets the pre-caustic the non-zero normal, n, to the pre-level surface is a linear combination of eigenvectors corresponding to non-zero eigenvalues of $(I + tS_0''(\boldsymbol{x}_0))$. The eigenvector of $(I + tS_0''(\boldsymbol{x}_0))$ corresponding to eigenvalue zero, e_0, will be orthogonal to these eigenvectors. Hence since T_{x_0} is only one dimensional we must have $T_{x_0} =< e_0 >$. □

Lemma 2.2.4. *Assume that at a point* $\boldsymbol{x}_0$ *on the pre-level surface we have* $|\nabla S_0(\boldsymbol{x}_0)| = 0$, $\boldsymbol{x}_0$ *being a singular point with tangent plane in more than one direction, and* $\dim\left(\mathrm{Ker}\left(I + tS_0''(\boldsymbol{x}_0)\right)\right) = 1$. *Then*

i). if $x_0 \in \Phi_t^{-1}C_t$ *the image point* $\Phi_t(x_0)$ *where the level surface meets the caustic is a singular point with tangent plane in one direction, namely a cusp,* *ii). if $x_0 \notin \Phi_t^{-1}C_t$ the image point $\Phi_t(x_0)$ is a singular point with tangent plane in two or more directions.*

Proof. First observe that if $|\nabla S_0(\boldsymbol{x}_0)| = 0$ then it follows from Equation (2.2.4) that $\boldsymbol{x}_0$ is a singular point of the pre-level surface. If it is a double point, then it will typically be a node with two different directions of the tangent plane. Moreover, observing that for $\boldsymbol{x}_0 = \Phi_t^{-1}\boldsymbol{x}$ we have

$$\nabla_{\boldsymbol{x}}\mathcal{A}(\boldsymbol{x}_0, \boldsymbol{x}, t) = \frac{(x - x_0)}{t} = \nabla_{\boldsymbol{x}_0} S_0(\boldsymbol{x}_0) \ ,$$

so that if $|\nabla S_0(\boldsymbol{x}_0)| = 0$, then at the image point $\boldsymbol{x} = \Phi_t \boldsymbol{x}_0$ we have $|\nabla_{\boldsymbol{x}}\mathcal{A}(\boldsymbol{x}_0, \boldsymbol{x}, t)| = 0$ meaning $\boldsymbol{x}$ is also a singular point.

In the first case, when $\boldsymbol{x}_0 \in \Phi_t^{-1}C_t$, let t_i for $i = 1, 2, \ldots, k$ be the k different directions at $\boldsymbol{x}_0$ of the tangent plane to the pre-level surface where it meets the pre-caustic. Since $D\Phi_t(\boldsymbol{x}_0)$ annihilates the zero eigenvector e_0 on the pre-caustic, it follows that each of the t_i must be mapped into $(I + tS_0''(\boldsymbol{x}_0))e_0^{\perp}$, where $e_0^{\perp}$ is the non-zero eigenvector of $(I + tS_0''(\boldsymbol{x}_0))$. Thus each of the t_i's get mapped into the same direction as $e_0^{\perp}$ and since $\Phi_t(x_0)$ is a singular point it must be a cusp.

In the second case, the k different directions t_i are mapped into the k different directions $(I + tS_0''(\boldsymbol{x}_0))t_i$ for $i = 1, 2, \ldots, k$. □

Remark 2.2.2. If the singular point in Lemma 2.2.4 is a double point then the lemma may be written in terms of nodes. Namely, if $\boldsymbol{x}_0$ is a node of the pre-level surface, then $\boldsymbol{x}_0 \in \Phi_t^{-1}C_t$ implies $\Phi_t\boldsymbol{x}_0$ is a cusped double point, whilst $\boldsymbol{x}_0 \notin \Phi_t^{-1}C_t$ implies $\Phi_t\boldsymbol{x}_0$ is a node.

What happens in the case when $|(I + tS_0''(\boldsymbol{x}_0))\nabla S_0(\boldsymbol{x}_0)| \neq 0$ is made clear in the following proposition.

Proposition 2.2.5. *Assume that $|(I + tS_0''(\boldsymbol{x}_0))\, \nabla S_0(\boldsymbol{x}_0)| \neq 0$, so that $\boldsymbol{x}_0$ is not a singular point of the pre-level surface. Then $\Phi_t(\boldsymbol{x}_0)$ can only be a generalised cusp of the level surface if $\Phi_t(\boldsymbol{x}_0) \in C_t$. Moreover if $\boldsymbol{x} = \Phi_t(\boldsymbol{x}_0) \in \Phi_t\left(\Phi_t^{-1}C_t \cap \Phi_t^{-1}H_t\right)$, then $\boldsymbol{x}$ will be a generalised cusp of the level surface.*

Proof. Let the pre-level surface be parameterised as $x_0 = x_0(s)$ and let $x_0(\tilde{s})$ be a point of intersection of the pre-curves. We write $x(s) = \Phi_t(x_0(s))$ and assume that x_0 and x are differentiable in s.

Since $n(\boldsymbol{x}_0) \neq 0$ we have $\frac{dx_0}{ds}(s)\big|_{s=\tilde{s}} \neq 0$ and it follows that

$$\begin{aligned} \left.\frac{dx}{ds}(s)\right|_{s=\tilde{s}} &= \left[(D\Phi_t(x_0(s)))\,\frac{dx_0}{ds}(s)\right]_{s=\tilde{s}} \\ &= \left[(I + tS_0''(x_0(s)))\,\frac{dx_0}{ds}(s)\right]_{s=\tilde{s}} \ . \end{aligned} \tag{2.2.5}$$

For this to be zero it is necessary that $\mathrm{Det}[I + tS_0''] = 0$, which means $\boldsymbol{x}_0 \in \Phi_t^{-1}C_t$ so that $\boldsymbol{x} = \Phi_t(\boldsymbol{x}_0) \in C_t$. Alternatively, if $\boldsymbol{x}_0 \in \Phi_t^{-1}C_t$ it follows immediately from Lemma 2.2.3 and Equation (2.2.5) that

$$\left.\frac{dx}{ds}(s)\right|_{s=\tilde{s}} = 0 \ .$$

□

2.3 The Cusp Singularity

As an example of the results in the previous section, we consider the initial function $S_0(\boldsymbol{x}_0) = \frac{x_0^2 y_0}{2}$ which gives rise to the cusp singularity. To obtain the pre-level surface we use the Eikonal equation from Equation (2.2.1), which gives

$$\frac{x_0^2}{2}\left\{t\left(y_0+\frac{1}{2t}\right)^2+\frac{x_0^2 t}{4}-\frac{1}{4t}\right\}=c\,.$$

If $c \equiv 0$ (the zero pre-level surface) this yields the line pair $x_0^2 = 0$ and the curve

$$y_0(x_0) = \frac{-1 \pm \sqrt{1-t^2x_0^2}}{2t}\,, \tag{2.3.1}$$

for $x_0^2 \leq \frac{1}{t^2}$. As may be seen in Figure 2.2 the zero pre-level surface consists of a line pair and ellipse. In addition the pre-caustic is given by

$$1 + ty_0 = t^2x_0^2\,,$$

so that

$$y_0(x_0) = \frac{1}{t}\left(t^2x_0^2 - 1\right)\,. \tag{2.3.2}$$

Now the mapping corresponding to the classical mechanical flow is given by

$$\Phi_t(\boldsymbol{x}_0) = \begin{pmatrix} x_0 \\ y_0 \end{pmatrix} + t\begin{pmatrix} x_0 y_0 \\ \frac{x_0^2}{2} \end{pmatrix}\,,$$

so that applying to Equation (2.3.1) yields the zero level surface as the line pair $x^2 = 0$ and the triple cusped hypocycloid (tricuspoid)

$$\begin{aligned} x(x_0) &= \frac{x_0 \pm x_0\sqrt{1-t^2x_0^2}}{2}\,, \\ y(x_0) &= \frac{t^2x_0^2 - 1 \pm x_0\sqrt{1-t^2x_0^2}}{2t}\,, \end{aligned}$$

for $x_0^2 \leq \frac{1}{t^2}$. Similarly applying Φ_t to Equation (2.3.2) yields the caustic as

$$\begin{aligned} x(x_0) &= t^2x_0^3\,, \\ y(x_0) &= \frac{3t}{2}x_0^2 - \frac{1}{t}\,, \end{aligned}$$

which is the semi-cubical parabolic cusp

$$8(yt+1)^3 = 27t^2x^2\,.$$

Observe that $\nabla S_0(\boldsymbol{x}_0) = (x_0y_0, \frac{x_0^2}{2})$ so that $\nabla S_0(\boldsymbol{x}_0) = 0$ at the points $(0, -\frac{1}{t})$ and $(0,0)$ on the zero pre-level surface. Both of these points have tangents planes in more than one direction. However $(0,0) \notin \Phi_t^{-1}C_t$ so that $\Phi_t(0,0) = (0,0)$ is a singular point with tangent

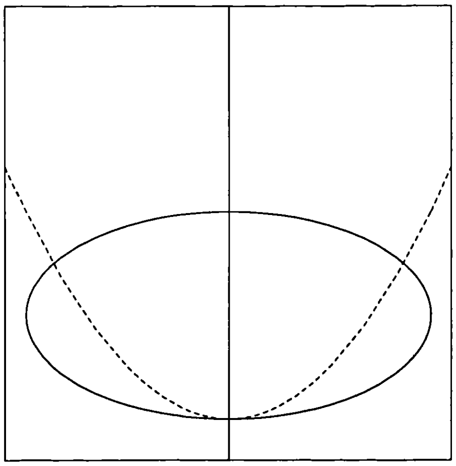

Figure 2.2: Zero pre-level surface and pre-caustic

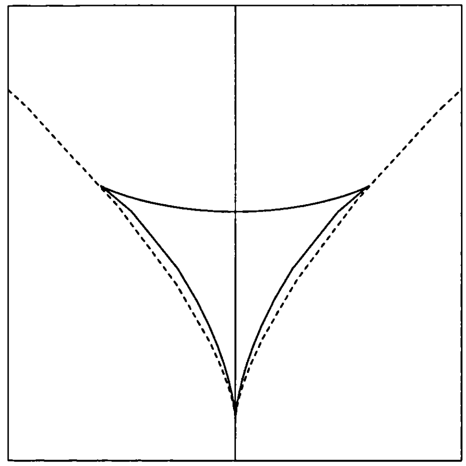

Figure 2.3: The tricuspoid and cusp

plane in more than one direction, whilst $(0,-\frac{1}{t}) \in \Phi_t^{-1}C_t$ so that $\Phi_t(0,-\frac{1}{t}) = (0,-\frac{1}{t})$ is a cusp. This may be seen in Figures 2.2 and 2.3 which show the pre-curves and image curves respectively at time $t=1$. The caustic is identified by the use of a broken line.

When $c \not\equiv 0$ the pre-level surface is given by the curve

$$y_0(x_0) = \frac{-x_0^2 \pm |x_0| \sqrt{8ct + x_0^2 - t^2x_0^4}}{2tx_0^2}, \tag{2.3.3}$$

for $x_0 \neq 0$ and $8ct + x_0^2 - t^2x_0^4 \geq 0$. In this case the sign of c affects the geometry of the (pre-)level surface. Observe that $8ct + x_0^2 - t^2x_0^4 = 0$ has solutions

$$x_0 = \pm\frac{1}{\sqrt{2}t}\left(1 \pm \sqrt{1+32ct^3}\right)^{\frac{1}{2}},$$

so that if $c > 0$ then only two of the solutions will be real meaning $8ct + x_0^2 - t^2x_0^4 \geq 0$ on one region which includes $x_0 = 0$. This results in the ellipse merging with the line pair. If $c < 0$ and $|c| < \frac{1}{32t^3}$ then all four solutions are real meaning $8ct + x_0^2 - t^2x_0^4 \geq 0$ on two regions neither of which includes $x_0 = 0$. This results in the appearance of two pebbles which reduce to two points as $|c| \nearrow \frac{1}{32t^3}$.

The corresponding level surface is given by

$$x(x_0) = \frac{x_0^2 \pm |x_0|\sqrt{8ct + x_0^2 - t^2x_0^4}}{2x_0},$$
$$y(x_0) = \frac{t^2x_0^4 - x_0^2 \pm |x_0|\sqrt{8ct + x_0^2 - t^2x_0^4}}{2tx_0^2},$$

for $x_0 \neq 0$ and $8ct + x_0^2 - t^2x_0^4 \geq 0$.

Proposition 2.3.1. *The pre-curves meet in*

i). two points if $c > 0$,

ii). three points if $c = 0$,

iii). four points if $-\frac{1}{32t^3} \leq c < 0$.

Proof. Writing the pre-caustic as $x_0(y_0) = \pm\frac{1}{t}\sqrt{1+ty_0}$, for $y_0 \geq -\frac{1}{t}$ and inserting into the pre-level surface yields

$$\frac{1}{8t^3} + \frac{3}{4t^2}y_0 + \frac{9}{8t}y_0^2 + \frac{y_0^3}{2} = c\ .$$

Define

$$F(y_0) := \frac{1}{8t^3} + \frac{3}{4t^2}y_0 + \frac{9}{8t}y_0^2 + \frac{y_0^3}{2} - c\ ,$$

so that the pre-curves meet at solutions $y_0 \geq -\frac{1}{t}$ of $F(y_0) = 0$.

Observe that at the local maximum $F(-\frac{1}{t}) = -c$ whilst at the local minimum $F(-\frac{1}{2t}) = -\frac{1}{32t^3} - c$. If $-\frac{1}{32t^3} \leq c < 0$ then $F(y_0) = 0$ has three solutions, two of which are greater than $-\frac{1}{t}$. Thus the pre-curves meet in $2+2=4$ points. If $c = 0$, then $F(y_0) = 0$ has two solutions $y_0^{(1)} = -\frac{1}{t}$ and $y_0^{(2)} > -\frac{1}{t}$. Thus the pre-curves meet in $1+2=3$ points. Finally if $c > 0$ then $F(y_0) = 0$ has one solution, which is greater than $-\frac{1}{t}$. Thus the pre-curves meet in $1+1=2$ points. □

Corollary 2.3.2. *The level surface* $S(x,t) = c$ *meets* C_t *in*

i). two generalised cusps if $c > 0$,

ii). three generalised cusps if $c = 0$,

iii). four generalised cusps if $-\frac{1}{32t^3} \leq c < 0$.

Figures 2.4 and 2.5 show the pre-level and level surfaces for $c = 0.01 > 0$ at $t = 1$ together with the caustic. The corresponding pictures for $c = -0.01 < 0$ at $t = 1$ are shown in Figures 2.6 and 2.7.

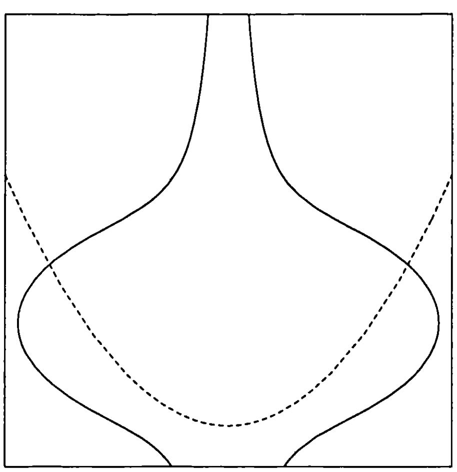

Figure 2.4: Pre-level surface ($c = 0.01$) and pre-caustic for the cusp singularity

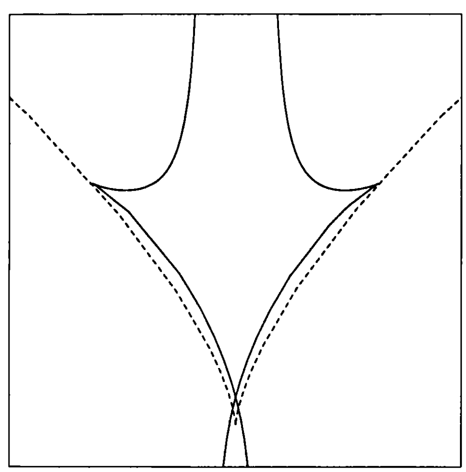

Figure 2.5: Level surface ($c = 0.01$) and caustic for the cusp singularity

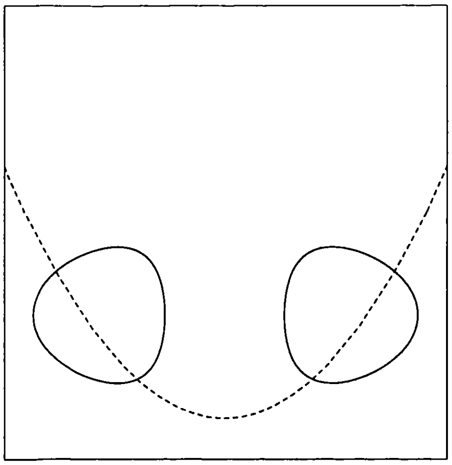

Figure 2.6: Pre-level surface ($c = -0.01$) and pre-caustic for the cusp singularity

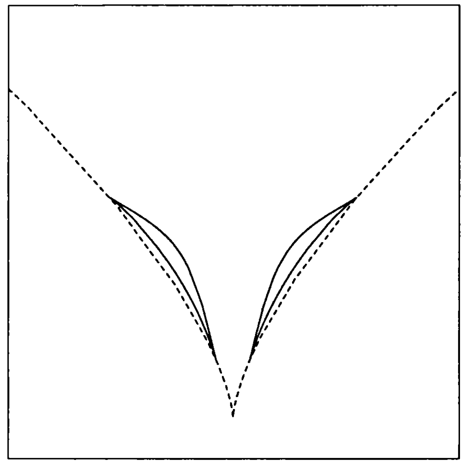

Figure 2.7: Level surface ($c = -0.01$) and caustic for the cusp singularity

2.4 Polynomial Swallowtail in Two Dimensions

In this section we attempt to find a polynomial initial condition that produces a caustic with the geometrical properties of a swallowtail. We consider an initial function of the form

$$S_0(\boldsymbol{x}_0) = f(x_0) + g(x_0)y_0 \ ,$$

with $f, g \in C^3$. A simple calculation yields the following result.

Lemma 2.4.1. *For the initial function $S_0(\boldsymbol{x}_0) = f(x_0) + g(x_0)y_0$ with $f, g \in C^3$ the pre-caustic is given by*

$$y_0(x_0) = \frac{-1 + t^2 g'(x_0)^2 - t f''(x_0)}{t g''(x_0)} \ , \tag{2.4.1}$$

for $g''(x_0) \neq 0$, whilst the pre-level surface is determined by

$$\frac{t}{2}\left(f'(x_0) + g'(x_0)y_0\right)^2 + \frac{t}{2}g(x_0)^2 + f(x_0) + g(x_0)y_0 = c \ . \tag{2.4.2}$$

Moreover, the mapping Φ_t corresponding to the classical mechanical flow is given by

$$\boldsymbol{x} = \Phi_t \boldsymbol{x}_0 = \begin{pmatrix} x_0 \\ y_0 \end{pmatrix} + t \begin{pmatrix} f'(x_0) + g'(x_0)y_0 \\ g(x_0) \end{pmatrix} \ .$$

All important in the derivation of an appropriate initial function is the following result.

Lemma 2.4.2. *For the initial function $S_0(\boldsymbol{x}_0) = f(x_0) + g(x_0)y_0$, with $f, g \in C^3$, the number of generalised cusps on the caustic is determined by the zeros of $F(x_0) = 0$ where*

$$F(x_0) := \frac{t}{g'(x_0)} \frac{d}{dx_0}\left(\frac{g'(x_0)^3}{g''(x_0)}\right) - \frac{d}{dx_0}\left(\frac{f''(x_0)}{g''(x_0)}\right) + \frac{1}{t}\frac{g'''(x_0)}{g''(x_0)^2} \ . \tag{2.4.3}$$

Proof. From Equation (2.2.5) in the proof of Proposition 2.2.5 we know that the image curve will have a generalised cusp when

$$(I + tS_0'')\,\frac{d\boldsymbol{x}_0}{ds}(s) = 0\ ,$$

which in our case is

$$\begin{pmatrix} 1 + t(f''(x_0(s)) + g''(x_0(s))y_0(s)) & tg'(x_0(s)) \\ tg'(x_0(s)) & 1 \end{pmatrix} \frac{d\boldsymbol{x}_0}{ds}(s) = 0\ .$$

Since we are interested in the caustic we use the parametrisation described in Lemma 2.4.1, namely $\boldsymbol{x}_0(s) = (s, y_0(s))$ where $y_0(s)$ is given by Equation (2.4.1). Thus we have

$$\begin{pmatrix} 1 + t(f''(s) + g''(s)y_0(s)) + tg'(s)y_0'(s) \\ tg'(s) + y_0'(s) \end{pmatrix} = \begin{pmatrix} 0 \\ 0 \end{pmatrix}\ ,$$

which on substitution of our expression for $y_0(s)$ yields the equations

$$\begin{aligned} tg'(s)(y_0'(s) + tg'(s)) &= 0\ , \\ y_0'(s) + tg'(s) &= 0\ . \end{aligned}$$

Assuming $g'(s) \neq 0$, it follows that we will obtain generalised cusps at the zeros of

$$F(s) := y_0'(s) + tg'(s)\ ,$$

which on insertion of the expression for $y_0'(s)$ yields the right hand side of Equation (2.4.3). □

2.4.1 The Pre-Caustic and Caustic

In order to obtain a caustic with the geometrical properties of a two dimensional swallow-tail we require that F has two zeros and the image curve has a point of self intersection. Observe that if we take $f(x_0) = \alpha x_0^5$ and $g(x_0) = \beta x_0^2$ for $\alpha, \beta \neq 0$, then we obtain

$$F(x_0) = t\beta^2 x_0 - 5\alpha x_0^2\ ,$$

so that

$$F(x_0) = 0 \qquad \Longrightarrow \qquad x_0 = 0 \text{ and } x_0 = \frac{t\beta^2}{5\alpha}\ .$$

For simplicity we take $\alpha > 0$ and set $\beta \equiv 1$ in what follows. From Lemma 2.4.1 we see that the pre-caustic is given by

$$y_0(x_0) = \frac{-1 + 4t^2x_0^2 - 20\alpha t x_0^3}{2t}\ , \tag{2.4.4}$$

whilst our mapping Φ_t is given by

$$\Phi_t(\boldsymbol{x}_0) = \begin{pmatrix} x_0 \\ y_0 \end{pmatrix} + t\begin{pmatrix} 5\alpha x_0^4 + 2x_0y_0 \\ x_0^2 \end{pmatrix}\ . \tag{2.4.5}$$

Thus the caustic C_t is given by

$$\begin{aligned} x(x_0) &= -15\alpha t x_0^4 + 4t^2 x_0^3 , \\ y(x_0) &= -\frac{1}{2t} + 3t x_0^2 - 10\alpha x_0^3 . \end{aligned} \tag{2.4.6}$$

Hence the generalised cusps will occur at

$$\Phi_t \left(0, y_0(0)\right) = \left(0, -\frac{1}{2t}\right) ,$$

and

$$\Phi_t \left(\frac{t}{5\alpha}, y_0\left(\frac{t}{5\alpha}\right)\right) = \left(\frac{t^5}{125\alpha^3}, -\frac{1}{2t} + \frac{t^3}{25\alpha^2}\right) ,$$

where for large α the cusps become increasingly close. Moreover solving the equations $x(s_1) = x(s_2)$ and $y(s_1) = y(s_2)$ for $s_1 \neq s_2$ yields $s_1 = t\left(\frac{1-\sqrt{3}}{10\alpha}\right)$ and $s_2 = t\left(\frac{1+\sqrt{3}}{10\alpha}\right)$. Thus C_t has a point of self intersection at

$$\boldsymbol{x} = \left(-\frac{t^5}{500\alpha^3}, -\frac{1}{2t} + \frac{t^3}{50\alpha^2}\right) .$$

Hence for all $t > 0$ and $\alpha \neq 0$ we will have a polynomial swallowtail. Moreover, the point of self intersection lies vertically half way between the generalised cusps.

Remark 2.4.1. Observe that $(x^{\alpha}(x_0), y^{\alpha}(x_0)) = (-x^{-\alpha}(-x_0), y^{-\alpha}(-x_0))$ so that the caustic for $\alpha < 0$ will simply be the mirror image of the case $\alpha > 0$ about the line $x = 0$.

Proposition 2.4.3. *For all $t > 0$ and $\alpha \neq 0$ the initial function $S_0(\boldsymbol{x}_0) = \alpha x_0^5 + x_0^2 y_0$ produces a* ***polynomial swallowtail*** *singularity with generalised cusps at $(0, -\frac{1}{2t})$ and $(\frac{t^2}{125\alpha^3}, -\frac{1}{2t} + \frac{t^3}{25\alpha^2})$ and self intersection point $(-\frac{t^5}{500\alpha^3}, -\frac{1}{2t} + \frac{t^3}{50\alpha^2})$.*

In Figures 2.8 and 2.9 the pre-caustic and caustic are shown for $\alpha = 0.2$ and $t = 1$.

2.4.2 Implicit Equation for the Polynomial Swallowtail

Alternatively, instead of obtaining the caustic in parametric form, we may obtain a single equation for the shockwave by considering the integral

$$I = \iint T_0(\boldsymbol{x_0}) \exp\left(-\frac{\mathcal{A}(\boldsymbol{x}_0, \boldsymbol{x}, t)}{\mu^2}\right) \mathrm{d}^2\boldsymbol{x_0} ,$$

as $\mu \sim 0$ with $T_0 \in C_0^{\infty}$, where in our case

$$\mathcal{A}(\boldsymbol{x}_0, \boldsymbol{x}, t) = \frac{(x - x_0)^2}{2t} + \frac{(y - y_0)^2}{2t} + \alpha x_0^5 + x_0^2 y_0 .$$

It follows from Laplace's result that after doing the y_0 integration we obtain

$$I \sim \int T_0(x_0, y - t x_0^2) \exp\left(-\frac{1}{\mu^2}\tilde{\mathcal{A}}(x_0, \boldsymbol{x}, t)\right) \mathrm{d}x_0 ,$$

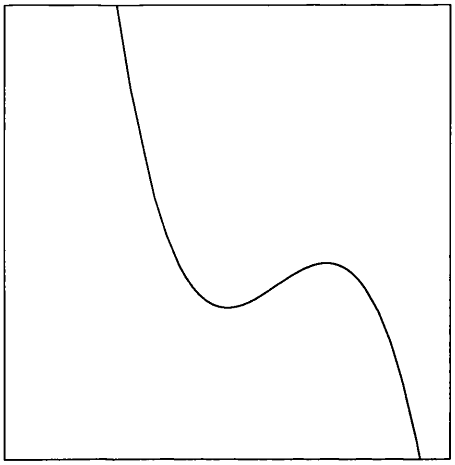

Figure 2.8: Pre-Caustic at $t = 1$ with $\alpha = 0.2$

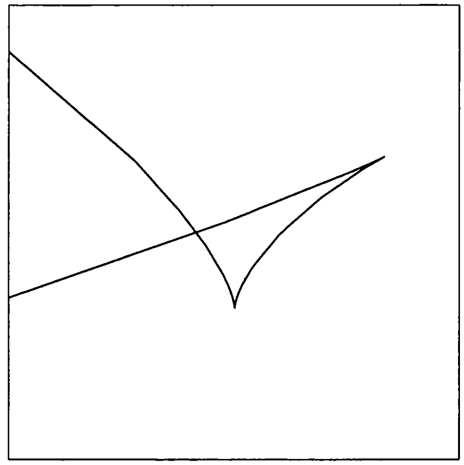

Figure 2.9: Polynomial Swallowtail at $t = 1$ with $\alpha = 0.2$

as $\mu \sim 0$ where

$$\tilde{\mathcal{A}}(x_0, x, t) = \alpha x_0^5 - \frac{t}{2}x_0^4 + x_0^2\left(\frac{1}{2t} + y\right) - \frac{x_0 x}{t} + \frac{x^2}{2t} .$$

This is the generating function of our two dimensional polynomial swallowtail. To obtain the equation of the shockwave we need to eliminate x_0 from $\frac{\partial \tilde{\mathcal{A}}}{\partial x_0} = 0$ and $\frac{\partial^2 \tilde{\mathcal{A}}}{\partial x_0^2} = 0$. Namely we must eliminate x_0 from

$$5\alpha x_0^4 - 2tx_0^3 + 2x_0\left(\frac{1}{2t} + y\right) - \frac{x}{t} = 0 ,$$

and

$$20\alpha x_0^3 - 6tx_0^2 + 2\left(\frac{1}{2t} + y\right) = 0 .$$

After some simplification this gives the equation of the shockwave for the two dimensional swallowtail

$$\begin{aligned} 8tx\left(54t^5 x - 15t^2(1+2ty)^2\alpha - 1200tx(1+2ty)\alpha^2 + 4000x^2\alpha^3\right) \\ = (1+2ty)^3\left(32t^4 - 675(1+2ty)\alpha^2\right) . \end{aligned}$$

2.4.3 The Zero Pre-Level and Zero Level Surface

It follows from Lemma 2.4.1 that the pre-level surface is given by

$$x_0^2\left(\frac{t}{2}\left(25\alpha^2 x_0^6 + 20\alpha x_0^3 y_0 + 4y_0^2 + x_0^2\right) + \alpha x_0^3 + y_0\right) = c .$$

Initially considering the case $c \equiv 0$ we see that the zero pre-level surface consists of the line pair $x_0^2 = 0$ and

$$y_0(x_0) = \frac{-1 - 10\alpha t x_0^3 \pm \sqrt{12\alpha t x_0^3 - 4t^2 x_0^2 + 1}}{4t} ,$$

for $12\alpha t x_0^3 - 4t^2 x_0^2 + 1 \geq 0$. Applying the flow mapping Φ_t to this yields the zero level surface as the line pair $x^2 = 0$ and

$$x(x_0) = \frac{x_0}{2}\left(1 \pm \sqrt{12\alpha t x_0^3 - 4t^2 x_0^2 + 1}\right) ,$$
$$y(x_0) = \frac{1}{4t}\left(4t^2 x_0^2 - 1 - 10\alpha t x_0^3 \pm \sqrt{12\alpha t x_0^3 - 4t^2 x_0^2 + 1}\right) .$$

Proposition 2.4.4. *For the initial function $S_0(\boldsymbol{x}_0) = x_0^5 + x_0^2 y_0$ the (pre-)zero level surface will consist of*

i). a line pair and one component if $t \leq 3^{\frac{5}{4}} \frac{\sqrt{\alpha}}{2}$,

ii). a line pair and two components if $t > 3^{\frac{5}{4}} \frac{\sqrt{\alpha}}{2}$.

Proof. Let $\mathcal{D}_t(x_0) := 12\alpha t x_0^3 - 4t^2 x_0^2 + 1$ be the discriminant in the expression for the zero pre-level surface. Then it may easily be shown that $\mathcal{D}_t(x_0) \geq 0$ on only one region if $1 - \frac{16t^4}{243\alpha^2} \geq 0$ whilst $\mathcal{D}_t(x_0) \geq 0$ on two regions if $1 - \frac{16t^4}{243\alpha^2} < 0$. Hence the zero pre-level surface will consist of one region for $t \leq \frac{3^{\frac{5}{4}}\sqrt{\alpha}}{2}$ and two regions for $t > \frac{3^{\frac{5}{4}}\sqrt{\alpha}}{2}$. □

Proposition 2.4.4 is illustrated in Figures 2.10 and 2.11 which show a time series for the zero (pre-)level surface with $\alpha = 0.2$. Observe that for $t \leq 3^{\frac{5}{4}} \frac{\sqrt{\alpha}}{2}$ the zero pre-level

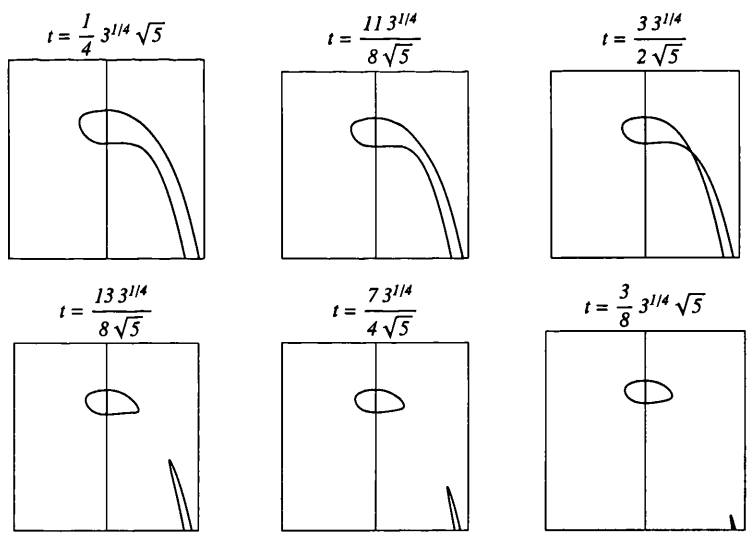

Figure 2.10: Zero pre-level surface for the polynomial swallowtail

surface consists of a line pair and worm whilst the zero level surface consists of a line pair and swallowtail shaped curve. However, for $t > 3^{\frac{5}{4}} \frac{\sqrt{\alpha}}{2}$ the worm separates into a pebble and worm whilst the swallowtail shaped curve separates into an arc and tricuspoid.

Alternatively, instead of parametric equations we may obtain a single equation for the level surface by observing that after doing the y_0 integration it follows from Laplace's result that

$$\mathcal{A}(x_0, \boldsymbol{x}, t) = \frac{x_0^2}{2t} - \frac{t x_0^4}{2} + x_0^5 - \frac{x_0 x}{t} + \frac{x^2}{2t} + x_0^2 y .$$

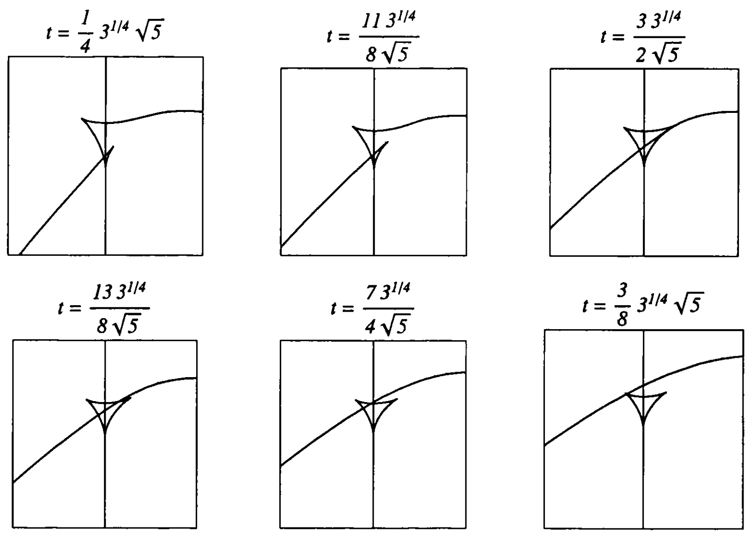

Figure 2.11: Zero level surface for the polynomial swallowtail

In order to obtain the zero level surface we now eliminate x_0 from

$$\mathcal{A}(x_0, \boldsymbol{x}, t) = 0 \qquad \text{and} \qquad \frac{\partial \mathcal{A}}{\partial x_0} = 0 \, .$$

After some simplification this gives the equation of the zero level surface as

$$\begin{aligned} \frac{x^2}{16t^5}\big(54(x^3+y) - 16t^7(x^2+y^2)^2 + t(-27x^2 + 3125x^6 + 3800x^3y + 432y^2) - \\ 2t^2(1250x^5 + 597x^2y + 4500x^3y^2 - 648y^3) + 8t^6(5x^2y - 3y^3) + \\ t^5(x^2 + 80x^3y - 12y^2 - 48xy^3) + 6t^3(75x^4 - 2xy - 230x^2y^2 + 288y^4) + \\ 2t^4(2x^3 - y + 500x^4y - 24xy^2 + 900x^2y^3 + 432y^5)\big) = 0 \, . \end{aligned}$$

Observe that we have a factor x^2 producing a line pair, a feature missing from the non-polynomial swallowtail in [14] which possesses a single line since the other has fused with the rest of the curve.

2.4.4 The Pre-Level and Level Surfaces

When $c \neq 0$ the pre-level surface is given by

$$y_0(x_0) = \frac{-10\alpha t x_0^5 - x_0^2 \pm |x_0|\sqrt{12\alpha t x_0^5 - 4t^2x_0^4 + x_0^2 + 8ct}}{4tx_0^2} \, ,$$

for $x_0 \neq 0$ and $12\alpha t x_0^5 - 4t^2x_0^4 + x_0^2 + 8ct \geq 0$. Moreover applying Φ_t yields the level surface as

$$x(x_0) = \frac{1}{2x_0}\left(x_0^2 \pm |x_0|\sqrt{12\alpha t x_0^5 - 4t^2x_0^4 + x_0^2 + 8ct}\right) \, ,$$

$$y(x_0) = \frac{1}{4tx_0^2}\left(-10\alpha t x_0^5 + 4t^2x_0^4 - x_0^2 \pm |x_0|\sqrt{12\alpha t x_0^5 - 4t^2x_0^4 + x_0^2 + 8ct}\right) \, ,$$

for $x_0 \neq 0$ and $12\alpha t x_0^5 - 4t^2x_0^4 + x_0^2 + 8ct \geq 0$. The geometry in the case when $c \not\equiv 0$ differs from the zero pre-level surface as the following proposition now explains.

Proposition 2.4.5. *If $t < \frac{3^{\frac{5}{4}}}{2}\sqrt{\alpha}$ and $|c|$ is sufficiently small then*

i). if $c > 0$ the pre-level surface consists of a worm fused with the line pair,

ii). if $c < 0$ the pre-level surface consists of two components, namely a pebble and worm.

If $t > \frac{3^{\frac{5}{4}}}{2}\sqrt{\alpha}$ and $|c|$ is sufficiently small then

i). if $c > 0$ the pre-level surface consists of a pebble fused with the line pair and a worm,

ii). if $c < 0$ the pre-level surface consists of two pebbles and a worm.

Proof. Denoting the discriminant by $\mathcal{D}_t(x_0) := 12\alpha t x_0^5 - 4t^2x_0^4 + x_0^2 + 8ct$ it follows that $\mathcal{D}_t'(x_0) = 2x_0 g(x_0)$ where $g(x_0) := 30\alpha t x_0^3 - 8t^2x_0^2 + 1$. Now $g(x_0)$ has a maximum at $x_0 = 0$ and a minimum at $x_0 = \frac{8t}{45\alpha}$, at which $g(0) = 1$ and $g(\frac{8t}{45\alpha}) = 1 - \frac{512t^4}{6075\alpha^2}$.

Case 1: $t \leq \frac{3}{4}\left(\frac{3}{2}\right)^{\frac{1}{4}}\sqrt{5\alpha}$
The local maximum and minimum are non-negative so that $g(x_0) = 0$ has one real non-repeated solution $x_0 = u_1 < 0$. Thus $\mathcal{D}_t(x_0)$ has a maximum at $x_0 = u_1$ and a minimum at $x_0 = 0$ where $\mathcal{D}_t(0) = 8ct$. If $c > 0$ then $\mathcal{D}_t(x_0) \geq 0$ on only one region which includes $x_0 = 0$, so that the pre-level surface consists of one component fused with the line pair. If $c < 0$ and $|c|$ is sufficiently small so that $\mathcal{D}_t(u_1) > 0$, i.e. c must satisfy $\left|\frac{\mathcal{D}_t(u_1)}{8ct} - 1\right| \geq 1$, then $\mathcal{D}_t(x_0) \geq 0$ on two regions, neither of which contains $x_0 = 0$. This results in the appearance of a pebble and worm.

Case 2: $t > \frac{3}{4}\left(\frac{3}{2}\right)^{\frac{1}{4}}\sqrt{5\alpha}$ and $t < \frac{3^{\frac{5}{4}}}{2}\sqrt{\alpha}$
For $t > \frac{3}{4}\left(\frac{3}{2}\right)^{\frac{1}{4}}\sqrt{5\alpha}$, $g(x_0) = 0$ will have three real solutions u_1, u_2, u_3 where $u_1 < 0$ and $u_3 > u_2 > 0$. It follows that $\mathcal{D}_t(x_0)$ will have local maxima at $x_0 = u_1$ and $x_0 = u_2$, and local minima at $x_0 = 0$ and $x_0 = u_3$.

We begin by showing that $\mathcal{D}_t(0) < \mathcal{D}_t(u_3)$. Using the fact that $\mathcal{D}_t'(u_3) = 0$ this is equivalent to showing $u_3 < \frac{\sqrt{3}}{2t}$. Observing that $\alpha > \frac{4t^2}{9\sqrt{3}}$ we see

$$\frac{8t}{45\alpha} < \frac{2\sqrt{3}}{5t} < \frac{\sqrt{3}}{2t},$$

and

$$g\left(\frac{\sqrt{3}}{2t}\right) = -5 + \frac{45\sqrt{3}}{4t^2}\alpha > 0 .$$

Hence since $g(\frac{8t}{45\alpha}) < 0$ and g is increasing for $x_0 > \frac{8t}{45\alpha}$ it follows that $u_3 < \frac{\sqrt{3}}{2t}$. Thus $\mathcal{D}_t(0) < \mathcal{D}_t(u_3)$. Assuming $|c|$ is sufficiently small so that $\mathcal{D}_t(u_3) > 0$ we arrive at the same conclusion as Case 1.

Case 3: $t > \frac{3^{\frac{5}{4}}}{2}\sqrt{\alpha}$
Here we show that $\mathcal{D}_t(u_3) < \mathcal{D}_t(0)$ or equivalently $u_3 > \frac{\sqrt{3}}{2t}$. Observing that $\alpha < \frac{4t^2}{9\sqrt{3}}$ we see

$$g\left(\frac{\sqrt{3}}{2t}\right) = -5 + \frac{45\sqrt{3}}{4t^2}\alpha < 0 .$$

Since $g(x_0) > 0$ for $x_0 > u_3$ it follows immediately that $u_3 > \frac{\sqrt{3}}{2t}$ so that $\mathcal{D}_t(u_3) < \mathcal{D}_t(0)$. Assume $|c|$ is sufficiently small so that $\mathcal{D}_t(u_3) < 0$ and $\mathcal{D}_t(u_1), \mathcal{D}_t(u_2) > 0$. If $c > 0$ then $\mathcal{D}_t(x_0) \geq 0$ on two regions one of which contains $x_0 = 0$. Thus we obtain a pebble fused with the line pair and a worm. If $c < 0$ then $\mathcal{D}_t(x_0) \geq 0$ on three regions none of which include $x_0 = 0$. This results in the appearance of two pebbles and a worm. □

The above Proposition is illustrated in Figures 2.12 - 2.15 where we have set $\alpha = 0.2$ and $t = 1$ so that $t > \frac{3^{\frac{5}{4}}}{2}\sqrt{\alpha}$. Figures 2.12 and 2.13 show the pre-level surface and level surface for $c = 0.005$, whilst Figures 2.14 and 2.15 show the pre-level surface and level surface for $c = -0.005$.

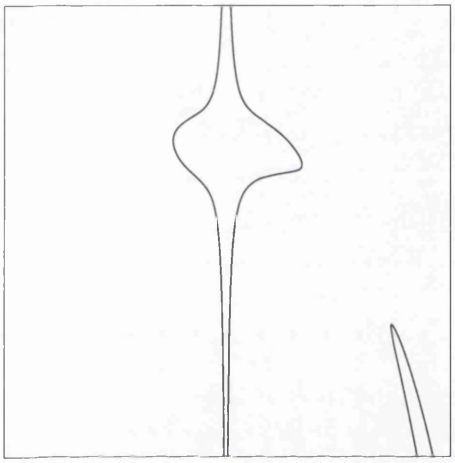

Figure 2.12: Pre-level surface ($c = 0.005$)

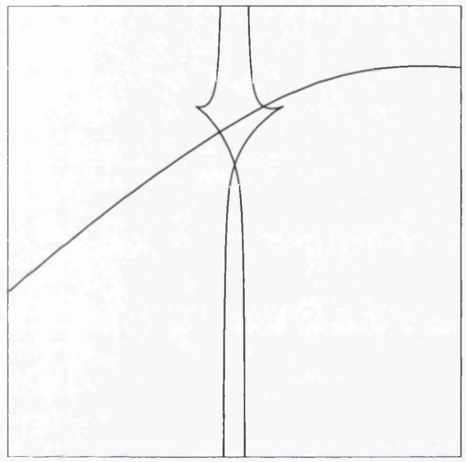

Figure 2.13: Level surface ($c = 0.005$)

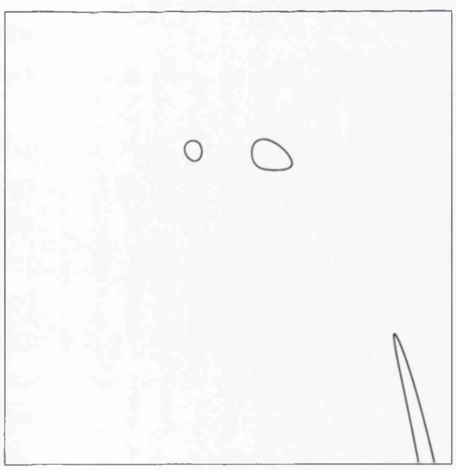

Figure 2.14: Pre-level surface ($c = -0.005$)

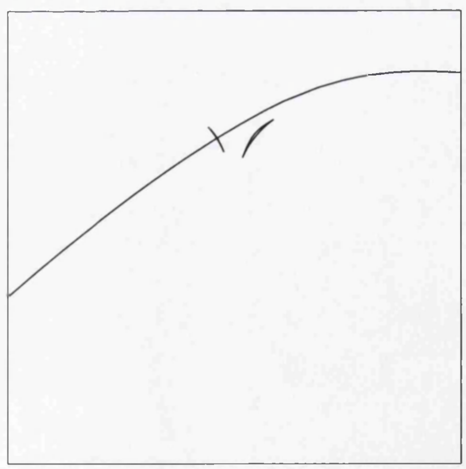

Figure 2.15: Level surface ($c = -0.005$)

2.4.5 Intersection of the Caustic and Zero-Level Surface

The basic idea of Proposition 2.2.5 is that the level surface will meet the caustic in a generalised cusp at α if and only if at least one inverse image point $\Phi_t^{-1}\alpha$ is a common point on the pre-curves. Hence points $\boldsymbol{x}$ at a generalised cusp on the level surface must satisfy

$$\mathcal{A}(\tilde{\boldsymbol{x}}_0(\boldsymbol{x},t),\boldsymbol{x},t)=0 \qquad \text{and} \qquad \mathrm{Det}\left(\mathcal{A}''_{\boldsymbol{x}_0}(\tilde{\boldsymbol{x}}_0(\boldsymbol{x},t),\boldsymbol{x},t)\right)=0\ ,$$

where we are using our usual nomenclature. The points $\boldsymbol{x}$ satisfying the above must lie on both the caustic and the level surface. Clearly in three dimensions we will obtain the intersection of two surfaces, namely a curve, whereas in the case of two dimensions they will meet in a finite number of points. In both cases the points or curve of intersection will evolve in time.

Let us consider our example of the polynomial swallowtail for zero-level surfaces. In Figure 2.16 we have plotted the pre-curves at $t=1$ with $\alpha=0.2$, using a broken line to distinguish the pre-caustic. Applying the mapping Φ_t yields the image curves shown in 2.17.

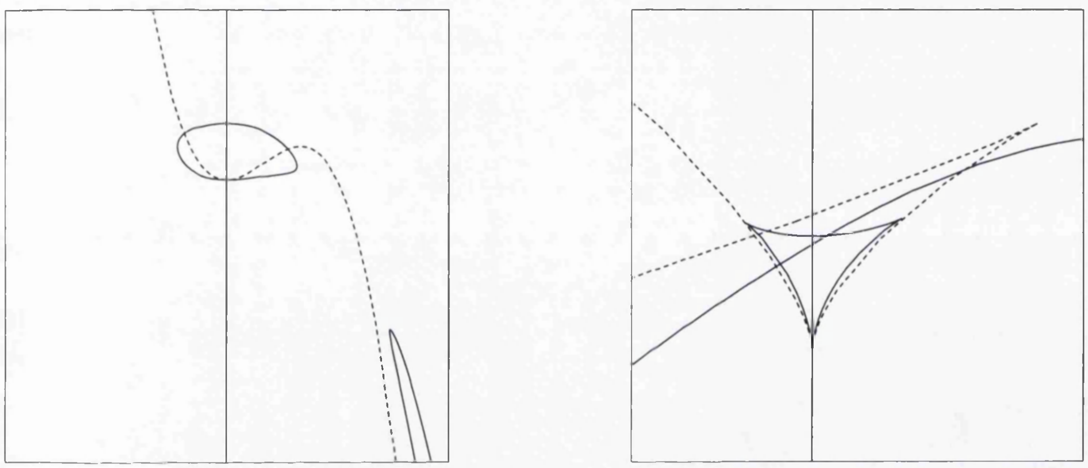

Figure 2.16: Pre-caustic and zero pre-level surface

Figure 2.17: Caustic and zero level surface

Notice that the pre-curves have three distinct points of intersection, one of which is a singular point of the zero pre-level surface. Moreover the zero level surface meets the caustic in eight places (three generalised cusps and five non-cusped intersection points). We remark that this observation does not contradict Proposition 2.2.5, for if α_i are non-cusped points of intersection of the image curves then $\Phi_t^{-1}\alpha_i \notin \Phi_t^{-1}C_t \cap \Phi_t^{-1}H_t$. This is illustrating the fact that $\Phi_t^{-1}C_t \cap \Phi_t^{-1}H_t \subset \Phi_t^{-1}(C_t \cap H_t)$ but the opposite inclusion does not hold.

We shall have more to say on the number of common points of pre-curves in Chapters 3 and 5.

2.5 Polynomial Swallowtail in Three Dimensions

In order to obtain a polynomial swallowtail in three dimensions our initial instinct is to extend our result obtained in two dimensions by considering an initial function of the form

$$S_0(\boldsymbol{x_0})=x_0^5+f(x_0)y_0+x_0^2z_0\ . \qquad (2.5.1)$$

Taking $y(x_0) = K$ to be constant it can be shown by the same method as the two dimensional case that generalised cusps will occur at the zeros of the function

$$F(x_0) = \frac{t}{2}\left(12x_0 + 3f'(x_0)f''(x_0) + f(x_0)f'''(x_0)\right) - \frac{1}{2}\left(60x_0^2 + f'''(x_0)K\right) . \qquad (2.5.2)$$

In order for us to obtain a three dimensional swallowtail we require that there must exist C such that $F(x_0) = 0$ has two solutions for $K > C$ and no solutions for $K < C$ or vice versa. The reason for this is that taking sections of a three dimensional swallowtail must produce a two dimensional swallowtail (2 cusps) prior to a certain point and a parabola (0 cusps) after it. Immediately we see from Equation (2.5.2) that $f(x_0)$ must be a polynomial of degree greater than or equal to 3. But if $f \sim x^n$ for $n \geq 3$ then $f' \sim x^{n-1}$, $f'' \sim x^{n-2}$ and $f''' \sim x^{n-3}$. Thus $\deg(f'f'') = \deg(ff''') = 2n-3$ so $F(x_0)$ will be a polynomial of odd degree and as a result will have at least one real root for all values of K. Hence there is no possibility that an initial function of the form in Equation (2.5.1) will produce a three dimensional polynomial swallowtail.

Let us instead consider a more general initial function of the form

$$S_0(\boldsymbol{x_0}) = f(x_0) + g(x_0)y_0 + h(x_0)z_0 .$$

A simple calculation yields the following result.

Lemma 2.5.1. *For the initial function $S_0(\boldsymbol{x_0}) = f(x_0)+g(x_0)y_0+h(x_0)z_0$, with $f, g, h \in C^3$ the pre-caustic is given by*

$$z_0(x_0, y_0) = \frac{1}{th''(x_0)}\left(t^2\left(g'(x_0)^2 + h'(x_0)^2\right) - t\left(f''(x_0) + y_0 g''(x_0)\right) - 1\right) ,$$

for $h''(x_0) \neq 0$, whilst the pre-level surface is determined by

$$\frac{t}{2}\left(f'(x_0) + g'(x_0)y_0 + h'(x_0)z_0\right)^2 + \frac{t}{2}g(x_0)^2 + \frac{t}{2}h(x_0)^2 + f(x_0) + g(x_0)y_0 + h(x_0)z_0 = c .$$

Moreover the mapping Φ_t corresponding to the classical mechanical flow is given by

$$\boldsymbol{x} = \Phi_t \boldsymbol{x}_0 = \begin{pmatrix} x_0 \\ y_0 \\ z_0 \end{pmatrix} + t \begin{pmatrix} f'(x_0) + g'(x_0)y_0 + h'(x_0)z_0 \\ g(x_0) \\ h(x_0) \end{pmatrix} .$$

Lemma 2.5.2. *For the initial function $S_0(\boldsymbol{x_0}) = f(x_0)+g(x_0)y_0+h(x_0)z_0$ where $f, g, h \in C^3$ the number of generalised cusps on the slice $y = K$ of the caustic is determined by the zeros of $F(x_0) = 0$ where omitting the x_0 variable for brevity we have*

$$F(x_0) := t\left\{\frac{1}{h'}\frac{d}{dx_0}\left(\frac{h'^3}{h''}\right) + \frac{1}{g'}\frac{d}{dx_0}\left(\frac{g'^3}{h''}\right) + g\frac{d}{dx_0}\left(\frac{g''}{h''}\right)\right\} - \frac{d}{dx_0}\left(\frac{f''}{h''}\right) - K\frac{d}{dx_0}\left(\frac{g''}{h''}\right) + \frac{1}{t}\frac{h'''}{h''^2} . \qquad (2.5.3)$$

Proof. For the slice $y = K$ we have

$$y_0(x_0) = K - tg(x_0) ,$$
$$z_0(x_0) = \frac{1}{th''(x_0)}\left(t^2(g'(x_0)^2 + h'(x_0)^2) - t(f''(x_0) + (K - tg(x_0))g''(x_0)) - 1\right) ,$$

which may be differentiated to give

$$y_0'(x_0) = -tg' ,$$
$$z_0'(x_0) = \frac{1}{th''^2}\Big(h''\left[2t^2\left(g'g'' + h'h''\right) - t\left(f''' + g'''(K - tg) - tg'g''\right)\right]$$
$$- h'''\left[t^2(g'^2 + h'^2) - t(f'' + (K - tg)g'') - 1\right]\Big) .$$

The cusp condition $(I + tS_0''(\boldsymbol{x}_0(s)))\frac{d\boldsymbol{x}_0(s)}{ds} = 0$ combined with our expressions for $y_0(s)$, $y_0'(s)$ and $z_0(s)$ yields the equations

$$th'(s)(th'(s) + z_0'(s)) = 0 ,$$
$$th'(s) + z_0'(s) = 0 .$$

Since by assumption $h'(s) \neq 0$ we see that generalised cusps are obtained at the zeros of

$$F(x_0) := th'(x_0) + z_0'(x_0) ,$$

which on inserting our expression for $z_0'(x_0)$ yields Equation (2.5.3). □

Proposition 2.5.3. *The initial function $S_0(\boldsymbol{x}_0) = x_0^7 + x_0^3y_0 + x_0^2z_0$ produces a three dimensional swallowtail singularity. We call this a* ***three dimensional polynomial swallowtail****.*

Proof. With $f(x_0) = x_0^7$, $g(x_0) = x_0^3$ and $h(x_0) = x_0^2$, Equation (2.5.3) reduces to

$$F(x_0) = -105x_0^4 + 30tx_0^3 + 6tx_0 - 3K ,$$

which is equivalent to considering the zeros of

$$G(x_0) := 35x_0^4 - 10tx_0^3 - 2tx_0 + K .$$

We need to show that $G(x_0) = 0$ will have either two or zero real solutions depending on the value of K.

Observe that $G'(x_0) = 140x_0^3 - 30tx_0^2 - 2t$ has a maximum at $x_0 = 0$ and a minimum at $x_0 = \frac{t}{7}$. Moreover $G'(0) = -2t < 0$ so that $G'(x_0) = 0$ has only one real solution, say $\tilde{x}_0(t)$. Clearly $G(x_0)$ will have a global minimum at $\tilde{x}_0(t)$ so that if $G(\tilde{x}_0(t)) < 0$ then $G(x_0) = 0$ has two real solutions whilst if $G(\tilde{x}_0(t)) > 0$ then $G(x_0) = 0$ has no real solutions.

Namely if $\mathcal{R}(t) := \tilde{x}_0(t)\left(2t + 10t\tilde{x}_0(t)^2 - 35\tilde{x}_0(t)^3\right)$ then $G(x_0) = 0$ will have two solutions when $K < \mathcal{R}(t)$ and none when $K > \mathcal{R}(t)$. Solving the cubic $G'(x_0) = 0$ shows that

$$\tilde{x}_0(t) = \frac{1}{14}\left(t + \left(\frac{5t^5}{98 + 5t^2 + 14\sqrt{49 + 5t^2}}\right)^{\frac{1}{3}} + t^{\frac{1}{3}}\left(\frac{98 + 5t^2 + 14\sqrt{49 + 5t^2}}{5}\right)^{\frac{1}{3}}\right) .$$

□

Recalling that Thom classifies the swallowtail singularity by $x_0^5 + ux_0^3 + vx_0^2 + wx_0$ it would appear advantageous if we could obtain an initial polynomial function of degree 5. The following corollary shows that this is not possible.

Corollary 2.5.4. *The initial function* $S_0(\boldsymbol{x}_0) = x_0^7 + x_0^3 y_0 + x_0^2 z_0$ *is the simplest polynomial that gives rise to a polynomial swallowtail.*

Proof. Performing the derivatives in Equation (2.5.3), the function $F(x_0)$ determining the number of cusps on the three dimensional image curve becomes

$$F(x_0) = \frac{1}{h''^2}\Big\{t\left(3h''g'g'' + 3h'h''^2 + h''gg''' - h'''g'^2 - h'''h'^2 - h'''gg''\right) - \left(h''f''' + h''g'''K - h'''f'' - h'''g''K\right) + \frac{h'''}{t}\Big\}\,, \quad (2.5.4)$$

where the x_0 variable has been omitted for brevity.

Note that since any polynomial of odd degree will always have at least one real solution and we require that $h''(x_0) \neq 0$ for all x_0 it is necessary that $h(x_0)$ must be of even degree. Let $f(x_0)$, $g(x_0)$ and $h(x_0)$ be polynomials of degree l, m and $2n$ respectively. Since $h''(x_0) \neq 0$ for all x_0 we may consider the equation

$$t\left(3h''g'g'' + 3h'h''^2 + h''gg''' - h'''g'^2 - h'''h'^2 - h'''gg''\right) - \left(h''f''' + h''g'''K - h'''f'' - h'''g''K\right) + \frac{h'''}{t} = 0\,. \quad (2.5.5)$$

There are two cases that we need to consider:

Case 1 : $n = 1$

The coefficient of K in $F(x_0)$ is given by $h'''g'' - h''g'''$ and since $h'''(x_0) = 0$ we require that $m \geq 3$ in order that the coefficient of K doesn't disappear. Hence we have

$$\left.\begin{array}{r}\deg(h''g'g'')\\ \deg(h''gg''')\end{array}\right\} = 2m-3 \qquad \deg(h'h''^2) = 1$$

$$\deg(h''f''') = l-3 \qquad \deg(h''g''') = m-3$$

Clearly $3h''g'g'' + h''gg''' \not\equiv 0$, so in order that F be of even degree we must choose l such that $l-3$ is even and $l-3 > 2m-3$, namely $l > 2m$. Hence in the *best* case scenario we will have $m = 3$ and $l = 7$.

Case 2 : $n \geq 2$

In order that the coefficient of K doesn't disappear we must have $m \geq 2$. For $m > 2$ we have

$$\left.\begin{array}{r}\deg(h''g'g'')\\ \deg(h''gg''')\\ \deg(h'''g'^2)\\ \deg(h'''gg'')\end{array}\right\} = 2n+2m-5 \qquad \left.\begin{array}{r}\deg(h'h''^2)\\ \deg(h'''h'^2)\end{array}\right\} = 6n-5$$

$$\left.\begin{array}{r}\deg(h''g''')\\ \deg(h'''g'')\end{array}\right\} = 2n+m-5 \qquad \left.\begin{array}{r}\deg(h''f''')\\ \deg(h'''f'')\end{array}\right\} = 2n+l-5$$

with the only difference for $m = 2$ being that $h''gg''' = h''g''' \equiv 0$. Observing that $3h'h''^2 - h'''h'^2 \not\equiv 0$ it follows that for F to be of even degree we must choose l such that $2n + l - 5$ is even and $2n + l - 5 > 6n - 5$, namely $l > 4n$. In the *best* case scenario this will yield $l = 9$.

Hence the simplest polynomial we may use is $S_0(\boldsymbol{x_0}) = x_0^7 + x_0^3 y_0 + x_0^2 z_0$. □

Remark 2.5.1. The initial condition for generating a polynomial swallowtail is not unique. For example $S_0(\boldsymbol{x_0}) = x_0^{2n-1} + x_0^3 y_0 + x_0^2 z_0$ will produce a swallowtail for any $n \geq 4$.

2.6 Caustic and Level Surface for the Three Dimensional Polynomial Swallowtail

With $S_0(\boldsymbol{x_0}) = x_0^7 + x_0^3 y_0 + x_0^2 z_0$ it follows immediately from Lemma 2.5.1 that the pre-caustic is

$$z_0(x_0, y_0) = -\frac{1}{2t}\left(42tx_0^5 - 9t^2x_0^4 - 4t^2x_0^2 + 6ty_0x_0 + 1\right) . \tag{2.6.1}$$

Moreover the mapping Φ_t is given by

$$\boldsymbol{x} = \Phi_t \boldsymbol{x_0} = \begin{pmatrix} x_0 \\ y_0 \\ z_0 \end{pmatrix} + t \begin{pmatrix} 7x_0^6 + 3x_0^2 y_0 + 2x_0 z_0 \\ x_0^3 \\ x_0^2 \end{pmatrix} , \tag{2.6.2}$$

so that the caustic is

$$\begin{aligned} x(x_0, y_0) &= x_0^2 t(-35x_0^4 + 9tx_0^3 + 4tx_0 - 3y_0) , \\ y(x_0, y_0) &= y_0 + tx_0^3 , \\ z(x_0, y_0) &= -21x_0^5 + \frac{9}{2}tx_0^4 + 3tx_0^2 - 3y_0x_0 - \frac{1}{2t} . \end{aligned} \tag{2.6.3}$$

These are illustrated in Figures 2.18 and 2.19 which show the pre-caustic and caustic respectively at time $t = 1$. The swallowtail shape can be clearly seen in the picture of the caustic.

Using Lemma 2.5.1 once more we see that the zero pre-level surface is given by

$$x_0^2\left(t\left(7x_0^5 + 3x_0y_0 + 2z_0\right)^2 + tx_0^4 + tx_0^2 + 2x_0^5 + 2x_0y_0 + 2z_0\right) = 0 . \tag{2.6.4}$$

Thus the zero pre-level surface consists of the line pair $x_0^2 = 0$ and the surface

$$z_0(x_0, y_0) = \frac{1}{4t}\left(-14tx_0^5 - 6tx_0y_0 - 1 \pm \sqrt{20tx_0^5 - 4t^2x_0^4 - 4t^2x_0^2 + 4tx_0y_0 + 1}\right) ,$$

for $20tx_0^5 - 4t^2x_0^4 - 4t^2x_0^2 + 4ty_0x_0 + 1 \geq 0$. Applying the mapping Φ_t we see that the zero level surface is given by the line pair $x^2 = 0$ and the surface

$$\begin{aligned} x(x_0, y_0) &= \frac{x_0}{2}\left(1 \pm \sqrt{20tx_0^5 - 4t^2x_0^4 - 4t^2x_0^2 + 4tx_0y_0 + 1}\right) , \\ y(x_0, y_0) &= y_0 + tx_0^3 , \\ z(x_0, y_0) &= \frac{1}{4t}\left(-14tx_0^5 + 4t^2x_0^2 - 6ty_0x_0 - 1 \pm \sqrt{20tx_0^5 - 4t^2x_0^4 - 4t^2x_0^2 + 4tx_0y_0 + 1}\right) , \end{aligned}$$

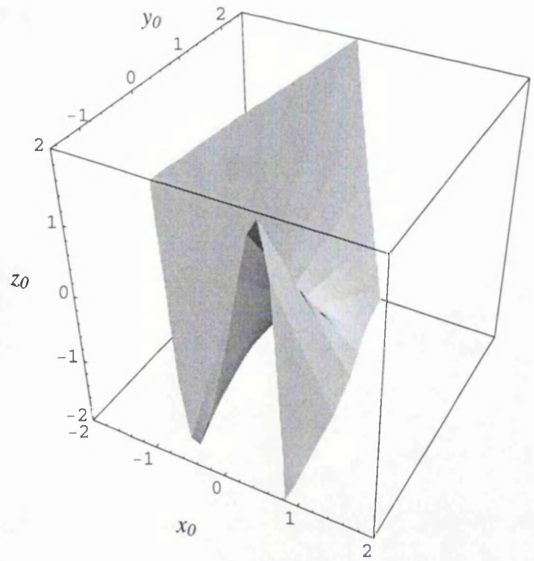

Figure 2.18: Pre-caustic at $t = 1$

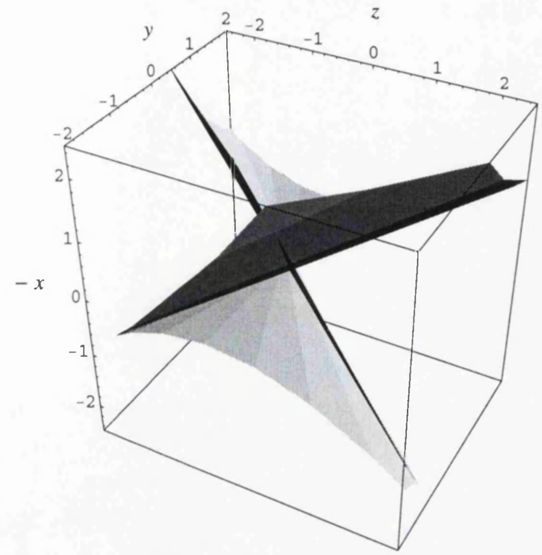

Figure 2.19: Caustic at $t = 1$

for $20tx_0^5 - 4t^2x_0^4 - 4t^2x_0^2 + 4ty_0x_0 + 1 \geq 0$. These are illustrated in Figures 2.20 and 2.21 which show the zero pre-level surface and zero level surface respectively at time $t = 1$.

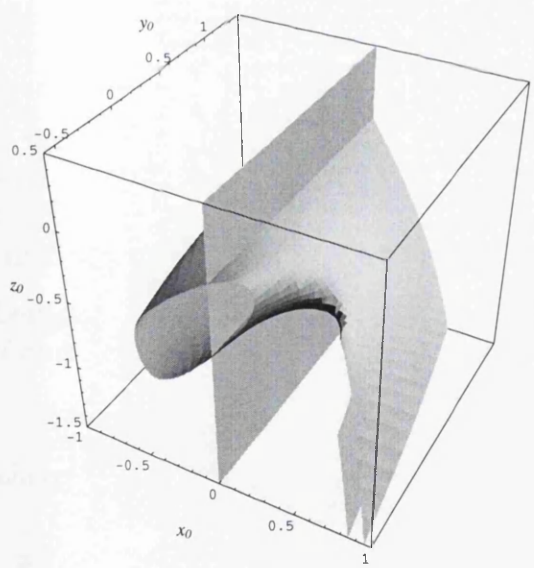

Figure 2.20: Zero pre-level surface at $t = 1$

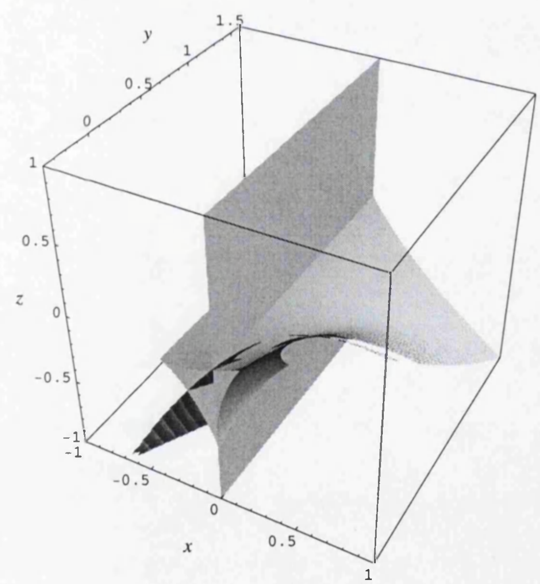

Figure 2.21: Zero level surface at $t = 1$

In order to clarify what is occurring we have plotted a series of slices $y = K$ of the caustic and zero level surface and the corresponding pre-images. Namely for the image curves we have plotted the slices $(x(x_0, K - tx_0^3), z(x_0, K - tx_0^3))$ with the corresponding slices $(x_0, z_0(x_0, K - tx_0^3))$ being plotted for the pre-images. The pre-curves and image curves are shown in Figures 2.22 and 2.23 respectively, where a broken line has been used to identify $\Phi_t^{-1}C_t$ and C_t. All our plots are for $t = 1$ so that $\mathcal{R}(1) \approx 0.605344$, where $\mathcal{R}$

is the function defined in the proof of Proposition 2.5.3.

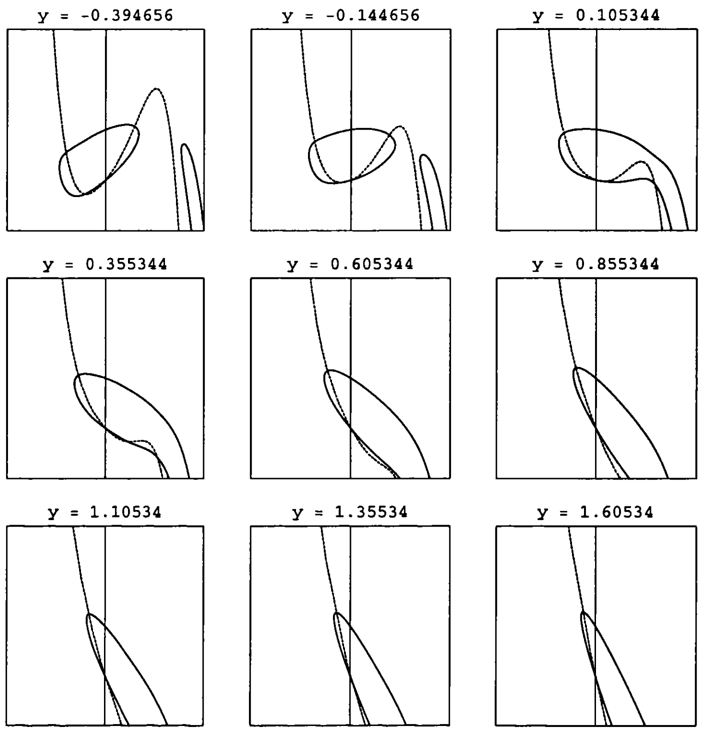

Figure 2.22: Slices of pre-caustic and zero pre-level surface

It may be observed from Figures 2.22 and 2.23 that depending on the slice, the (pre-) level surface consists of either one or two components. Letting $\mathcal{D}_t(x_0) := 20tx_0^5 - 4t^2x_0^4 - 4t^2x_0^2 + 4tx_0y_0 + 1$ we arrive at the following lemma which provides a condition for the number of components.

Lemma 2.6.1. *A slice $y = K$ of the zero (pre-) level surface consists of two components if and only if K satisfies the inequalities*

$$K < 2\tilde{x}_0(t)t + 8\tilde{x}_0(t)^3t - 25\tilde{x}_0(t)^4 \ , \tag{2.6.5}$$

where

$$\tilde{x}_0(t) = \frac{2t}{25} + \frac{1}{25}\left(\frac{4^4t^6}{625t + 32t^3 - 25t\sqrt{625 + 64t^2}}\right)^{\frac{1}{3}} + \frac{1}{25}\left(\frac{625t + 32t^3 - 25t\sqrt{625 + 64t^2}}{4}\right)^{\frac{1}{3}} \ , \tag{2.6.6}$$

and

$$K < \frac{8y^2u_2^4 + 12t^2u_2^2 - 5}{16tu_2} \ , \tag{2.6.7}$$

where u_2 is a stationary point which is a local minimiser of $\mathcal{D}_t(x_0, K - tx_0^3)$. Otherwise the slice consists of one component.

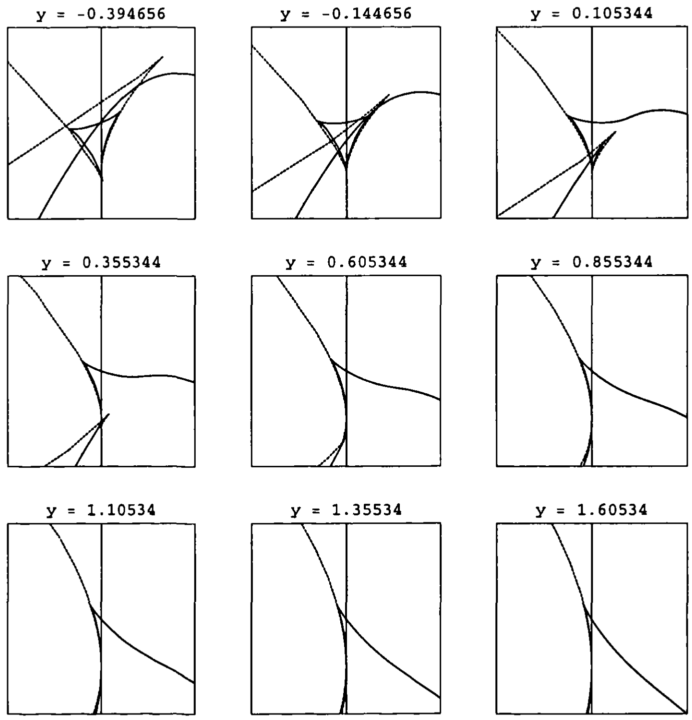

Figure 2.23: Slices of caustic and zero level surface

Proof. We have

$$\mathcal{D}_t(x_0, K - tx_0^3) = 20tx_0^5 - 8t^2x_0^4 - 4t^2x_0^2 + 4Kx_0t + 1 ,$$

which has first two derivatives

$$\begin{aligned} \mathcal{D}_t' &= 100tx_0^4 - 32t^2x_0^3 - 8t^2x_0 + 4Kt , \\ \mathcal{D}_t'' &= 400tx_0^3 - 96t^2x_0^2 - 8t^2 . \end{aligned}$$

Observe that $\mathcal{D}_t''$ has a maximum at $x_0 = 0$ and minimum at $x_0 = \frac{4t}{25}$, at which $\mathcal{D}_t''(0) = -8t^2 < 0$ and $\mathcal{D}_t''(\frac{4t}{25}) = -\frac{512}{625}t^4 - 8t^2 < 0$. Hence $\mathcal{D}_t''(x_0) = 0$ has only one real solution $\tilde{x}_0(t) > 0$ which is given by Equation (2.6.6). Clearly for $\mathcal{D}_t$ to have stationary points it is necessary that $\mathcal{D}_t'(\tilde{x}_0(t)) < 0$. If this holds then $\mathcal{D}_t'(x_0) = 0$ will have two solutions $u_1 < u_2$. Moreover $\mathcal{D}_t(x_0)$ has a local maximum at u_1 and since $\mathcal{D}_t$ is concave down for $x_0 < \tilde{x}_0(t)$ it follows that $\mathcal{D}_t(u_1) > \mathcal{D}_t(0) > 0$. Thus there will be two parts to the zero level surface if and only if $\mathcal{D}_t(u_2) < 0$. Using the fact that $\mathcal{D}_t'(u_2) = 0$ this condition reduces to Equation (2.6.7). □

2.6.1 Curves of Intersection of the Swallowtail and Level Surface

The geometrical relationship between cusped meeting points of the image surfaces and common points of the pre-curves may be extended to the three dimensional case, as shown in [15]. Let us consider the intersection of the swallowtail and zero level surface where of course we will now obtain curves of intersection as opposed to points.

First observe that for the line pair $x_0^2 = 0$ the curves will meet at $z_0(0, y_0) = -\frac{1}{2t}$ giving $x_0 = 0, y_0 \in \mathbb{R}, z_0 = -\frac{1}{2t}$. Applying Φ_t yields the straight line

$$x(x_0) = 0 \ , \ y(x_0) \in \mathbb{R} \ , \ z(x_0) = -\frac{1}{2t} \ . \tag{2.6.8}$$

For the rest of the pre-level surface we see it shall meet the pre-caustic when

$$x_0^5 + x_0 y_0 + z_0(x_0, y_0) + \frac{t}{2}\left(x_0^2 + x_0^4 + \left(7x_0^5 + 3x_0 y_0 + 2z_0(x_0, y_0)\right)^2\right) = 0 \ ,$$

where $z_0(x_0, y_0)$ is the pre-caustic given by Equation (2.6.1). This reduces to a quadratic

$$-\frac{3t}{2}x_0^2 + 4t(2t^2 - 1)x_0^4 + 15x_0^5 + 36t^3x_0^6 - 140t^2x_0^7 + \frac{81t^3}{2}x_0^8 - 315t^2x_0^9 + \frac{1225t}{2}x_0^{10}$$
$$+ y_0\left(x_0 - 12t^2x_0^3 - 27t^2x_0^5 + 105tx_0^6\right) + y_0^2\left(\frac{9t}{2}x_0^2\right) = 0 \ ,$$

which may be solved to give

$$y_0(x_0) = \frac{1}{9tx_0}\left(-1 + 12t^2x_0^2 + 27t^2x_0^4 - 105tx_0^5 \pm \sqrt{1 + 3t^2x_0^2 + 18t^2x_0^4 - 60tx_0^5}\right) \ .$$

To obtain the equation of the cusped curve we simply apply Φ_t. This yields, for the positive root, the curve

$$\begin{aligned}
x(x_0) &= \frac{x_0}{3}\left(1 - \sqrt{1 + 3t^2x_0^2 + 18t^2x_0^4 - 60tx_0^5}\right) \ , \\
y(x_0) &= \frac{-105tx_0^5 + 36t^2x_0^4 + 12t^2x_0^2 - 1 + \sqrt{1 + 3t^2x_0^2 + 18t^2x_0^4 - 60tx_0^5}}{9tx_0} \ , \\
z(x_0) &= \frac{84tx_0^5 - 27t^2x_0^4 - 6t^2x_0^2 - 1 - 2\sqrt{1 + 3t^2x_0^2 + 18t^2x_0^4 - 60tx_0^5}}{6t} \ ,
\end{aligned} \tag{2.6.9}$$

whilst for the negative root we obtain the two curves ($x_0 < 0$, $x_0 > 0$)

$$\begin{aligned}
x(x_0) &= \frac{x_0}{3}\left(1 + \sqrt{1 + 3t^2x_0^2 + 18t^2x_0^4 - 60tx_0^5}\right) \ , \\
y(x_0) &= \frac{-105tx_0^5 + 36t^2x_0^4 + 12t^2x_0^2 - 1 - \sqrt{1 + 3t^2x_0^2 + 18t^2x_0^4 - 60tx_0^5}}{9tx_0} \ , \\
z(x_0) &= \frac{84tx_0^5 - 27t^2x_0^4 - 6t^2x_0^2 - 1 + 2\sqrt{1 + 3t^2x_0^2 + 18t^2x_0^4 - 60tx_0^5}}{6t} \ .
\end{aligned} \tag{2.6.10}$$

2.6.2 Form of the Generating Function

We know that the generic three dimensional swallowtail has a generating function of the form

$$V(x_0) = x_0^5 + ux_0^3 + vx_0^2 + wx_0 \ . \tag{2.6.11}$$

From the outset it seems intuitively obvious that the initial function $S_0(\boldsymbol{x}_0) = x_0^7 + x_0^3 y_0 + x_0^2 z_0$ will not give rise to the function in Equation (2.6.11). Let us now discover what the analogue is in our case.

We begin by considering the integral

$$u^\mu(\boldsymbol{x}, t) = \left(2\pi t\mu^2\right)^{-\frac{3}{2}} \iiint_{\mathbb{R}^3} T_0(\boldsymbol{x}_0) \exp\left(-\frac{\mathcal{A}(\boldsymbol{x}_0, \boldsymbol{x}, t)}{\mu^2}\right) \mathrm{d}^3\boldsymbol{x}_0 , \tag{2.6.12}$$

where

$$\mathcal{A}(\boldsymbol{x}_0, \boldsymbol{x}, t) = \frac{(x - x_0)^2}{2t} + \frac{(y - y_0)^2}{2t} + \frac{(z - z_0)^2}{2t} + x_0^7 + x_0^3 y_0 + x_0^2 z_0 ,$$

and the convergence factor $T_0(\boldsymbol{x}_0) \in C_0^\infty(\mathbb{R}^3)$. Write

$$\mathcal{A}(\boldsymbol{x}_0, \boldsymbol{x}, t) = \frac{(x - x_0)^2}{2t} + \frac{y^2}{2t} + \frac{z^2}{2t} + x_0^7 + \frac{G(y_0)}{t} + \frac{H(z_0)}{t} ,$$

where

$$G(y_0) := \frac{1}{2}\left(y_0^2 - 2y_0(y - tx_0^3)\right) ,$$

and

$$H(z_0) := \frac{1}{2}\left(z_0^2 - 2z_0(z - tx_0^2)\right) .$$

If $\tilde{y}_0$ and $\tilde{z}_0$ denote the non-degenerate critical points which minimise G and H respectively, then by Laplace's method

$$\begin{aligned} u \sim \left(2\pi t\mu^2\right)^{-\frac{3}{2}} \int_{\mathbb{R}} \Bigg[T_0(x_0, \tilde{y}_0, \tilde{z}_0) \exp\left\{-\frac{1}{\mu^2}\left(\frac{(x - x_0)^2}{2t} + \frac{y^2}{2t} + \frac{z^2}{2t} + x_0^7 + \frac{G(\tilde{y}_0)}{t} + \frac{H(\tilde{z}_0)}{t}\right)\right\} \\ \times \int_{\mathbb{R}} \exp\left\{-\frac{1}{2\mu^2 t} H''(\tilde{z}_0)(z_0 - \tilde{z}_0)^2\right\} \mathrm{d}z_0 \\ \times \int_{\mathbb{R}} \exp\left\{-\frac{1}{2\mu^2 t} G''(\tilde{y}_0)(y_0 - \tilde{y}_0)^2\right\} \mathrm{d}y_0 \Bigg] \mathrm{d}x_0 , \end{aligned}$$

as $\mu \sim 0$. Assuming $G''(\tilde{y}_0) > 0$ and $H''(\tilde{z}_0) > 0$ we obtain

$$\begin{aligned} u \sim \left(2\pi t\mu^2\right)^{-\frac{1}{2}} \int_{\mathbb{R}} T_0(x_0, \tilde{y}_0, \tilde{z}_0) \left[G''(\tilde{y}_0) H''(\tilde{z}_0)\right]^{-\frac{1}{2}} \\ \times \exp\left\{-\frac{1}{\mu^2}\left(\frac{(x - x_0)^2}{2t} + \frac{y^2}{2t} + \frac{z^2}{2t} + x_0^7 + \frac{G(\tilde{y}_0)}{t} + \frac{H(\tilde{z}_0)}{t}\right)\right\} \mathrm{d}x_0 . \end{aligned}$$

In our example

$$\tilde{y}_0 = y - tx_0^3 \qquad \text{and} \qquad \tilde{z}_0 = z - tx_0^2 ,$$

so that

$$u \sim \left(2\pi t\mu^2\right)^{-\frac{1}{2}} \int_{\mathbb{R}} T_0(x_0, \tilde{y}_0, \tilde{z}_0) \left[G''(\tilde{y}_0) H''(\tilde{z}_0)\right]^{-\frac{1}{2}}$$

$$\times \exp\left\{-\frac{1}{\mu^2}\left(x_0^7 - \frac{t}{2}x_0^6 - \frac{t}{2}x_0^4 + x_0^3 y + x_0^2\left(z + \frac{1}{2t}\right) - \frac{x}{t}x_0 + \frac{x^2}{2t}\right)\right\} \mathrm{d}x_0 \ .$$

Thus our polynomial swallowtail has a generating function of the form

$$V(x_0) = x_0^7 + Ax_0^6 + Bx_0^4 + Cx_0^3 + Dx_0^2 + Ex_0 \ .$$

Chapter 3

The Stochastic Polynomial Swallowtail

In this chapter we are primarily concerned with the stochastic viscous Burgers equation in the case $V \equiv 0$ and the corresponding heat equation. The noise is introduced by means of a one dimensional Wiener process W_t on the probability space $\{\Omega, \mathcal{F}, \mathbb{P}\}$ which in our case will act in a fixed general direction. Analogous results of the geometrical relationship in the deterministic case are discussed and we consider the examples of the cusp and polynomial swallowtail in the stochastic setting. The chapter concludes with a result concerning the expected number of cusped meeting points of the level surface and caustic.

3.1 Introduction

Here we are considering the stochastic Burgers equation for the velocity fields $v^\mu = v^\mu(\boldsymbol{x}, t)$, $\boldsymbol{x} \in \mathbb{R}^d$, $t > 0$

$$\frac{\partial v^\mu}{\partial t}(\boldsymbol{x}, t) + (v^\mu \cdot \nabla)\, v^\mu = \frac{\mu^2}{2}\Delta v^\mu - \nabla V(\boldsymbol{x}) - \varepsilon \nabla k(\boldsymbol{x}, t)\dot{W}_t \,,$$

with initial velocity $v^\mu(\boldsymbol{x}, 0) = \nabla S_0(\boldsymbol{x})$ where μ^2 is the coefficient of viscosity and $V, k \in C^2$. Applying the logarithmic Hopf-Cole transformation $v^\mu = -\mu^2 \nabla \ln u^\mu$ we obtain the Stratonovich type heat equation

$$\frac{\partial u^\mu}{\partial t} = \frac{\mu^2}{2}\Delta u^\mu + \frac{1}{\mu^2}V(x)u^\mu + \frac{\varepsilon}{\mu^2}k(x, t)u^\mu \circ \dot{W}_t \,,$$

where $u^\mu(x, 0) = \exp\left(-\frac{S_0(x)}{\mu^2}\right)$.

Consider a curve $\gamma = \{X(s) : s \leq t, X(0) = 0, \dot{X}(0) = p_0\}$ where X_s is adapted with respect to $\mathcal{F}_s$. The stochastic action $A[\gamma]$ is given by

$$\begin{aligned} A[\gamma] &= A[x_0, p_0, t] \\ &= \int_0^t \left(\frac{1}{2}\dot{X}^2(s) - V(X(s))\right) \mathrm{d}s - \varepsilon \int_0^t k(X(s), s)\,\mathrm{d}W_s \,, \end{aligned}$$

where $X_s = X(s, x_0, p_0)$ must satisfy the second order stochastic differential equation

$$\mathrm{d}\dot{X}(s) = -\nabla V(X(s))\,\mathrm{d}s - \varepsilon \nabla k(X(s), s)\,\mathrm{d}W_s \ , \tag{3.1.1}$$

for $s \in [0, t]$ with $X(0) = x_0$, $\dot{X}(0) = p_0$. Here p_0 is an as yet unspecified function of x_0.

Lemma 3.1.1. *Assume $S_0, V \in C^2$ and $k(x,t) \in C^{2,0}$, ∇V, ∇k are Lipschitz and all second derivatives with respect to space variables of V and k are bounded. If $\dot{X}_s$ satisfies Equation* (3.1.1) *and p_0 is possibly x_0 dependent then*

$$\frac{\partial A}{\partial x_0^\alpha}(x_0, p_0, t) = \dot{X}(t)\frac{\partial X(t)}{\partial x_0^\alpha} - \dot{X}_\alpha(0) \ , \tag{3.1.2}$$

almost surely.

Proof. See [15]. □

We set

$$X(s, x_0, x) = X(s, x_0, p_0)|_{p_0 = p(x_0, x, t)} \ ,$$

where $p_0 = p(x_0, x, t)$ is the random minimiser of $A(x_0, p_0, t)$ with $X(t, x_0, p_0) = x$ which we assume to be unique. Note that we are also assuming here that the map $\mathbb{R}^n \to \mathbb{R}^n$ where $p_0 \mapsto X(t, x_0, p_0) = X_{t,x_0}(p_0)$ is onto.

Similarly setting

$$A(x_0, x, t) = A(x_0, p_0, t)|_{p_0 = p(x_0, x, t)} \ ,$$

it follows from Lemma 3.1.1 that

$$\left.\frac{\partial}{\partial x_0^\alpha}\right|_{\text{fixed } (x,t)} A(x_0, x, t) = -\dot{X}_\alpha(0) \ ,$$

for $\alpha = 1, 2, \ldots, d$. Hence if we define the stochastic action corresponding to the initial momentum $\nabla S_0(x_0)$ by

$$\mathcal{A}(x_0, x, t) = A(x_0, x, t) + S_0(x_0) \ ,$$

then

$$\left.\frac{\partial}{\partial x_0^\alpha}\right|_{\text{fixed } (x,t)} \mathcal{A}(x_0, x, t) = 0 \ ,$$

for $\alpha = 1, 2, \ldots, d$ defines the classical mechanical flow map Φ_t with $x = \Phi_t(x_0)$.

3.2 Geometrical Result of Truman, Davies and Zhao

Here we provide a brief account of the main geometrical results obtained by Truman, Davies and Zhao in [15] and [14] for random caustics and level surfaces. We omit all proofs and only consider the two dimensional case. Interested readers are referred to the original account in [15] where full proofs and arguments in higher dimensions may be found.

We begin by assuming that

$$\mathrm{Det}\left[\frac{\partial^2 \mathcal{A}}{\partial x_0 \partial x}(x_0, x, t)\right] \neq 0 \;, \tag{3.2.1}$$

for $x_0, x \in \mathbb{R}^2$. Although this assumption may be weakened it is sufficient for the situations we will consider.

Lemma 3.2.1. *The classical flow map $x = \Phi_t(x_0)$ is a differentiable map from $\Phi_t^{-1}H_t$ to H_t with Fréchet derivative*

$$D\Phi_t(x_0) = \left(-\frac{\partial^2 \mathcal{A}}{\partial x \partial x_0}(x_0, x, t)\right)^{-1} \left(\frac{\partial^2 \mathcal{A}}{\partial x_0^2}(x_0, x, t)\right) \;,$$

if $\mathcal{A}$ is C^3 in space variables.

Proposition 3.2.2. *The normal to the pre-level surface at x_0 is to within a scalar multiplier given by*

$$n(x_0) = -\left(\frac{\partial^2 \mathcal{A}}{\partial x_0^2}\right)\left(\frac{\partial^2 \mathcal{A}}{\partial x_0 \partial x}\right)^{-1} \dot{X}(t, x_0, \nabla S_0(x_0)) \;.$$

Corollary 3.2.3. *In two dimensions consider a point $x_0 \in \Phi_t^{-1}C_t \cap \Phi_t^{-1}H_t$ where $n(x_0) \neq 0$ and $\mathrm{Ker}\left(\frac{\partial^2 \mathcal{A}}{\partial x_0^2}(x_0, \Phi_t(x_0), t)\right) =< e_0 >$, e_0 being the zero eigenvector. Then the tangent plane to the pre-level surface at x_0, T_{x_0}, is spanned by e_0.*

Proposition 3.2.4. *Consider a point $x_0 \in \Phi_t^{-1}H_t$ where $n(x_0) \neq 0$ so that $\Phi_t^{-1}H_t$ does not have a cusp at x_0. Then H_t will have a cusp at $x = \Phi_t(x_0)$ if $\Phi_t(x_0) \in C_t$. Moreover, if $x = \Phi_t(x_0) \in \Phi_t\{\Phi_t^{-1}C_t \cap \Phi_t^{-1}H_t\}$, then H_t will have a generalised cusp at x.*

The point here is that under the assumption in Equation (3.2.1) the geometrical results discussed in the deterministic case still hold true in the random setting.

3.3 Explicit Form of the Noisy Heat Kernel

In the section we will derive an explicit form for the noisy heat kernel when $V(x) \equiv 0$ and $k(x, t) = x$. We shall illustrate two possible methods that may be used and prove the equivalence of the results obtained. Variations of the explicit heat kernel discussed here may be found in a number of works, see for instance [53].

Method 1

For $V(x) \equiv 0$ and $k(x, t) = x$ the Stratonovich type heat equation reduces to

$$\partial u = \frac{\mu^2}{2}\Delta u \,\mathrm{d}t + \varepsilon\frac{x}{\mu^2} u \circ \mathrm{d}W_t \;. \tag{3.3.1}$$

If we define $g_t(x, x_0)$ by

$$\ln g_t(x,x_0) := \ln t^{-\frac{1}{2}} - \frac{(x-x_0)^2}{2t\mu^2} + \frac{\varepsilon}{t\mu^2}\int_0^t (x-x_0)s\,\mathrm{d}W_s + \varepsilon\frac{x_0}{\mu^2}W_t\ , \tag{3.3.2}$$

then on differentiating with respect to t we obtain

$$\begin{aligned}\frac{\partial g_t}{g_t} &= -\frac{1}{2}\frac{dt}{t} + \frac{(x-x_0)^2}{2t^2\mu^2}dt - \frac{\varepsilon}{t^2\mu^2}dt\int_0^t (x-x_0)s\,\mathrm{d}W_s + \varepsilon\frac{(x-x_0)}{\mu^2}\circ\partial W_t + \varepsilon\frac{x_0}{\mu^2}\circ\partial W_t \\ &= -\frac{1}{2}\frac{dt}{t} + \frac{(x-x_0)^2}{2t^2\mu^2}dt - \frac{\varepsilon}{t^2\mu^2}dt\int_0^t (x-x_0)s\,\mathrm{d}W_s + \varepsilon\frac{x}{\mu^2}\circ\partial W_t\ . \qquad (3.3.3)\end{aligned}$$

Differentiating Equation (3.3.2) with respect to x gives

$$\frac{g_t'}{g_t} = -\frac{(x-x_0)}{t\mu^2} + \frac{\varepsilon}{t\mu^2}\int_0^t s\,\mathrm{d}W_s\ ,$$

and on differentiating again we obtain

$$\begin{aligned}\frac{g_t''}{g_t} &= \left(\frac{g_t'}{g_t}\right)^2 - \frac{1}{t\mu^2} \\ &= -\frac{1}{t\mu^2} + \frac{1}{\mu^4}\left\{\frac{(x-x_0)}{t} - \frac{\varepsilon}{t}\int_0^t s\,\mathrm{d}W_s\right\}^2\ .\end{aligned} \tag{3.3.4}$$

Thus from Equations (3.3.3) and (3.3.4) we see that

$$\begin{aligned}&\frac{\mu^2}{2}\frac{g_t''}{g_t}dt + \varepsilon\frac{x}{\mu^2}\circ\partial W_t \\ &= -\frac{1}{2}\frac{dt}{t} + \frac{dt}{2\mu^2}\left\{\frac{(x-x_0)^2}{t^2} + \frac{\varepsilon^2}{t^2}\left(\int_0^t s\,\mathrm{d}W_s\right)^2 - \frac{2\varepsilon(x-x_0)}{t}\int_0^t s\,\mathrm{d}W_s\right\} + \varepsilon\frac{x}{\mu^2}\circ\partial W_t \\ &= \frac{\partial g_t}{g_t} + \frac{\varepsilon^2 dt}{2t^2\mu^2}\left(\int_0^t s\,\mathrm{d}W_s\right)^2\ . \qquad (3.3.5)\end{aligned}$$

Observe that

$$\int_0^t s\,\mathrm{d}W_s = W\left(\int_0^u s^2\,\mathrm{d}s\right) = W\left(\frac{u^3}{3}\right) \sim \left(\frac{u^3}{3}\right)^{\frac{1}{2}} = \frac{u^{\frac{3}{2}}}{3^{\frac{1}{2}}}\ ,$$

for large u, so that the integral

$$\int_0^t \frac{\mathrm{d}u}{2\mu^2u^2}\left(\int_0^u s\,\mathrm{d}W_s\right)^2\ ,$$

is well defined as $\mu \sim 0$. Since

$$\begin{aligned}&\partial\left(g_t\exp\left\{\int_0^t \frac{\mathrm{d}u}{2\mu^2u^2}\left(\int_0^u s\,\mathrm{d}W_s\right)^2\right\}\right) \\ &\qquad = g_t\exp\left\{\int_0^t \frac{\mathrm{d}u}{2\mu^2u^2}\left(\int_0^u s\,\mathrm{d}W_s\right)^2\right\}\frac{\mathrm{d}t}{2\mu^2t^2}\left(\int_0^t s\,\mathrm{d}W_s\right)^2 \\ &\qquad\qquad + \exp\left\{\int_0^t \frac{\mathrm{d}u}{2\mu^2u^2}\left(\int_0^u s\,\mathrm{d}W_s\right)^2\right\}\partial g_t\ ,\end{aligned}$$

we may write (3.3.5) as

$$\frac{\mu^2}{2}\frac{g_t''}{g_t}dt + \varepsilon\frac{x}{\mu^2}\circ\partial W_t$$
$$= g_t^{-1}\exp\left\{-\varepsilon^2\int_0^t \frac{\mathrm{d}u}{2\mu^2u^2}\left(\int_0^u s\,\mathrm{d}W_s\right)^2\right\}\partial\left(g_t\exp\left\{\varepsilon^2\int_0^t\frac{\mathrm{d}u}{2\mu^2u^2}\left(\int_0^u sdW_s\right)^2\right\}\right). \tag{3.3.6}$$

Thus if we define

$$G_t(x,x_0) := (2\pi\mu^2)^{-\frac{1}{2}}\exp\left\{\varepsilon^2\int_0^t\frac{du}{2\mu^2u^2}\left(\int_0^u sdW_s\right)^2\right\}g_t(x,x_0)\ ,$$

then the right hand side of Equation (3.3.6) may be written as

$$(2\pi\mu^2)^{-\frac{1}{2}}G_t^{-1}\partial\left((2\pi\mu^2)^{\frac{1}{2}}G_t\right) = \frac{\partial G_t}{G_t}\ , \tag{3.3.7}$$

and so we have

$$\frac{\mu^2}{2}\frac{G_t''}{G_t}dt + \varepsilon\frac{x}{\mu^2}\circ\partial W_t = \frac{\mu^2}{2}\frac{g_t''}{g_t} + \varepsilon\frac{x}{\mu^2}\circ\partial W_t$$
$$= \frac{\partial G_t}{G_t}\ .$$

Thus, after applying the integration by parts result, we see that the Stratonovich type heat equation with zero potential has heat kernel

$$G_t(x,x_0) = \frac{1}{(2\pi\mu^2t)^{\frac{1}{2}}}\exp\left\{-\frac{(x-x_0)^2}{2t\mu^2} + \varepsilon\frac{xW_t}{\mu^2} - \varepsilon\frac{(x-x_0)}{t\mu^2}\int_0^t W_s\,\mathrm{d}s\right.$$
$$\left. + \varepsilon^2\int_0^t\frac{du}{2\mu^2u^2}\left(\int_0^u sdW_s\right)^2\right\}\ . \tag{3.3.8}$$

Hence, if $u^\mu(x,0) = \exp\left(-\frac{S_0(x_0)}{\mu^2}\right)$, then the solution is given by

$$u^\mu(x,t) = \int_{\mathbb{R}} G_t(x,x_0)F(x_0)\,\mathrm{d}x_0\ ,$$

where $F(x_0) = \exp\left\{-\frac{1}{\mu^2}S_0(x_0)\right\}$. This may be written as

$$u^\mu(x,t) = (2\pi\mu^2t)^{-\frac{1}{2}}\int_{\mathbb{R}}\exp\left(-\frac{1}{\mu^2}\mathcal{A}(x_0,x,t)\right)\,\mathrm{d}x_0\ ,$$

where the phase function $\mathcal{A}$ is given by

$$\mathcal{A}(x,x_0,t) = \frac{(x-x_0)^2}{2t} - \varepsilon xW_t + \varepsilon\frac{(x-x_0)}{t}\int_0^t W_s\,\mathrm{d}s - \varepsilon^2\int_0^t\frac{\mathrm{d}u}{2u^2}\left(\int_0^u s\,\mathrm{d}W_s\right)^2 + S_0(x_0)\ . \tag{3.3.9}$$

Method 2

The stochastic action in this case reduces to

$$A(x_0,p_0,t) = \frac{1}{2}\int_0^t \dot{X}^2(s)\,\mathrm{d}s - \varepsilon\int_0^t X(s)\,\mathrm{d}W_s\ ,$$

where $X_s = X(s, x_0, p_0)$ satisfies the Euler Lagrange equation

$$\mathrm{d}\dot{X}(s) = -\varepsilon\,\mathrm{d}W_s\ , \tag{3.3.10}$$

with $\dot{X}(0) = p_0$, $X(0) = x_0$. From Equation (3.3.10) we obtain

$$\dot{X}(s) = p_0 - \varepsilon W_s\ ,$$

and

$$X(s) = x_0 + sp_0 - \varepsilon\int_0^s W_u\,\mathrm{d}u\ . \tag{3.3.11}$$

Thus

$$\begin{aligned} A(x_0,p_0,t) &= \frac{1}{2}\int_0^t \left(p_0^2 + \varepsilon^2 W_s^2 - 2p_0\varepsilon W_s\right)\mathrm{d}s - \varepsilon\int_0^t \left(x_0 + sp_0 - \varepsilon\int_0^s W_u\,\mathrm{d}u\right)\mathrm{d}W_s \\ &= \frac{t}{2}p_0^2 + \frac{\varepsilon^2}{2}\int_0^t W_s^2\,\mathrm{d}s - \varepsilon p_0 t W_t - \varepsilon x_0 W_t + \varepsilon^2\int_0^t \left(\int_0^s W_u\,\mathrm{d}u\right)\mathrm{d}W_s\ . \end{aligned}$$

By integration by parts

$$\varepsilon^2\int_0^t\left(\int_0^s W_u\,\mathrm{d}u\right)\mathrm{d}W_s = \varepsilon^2 W_t\int_0^t W_u\,\mathrm{d}u - \varepsilon^2\int_0^t W_s^2\,\mathrm{d}s\ ,$$

so that

$$A(x_0,p_0,t) = \frac{t}{2}p_0^2 - \varepsilon p_0 t W_t - \varepsilon x_0 W_t + \varepsilon^2 W_t\int_0^t W_u\,\mathrm{d}u - \frac{\varepsilon^2}{2}\int_0^t W_s^2\,\mathrm{d}s\ .$$

But from Equation (3.3.11)

$$p(x_0,x,t) = \frac{x-x_0}{t} + \frac{\varepsilon}{t}\int_0^t W_u\,\mathrm{d}u\ ,$$

so that

$$\begin{aligned} \mathcal{A}(x_0,x,t) &= A(x_0,p_0,t)\big|_{p_0=p(x_0,x,t)} + S_0(x_0) \\ &= \frac{(x-x_0)^2}{2t} + \varepsilon\frac{(x-x_0)}{t}\int_0^t W_u\,\mathrm{d}u - \varepsilon x W_t + \frac{\varepsilon^2}{2t}\left(\int_0^t W_u\,\mathrm{d}u\right)^2 \\ &\qquad - \frac{\varepsilon^2}{2}\int_0^t W_u^2\,\mathrm{d}u + S_0(x_0)\ . \end{aligned} \tag{3.3.12}$$

We shall see shortly that the results obtained by the two different methods are almost surely equal.

3.4 Equivalence with Earlier Result

In his recent thesis [41], B. Reynolds obtained the stochastic heat kernel for Equation (3.3.1) by allowing $\omega \searrow 0$ in the stochastic Mehler kernel obtained in [52] by Truman and Zastawniak. This gave a Stratonovich type stochastic heat kernel, namely

$$G_t(x,x_0) = \left(2\pi\mu^2 t\right)^{-\frac{1}{2}} \exp\left\{ -\frac{(x-x_0)^2}{2t\mu^2} + \varepsilon\frac{xW_t}{\mu^2} - \frac{\varepsilon}{t\mu^2}(x-x_0)\int_0^t W_r\,\mathrm{d}r \right. \\ \left. + \frac{\varepsilon^2}{\mu^2}\int_0^t \left[\int_0^r s\left(1-\frac{r}{t}\right)\circ\partial W_s\right]\circ\partial W_r \right\}.$$

Equivalence with our Itô type stochastic heat kernel, Equation (3.3.8), is provided by the Lemma below.

Lemma 3.4.1. *If*

$$X_t(\omega) := \int_0^t \left(\int_0^r s\left(1-\frac{r}{t}\right)\circ\partial W_s\right)\circ\partial W_r\ ,$$

and

$$Y_t(\omega) := \int_0^t \frac{1}{2r^2}\left(\int_0^r s\,\mathrm{d}W_s\right)^2 \mathrm{d}r\ ,$$

then $X_t(\omega) = Y_t(\omega)$ *almost surely.*

Proof. Using integration by parts on X_t yields

$$\begin{aligned} X_t(\omega) &= \left[W_r\int_0^r s\left(1-\frac{r}{t}\right)\circ\partial W_s\right]_0^t - \int_0^t W_r\partial_r\left\{\int_0^r s\left(1-\frac{r}{t}\right)\circ\partial W_s\right\} \\ &= -\int_0^t W_r\left\{-\frac{dr}{t}\int_0^r s\circ\partial W_s + r\left(1-\frac{r}{t}\right)\circ\partial W_r\right\} \\ &= \int_0^t \frac{W_r}{t}\left\{rW_r - \int_0^r W_s\,\mathrm{d}s\right\}\mathrm{d}r - \int_0^t r\left(1-\frac{r}{t}\right)\circ\partial\left(\frac{W_r^2}{2}\right) \\ &= \int_0^t \frac{r}{t}W_r^2\,\mathrm{d}r - \frac{1}{t}\int_0^t\left(W_r\int_0^r W_s\,\mathrm{d}s\right)\mathrm{d}r \\ &\qquad -\left\{\left[\frac{W_r^2}{2}r\left(1-\frac{r}{t}\right)\right]_0^t - \int_0^t\frac{1}{2}W_r^2\left(1-\frac{2r}{t}\right)\mathrm{d}r\right\} \\ &= \frac{1}{2}\int_0^t W_r^2\,\mathrm{d}r - \frac{1}{t}\int_0^t\left(W_r\int_0^r W_s\,\mathrm{d}s\right)\mathrm{d}r\ . \end{aligned}$$

Whilst the process Y_t may be written as

$$\begin{aligned} Y_t(\omega) &= \frac{1}{2}\int_0^t\left\{W_r - \frac{1}{r}\int_0^r W_s\,\mathrm{d}s\right\}^2\mathrm{d}r \\ &= \frac{1}{2}\int_0^t W_r^2\,\mathrm{d}r - \int_0^t\left(\frac{1}{r}W_r\int_0^r W_s\,\mathrm{d}s\right)\mathrm{d}r + \frac{1}{2}\int_0^t\frac{1}{r^2}\left(\int_0^r W_s\,\mathrm{d}s\right)^2\mathrm{d}r\ . \end{aligned}$$

However

$$\frac{1}{2}\int_0^t \frac{1}{r^2}\left(\int_0^r W_s\,\mathrm{d}s\right)^2 \mathrm{d}r = -\frac{1}{2}\int_0^t \left(\int_0^r W_s\,\mathrm{d}s\right)^2 \mathrm{d}\left(\frac{1}{r}\right)$$
$$= -\frac{1}{2}\left[\frac{1}{r}\left(\int_0^r W_s\,\mathrm{d}s\right)^2\right]_0^t + \int_0^t \frac{1}{r}\left(\int_0^r W_s\,\mathrm{d}s\right) W_r\,\mathrm{d}r$$
$$= -\frac{1}{2t}\left(\int_0^t W_r\,\mathrm{d}r\right)^2 + \int_0^t \frac{1}{r}W_r\left(\int_0^r W_s\,\mathrm{d}s\right)\mathrm{d}r\,.$$

and we have

$$Y_t(\omega) = \frac{1}{2}\int_0^t W_r^2\,\mathrm{d}r - \frac{1}{2t}\left(\int_0^t W_r\,\mathrm{d}r\right)^2\,. \tag{3.4.1}$$

But we know

$$\mathrm{d}\left\{\left(\int_0^r W_s\,\mathrm{d}s\right)^2\right\} = 2W_r\left(\int_0^r W_s\,\mathrm{d}s\right)\mathrm{d}r\,,$$

so that

$$\left(\int_0^t W_s\,\mathrm{d}s\right)^2 = 2\int_0^t W_r\left(\int_0^r W_s\,\mathrm{d}s\right)\mathrm{d}r\,,$$

which when inserted in Equation (3.4.1) completes the proof. □

Remark 3.4.1. Note that Equation (3.4.1) proves the equivalence of the expressions in Equation (3.3.9) and Equation (3.3.12). Thus we have three equivalent forms of the stochastic heat kernel.

Using our explicit heat kernels we observe that in $\mathbb{R}^3$ we have

$$\frac{\partial \mathcal{A}}{\partial \boldsymbol{x}_0} = \left(\frac{x_0 - x}{t} - \frac{\varepsilon}{t}\int_0^t W_u\,\mathrm{d}u + \frac{\partial S_0}{\partial x_0}, \frac{y_0 - y}{t} + \frac{\partial S_0}{\partial y_0}, \frac{z_0 - z}{t} + \frac{\partial S_0}{\partial z_0}\right)\,,$$

so that

$$\mathrm{Det}\left[\frac{\partial^2 \mathcal{A}}{\partial \boldsymbol{x}\partial \boldsymbol{x}_0}\right] = \mathrm{Det}\begin{bmatrix} -\frac{1}{t} & 0 & 0 \\ 0 & -\frac{1}{t} & 0 \\ 0 & 0 & -\frac{1}{t}\end{bmatrix} = -\frac{1}{t^3} \neq 0\,,$$

for all $t > 0$. Hence the assumption made in Equation (3.2.1) is always true for $V \equiv 0$ and $k = x$.

3.5 Explicit Examples

We begin with a proposition relating the random and deterministic caustic where superscript zeros and epsilons are used to represent deterministic and random situations respectively.

Proposition 3.5.1. *The random caustic is determined by*

$$\text{Det}\left.\frac{\partial X^0(t)}{\partial x_0}\right|_{x_0=x_0^0(x,t)|_{x=x+\varepsilon\int_0^t W_s\,ds}} = 0\ ,$$

where

$$\text{Det}\left.\frac{\partial X^0(t)}{\partial x_0}\right|_{x_0=x_0^0(x,t)} = 0\ ,$$

is the caustic in the deterministic case.

Proof. In the deterministic case $X^0(s) = x_0 + sS_0'(x_0)$, so that from

$$X^0(t) = x = x_0 + tS_0'(x_0)\ ,$$

we may obtain $x_0 = x_0^0(x,t)$. Similarly in the stochastic case we have $X^\varepsilon(s) = x_0 + sS_0'(x_0) - \varepsilon\int_0^s W_u\,du$ so that from

$$X^\varepsilon(t) = x = x_0 + tS_0'(x_0) - \varepsilon\int_0^t W_u\,du\ ,$$

we obtain

$$x_0 = x_0^\varepsilon(x,t) = x_0^0(x+\varepsilon\int_0^t W_u\,du, t)\ .$$

Trivially

$$\frac{\partial X^\varepsilon}{\partial x_0}(t) = 1 + tS_0''(x_0) = \frac{\partial X^0(t)}{\partial x_0}\ ,$$

so that the pre-caustics are identical. Hence the random caustic is given by

$$\begin{aligned}
&\text{Det}\left.\frac{\partial X^\varepsilon}{\partial x_0}(t)\right|_{x_0=x_0^\varepsilon(x,t)} = 0\ ,\\
\Longrightarrow\quad &\text{Det}\left.\frac{\partial X^\varepsilon}{\partial x_0}(t)\right|_{x_0=x_0^0(x+\varepsilon\int_0^t W_u\,du,t)} = 0\ ,\\
\Longrightarrow\quad &\text{Det}\left.\frac{\partial X^0}{\partial x_0}(t)\right|_{x_0=x_0^0(x+\varepsilon\int_0^t W_u\,du,t)} = 0\ ,\\
\Longrightarrow\quad &\text{Det}\left.\frac{\partial X^0}{\partial x_0}(t)\right|_{x_0=x_0^0(x,t)|_{x=x+\varepsilon\int_0^t W_u\,du}} = 0\ .
\end{aligned}$$

Thus the noise simply displaces the caustic by the random quantity $\varepsilon\int_0^t W_u\,du$. □

We may of course consider the slightly more general case of noise in a fixed general direction as opposed to parallel to the x-direction. Namely we are considering a random force of the form

$$\varepsilon\nabla k(\boldsymbol{x},t)\dot{W}_t = \varepsilon(\cos\theta,\sin\theta)\dot{W}_t\ , \tag{3.5.1}$$

for fixed θ, so that $k(\boldsymbol{x},t) = x\cos\theta + y\sin\theta$. Choosing to work in a (ξ,η) coordinate system where

$$\begin{pmatrix}\xi\\ \eta\end{pmatrix} = \begin{pmatrix}\cos\theta & \sin\theta\\ -\sin\theta & \cos\theta\end{pmatrix}\begin{pmatrix}x\\ y\end{pmatrix},$$

the noise is parallel to ξ so that the heat kernel is given by

$$\tilde{\mathcal{A}}(\boldsymbol{\xi},\boldsymbol{\xi}_0,t) = \frac{|\boldsymbol{\xi}-\boldsymbol{\xi}_0|^2}{2t} - \varepsilon\xi W_t + \varepsilon\frac{(\xi-\xi_0)}{t}\int_0^t W_u\,\mathrm{d}u - \varepsilon^2\int_0^t \frac{\mathrm{d}u}{2u^2}\left(\int_0^u s\,\mathrm{d}W_s\right)^2 + \tilde{S}_0(\boldsymbol{\xi}_0),$$

where

$$\tilde{S}_0(\boldsymbol{\xi}_0) = S_0(x_0(\xi_0,\eta_0), y_0(\xi_0,\eta_0)) = S_0(\xi_0\cos\theta - \eta_0\sin\theta, \eta_0\cos\theta + \xi_0\sin\theta).$$

In this new coordinate system the pre-caustic is determined by $\mathrm{Det}[I + t\tilde{S}_0''] = 0$ and the random caustic is simply the deterministic caustic plus a random displacement $\varepsilon\int_0^t W_u\,du$ in the direction ξ.

Remark 3.5.1. It may be shown that $\mathrm{Det}[I + t\tilde{S}_0''(\boldsymbol{\xi}_0)] = \mathrm{Det}[I + tS_0''(\boldsymbol{x}_0)]$ so that for the more general potential in Equation (3.5.1) the pre-caustic in the (x,y) coordinate system is still determined by $\mathrm{Det}[I + tS_0''(\boldsymbol{x}_0)] = 0$.

Proposition 3.5.2. *For the two dimensional Burgers equation with potential of the form* $(x\cos\theta + y\sin\theta)\dot{W}_t$, *the (pre-)level surface,* $\mathcal{S}(\boldsymbol{x},t) = c$, *of Hamilton's principal function is given by*

$$\frac{t}{2}\left|\nabla_{(\xi_0,\eta_0)}\tilde{S}_0(\boldsymbol{\xi}_0)\right|^2 + \tilde{S}_0(\boldsymbol{\xi}_0) - \left(\xi_0 + t\frac{\partial\tilde{S}_0}{\partial\xi_0} - \varepsilon\int_0^t W_u\,\mathrm{d}u\right)\varepsilon W_t - \frac{\varepsilon^2}{2}\int_0^t W_u^2\,\mathrm{d}u = c\,, \quad (3.5.2)$$

where $\boldsymbol{\xi} = \begin{pmatrix}\cos\theta & \sin\theta\\ -\sin\theta & \cos\theta\end{pmatrix}\boldsymbol{x}$.

Proof. The stochastic flow mapping Φ_t^ε is determined by $\nabla_{\boldsymbol{\xi}}\tilde{\mathcal{A}} = 0$ which yields

$$\boldsymbol{\xi} = \boldsymbol{\xi}_0 + t\nabla\tilde{S}_0(\boldsymbol{x}_0) - \begin{pmatrix}\varepsilon\\ 0\end{pmatrix}\int_0^t W_u\,\mathrm{d}u\,.$$

Thus using our explicit formula for $\mathcal{A}(\boldsymbol{\xi},\boldsymbol{\xi}_0,t)$ we see that the pre-level surface is given by

$$\frac{1}{2t}\left|t\nabla\tilde{S}_0 - \begin{pmatrix}\varepsilon\\ 0\end{pmatrix}\int_0^t W_u\,\mathrm{d}u\right|^2 - \varepsilon\left(\xi_0 + t\frac{\partial\tilde{S}_0}{\partial\xi_0} - \varepsilon\int_0^t W_u\,\mathrm{d}u\right)W_t$$
$$+\frac{\varepsilon}{t}\left(t\frac{\partial\tilde{S}_0}{\partial\xi_0} - \varepsilon\int_0^t W_u\,\mathrm{d}u\right)\int_0^t W_u\,\mathrm{d}u - \varepsilon^2\int_0^t\frac{\mathrm{d}u}{2u^2}\left(\int_0^u s\,\mathrm{d}W_s\right)^2 + \tilde{S}_0(\boldsymbol{\xi}_0) = c\,,$$

which reduces to

$$\frac{t}{2}\left|\nabla\tilde{S}_0\right|^2 - \frac{\varepsilon^2}{2t}\left(\int_0^t W_u\,\mathrm{d}u\right)^2 - \varepsilon\left(\xi_0 + t\frac{\partial\tilde{S}_0}{\partial\xi_0} - \varepsilon\int_0^t W_u\,\mathrm{d}u\right)W_t$$
$$- \varepsilon^2\int_0^t \frac{\mathrm{d}u}{2u^2}\left(\int_0^u s\,\mathrm{d}W_s\right)^2 + \tilde{S}_0(\boldsymbol{\xi}_0) = c\,.$$

Finally using the fact that

$$\int_0^t \frac{\mathrm{d}u}{2u^2}\left(\int_0^u s\,\mathrm{d}W_s\right)^2 = \frac{1}{2}\int_0^t W_u^2\,\mathrm{d}u - \frac{1}{2t}\left(\int_0^t W_u\,\mathrm{d}u\right)^2\,,$$

yields the required result. □

For explicit examples it is often easier to work in the (x, y) coordinate system since this allows us to obtain the pre-level surface in the form $y_0(x_0)$. In this setting Equation (3.5.2) becomes

$$\frac{t}{2}\left|\nabla S_0\right|^2 + S_0(\boldsymbol{x}_0) - < C(\theta), \boldsymbol{x}_0 + t\nabla S_0 > \varepsilon W_t + \varepsilon^2 W_t\int_0^t W_u\,\mathrm{d}u - \frac{\varepsilon^2}{2}\int_0^t W_u^2\,\mathrm{d}u = c\,, \tag{3.5.3}$$

where $C(\theta) := (\cos\theta, \sin\theta)$. Similarly the flow Φ_t^ε is given by

$$\Phi_t^\varepsilon(x_0) = \boldsymbol{x}_0 + t\nabla S_0(\boldsymbol{x}_0) - \varepsilon C(\theta)\int_0^t W_u\,\mathrm{d}u\,.$$

Remark 3.5.2. Observe that if $p^\varepsilon(x_0, y_0)$ denotes the expression on the left hand side of Equation (3.5.3) then

$$\mathbb{E}\left[p^\varepsilon(x_0, y_0)\right] = p^0(x_0, y_0) + \varepsilon^2\mathbb{E}\left[\int_0^t W_t W_u\,\mathrm{d}u\right] - \frac{\varepsilon^2}{2}\int_0^t \mathbb{E}\left[W_u^2\right]\,\mathrm{d}u$$
$$= p^0(x_0, y_0) + \frac{\varepsilon^2}{4}t^2\,.$$

3.5.1 The Cusp

For $S_0(\boldsymbol{x}_0) = \frac{1}{2}x_0^2 y_0$ the pre-caustic is given by $y_0(x_0) = \frac{1}{t}(t^2x_0^2 - 1)$ and

$$\Phi_t^\varepsilon(\boldsymbol{x}_0) = \begin{pmatrix} x_0 \\ y_0 \end{pmatrix} + t\begin{pmatrix} x_0 y_0 \\ \frac{x_0^2}{2} \end{pmatrix} - \varepsilon\begin{pmatrix} \cos\theta \\ \sin\theta \end{pmatrix}\int_0^t W_u\,\mathrm{d}u\,,$$

so that the stochastic caustic will be

$$x(x_0) = t^2x_0^3 - \varepsilon\cos\theta\int_0^t W_u\,\mathrm{d}u\,,$$
$$y(x_0) = \frac{3t}{2}x_0^2 - \frac{1}{t} - \varepsilon\sin\theta\int_0^t W_u\,\mathrm{d}u\,.$$

For the pre-level surface we have

$$\frac{t}{2}\left(x_0^2y_0^2+\frac{1}{4}x_0^4\right)+\frac{1}{2}x_0^2y_0-\cos\theta\left(x_0+tx_0y_0\right)\varepsilon W_t$$
$$-\sin\theta\left(y_0+\frac{t}{2}x_0^2\right)\varepsilon W_t+\varepsilon^2\left(W_t\int_0^t W_u\,\mathrm{d}u-\frac{1}{2}\int_0^t W_u^2\,\mathrm{d}u\right)=c\,,$$

which is simply a quadratic in y_0, namely

$$y_0^2\left(\frac{x_0^2t}{2}\right)+y_0\left(\frac{x_0^2}{2}-\varepsilon tx_0W_t\cos\theta-\varepsilon W_t\sin\theta\right)$$
$$+\frac{t}{8}x_0^4-x_0\cos\theta\varepsilon W_t-\frac{x_0^2t}{2}\sin\theta\varepsilon W_t+\varepsilon^2\left(W_t\int_0^t W_u\,\mathrm{d}u-\frac{1}{2}\int_0^t W_u^2\,\mathrm{d}u\right)-c=0\,.$$

Solving this quadratic yields

$$y_0(x_0)=\frac{1}{2x_0^2t}\left\{-x_0^2\pm\sqrt{\mathcal{D}_t}\right\}+\frac{\varepsilon W_t\cos\theta}{x_0}+\frac{\varepsilon W_t\sin\theta}{x_0^2t}\,,$$

for $x_0\neq 0$ and $\mathcal{D}_t\geq 0$, where

$$\mathcal{D}_t:=8ctx_0^2+x_0^4-t^2x_0^6-4\varepsilon x_0^2W_t\left(\sin\theta\left(1-x_0^2t\right)-x_0t\cos\theta\right)$$
$$+4\varepsilon^2\left(W_t^2\left(tx_0\cos\theta+\sin\theta\right)^2-2tx_0^2\left(W_t\int_0^t W_u\,\mathrm{d}u-\frac{1}{2}\int_0^t W_u^2\,\mathrm{d}u\right)\right)\,.$$

Hence applying the mapping Φ_t^ε yields the level surface

$$x(x_0)=\frac{1}{2x_0}\left\{x_0^2\pm\sqrt{\mathcal{D}_t}\right\}+\varepsilon\cos\theta\int_0^t u\,\mathrm{d}W_u+\varepsilon\sin\theta\frac{W_t}{x_0}$$
$$y(x_0)=\frac{1}{2x_0^2t}\left\{x_0^4t^2-x_0^2\pm\sqrt{\mathcal{D}_t}\right\}-\varepsilon\sin\theta\left(\int_0^t W_u\,\mathrm{d}u-\frac{W_t}{x_0^2t}\right)+\varepsilon\cos\theta\frac{W_t}{x_0}$$

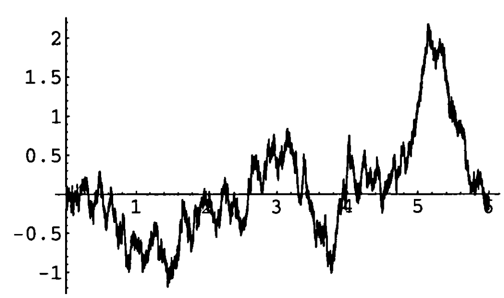

Figure 3.1: Brownian Motion Sample Path

In order to obtain plots of the random caustic and level surface we use a Brownian Motion simulation in Mathematica (see Appendix A) that can be used to produce the random terms. Fixing $\omega\in\Omega$ we consider the sample path $t\longrightarrow W_t(\omega)$ of W_t shown in Figure 3.1.

In Figure 3.2 we have illustrated the pre-curves for $t=1,2,\ldots,6$ where $\theta=\frac{\pi}{8}$, $\varepsilon=\frac{1}{10}$ and $c\equiv 0$. As per usual the pre-caustic is identified by the use of a broken line. The corresponding image curves are shown in Figure 3.3.

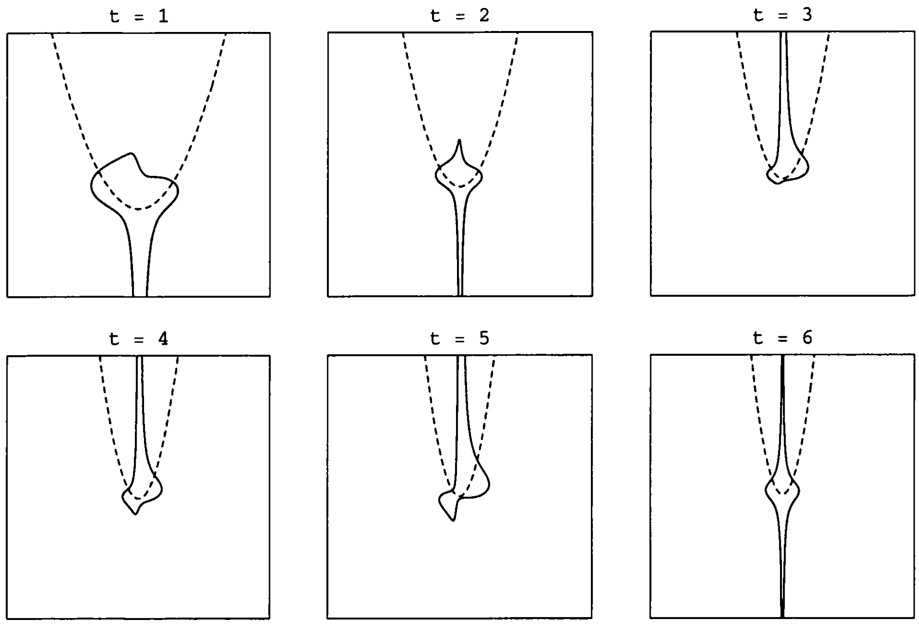

Figure 3.2: Pre-Curves for the stochastic cusp with $\theta = \frac{\pi}{8}$, $\varepsilon = \frac{1}{10}$ and $c \equiv 0$

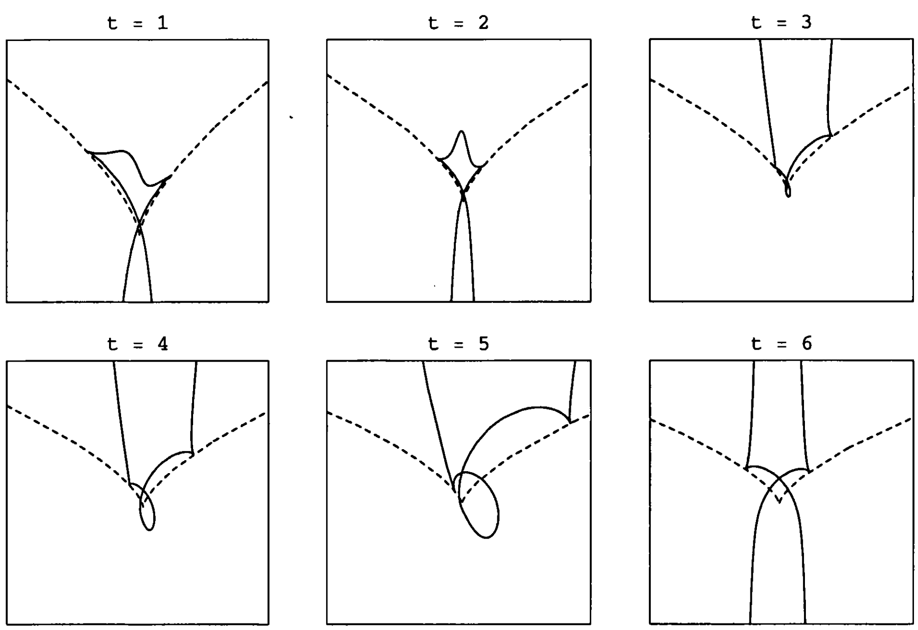

Figure 3.3: Image-Curves for the stochastic cusp with $\theta = \frac{\pi}{8}$, $\varepsilon = \frac{1}{10}$ and $c \equiv 0$

3.5.2 The Polynomial Swallowtail

For $S_0(\boldsymbol{x}_0) = x_0^5 + x_0^2 y_0$, the pre-caustic is given by $y_0(x_0) = -\frac{1}{2t} + 2tx_0^2 - 10x_0^3$ and

$$\Phi_t^\varepsilon(\boldsymbol{x}_0) = \begin{pmatrix} x_0 \\ y_0 \end{pmatrix} + t \begin{pmatrix} 5x_0^4 + 2x_0 y_0 \\ x_0^2 \end{pmatrix} - \varepsilon \begin{pmatrix} \cos\theta \\ \sin\theta \end{pmatrix} \int_0^t W_u \, \mathrm{d}u \, ,$$

so that the random caustic is given by

$$x(x_0) = -15tx_0^4 + 4t^2 x_0^3 - \varepsilon \cos\theta \int_0^t W_u \, \mathrm{d}u \, ,$$

$$y(x_0) = -\frac{1}{2t} + 3tx_0^2 - 10x_0^3 - \varepsilon \sin\theta \int_0^t W_u \, \mathrm{d}u \, .$$

For the pre-level surface we have

$$\frac{t}{2}\left\{\left(5x_0^4 + 2x_0 y_0\right)^2 + x_0^4\right\} + x_0^5 + x_0^2 y_0 - \cos\theta\left(x_0 + t\left(5x_0^4 + 2x_0 y_0\right)\right)\varepsilon W_t$$
$$- \sin\theta\left(y_0 + tx_0^2\right)\varepsilon W_t + \varepsilon^2\left(W_t \int_0^t W_u \, \mathrm{d}u - \frac{1}{2}\int_0^t W_u^2 \, \mathrm{d}u\right) = c \, ,$$

which reduces to the quadratic

$$y_0^2(2x_0^2 t) + y_0\left(10tx_0^5 + x_0^2 - 2tx_0\varepsilon W_t \cos\theta - \varepsilon W_t \sin\theta\right)$$
$$+ \frac{25t}{2}x_0^8 + \frac{t}{2}x_0^4 + x_0^5 + \varepsilon^2\left(W_t \int_0^t W_u \, \mathrm{d}u - \frac{1}{2}\int_0^t W_u^2 \, \mathrm{d}u\right)$$
$$- x_0 \varepsilon W_t \cos\theta - 5tx_0^4 \varepsilon W_t \cos\theta - tx_0^2 \varepsilon W_t \sin\theta - c = 0 \, .$$

Thus the pre-level surface is given by

$$y_0(x_0) = \frac{1}{4x_0^2 t}\left\{-10tx_0^5 - x_0^2 \pm \sqrt{\mathcal{D}_t}\right\} + \frac{\varepsilon W_t \cos\theta}{2x_0} + \frac{\varepsilon W_t \sin\theta}{4x_0^2 t} \, ,$$

for $x_0 \neq 0$ and $\mathcal{D}_t \geq 0$ where

$$\mathcal{D}_t := 12tx_0^7 - 4t^2 x_0^6 + x_0^4 + 8ctx_0^2 - 2\varepsilon W_t x_0^2\left(\sin\theta\left(1 - 4t^2 x_0^2 + 10tx_0^3\right) - 2tx_0 \cos\theta\right)$$
$$+ \varepsilon^2\left(W_t^2\left(2tx_0 \cos\theta + \sin\theta\right)^2 - 8x_0^2 t\left(W_t \int_0^t W_u \, \mathrm{d}u - \frac{1}{2}\int_0^t W_u^2 \, \mathrm{d}u\right)\right) \, .$$

Thus applying the random mapping $\Phi_t^\varepsilon(\boldsymbol{x}_0)$ to the pre-level surface gives the level surface as

$$x(x_0) = \frac{1}{2x_0}\left\{x_0^2 \pm \sqrt{\mathcal{D}_t}\right\} + \varepsilon \cos\theta \int_0^t u \, \mathrm{d}W_u + \frac{\varepsilon}{2x_0} W_t \sin\theta \, ,$$

$$y(x_0) = \frac{1}{4tx_0^2}\left\{-10tx_0^5 + 4t^2 x_0^4 - x_0^2 \pm \sqrt{\mathcal{D}_t}\right\} - \varepsilon \sin\theta\left(\int_0^t W_u \, \mathrm{d}u - \frac{W_t}{4tx_0^2}\right) + \varepsilon \cos\theta \frac{W_t}{2x_0} \, ,$$

for $x_0 \neq 0$ and $\mathcal{D}_t \geq 0$. In Figures 3.4 and 3.5 we have illustrated the pre-curves and image curves respectively using our sample path with $\theta = \frac{\pi}{8}$, $\varepsilon = \frac{1}{10}$ and $c \equiv 0$.

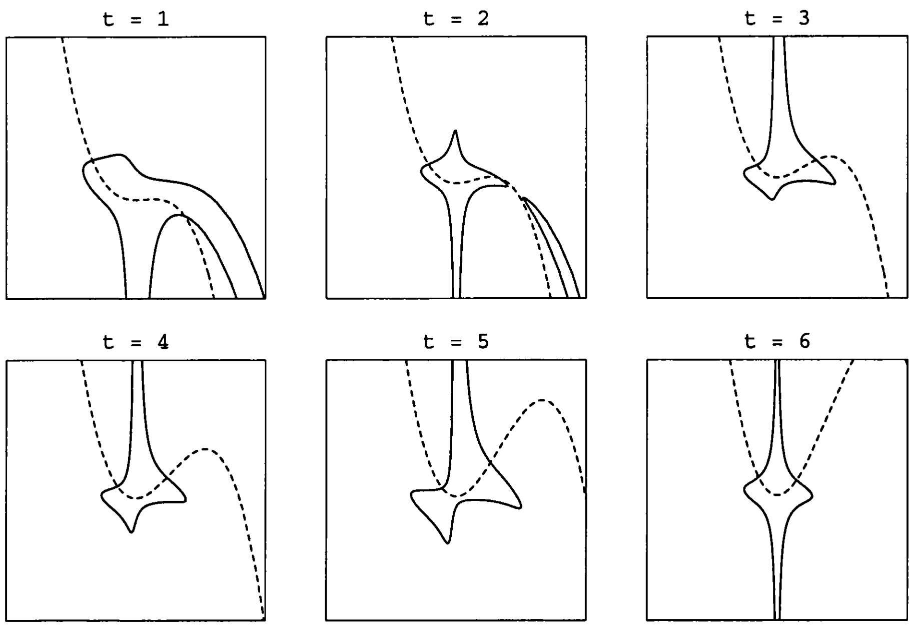

Figure 3.4: Pre-Curves for the polynomial swallowtail with $\theta = \frac{\pi}{8}$, $\varepsilon = \frac{1}{10}$ and $c \equiv 0$

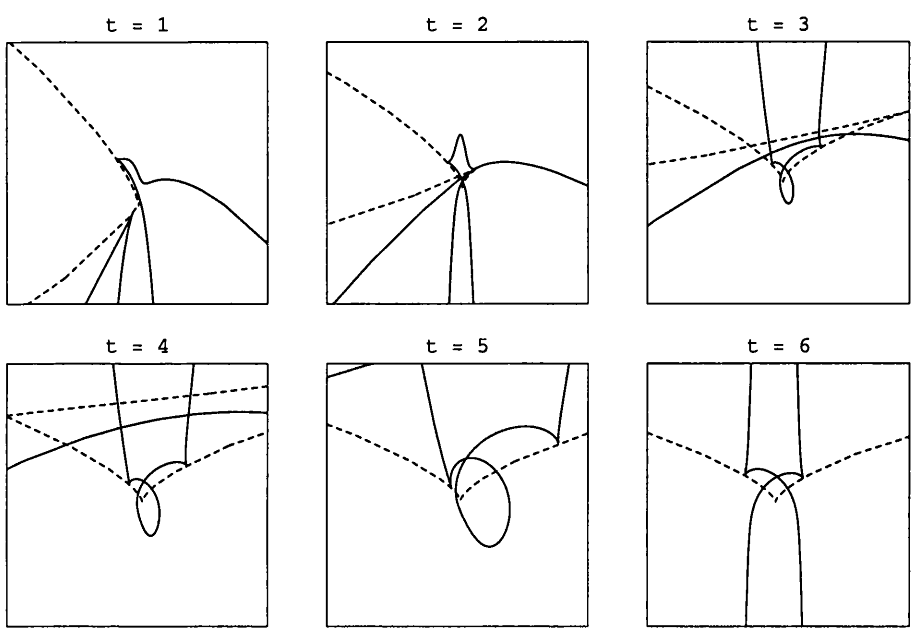

Figure 3.5: Image-Curves for the polynomial swallowtail with $\theta = \frac{\pi}{8}$, $\varepsilon = \frac{1}{10}$ and $c \equiv 0$

3.6 The Three Dimensional Setup

Here we consider the case of one dimensional noise in a general direction for a three dimensional coordinate system. If $\boldsymbol{e_x}, \boldsymbol{e_y}$ and $\boldsymbol{e_z}$ are the unit vectors of a right handed cartesian co-ordinate system at the stationary point O, and $\boldsymbol{e_w}$ is the unit vector parallel to the direction of the noise then we have the following situation,

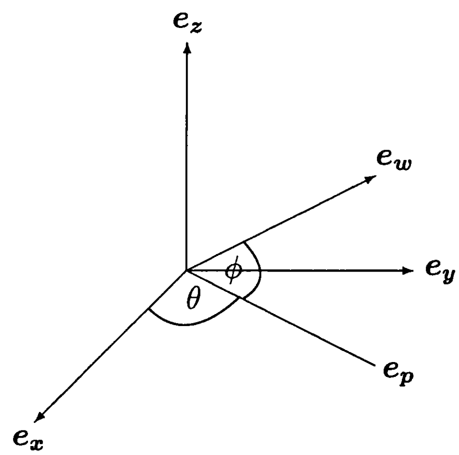

If $\boldsymbol{e_p}$ denotes the projection of $\boldsymbol{e_w}$ onto the xy plane then

$$\begin{aligned}\boldsymbol{e_w} &= \cos\phi \boldsymbol{e_p} + \sin\phi \boldsymbol{e_z} \\ &= \cos\phi\cos\theta \boldsymbol{e_x} + \cos\phi\sin\theta \boldsymbol{e_y} + \sin\phi \boldsymbol{e_z} \ .\end{aligned}$$

Thus we are considering a random force of the form

$$\nabla k(\boldsymbol{x}, t)\dot{W}_t = (\cos\phi\cos\theta, \cos\phi\sin\theta, \sin\phi)\, \dot{W}_t \ ,$$

where $W_t(\omega)$ is a one dimensional Wiener process. Hence setting

$$C(\phi, \theta) := (\cos\phi\cos\theta, \cos\phi\sin\theta, \sin\phi) \ ,$$

we obtain

$$\begin{aligned}\mathcal{A}(\boldsymbol{x}, \boldsymbol{x_0}, t) = \frac{|\boldsymbol{x} - \boldsymbol{x_0}|^2}{2t} - \langle \boldsymbol{x}, C(\phi,\theta)\rangle \varepsilon W_t + \frac{1}{t}\langle \boldsymbol{x} - \boldsymbol{x_0}, C(\phi,\theta)\rangle \varepsilon \int_0^t W_u \,\mathrm{du} \\ + \frac{\varepsilon^2}{2t}\left(\int_0^t W_u \,\mathrm{du}\right)^2 - \frac{\varepsilon^2}{2}\int_0^t W_u^2 \,\mathrm{du} + S_0(\boldsymbol{x_0}) \ .\end{aligned}$$

Proposition 3.6.1. *For the three dimensional Burgers equation with potential of the form* $(x\cos\phi\cos\theta + y\cos\phi\sin\theta + z\sin\phi)\,\dot{W}_t$, *the (pre-)level surface,* $\mathcal{S}(\boldsymbol{x}, t) = c$ *of Hamilton's principal function is given by*

$$\frac{t}{2}\left|\nabla S_0(\boldsymbol{x_0})\right|^2 + S_0(\boldsymbol{x_0}) + \varepsilon^2 W_t \int_0^t W_u \,\mathrm{du} - \frac{\varepsilon^2}{2}\int_0^t W_u^2 \,\mathrm{du} - \langle \boldsymbol{x_0} + t\nabla S_0(\boldsymbol{x_0}), C(\phi,\theta)\rangle \varepsilon W_t = c \ , \tag{3.6.1}$$

where $C(\phi,\theta) := (\cos\phi\cos\theta, \cos\phi\sin\theta, \sin\phi)$.

Proof. Observing that

$$\Phi_t^\varepsilon(\boldsymbol{x}_0) = \boldsymbol{x}_0 - C(\phi,\theta)\varepsilon \int_0^t W_u \, \mathrm{d}u + t\nabla S_0(\boldsymbol{x}_0) \ ,$$

if follows from our expression for $\mathcal{A}(\boldsymbol{x}, \boldsymbol{x}_0, t)$ that the pre-level surface is given by

$$\frac{1}{2t}\left|-C(\phi,\theta)\varepsilon \int_0^t W_u \, \mathrm{d}u + t\nabla S_0\right|^2 - \left\langle \boldsymbol{x}_0 - C(\phi,\theta)\varepsilon \int_0^t W_u \, \mathrm{d}u + t\nabla S_0, C(\phi,\theta)\right\rangle \varepsilon W_t$$
$$+ \frac{1}{t}\left\langle -C(\phi,\theta)\varepsilon \int_0^t W_u \, \mathrm{d}u + t\nabla S_0, C(\phi,\theta)\right\rangle \varepsilon \int_0^t W_u \, \mathrm{d}u + \frac{\varepsilon^2}{2t}\left(\int_0^t W_u \, \mathrm{d}u\right)^2$$
$$- \frac{\varepsilon^2}{2}\int_0^t W_u \, \mathrm{d}u + S_0(\boldsymbol{x}_0) = c \ .$$

Using the fact that $|C(\phi,\theta)| = 1$ yields the required result. □

Remark 3.6.1. Equation (3.6.1) is the analogue of the Eikonal equation obtained in the deterministic case. To obtain the level surface we must evaluate Equation (3.6.1) at $\boldsymbol{x}_0 = (\Phi_t^\varepsilon)^{-1}(\boldsymbol{x})$.

Let us now consider our archetypal examples in the three dimensional case: the butterfly and three dimensional polynomial swallowtail.

3.6.1 The Stochastic Butterfly

The butterfly is generated by taking $S_0(\boldsymbol{x}_0) = x_0^3 y_0 + x_0^2 z_0$ and is the three dimensional analogue of the cuspoidal two dimensional caustic. It is considered in detail in [14], [15], and [41]. We only consider it briefly and refer the interested reader to the aforementioned references.

Taking $S_0(\boldsymbol{x}_0) = x_0^3 y_0 + x_0^2 z_0$ we see

$$\Phi_t^\varepsilon(\boldsymbol{x}_0) = \begin{pmatrix} x_0 \\ y_0 \\ z_0 \end{pmatrix} + t\begin{pmatrix} 3x_0^2 y_0 + 2x_0 z_0 \\ x_0^3 \\ x_0^2 \end{pmatrix} - C(\phi,\theta)\varepsilon \int_0^t W_u \, \mathrm{d}u \ .$$

The pre-caustic is given by

$$z(x_0, y_0) = -\frac{1}{2t}\left(1 - 4t^2 x_0^2 - 9t^2 x_0^4 + 6t x_0 y_0\right) \ ,$$

so that the random caustic is

$$x(x_0,y_0) = 9t^2 x_0^5 + 4t^2 x_0^3 - 3t x_0^2 y_0 - \varepsilon\cos\theta\cos\phi \int_0^t W_u \, \mathrm{d}u \ ,$$
$$y(x_0,y_0) = y_0 + t x_0^3 - \varepsilon\cos\phi\sin\theta \int_0^t W_u \, \mathrm{d}u \ ,$$
$$z(x_0,y_0) = -\frac{1}{2t}\left(1 - 6t^2 x_0^2 - 9t^2 x_0^4 + 6t x_0 y_0\right) - \varepsilon\sin\phi \int_0^t W_u \, \mathrm{d}u \ .$$

Applying Proposition 3.6.1 and solving the resulting quadratic yields the pre-level surface

$$z_0(x_0,y_0)=\frac{1}{4tx_0^2}\left\{-x_0^2-6tx_0^3y_0\pm\sqrt{\mathcal{D}_t}\right\}+\frac{\varepsilon}{2x_0}\cos\theta\cos\phi W_t+\frac{\varepsilon}{4tx_0^2}\sin\phi W_t\ ,$$

for $x_0\neq 0$ and $\mathcal{D}_t\geq 0$ where

$$\begin{aligned}\mathcal{D}_t:=\varepsilon^2&\left(\left(2tx_0\cos\theta\cos\phi+\sin\phi\right)^2W_t^2-8tx_0^2W_t\int_0^t W_u\,\mathrm{d}u+4tx_0^2\int_0^t W_u^2\,\mathrm{d}u\right)\\&+2x_0^2W_t\varepsilon\left(2tx_0\cos\theta\cos\phi+4t\left(tx_0^3+y_0\right)\cos\phi\sin\theta-\left(1-4t^2x_0^2+6tx_0y_0\right)\sin\phi\right)\\&\qquad+x_0^2\left(8ct+x_0^2-4t^2x_0^4-4t^2x_0^6+4tx_0^3y_0\right)\ .\end{aligned}$$

Thus the level surface is given by

$$\begin{aligned}x(x_0,y_0)&=\frac{1}{2x_0}\left\{x_0^2\pm\sqrt{\mathcal{D}_t}\right\}+\varepsilon\cos\theta\cos\phi\int_0^t u\,\mathrm{d}W_u+\frac{\varepsilon}{2x_0}\sin\phi W_t\\y(x_0,y_0)&=y_0+tx_0^3-\varepsilon\cos\phi\sin\theta\int_0^t W_u\,\mathrm{d}u\\z(x_0,y_0)&=\frac{1}{4tx_0^2}\left\{4t^2x_0^4-x_0^2-6tx_0^3y_0\pm\sqrt{\mathcal{D}_t}\right\}+\frac{\varepsilon}{2x_0}\cos\theta\cos\phi W_t\\&\qquad+\varepsilon\sin\phi\left(\frac{W_t}{4tx_0^2}-\int_0^t W_u\,\mathrm{d}u\right)\ ,\end{aligned}$$

for $x_0\neq 0$ and $\mathcal{D}_t\geq 0$.

3.6.2 The Stochastic 3D Polynomial Swallowtail

For $S_0(\boldsymbol{x}_0)=x_0^7+x_0^3y_0+x_0^2z_0$ we have

$$\Phi_t^\varepsilon(\boldsymbol{x}_0)=\begin{pmatrix}x_0\\y_0\\z_0\end{pmatrix}+t\begin{pmatrix}7x_0^6+3x_0^2y_0+2x_0z_0\\x_0^3\\x_0^2\end{pmatrix}-\varepsilon C(\phi,\theta)\int_0^t W_u\,\mathrm{d}u\ .$$

Using our results from Chapter 2 we know that the pre-caustic is given by

$$z_0(x_0,y_0)=-\frac{1}{2t}\left\{1-4t^2x_0^2-9t^2x_0^4+42tx_0^5+6tx_0y_0\right\}\ ,$$

so that the random caustic is

$$\begin{aligned}x(x_0,y_0)&=x_0^2t\left(-35x_0^4+9tx_0^3+4tx_0-3y_0\right)-\varepsilon\cos\theta\cos\phi\int_0^t W_u\,\mathrm{d}u\ ,\\y(x_0,y_0)&=y_0+tx_0^3-\varepsilon\cos\phi\sin\theta\int_0^t W_u\,\mathrm{d}u\ ,\\z(x_0,y_0)&=-21x_0^5+\frac{9}{2}tx_0^4+3tx_0^2-3x_0y_0-\frac{1}{2t}-\varepsilon\sin\phi\int_0^t W_u\,\mathrm{d}u\ .\end{aligned}$$

Applying Proposition 3.6.1 and solving the resulting quadratic yields the pre-level surface

$$z_0(x_0,y_0) = \frac{1}{4tx_0^2}\left\{-14tx_0^7 - 6tx_0^3y_0 - x_0^2 \pm \sqrt{\mathcal{D}_t}\right\} + \frac{\varepsilon}{2x_0}\cos\theta\cos\phi W_t + \frac{\varepsilon}{4tx_0^2}\sin\phi W_t ,$$

for $x_0 \neq 0$ and $\mathcal{D}_t \geq 0$ where

$$\begin{aligned}\mathcal{D}_t := \varepsilon^2 &\left(\left(2tx_0\cos\theta\cos\phi + \sin\phi\right)^2 W_t^2 - 8tx_0^2 W_t \int_0^t W_u\,\mathrm{d}u + 4tx_0^2\int_0^t W_u^2\,\mathrm{d}u\right)\\ &+ 2x_0^2 W_t\varepsilon\Big(2tx_0\cos\theta\cos\phi + 4t\left(tx_0^3+y_0\right)\cos\phi\sin\theta\\ &\qquad - \left(1 - 4t^2x_0^2 + 14tx_0^5 + 6tx_0y_0\right)\sin\phi\Big)\\ &\qquad\qquad + x_0^2\left(8ct + x_0^2\left(1 - 4t^2x_0^2 - 4t^2x_0^4 + 20tx_0^5 + 4tx_0y_0\right)\right) .\end{aligned}$$

Thus applying $\Phi_t^\varepsilon(\boldsymbol{x}_0)$ we obtain the level surface,

$$\begin{aligned}x(x_0,y_0) &= \frac{1}{2x_0}\left\{x_0^2 \pm \sqrt{\mathcal{D}_t}\right\} + \frac{\varepsilon}{2x_0}\sin\phi W_t + \varepsilon\cos\theta\cos\phi\int_0^t u\,\mathrm{d}W_u ,\\ y(x_0,y_0) &= y_0 + tx_0^3 - \varepsilon\cos\phi\sin\theta\int_0^t W_u\,\mathrm{d}u ,\\ z(x_0,y_0) &= \frac{1}{4tx_0^2}\left\{4t^2x_0^4 - 14tx_0^7 - 6tx_0^3y_0 - x_0^2 \pm \sqrt{\mathcal{D}_t}\right\} + \frac{\varepsilon}{2x_0}\cos\theta\cos\phi W_t\\ &\qquad + \varepsilon\sin\phi\left(\frac{W_t}{4tx_0^2} - \int_0^t W_u\,\mathrm{d}u\right) ,\end{aligned}$$

for $x_0 \neq 0$ and $\mathcal{D}_t \geq 0$.

3.7 Cusped Meeting Points

In the remainder of this chapter we study the number of cusps on level surfaces of Hamilton's principal function in the two dimensional setting. We begin by contradicting the title of this chapter by considering the deterministic situation.

We know that for an initial function of the form $S_0(\boldsymbol{x}_0) = f(x_0) + g(x_0)y_0$ the pre-caustic is given by

$$y_0(x_0) = \frac{1}{tg''(x_0)}\left(t^2 g'(x_0)^2 - tf''(x_0) - 1\right) , \tag{3.7.1}$$

whilst the pre-level surface is

$$\frac{t}{2}\left\{\left(f'(x_0) + g'(x_0)y_0\right)^2 + g(x_0)^2\right\} + f(x_0) + g(x_0)y_0 = c . \tag{3.7.2}$$

If $y_1^0(x_0,t)$ and $y_2^0(x,t)$ are solutions of the quadratic Equation (3.7.2), then we know from the geometrical result considered in Chapter 2 that the number of cusps, $\mathcal{N}_C(t)$, on level surfaces of Hamilton's principal function will be given by the number of x_0's for which

$y_1^0(x,t) = y_0(x_0)$ plus the number of x_0's for which $y_2^0(x,t) = y_0(x_0)$. Thus if we denote the left hand side of Equation (3.7.2) by $p(x_0, y_0)$ then the number of cusps on $\mathcal{S}(x,t) = c$ is given by

$$\mathcal{N}_C(t) = \{\#x_0 : p(x_0, y_0(x_0)) = c\} \ .$$

Substituting in the expression from Equation (3.7.1) and omitting the x_0 variable for brevity yields

$$p(x_0, y_0(x_0)) = \frac{t}{2}\left\{\left(f' + \frac{g'}{tg''}\left(t^2 g'^2 - tf'' - 1\right)\right)^2 + g^2\right\} + f + \frac{g}{tg''}\left(t^2 g'^2 - tf'' - 1\right) \ .$$

Thus setting $F_0(x_0, t) := p(x_0, y_0(x_0))$ for fixed $t > 0$, we are interested in the number of x_0 satisfying $F_0(x_0, t) = c$.

In [31], Mark Kac proved the following lemma concerning the number of zeros of a function $f(x_0)$. Here we provide an account of the result and accompanying proof.

Lemma 3.7.1 (Kac's Lemma). *If $f(x)$ is continuous for $a \le x \le b$ and continuously differentiable for $a < x < b$ then assuming $f(x)$ has a finite number of turning points the number of zeros of $f(x)$ in (a, b) is given by*

$$n(a, b; f) = (2\pi)^{-1} \int_{-\infty}^{\infty} \int_a^b \cos\left[\xi f(x)\right] |f'(x)| \, \mathrm{d}x \, \mathrm{d}\xi \ ,$$

where multiple zeros are counted once and if either a or b is a zero it is counted as $\frac{1}{2}$.

Proof. Let $\alpha_0 = a \le \alpha_1 < \alpha_2 < \cdots < \alpha_k \le b = \alpha_{k+1}$ be the abscissae of the turning points. The we may split the integral as follows,

$$\begin{aligned}
\int_a^b \cos\left[\xi f(x)\right] |f'(x)| \, \mathrm{d}x &= \sum_{j=1}^{k} \int_{\alpha_j}^{\alpha_{j+1}} \cos\left[\xi f(x)\right] |f'(x)| \, \mathrm{d}x \\
&= \sum_{j=1}^{k} \pm \int_{\alpha_j}^{\alpha_{j+1}} \cos\left[\xi f(x)\right] f'(x) \, \mathrm{d}x \\
&= \sum_{j=0}^{k} \pm \frac{1}{\xi}\left[\sin[\xi f(\alpha_{j+1})] - \sin[\xi f(\alpha_j)]\right] \ ,
\end{aligned}$$

where a $+$ sign is attached if $f(x)$ is increasing on (α_j, α_{j+1}) and a $-$ sign is attached if $f(x)$ is decreasing. Hence if $n(a, b; f)$ denotes the number of zeros of $f(x)$ in (a, b) then

$$\begin{aligned}
&(2\pi)^{-1} \int_{-\infty}^{\infty} \int_a^b \cos\left[\xi f(x)\right] |f'(x)| \, \mathrm{d}x \, \mathrm{d}\xi \\
&\quad = \sum_{j=0}^{k} \pm (2\pi)^{-1} \int_{-\infty}^{\infty} \frac{1}{\xi}\left[\sin[\xi f(\alpha_{j+1})] - \sin[\xi f(\alpha_j)]\right] \mathrm{d}\xi \\
&\quad = \sum_{j=0}^{k} \pm \frac{1}{2}\left[\operatorname{sgn} f(\alpha_{j+1}) - \operatorname{sgn} f(\alpha_j)\right] \\
&\quad = n(a, b; f) \ .
\end{aligned}$$

□

Remark 3.7.1. The above lemma was actually first proved by Kac in [30] whilst studying the distribution of values of trigonometric sums with linearly independent frequencies.

Let us consider the function $F_0(x_0, t)$ defined earlier for fixed $t > 0$. Since we are dealing with a polynomial there will exist $a \in \mathbb{R}$ such that $|F_0(x_0, t) - c| > 0$ for $x_0 \in (-\infty, -a] \cup [a, \infty)$. Thus it follows from Kac's Lemma that

$$\mathcal{N}_C(t) = (2\pi)^{-1} \int_{-\infty}^{\infty} \int_{-a}^{a} \cos[\xi(F_0(x_0, t) - c)]\, |F_0'(x_0, t)|\, \mathrm{d}x_0\, \mathrm{d}\xi \; .$$

Let us see how this works for the cusp and polynomial swallowtail in which we shall obtain explicit values for the constant $a \in \mathbb{R}$.

3.7.1 Cusp

For $S_0(\boldsymbol{x}_0) = \frac{1}{2}x_0^2 y_0$ we have

$$F_0(x_0, t) = x_0^4 \left(\frac{t^3 x_0^2}{2} - \frac{3t}{8} \right) \; .$$

Lemma 3.7.2. *For fixed $t > 0$, any real solutions of $F_0(x_0, t) = c$ lie in the interval $(-a, a)$ where*

$$a := \frac{\sqrt{3}}{2t} + \left(\frac{2}{t^3}|c| \right)^{\frac{1}{6}} \; .$$

Proof. We begin by observing that $F_0(x_0, t) = 0$ has solutions $x_0 = 0$ and $x_0 = \pm\frac{\sqrt{3}}{2t}$. Setting $x^* = \frac{\sqrt{3}}{2t}$ and $c^* = \left(\frac{2}{t^3}|c|\right)^{\frac{1}{6}}$ we obtain

$$\begin{aligned} F(x^* + c^*) &= (x^* + c^*)^4 \left(\frac{t^3}{2}(x^* + c^*)^2 - \frac{3t}{8} \right) \\ &> c^{*4} \left(\frac{t^3}{2}x^{*2} + \frac{t^3}{2}c^{*2} - \frac{3t}{8} \right) \\ &= \frac{t^3}{2}c^{*6} = |c| \; , \end{aligned}$$

and by symmetry $F(-x^* - c^*) > |c|$. ☐

Thus we immediately have the following result.

Proposition 3.7.3. *For fixed $t > 0$ and initial condition $S_0(\boldsymbol{x}_0) = \frac{1}{2}x_0^2 y_0$, the number of cusps on level surfaces, $S(\boldsymbol{x}, t) = c$, of Hamilton's principal function is given by*

$$\mathcal{N}_C(t) = \frac{3t}{2\pi} \int_{-\infty}^{\infty} \int_{-a}^{a} \cos\left[\xi \left(\frac{t^3 x_0^6}{2} - \frac{3t x_0^4}{8} - c \right) \right] \left| t^2 x_0^5 - \frac{x_0^3}{2} \right| \mathrm{d}x_0\, \mathrm{d}\xi \; ,$$

where $a := \frac{\sqrt{3}}{2t} + \left(\frac{2}{t^3}|c|\right)^{\frac{1}{6}}$.

3.7.2 Polynomial Swallowtail

For $S_0(\boldsymbol{x}_0) = x_0^5 + x_0^2 y_0$ we have

$$F_0(x_0, t) = \frac{225}{2} t x_0^8 - 60t^2 x_0^7 + 8t^3 x_0^6 + 6x_0^5 - \frac{3t}{2} x_0^4 \,.$$

Lemma 3.7.4. *For fixed $t > 0$, any real solutions of $F_0(x_0, t) = c$ lie in the interval $(-a, a)$ where*

$$a := \max\left\{\frac{8t}{15}, \frac{3 + \sqrt{12t^4 + 9}}{8t^3}\right\} + \left(\frac{2}{225t}|c|\right)^{\frac{1}{8}} \,.$$

Proof. Define $\alpha(x_0) := \frac{225}{2} t x_0^8 - 60t^2 x_0^7$ and $\beta(x_0) = 8t^3 x_0^6 + 6x_0^5 - \frac{3t}{2} x_0^4$, so that $F_0(x_0, t) = \alpha(x_0) + \beta(x_0)$. Now $\alpha(x_0) = 0$ has solutions $x_0 = 0$ and $x_0 = \frac{8t}{15}$, so that $\alpha(x_0) > 0$ for $|x_0| > \frac{8t}{15}$.

Similarly $\beta(x_0) = 0$ has solutions $x_0 = 0$ and $x_0 = \frac{1}{8t^3}\left(-3 \pm \sqrt{9 + 12t^4}\right)$. Taking the magnitude of the largest we see $\beta(x_0) > 0$ for $|x_0| > \frac{1}{8t^3}\left(3 + \sqrt{9 + 12t^4}\right)$. Hence setting

$$x^* = \max\left\{\frac{8t}{15}, \frac{3 + \sqrt{12t^4 + 9}}{8t^3}\right\} \qquad \text{and} \qquad c^* = \left(\frac{2}{225t}|c|\right)^{\frac{1}{8}} \,,$$

we see

$$\begin{aligned}
\alpha(x^* + c^*) + \beta(x^* + c^*) &> (x^* + c^*)^7 \left(\frac{225}{2} t(x^* + c^*) - 60t^2\right) \\
&> c^{*7}\left(\frac{225t}{2} x^* + \frac{225t}{2} c^* - 60t^2\right) \\
&\geq \frac{225t}{2} c^{*8} = |c| \qquad\qquad \text{since } x^* \geq \tfrac{8t}{15}.
\end{aligned}$$

By a similar method it may be shown that $\alpha(-x^* - c^*) + \beta(-x^* - c^*) > |c|$, so that for $|x_0| \geq x^* + c^*$ we have $F_0(x_0, t) > c$ as required. □

Proposition 3.7.5. *For fixed $t > 0$ and initial function $S_0(\boldsymbol{x}_0) = x_0^5 + x_0^2 y_0$, the number of cusps on the level surface, $\mathcal{S}(\boldsymbol{x}, t) = c$, of Hamilton's principal function is given by*

$$\begin{aligned}
\mathcal{N}_C(t) = \frac{3}{\pi} \int_{-\infty}^{\infty} \int_{-a}^{a} x_0^2 \cos\left[\xi\left(\frac{225}{2} t x_0^8 - 60t^2 x_0^7 + 8t^3 x_0^6 + 6x_0^5 - \frac{3t}{2} x_0^4 - c\right)\right] \\
\times \left|x_0\left(150 t x_0^4 - 70t^2 x_0^3 + 8t^3 x_0^2 + 5x_0 - t\right)\right| \, \mathrm{d}x_0 \, \mathrm{d}\xi \,, \quad (3.7.3)
\end{aligned}$$

where $a := \max\left\{\frac{8t}{15}, \frac{3+\sqrt{12t^4+9}}{8t^3}\right\} + \left(\frac{2}{225t}|c|\right)^{\frac{1}{8}}$.

Let us now return to the stochastic situation. For the sake of simplicity we only consider the case of noise parallel to the x-axis. However there is no reason why the following argument may not be extended to the case of one dimensional noise parallel to a fixed general direction.

From Proposition 3.5.2 with $\theta = 0$ the pre-level surface for $S_0(\boldsymbol{x}_0) = f(x_0) + g(x_0)y_0$ is given by

$$\frac{t}{2}\left\{(f' + g'y_0))^2 + g^2\right\} + f + gy_0 - \left(x_0 + t\,(f' + g'y_0) - \varepsilon \int_0^t W_u\,\mathrm{d}u\right)\varepsilon W_t - \frac{\varepsilon^2}{2}\int_0^t W_u^2\,\mathrm{d}u = c\,.$$

Consider the function

$$F_\varepsilon(x_0, u, v, w) := \frac{t}{2}\left\{(f' + g'y_0(x_0))^2 + g^2\right\} + f + gy_0(x_0) - \frac{\varepsilon^2}{2}w - (x_0 - \varepsilon v + tf' + tg'y_0(x_0))\,\varepsilon u\,,$$

where f and g are polynomials in x_0 and $y_0(x_0)$ is the pre-caustic. Using the expression for the pre-caustic from Equation (3.7.1) we obtain

$$F_\varepsilon(x_0, u, v, w) = \frac{t}{2}\left\{\left(f' + \frac{g'}{tg''}\left(t^2g'^2 - tf'' - 1\right)\right)^2 + g^2\right\} + f + \frac{g}{tg''}\left(t^2g'^2 - tf'' - 1\right) - \frac{\varepsilon^2}{2}w - \left(x_0 - \varepsilon v + tf' + \frac{g'}{g''}\left(t^2g'^2 - tf'' - 1\right)\right)\varepsilon u\,. \quad (3.7.4)$$

Then for fixed $t > 0$ and initial function $S_0(\boldsymbol{x}_0) = f(x_0) + g(x_0)y_0$, the number of cusped meeting points of the level surface H_t with the caustic C_t in the presence of white noise parallel to the x-axis is given by

$$\mathcal{N}_C(t) := \left\{\# x_0 : F_\varepsilon\left(x_0, W_t, \textstyle\int_0^t W_u\,\mathrm{d}u, \int_0^t W_u^2\,\mathrm{d}u\right) = c\right\}\,. \quad (3.7.5)$$

In order to analyse the random quantity $\mathcal{N}_C(t)$ it is necessary to study a random polynomial. We remark at the outset that it has been proved in [6] that the number of zeros of a random polynomial is a measurable quantity. There is much literature on the subject of random polynomials, see for instance the papers [29], [28] and [17], but these are largely concerned with the case when the polynomial has normally distributed independent coefficients. Unfortunately this assertion is false for our polynomial $F_\varepsilon\left(x_0, W_t, \int_0^t W_u\,\mathrm{d}u, \int_0^t W_u^2\,\mathrm{d}u\right)$.

By Kac's Lemma it follows that for fixed $t > 0$ the number of cusps in the vertical strip $[a, b]$ is given by

$$\mathcal{N}_C(\omega)(a, b) = (2\pi)^{-1}\int_{-\infty}^{\infty}\int_a^b \cos\left[\xi\left(F_\varepsilon\left(x_0, W_t, \textstyle\int_0^t W_u\,\mathrm{d}u, \int_0^t W_u^2\,\mathrm{d}u\right) - c\right)\right] \times \left|\frac{\partial F_\varepsilon}{\partial x_0}\left(x_0, W_t, \textstyle\int_0^t W_u\,\mathrm{d}u, \int_0^t W_u^2\,\mathrm{d}u\right)\right| \mathrm{d}x_0\,\mathrm{d}\xi\,. \quad (3.7.6)$$

Thus if $\boldsymbol{u} = (u, v, w)$ then the expected number of cusped meeting points at fixed time $t > 0$ is

$$\mathbb{E}\left[\mathcal{N}_C(\omega)(a,b)\right] = (2\pi)^{-1}\int_{-\infty}^{\infty}\int_a^b \mathbb{E}\Big[\cos\left[\xi\left(F_\varepsilon\left(x_0, W_t, \textstyle\int_0^t W_u\,\mathrm{d}u, \int_0^t W_u^2\,\mathrm{d}u\right) - c\right)\right] \times \left|\frac{\partial F_\varepsilon}{\partial x_0}\left(x_0, W_t, \textstyle\int_0^t W_u\,\mathrm{d}u, \int_0^t W_u^2\,\mathrm{d}u\right)\right|\Big]\,\mathrm{d}x_0\,\mathrm{d}\xi$$

$$= (2\pi)^{-1}\int_{-\infty}^{\infty}\int_a^b \int_{\mathbb{R}^3} \cos\left[\xi(F_\varepsilon(x_0,\boldsymbol{u}) - c)\right]\left|\frac{\partial F_\varepsilon}{\partial x_0}(x_0,\boldsymbol{u})\right| f_X(\boldsymbol{u})\,\mathrm{d}^3\boldsymbol{u}\,\mathrm{d}x_0\,\mathrm{d}\xi\ ,$$

where $f_X(u,v,w)$ is the joint density function of

$$X_t := \left(W_t, \int_0^t W_u\,\mathrm{d}u, \int_0^t W_u^2\,\mathrm{d}u\right)\ .$$

The challenge is to determine the function $f_X(u,v,w)$.

Consider a random variable $X:\Omega\to\mathbb{R}^n$, then the function L_X defined by

$$L_X(\boldsymbol{\theta}) = \mathbb{E}\left[\exp\left(-\langle\boldsymbol{\theta}, X\rangle\right)\right] = \int_{\mathbb{R}^n} e^{-\langle\boldsymbol{\theta},\boldsymbol{x}\rangle}\mathbb{P}\left[X\in\,\mathrm{d}\boldsymbol{x}\right] = \int_{\mathbb{R}^n} e^{-\langle\boldsymbol{\theta},\boldsymbol{x}\rangle} f_X(\boldsymbol{x})\,\mathrm{d}\boldsymbol{x}\ , \qquad (\theta\in\mathbb{C})$$

is the Laplace Transform of X, or more precisely of the measure $\mathbb{P}\left[X\in\,\mathrm{d}\boldsymbol{x}\right]$. In particular if we set $\theta = -i\lambda$ for $\lambda\in\mathbb{R}$ then we obtain the characteristic function

$$\varphi_X(\boldsymbol{\lambda}) = L_X(-i\boldsymbol{\lambda}) = \int_{\mathbb{R}^n} e^{i\langle\boldsymbol{\lambda},\boldsymbol{x}\rangle} f_X(\boldsymbol{x})\,\mathrm{d}\boldsymbol{x}\ ,$$

which is the Fourier transform of the measure $\mathbb{P}\left[X\in\,\mathrm{d}\boldsymbol{x}\right]$. Hence it follows from the Fourier inversion theorem that knowledge of $\varphi_X(\boldsymbol{\lambda})$ allows us to determine $f_X(\boldsymbol{x})$ uniquely.

We begin by considering the quantity

$$\mathbb{E}\left[\exp\left\{-\lambda_1 W_t - \lambda_2\int_0^t W_u\,\mathrm{d}u - \lambda_3\int_0^t W_u^2\,\mathrm{d}u\right\}\right]\ .$$

Much work has been done on developing methods for the computation of the laws of quadratic functionals of the Wiener process, see for example [16], [12] and [40].

Following the work of Dean and Jansons in [16], we remark that a Brownian motion started at some point x and conditioned to be at y at time t is called a Brownian bridge on $[0,t]$ between x and y. It has the representation $\beta_s + x + (y-x)\frac{s}{t}$ where $(\beta)_{0\le s\le t}$ is the standard Brownian bridge on $[0,t]$, namely one that starts and ends at zero. It follows from Lemma 6 in [16], that the general form of the law of the quadratic functional for a path with both end points fixed at arbitrary points is given by

$$\mathbb{E}^{x\to y}\left[\exp\left\{-\frac{\alpha^2}{2}\int_0^t W_u^2\,\mathrm{d}u\right\}\right]$$
$$=\sqrt{\frac{\alpha t}{\sinh(\alpha t)}}\exp\left\{-\frac{1}{2}\alpha\coth(\alpha t)\left(x^2+y^2-2xy\,\mathrm{sech}(\alpha t)\right)+\frac{1}{2t}(x-y)^2\right\}\ . \quad (3.7.7)$$

Remark 3.7.2. The essence of the proof of Equation (3.7.7) is to observe

$$\mathbb{E}^{x\to y}\left[\exp\left\{-\frac{\alpha^2}{2}\int_0^t W_u^2\,\mathrm{d}u\right\}\right]=\mathbb{E}\left[\exp\left\{-\frac{\alpha^2}{2}\int_0^t\left(\beta_u+x+(y-x)\frac{u}{t}\right)^2\mathrm{d}u\right\}\right]\ ,$$

and use the so-called Fundamental Theorem of Statistics.

Let us consider the expression

$$\hat{\phi}(\xi):=\mathbb{E}\left[\exp\left\{-\int_0^t W_u^2\,\mathrm{d}\mu+(2\rho)^{\frac{1}{2}}\xi\int_0^t W_u\,\mathrm{d}\mu-\lambda W_t\right\}\right]\ ,$$

where $\rho=(\int_0^t \mathrm{d}\mu)^{-1}$ and $\mathrm{d}\mu=\frac{\alpha^2}{2}\,\mathrm{d}u$. Now

$$\begin{aligned}\hat{\phi}(\xi)&=\exp\left\{\frac{\xi^2}{2}\right\}\mathbb{E}^0\left[\exp\left\{-\left(\int_0^t\left(W_u-\xi\sqrt{\frac{\rho}{2}}\right)^2\mathrm{d}\mu+\lambda W_t\right)\right\}\right]\\&=\exp\left\{\frac{\xi^2}{2}\right\}\mathbb{E}^{-\xi\sqrt{\frac{\rho}{2}}}\left[\exp\left\{-\left(\int_0^t W_u^2\,\mathrm{d}\mu+\lambda W_t+\lambda\xi\sqrt{\frac{\rho}{2}}\right)\right\}\right]\\&=\frac{1}{\sqrt{2\pi t}}\exp\left\{\frac{\xi^2}{2}\right\}\int_{\mathbb{R}}e^{-\frac{y^2}{2t}}\mathbb{E}^{-\xi\sqrt{\frac{\rho}{2}}\to y-\xi\sqrt{\frac{\rho}{2}}}\left[\exp\left\{-\left(\int_0^t W_u^2\,\mathrm{d}\mu+\lambda y\right)\right\}\right]\mathrm{d}y\ .\end{aligned}$$

But using Equation (3.7.7) we obtain

$$\begin{aligned}\hat{\phi}(\xi)&=\sqrt{\frac{\alpha}{2\pi\sinh(\alpha t)}}\exp\left\{\frac{\xi^2}{2}\right\}\int_{\mathbb{R}}\exp\left\{-\frac{\xi^2}{\alpha t}\tanh\left(\frac{\alpha t}{2}\right)+\frac{\xi y}{\sqrt{t}}\tanh\left(\frac{\alpha t}{2}\right)\right.\\&\qquad\left.-\frac{y^2\alpha}{2}\coth(\alpha t)-\lambda y\right\}\mathrm{d}y\\&=\sqrt{\frac{1}{\cosh(\alpha t)}}\exp\left\{\frac{\xi^2}{2}\right\}\exp\left\{\frac{1}{\alpha t}\left[\mathrm{sech}(\alpha t)\sinh\left(\frac{\alpha t}{2}\right)\left((t\lambda^2-\xi^2)\cosh\left(\frac{\alpha t}{2}\right)\right.\right.\right.\\&\qquad\left.\left.\left.-2\lambda\xi\sqrt{t}\sinh\left(\frac{t\alpha}{2}\right)\right)\right]\right\}\ ,\end{aligned}$$

for $\mathrm{Re}[\alpha\coth(\alpha t)]>0$. After slightly more simplification this yields

$$\mathbb{E}\left[\exp\left\{-\frac{\alpha^2}{2}\int_0^t W_u^2\,\mathrm{d}u+\frac{\alpha\xi}{\sqrt{t}}\int_0^t W_u\,\mathrm{d}u-\lambda W_t\right\}\right]$$
$$=\sqrt{\frac{1}{\cosh(\alpha t)}}\exp\left\{\frac{\xi^2}{2}+\frac{\lambda\xi}{\alpha\sqrt{t}}(\mathrm{sech}(\alpha t)-1)+\frac{\tanh(\alpha t)}{2t\alpha}(t\lambda^2-\xi^2)\right\}\ .$$

In order to obtain the required characteristic function we set $i\lambda_1 = -\frac{\alpha^2}{2}$, $i\lambda_2 = \frac{\alpha\xi}{\sqrt{t}}$ and $i\lambda_3 = -\lambda$. This yields

$$\alpha = \pm\sqrt{\lambda_1}(1-i) \, ,$$
$$\xi = \pm(i-1)\frac{\lambda_2}{2}\sqrt{\frac{t}{\lambda_1}} \, ,$$
$$\lambda = -i\lambda_3 \, .$$

We remark that both signs yield the same expression for our characteristic function, namely

$$\varphi_X(\boldsymbol{\lambda}) = \sqrt{\frac{1}{\cosh\left(\sqrt{\lambda_1}(1-i)t\right)}} \exp\left\{ -\frac{i\lambda_2^2 t}{4\lambda_1} + i\frac{\lambda_2\lambda_3}{2\lambda_1}\left(\operatorname{sech}\left(\sqrt{\lambda_1}(1-i)t\right) - 1\right) - \tanh\left(\sqrt{\lambda_1}(1-i)t\right)\frac{(1+i)}{4\sqrt{\lambda_1}}\left(\lambda_3^2 - i\frac{\lambda_2^2}{2\lambda_1}\right)\right\} ,$$

where we may write

$$\cosh(\sqrt{\lambda_1}(1-i)t) = \frac{\exp\left\{2\sqrt{\lambda_1}(1-i)t\right\} + 1}{2\exp\left\{\sqrt{\lambda_1}(1-i)t\right\}} ,$$

and

$$\tanh(\sqrt{\lambda_1}(1-i)t) = \frac{\exp\left\{2\sqrt{\lambda_1}(1-i)t\right\} - 1}{\exp\left\{2\sqrt{\lambda_1}(1-i)t\right\} + 1} .$$

Hence for $\boldsymbol{u} = (u, v, w)$ we have

$$\mathbb{E}\left[\mathcal{N}_C(\omega)(a,b)\right] = (2\pi)^{-1}\int_{-\infty}^{\infty}\int_a^b \int_{\mathbb{R}^3} \cos\left[\xi(F_\varepsilon(x_0,\boldsymbol{u}) - c)\right]\left|\frac{\partial F_\varepsilon}{\partial x_0}(x_0,\boldsymbol{u})\right| f_X(\boldsymbol{u})\,\mathrm{d}^3\boldsymbol{u}\,\mathrm{d}x_0\,\mathrm{d}\xi ,$$

where

$$f_X(\boldsymbol{u}) = \frac{1}{(2\pi)^3}\int_{\mathbb{R}^3} e^{-i(\lambda_1 u + \lambda_2 v + \lambda_3 w)}\varphi_X(\boldsymbol{\lambda})\,\mathrm{d}^3\boldsymbol{\lambda}$$
$$= \frac{1}{(2\pi)^3}\int_{\mathbb{R}^3} \sqrt{\frac{1}{\cosh\left(\sqrt{\lambda_1}(1-i)t\right)}} \exp\left\{ -\frac{i\lambda_2^2 t}{4\lambda_1} + i\frac{\lambda_2\lambda_3}{2\lambda_1}\left(\operatorname{sech}\left(\sqrt{\lambda_1}(1-i)t\right) - 1\right) - \tanh\left(\sqrt{\lambda_1}(1-i)t\right)\frac{(1+i)}{4\sqrt{\lambda_1}}\left(\lambda_3^2 - i\frac{\lambda_2^2}{2\lambda_1}\right) - i\left(\lambda_1 u + \lambda_2 v + \lambda_3 w\right)\right\}\mathrm{d}^3\boldsymbol{\lambda} .$$

Chapter 4

On the Hot and Cool Parts of the Polynomial Swallowtail

In this chapter we investigate the behaviour of the solution of the heat equation $u^\mu(\boldsymbol{x},t)$ as we cross the zero level surface of Hamilton's principal function and the caustic. Beginning with a discussion of the multiplicity of Φ_t^{-1} we proceed to introduce the notion of hot and cool parts of the caustic and illustrate how these are connected to exponential discontinuity in $u^0(\boldsymbol{x},t)$. A new method is developed to determine whether a point on the caustic is hot or cool and this is applied to provide a full description for the cusp and polynomial swallowtail. The effect of one dimensional noise parallel to a fixed direction is considered and shown to displace the hot and cool sections bodily with the caustic.

4.1 Introduction

In this chapter we are guided by the recent paper [15] particularly with reference to their results on the exponential discontinuity of $u^0(\boldsymbol{x},t)$ for the cusp example.

Let C_t and H_t respectively denote the caustic surface and zero level surface of Hamilton's principal function. The pre-surfaces are simply the algebraic pre-images of C_t and H_t under the classical flow map Φ_t, which we denote by $\Phi_t^{-1}C_t$ and $\Phi_t^{-1}H_t$.

Consider a non-degenerate critical point $\tilde{\boldsymbol{x}}$ where the multiplicity of $\Phi_t^{-1}\{\tilde{\boldsymbol{x}}\}$ has the finite value $n = n(\tilde{\boldsymbol{x}})$. Denoting the elements of $\Phi_t^{-1}\{\tilde{\boldsymbol{x}}\}$ by $x_0^i(\tilde{\boldsymbol{x}},t)$ where $x_0^i(\tilde{\boldsymbol{x}},t) \neq x_0^j(\tilde{\boldsymbol{x}},t)$ for $i \neq j$ we have

$$\Phi_t^{-1}\{\tilde{\boldsymbol{x}}\} = \left\{\boldsymbol{x}_0^1(\tilde{\boldsymbol{x}},t),\ldots,\boldsymbol{x}_0^n(\tilde{\boldsymbol{x}},t)\right\} .$$

From this it may be deduced that

$$u^\mu(\tilde{\boldsymbol{x}},t) \sim \sum_{i=1}^{n} \theta_i \exp\left\{-\frac{S_i(\tilde{\boldsymbol{x}},t)}{\mu^2}\right\} ,$$

where

$$S_i(\tilde{\boldsymbol{x}},t) := \mathcal{A}(\boldsymbol{x}_0^i(\tilde{\boldsymbol{x}},t),\tilde{\boldsymbol{x}},t) = A\left(\boldsymbol{x}_0^i(\tilde{\boldsymbol{x}},t),\tilde{\boldsymbol{x}},t\right) + S_0\left(\boldsymbol{x}_0^i(\tilde{\boldsymbol{x}},t)\right) , \tag{4.1.1}$$

for $i = 1, 2, \ldots, n$ and θ_i is an asymptotic series in μ^2. Details of this asymptotic series may be found in [54]. With this in mind we now conduct an analysis of the multiplicity of $\Phi_t^{-1}\{\tilde{x}\}$.

4.2 Analysis of the Multiplicity of $\Phi_t^{-1}\{\boldsymbol{x}\}$

Here we investigate how the cardinality of the set $\Phi_t^{-1}\{\boldsymbol{x}\}$, which we denote by $\left|\Phi_t^{-1}\{\boldsymbol{x}\}\right|$, depends upon the value $\boldsymbol{x}$ considered. We illustrate the connection between the multiplicity of $\Phi_t^{-1}\{\boldsymbol{x}\}$ and the location of $\boldsymbol{x}$ with respect to the caustic.

Consider the stochastic case in two dimensions with noise in a general direction where the phase function is given by

$$\begin{aligned}\mathcal{A}(\boldsymbol{x}_0, \boldsymbol{x}, t) = \frac{|\boldsymbol{x} - \boldsymbol{x}_0|^2}{2t} &- (x\cos\theta + y\sin\theta)\varepsilon W_t \\ &+ \frac{\varepsilon}{t}\left((x - x_0)\cos\theta + (y - y_0)\sin\theta\right)\int_0^t W_u \,\mathrm{d}u \\ &+ \frac{\varepsilon^2}{2t}\left(\int_0^t W_u \,\mathrm{d}u\right)^2 - \frac{\varepsilon^2}{2}\int_0^t W_u^2 \,\mathrm{d}u + S_0(\boldsymbol{x}_0) ,\end{aligned}$$

where $\boldsymbol{x}_0 = (x_0, y_0) \in \mathbb{R}^2$, $S_0(\boldsymbol{x}_0) \in C^2$ and θ is fixed. To obtain the corresponding results for the deterministic case one needs simply set $\varepsilon \equiv 0$. Choosing to work in a coordinate system (ξ, η) where

$$\begin{pmatrix}\xi \\ \eta\end{pmatrix} = \begin{pmatrix}\cos\theta & \sin\theta \\ -\sin\theta & \cos\theta\end{pmatrix}\begin{pmatrix}x \\ y\end{pmatrix} ,$$

reduces the phase function to

$$\begin{aligned}\tilde{\mathcal{A}}(\boldsymbol{\xi}_0, \boldsymbol{\xi}, t) = \frac{|\boldsymbol{\xi} - \boldsymbol{\xi}_0|^2}{2t} - \varepsilon\xi W_t + \frac{\varepsilon}{t}(\xi - \xi_0)\int_0^t W_u \,\mathrm{d}u + \frac{\varepsilon^2}{2t}\left(\int_0^t W_u \,\mathrm{d}u\right)^2 \\ - \frac{\varepsilon^2}{2}\int_0^t W_u^2 \,\mathrm{d}u + \tilde{S}_0(\boldsymbol{\xi}_0) ,\end{aligned}$$

where

$$\begin{aligned}\tilde{S}_0(\boldsymbol{\xi}_0) = \tilde{S}_0(\xi_0, \eta_0) &= S_0(x_0(\xi_0, \eta_0), y_0(\xi_0, \eta_0)) \\ &= S_0(\xi_0\cos\theta - \eta_0\sin\theta, \eta_0\cos\theta + \xi_0\sin\theta) .\end{aligned}$$

Recall from Chapter 3 that in the chosen coordinate system the pre-caustic equation is given by

$$\left(1 + t\frac{\partial^2\tilde{S}_0}{\partial\xi_0^2}(\boldsymbol{\xi}_0)\right)\left(1 + t\frac{\partial^2\tilde{S}_0}{\partial\eta_0^2}(\boldsymbol{\xi}_0)\right) - t^2\left(\frac{\partial^2\tilde{S}_0}{\partial\xi_0\partial\eta_0}(\boldsymbol{\xi}_0)\right)^2 = 0 .$$

Lemma 4.2.1. *Consider a fixed point $\boldsymbol{\xi} = (\xi, \eta)$ and define*

$$\zeta(\xi_0) := \xi_0 - \xi + t\frac{\partial\tilde{S}_0}{\partial\xi_0}(\xi_0, \eta_0(\eta, \xi_0)) - \varepsilon\int_0^t W_u \,\mathrm{d}u . \tag{4.2.1}$$

Assuming that $1+t\frac{\partial^2\tilde{S}_0}{\partial\eta_0^2}(\boldsymbol{\xi}_0)\neq 0$ *we may solve* $\eta=\eta_0+t\frac{\partial\tilde{S}_0}{\partial\eta_0}$ *to obtain a unique* $\eta_0(\eta,\xi_0)$ *and the values of* $\Phi_t^{-1}\{\boldsymbol{\xi}\}$ *are given by*

$$\left(\xi_0^i(\boldsymbol{\xi},\omega,t),\eta_0(\eta,\xi_0^i(\gamma,\omega,t))\right)\ ,$$

for $i=1,2,\ldots,n$ *where* $\xi_0^i(\boldsymbol{\xi},\omega,t)$ *are the solutions of* $\zeta(\xi_0)=0$.

Proof. The flow mapping Φ_t is determined by $\nabla\tilde{A}(\boldsymbol{\xi}_0,\boldsymbol{\xi},t)=0$, namely

$$\frac{\partial\tilde{A}}{\partial\xi_0}\boldsymbol{e}_{\xi_0}+\frac{\partial\tilde{A}}{\partial\eta_0}\boldsymbol{e}_{\eta_0}=0\ .$$

Thus we obtain

$$\begin{pmatrix}\xi\\ \eta\end{pmatrix}=\begin{pmatrix}\xi_0\\ \eta_0\end{pmatrix}+t\begin{pmatrix}\frac{\partial\tilde{S}_0}{\partial\xi_0}\\ \frac{\partial\tilde{S}_0}{\partial\eta_0}\end{pmatrix}-\varepsilon\begin{pmatrix}\int_0^t W_u\,\mathrm{d}u\\ 0\end{pmatrix}\ ,$$

so that assuming $\frac{\partial\eta}{\partial\eta_0}\neq 0$ we may invert the η-coordinate map to obtain $\eta_0(\eta,\xi_0)$. Substituting into the expression for ξ yields

$$\xi=\xi_0+t\frac{\partial\tilde{S}_0}{\partial\xi_0}(\xi_0,\eta_0(\eta,\xi_0))-\varepsilon\int_0^t W_u\,\mathrm{d}u\ ,$$

so that if $\boldsymbol{\xi}$ is fixed then the solutions $\xi_0^i(\boldsymbol{\xi},\omega,t)$ of the above will yield the values of $\Phi_t^{-1}\{\boldsymbol{\xi}\}$. □

Remark 4.2.1.

i). $\eta_0(\eta,\xi_0)$ is a purely deterministic function, a fact which will be of crucial importance shortly.

ii). The condition $1+t\frac{\partial^2\tilde{S}_0}{\partial\eta^2}\neq 0$ may be written in terms of S_0 as

$$1+t\left[\sin^2\theta\frac{\partial^2 S_0}{\partial x_0^2}-2\cos\theta\sin\theta\frac{\partial^2 S_0}{\partial x_0\partial y_0}+\cos^2\theta\frac{\partial^2 S_0}{\partial y_0^2}\right]_{(x_0,y_0)=(x_0(\xi_0,\eta_0),y_0(\xi_0,\eta_0))}\neq 0\ .$$

Lemma 4.2.2. *Under the assumptions of Lemma 4.2.1 a fixed point* $\boldsymbol{\xi}=(\xi,\eta)$ *is on the caustic* C_t *if and only if* $\zeta(\xi_0)=0$ *has a repeated solution* $\xi_0^r(\boldsymbol{\xi},t)$.

Proof. In order to obtain the η-coordinate of the caustic in terms of ξ_0 we substitute $\eta_0(\eta,\xi_0)$ into the pre-caustic equation giving

$$\left(1+t\frac{\partial^2\tilde{S}_0}{\partial\xi_0^2}(\xi_0,\eta_0(\eta,\xi_0))\right)\left(1+t\frac{\partial^2\tilde{S}_0}{\partial\eta_0^2}(\xi_0,\eta_0(\eta,\xi_0))\right)-t^2\left(\frac{\partial^2\tilde{S}_0}{\partial\xi_0\partial\eta_0}(\xi_0,\eta_0(\eta,\xi_0))\right)^2=0\ . \tag{4.2.2}$$

However differentiating $\eta=\eta_0(\eta,\xi_0)+t\frac{\partial\tilde{S}_0}{\partial\eta_0}(\xi_0,\eta_0(\eta,\xi_0))$ with respect to ξ_0 yields

$$-t\frac{\partial^2\tilde{S}_0}{\partial\xi_0\partial\eta_0}(\xi_0,\eta_0(\eta,\xi_0))=\frac{\partial\eta_0}{\partial\xi_0}(\eta,\xi_0)\left(1+t\frac{\partial^2\tilde{S}_0}{\partial\eta_0^2}(\xi_0,\eta_0(\eta,\xi_0))\right)\ , \tag{4.2.3}$$

which may be substituted into Equation (4.2.2) to give

$$\left(1+t\frac{\partial^2\tilde{S}_0}{\partial\xi_0^2}(\xi_0,\eta_0(\eta,\xi_0))\right)\left(1+t\frac{\partial^2\tilde{S}_0}{\partial\eta_0^2}(\xi_0,\eta_0(\eta,\xi_0))\right) \\ +t\frac{\partial\eta_0}{\partial\xi_0}(\eta,\xi_0)\left(1+t\frac{\partial^2\tilde{S}_0}{\partial\eta_0^2}(\xi_0,\eta_0(\eta,\xi_0))\right)\frac{\partial^2\tilde{S}_0}{\partial\xi_0\partial\eta_0}(\xi_0,\eta_0(\eta,\xi_0))=0\ .$$

Since by assumption $1+t\frac{\partial^2\tilde{S}_0}{\partial\eta_0^2}\neq 0$ the η coordinate of the caustic must satisfy

$$\left(1+t\frac{\partial^2\tilde{S}_0}{\partial\xi_0^2}(\xi_0,\eta_0(\eta,\xi_0))\right)+t\frac{\partial\eta_0}{\partial\xi_0}(\eta,\xi_0)\frac{\partial^2\tilde{S}_0}{\partial\xi_0\partial\eta_0}(\xi_0,\eta_0(\eta,\xi_0))=0\ . \tag{4.2.4}$$

But this is simply the equation $\zeta'(\xi_0)=0$. Thus if there exist $\xi_0^r(\boldsymbol{\xi},t)$ such that $\zeta(\xi_0^r(\boldsymbol{\xi},t))=\zeta'(\xi_0^r(\boldsymbol{\xi},t)=0$ then $\boldsymbol{\xi}\in C_t$. Alternatively if $\xi_0^i(\boldsymbol{\xi},\omega,t)$ are the solutions of $\zeta(\xi_0)=0$ but $\zeta'(\xi_0^i(\boldsymbol{\xi},\omega,t))\neq 0$ for all $i=1,2,\ldots,n$ then Equation (4.2.4) is not satisfied and so $\boldsymbol{\xi}\notin C_t$. □

Corollary 4.2.3. *If $\zeta(\xi_0^r(\boldsymbol{\xi},t))=\zeta'(\xi_0^r(\boldsymbol{\xi},t))=\zeta''(\xi_0^r(\boldsymbol{\xi},t))=0$ then C_t will have a generalised cusp at $\boldsymbol{\xi}$.*

Proof. If C_t is described by $(\xi(\xi_0),\eta(\xi_0))$ then the above simply says $(\dot{\xi}(\xi_0),\dot{\eta}(\xi_0))=0$ which is the condition for a generalised cusp. □

Corollary 4.2.4. *As we cross C_t the cardinality of $\Phi_t^{-1}\{\boldsymbol{\xi}\}$ changes by a multiple of* 2.

Proof. This is an immediate consequence of the fact that for $\boldsymbol{\xi}\in C_t$ the equation $\zeta(\xi_0)=0$ has a repeated solution. □

Let us see how this analysis works in practice for the deterministic case ($\varepsilon\equiv 0$) in the examples of the cusp and polynomial swallowtail.

4.2.1 Cusp

Here we take initial condition $S_0(\boldsymbol{x_0})=\frac{1}{2}x_0^2y_0$ and consider a fixed point $\tilde{\boldsymbol{x}}=(\tilde{x},\tilde{y})$. Then Equation (4.2.1) yields

$$\zeta(x_0)=x_0+t\left(x_0\tilde{y}-\frac{t}{2}x_0^3\right)-\tilde{x}\ ,$$

so that

$$\zeta'(x_0)=1+t\tilde{y}-\frac{3t^2}{2}x_0^2\ .$$

Clearly $\zeta'(x_0)=0$ has the solutions

$$\beta=x_0=\pm\frac{1}{t}\left(\frac{2}{3}(1+t\tilde{y})\right)^{\frac{1}{2}}\ ,$$

and it follows immediately that if $\tilde{y} \leq -\frac{1}{t}$ then $\zeta(x_0) = 0$ has only one solution, so $\left|\Phi_t^{-1}\{\tilde{\boldsymbol{x}}\}\right| = 1$.

Alternatively if $\tilde{y} > -\frac{1}{t}$ then $\zeta(x_0)$ has two stationary points, at which

$$\zeta(\beta) = -\tilde{x} \pm \frac{2}{3t}\sqrt{\frac{2}{3}}\,(1+t\tilde{y})^{\frac{3}{2}} \ .$$

Thus it follows that $\zeta(x_0) = 0$ will have

i). three solutions if and only if

$$-\frac{2}{3t}\sqrt{\frac{2}{3}}\,(1+t\tilde{y})^{\frac{3}{2}} < \tilde{x} < \frac{2}{3t}\sqrt{\frac{2}{3}}\,(1+t\tilde{y})^{\frac{3}{2}} \ ,$$

ii). two solutions if and only if

$$\tilde{x} = \pm\frac{2}{3t}\sqrt{\frac{2}{3}}\,(1+t\tilde{y})^{\frac{3}{2}} \ ,$$

iii). one solution otherwise.

This is summarised in Proposition 4.2.5 below and illustrated in Figure 4.1.

Proposition 4.2.5. *For the initial function $S_0(\boldsymbol{x}_0) = \frac{1}{2}x_0^2 y_0$ consider a fixed point $\tilde{\boldsymbol{x}} = (\tilde{x}, \tilde{y})$ on the image plane. The multiplicity of $\Phi_t^{-1}\{\tilde{\boldsymbol{x}}\}$ will be*

i). three if and only if $\tilde{\boldsymbol{x}}$ is inside the caustic,

ii). two if and only if $\tilde{\boldsymbol{x}}$ is on the caustic,

iii). one if and only if $\tilde{\boldsymbol{x}}$ is outside the caustic.

Remark 4.2.2. Along the caustic $\left|\Phi_t^{-1}(\tilde{\boldsymbol{x}})\right| = 2$ except at the cusp where $\left|\Phi_t^{-1}(\tilde{\boldsymbol{x}})\right| = 1$.

4.2.2 Polynomial Swallowtail

Let us now consider the more complicated example of the polynomial swallowtail with an arbitrary positive coefficient α. If $S_0(\boldsymbol{x}_0) = \alpha x_0^5 + x_0^2 y_0$ then for a fixed point $\tilde{\boldsymbol{x}} = (\tilde{x}, \tilde{y})$ we have

$$\zeta(x_0) = 5\alpha t x_0^4 - 2t^2 x_0^3 + x_0\,(1 + 2t\tilde{y}) - \tilde{x} \ , \tag{4.2.5}$$

so that

$$\zeta'(x_0) = 20\alpha t x_0^3 - 6t^2 x_0^2 + 1 + 2t\tilde{y} \ ,$$

and

$$\zeta''(x_0) = 60\alpha t x_0^2 - 12t^2 x_0 \ .$$

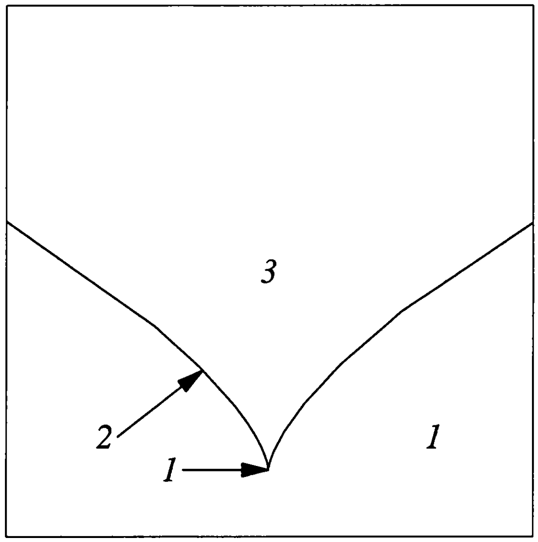

Figure 4.1: Multiplicity of Φ_t^{-1} for the cusp

Clearly the solutions of $\zeta''(x_0) = 0$ are $x_0 = 0$ and $x_0 = \frac{t}{5\alpha}$ so that $\zeta'(x_0)$ has a local maximum at $x_0 = 0$ and a local minimum at $x_0 = \frac{t}{5\alpha}$. The values of $\zeta'(x_0)$ at these points are

$$\zeta'(0) = 1 + 2t\tilde{y} \qquad \text{and} \qquad \zeta'(\frac{t}{5\alpha}) = -\frac{2t^4}{25\alpha^2} + 1 + 2t\tilde{y}\ .$$

This implies there are two cases that we need to consider:

Case 1 : If $\tilde{y} \leq \frac{-1}{2t}$ (below the lowest cusp) or $\tilde{y} \geq -\frac{1}{2t} + \frac{t^3}{25\alpha^2}$ (above the highest cusp) then $\zeta'(x_0) = 0$ has a single non-repeated solution β_1 and a repeated solution β_2 in the case of equality. Thus $\zeta(x_0)$ will look like Figure 4.2. Take $\tilde{x} = -\infty$ and consider moving

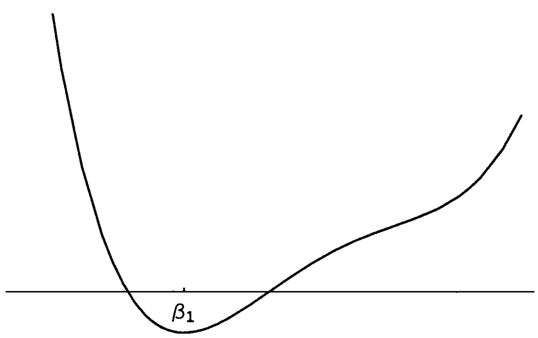

Figure 4.2: Shape of $\zeta(x_0)$ for case 1

horizontally to the right. The corresponding effect on Figure 4.2 is to begin with a graph contained wholly above $y = 0$ and proceed to move it vertically downwards. Initially $\zeta(x_0) = 0$ will have no real solutions so that to the left of the caustic $\Phi_t^{-1}(\tilde{\boldsymbol{x}}) = \phi$. When we hit the caustic $\zeta(x_0) = 0$ will have a single repeated solution $x_0 = \beta_1$ so that $\left|\Phi_t^{-1}(\tilde{\boldsymbol{x}})\right| = 1$. Finally to the right of the caustic $\zeta(x_0) = 0$ will have two distinct real solutions so that $\left|\Phi_t^{-1}(\tilde{\boldsymbol{x}})\right| = 2$.

Case 2 : If $-\frac{1}{2t} < \tilde{y} < -\frac{1}{2t} + \frac{t^3}{25\alpha^2}$ (we lie vertically between the cusps) then $\zeta'(x_0) = 0$ has three distinct solutions β_1, β_2 and β_3. Thus $\zeta(x_0)$ will look like Figure 4.3. Let us once

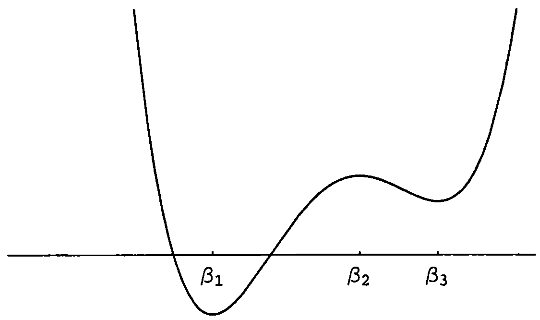

Figure 4.3: Shape of $\zeta(x_0)$ for case 2

again take $\tilde{x} = -\infty$ and consider moving horizontally to the right. Using the labelling scheme defined in Figure 4.4 we obtain the following. To the left of branch (A) the

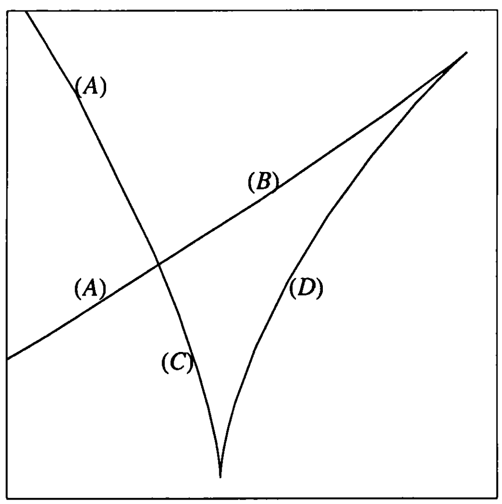

Figure 4.4: Labelling for caustic

equation $\zeta(x_0) = 0$ has no real solutions so that $\Phi_t^{-1}(\tilde{\boldsymbol{x}}) = \phi$. Assuming we reach branch (A) at a point other than the point of self intersection, $\zeta(x_0) = 0$ will have one repeated solution so that $\left|\Phi_t^{-1}(\tilde{\boldsymbol{x}})\right| = 1$. Between branches (A) and (B) or (A) and (C) we have $\left|\Phi_t^{-1}(\tilde{\boldsymbol{x}})\right| = 2$. On branches (B) or (C), $\left|\Phi_t^{-1}(\tilde{\boldsymbol{x}})\right| = 3$ away from the cusped points whilst at the cusped points $\left|\Phi_t^{-1}(\tilde{\boldsymbol{x}})\right| = 2$. In the caustic tail, i.e. between branches (B) and (D) or (C) and (D), we have $\left|\Phi_t^{-1}(\tilde{\boldsymbol{x}})\right| = 4$. Finally on branch (D), $\left|\Phi_t^{-1}(\tilde{\boldsymbol{x}})\right| = 3$, whilst to the right of the caustic $\left|\Phi_t^{-1}(\tilde{\boldsymbol{x}})\right| = 2$.

Note that if we reach branch (A) at the point of self intersection then $\zeta(x_0) = 0$ will have two repeated solutions so that $\left|\Phi_t^{-1}(\tilde{\boldsymbol{x}})\right| = 2$. Observe that as we move from left to right passing over the point of self intersection the multiplicity of $\Phi_t^{-1}(\tilde{\boldsymbol{x}})$ changes by $4 (= 2 \times 2)$.

Summarising the above cases yields the following proposition which is illustrated in Figure 4.5.

Proposition 4.2.6. *For the initial function* $S_0(\boldsymbol{x_0}) = \alpha x_0^5 + x_0^2 y_0$ *consider a fixed point* $\tilde{\boldsymbol{x}} = (\tilde{x}, \tilde{y})$ *on the image plane. The multiplicity of* $\Phi_t^{-1}\{\tilde{\boldsymbol{x}}\}$ *will be*

i). 4 if and only if $\tilde{\boldsymbol{x}}$ *lies inside the caustic tail,*

ii). 3 if and only if $\tilde{\boldsymbol{x}}$ *lies on the portion of the caustic prescribing the tail but not at a cusp or point of self intersection,*

iii). 2 if and only if $\tilde{\boldsymbol{x}}$ *lies outside the caustic or on the caustic at a cusp or point of self intersection,*

iv). 1 if and only if $\tilde{\boldsymbol{x}}$ *lies on the portion of the caustic not prescribing the tail,*

v). 0 if and only if $\tilde{\boldsymbol{x}}$ *is inside the caustic but not inside the tail.*

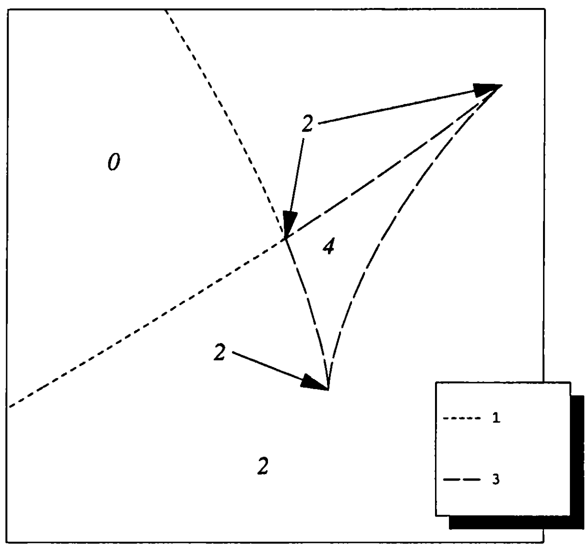

Figure 4.5: Multiplicity of Φ_t^{-1} for the polynomial swallowtail

4.3 Minimising Hamilton Function and the Wavefront

With $S_i(\boldsymbol{x}, t)$ defined by Equation (4.1.1), the zero level surface of Hamilton's principal function is given by

$$H_t = \{\boldsymbol{x} : S_i(\boldsymbol{x}, t) = 0, \text{ for some } i\} \ ,$$

where $i = 1, 2, \ldots, n$.

It is clear that the dominant term in Equation (4.1) comes from the minimising $\boldsymbol{x}_0^i(\boldsymbol{x}, t)$, thus we are concerned with

$$\mathcal{S}(\boldsymbol{x}, t) := \min_{i=1,2,\ldots,n} S_i(\boldsymbol{x}, t) \ .$$

Observe that the zero level set of the minimising Hamilton function,

$$\{\boldsymbol{x} : \mathcal{S}(\boldsymbol{x}, t) = 0\} \ , \tag{4.3.1}$$

will be part of H_t. Moreover $u^0(\boldsymbol{x}, t)$ switches smoothly from being exponentially large to exponentially small on $\mathcal{S}(\boldsymbol{x}, t) = 0$. The surface defined by Equation (4.3.1) is traditionally referred to as the wavefront. Note however that $u^0(\boldsymbol{x}, t)$ may also switch discontinuously from being exponentially large to exponentially small as we cross parts of the caustic. This will occur when the minimising S_i disappears.

4.3.1 Analysis of Discontinuity of $u^0(\boldsymbol{x}, t)$ for the Polynomial Swallowtail

In [15], Truman, Davies and Zhao were able to obtain a full description of the exponential discontinuity in u^0 for the cusp by first determining the number of negative S_i's in different regions of the superimposed caustic and zero level surface. Let us attempt a similar approach in the case of the polynomial swallowtail. To determine the number of negative S_i's in different regions we must:

- choose a point $\tilde{\boldsymbol{x}}$ in a particular region,
- solve $5\alpha t x_0^4 - 2t^2 x_0^3 + x_0(1 + 2t\tilde{y}) - \tilde{x} = 0$ to obtain $\boldsymbol{x}_0^i(\tilde{\boldsymbol{x}}, t)$ for $i = 1, 2, \ldots, n$,
- evaluate $Q(\tilde{\boldsymbol{x}}) := \#\{i : S_i(\tilde{\boldsymbol{x}}, t) < 0 \ , \ i = 1, 2, \ldots, n\}$.

To achieve the above we perform a numerical analysis using the *Mathematica* procedure outlined in Appendix B. Recalling from Chapter 2 that the topological nature of the zero level surface changes at $t = \alpha\frac{3^{\frac{5}{4}}}{2}$ we perform the analysis separately for $t < \alpha\frac{3^{\frac{5}{4}}}{2}$ and $t > \alpha\frac{3^{\frac{5}{4}}}{2}$. This yields the pictures in Figures 4.6 and 4.7.

In order to analyse Figures 4.6 and 4.7 we set up the labelling schemes shown in Figures 4.8 and 4.9 . Beginning with an analysis of $t < \frac{3^{\frac{5}{4}}}{2}$ we observe that only the top part (curve separating $A_1 \cup A_2$ and $B_1 \cup B_2$) and the lower branch (curve separating A_3 and B_3) of the zero level surface form part of the wavefront. The remainder of the picture is comprised of surfaces $\{\boldsymbol{x} : S_i(\boldsymbol{x}, t) = 0\}$ where S_i is not the minimum. Thus as we move from the region A_i to B_i $(i = 1, 2, 3)$ we see that u^μ smoothly switches from exponentially small to exponentially large.

In addition the portion of the line pair denoted by C corresponds to the minimising Hamilton function and hence forms part of the wavefront. As we move from A_1 to A_2, u^μ smoothly switches from exponentially small to $u^\mu \sim 1$ on C and then back to exponentially small. Similarly as we move from B_1 to B_2, u^μ smoothly switches from exponentially large to $u^\mu \sim 1$ on C and then back to exponentially large. Note that the remainder of the line pair comes from S_i which are not the minimum and hence does not contribute to the wavefront.

Let us now turn our attention to the behaviour of u as we cross the caustic C_t. As we move from D to A_3 we go from a region with four S_i's, two of which are negative, to a region with two S_i's, both of which are positive. Hence u^0 switches discontinuously from

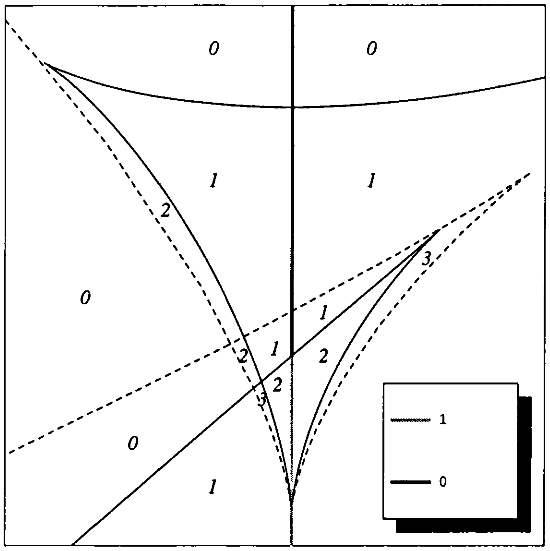

Figure 4.6: Number of negative S_i's for $t < \frac{3^{\frac{5}{4}}}{2}$.

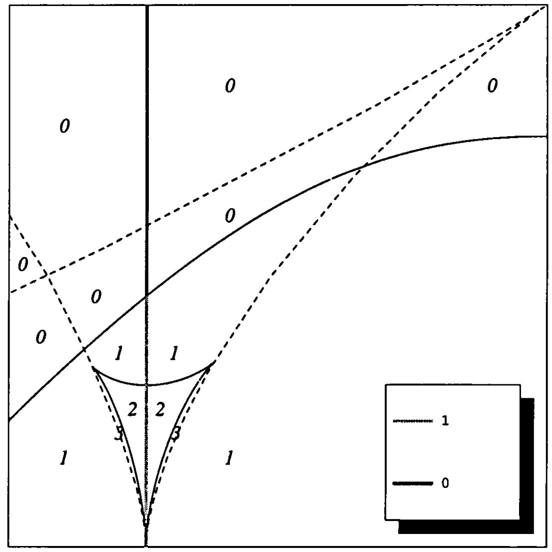

Figure 4.7: Number of negative S_i's for $t > \frac{3^{\frac{5}{4}}}{2}$.

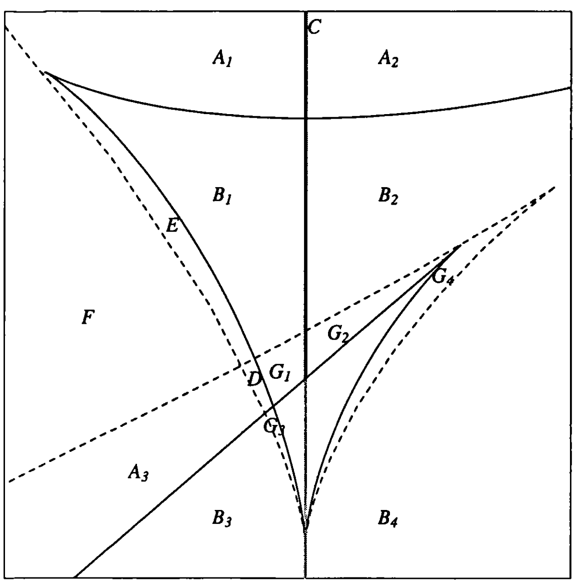

Figure 4.8: Labelling scheme for $t < \frac{3^{\frac{5}{4}}}{2}$.

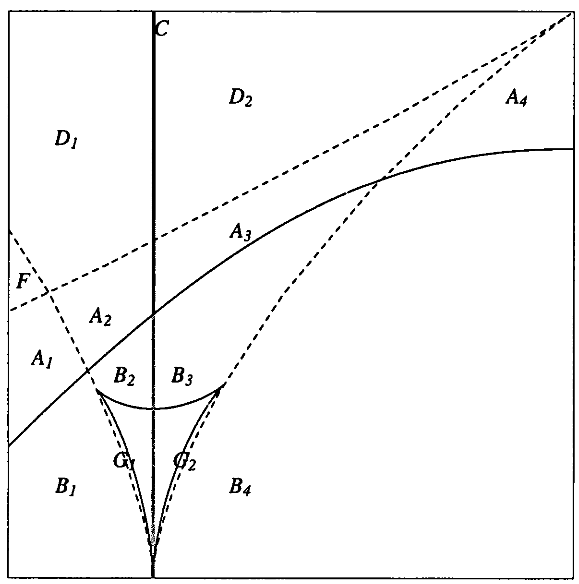

Figure 4.9: Labelling scheme for $t > \frac{3^{\frac{5}{4}}}{2}$.

exponentially large to exponentially small since the minimising S_i disappears. Note that this change cannot occur smoothly, for if we assume it does then the curve separating D and A_3 must be part of the zero level surface which is a contradiction.

Similarly as we pass from E or A_1 to F the minimising S_i disappears and so u^0 will be discontinuous along the portion of C_t between $E \cup A_1$ and F. A discussion of the behaviour of u^μ inside the region F may be found in Appendix C. This situation requires special attention since for $\tilde{\boldsymbol{x}} \in F$ we know $\nabla_{\boldsymbol{x}_0} \mathcal{A}(\boldsymbol{x}_0, \tilde{\boldsymbol{x}}, t) \neq 0$ for all $\boldsymbol{x}_0 \in \mathbb{R}$. Hence in F there is no minimising $\boldsymbol{x}_0(\tilde{\boldsymbol{x}}, t)$.

Finally we see that passing from G_i to B_i $(i = 1, 2)$ doesn't produce any interesting behaviour in u^0 since the minimising S_i carries over. However the behaviour as we pass from G_3 to B_3 or G_4 to B_4 cannot yet be determined. This difficulty will be rectified by a study of the hot and cool parts of the caustic.

A similar analysis may be performed for $t > \frac{3^{\frac{5}{4}}}{2}$, namely Figure 4.7. The main points here are that the tricorn does not form part of the wavefront but the arc separating $\bigcup_{i=1}^{4} A_i$ and $\bigcup_{i=1}^{4} B_i$ does. This is effectively brought about by the merging of the two parts of the wavefront in Figure 4.6.

In addition we observe that as we move from B_2 to B_1 or B_3 to B_4, the minimising S_i survives so that there is no discontinuity in u^0. However on crossing the remaining parts of the caustic tail the situation is not yet clear.

4.4 Hot and Cool Parts of the Caustic

If $\boldsymbol{x} \in \mathbb{R}^2$ and the initial function S_0 is smooth then it is possible to designate parts of the caustic as hot or cool. We now explain what is meant by a hot or cool part and moreover show how parts of the caustic are designated as such.

Consider a level surface $S_i(\boldsymbol{x}, t) = c$ which has a cusped point of intersection with the caustic at γ. Recall that the condition for $\{\boldsymbol{x} : S_i(\boldsymbol{x}, t) = c\}$ to have a cusp at γ is $\nabla S_i(\gamma, t) = 0$. Hence if the part of the level surface cusped at γ corresponds to the minimising $\tilde{\boldsymbol{x}}_0(\gamma, t)$ then the Burger's velocity field

$$v^0(\boldsymbol{x}, t) = \nabla S(\boldsymbol{x}, t) \to \nabla S_i(\gamma, t) = 0 \ ,$$

as $x \to \gamma$ from the cusped side of the caustic. We denote such points γ as *cool* since the Burger's fluid has zero velocity on one side of the caustic. Any points not satisfying the cool condition are classified as hot. It is important to note that we are only designating parts of one side of the caustic as hot or cool.

Recalling our discussion in the previous section we see that $u^0(\boldsymbol{x}, t)$ will be exponentially discontinuous as we cross cool parts of the caustic. This occurs because two $\boldsymbol{x}_0(\boldsymbol{x}, t)$'s are coalescing as the minimiser at the cusp and then disappearing. Hence the minimising surface on the cusped side of the caustic cannot be continued across the caustic causing an exponential discontinuity in $u^0(\boldsymbol{x}, t)$.

4.4.1 Hot and Cool Parts of the Polynomial Swallowtail

As we have just indicated, knowing how the number of S_i's, in particular the number of negative S_i's, changes as we cross the caustic is all important in determining the nature of parts of the caustic. Let us consider the different combinations which may occur as we cross C_t in the case of the polynomial swallowtail. The numbers in brackets represent the number of negative S_i's.

(i).

Prior to crossing C_t	4 (2)	4 (1)
After crossing C_t	2 (2)	2 (1)

Here the two cusped level surfaces coalescing corresponding to positive S_i's. However this is clearly not the minimum S_i since there are negative S_i present. Thus the side of C_t that we have approached is designated as hot.

(ii).

Prior to crossing C_t	2 (2)	2 (0)
After crossing C_t	0 (0)	0 (0)

Here the two cusped level surfaces coalescing correspond to the only S_i present. Hence the cusped level surface must correspond to the minimising $\boldsymbol{x}_0(\alpha, t)$, and so the side we are approaching is designated as cool.

(iii).

Prior to crossing C_t	4 (3)	4 (0)
After crossing C_t	2 (1)	2 (0)

In this situation there is no reason a priori why the minimiser should correspond to one of the coalescing surfaces. Thus we are as yet unable to determine whether such parts of the caustic are designated as hot or cool.

Observe that the method described in [15] by Truman, Davies and Zhao is sufficient to prove that the whole of the polynomial swallowtail is not cool. However it does not provide us with a full characterisation of the caustic as it did for the cusp example.

Let us illustrate some of the cases above for $t < \alpha\frac{3^{\frac{5}{4}}}{2}$ by choosing a point γ close to the caustic and looking at all the level surfaces passing through it. The behaviour of these level surfaces, especially the minimum, should re-enforce our comments about the caustic being hot or cool.

Using the labelling scheme from Figure 4.8 we proceed as follows. In Figure 4.10 we have chosen a point $\gamma \in A_1$ which lies close to the caustic. We know that there will be two level surfaces $S_i(\boldsymbol{x}, t) = c_i$ $(i = 1, 2)$ where $c_i = S_i(\gamma, t)$ passing though the point γ. The level surface corresponding to the minimiser is identified by the use of a lightly shaded curve.

It is clear that as γ tends to C_t the cusped level surfaces will coalesce. Moreover this cusped part of the level surface will correspond to the minimiser $\tilde{x}_0(\gamma, t)$. Hence we designate one side of this part of the caustic as cool. The above is an example of Case (ii).

In Figures 4.11 and 4.12 we have chosen a point $\gamma \in G_1$. Clearly as γ moves upwards towards C_t the cusped level surfaces in Figure 4.11 will coalesce, but this does not make the caustic cool since the cusped part of the level surface doesn't correspond to the minimiser $\tilde{x}_0(\gamma, t)$. The behaviour of the level surface corresponding to the minimiser is shown by the lightly shaded curve in Figure 4.12 and is not cusped at γ in the limit. Thus we designate one side of this part of the caustic as hot. This is an example of Case (i).

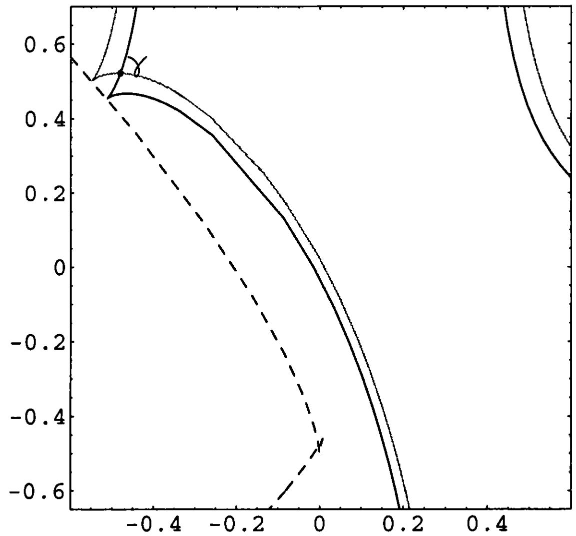

Figure 4.10: Level surfaces passing through $\gamma \in A_1$.

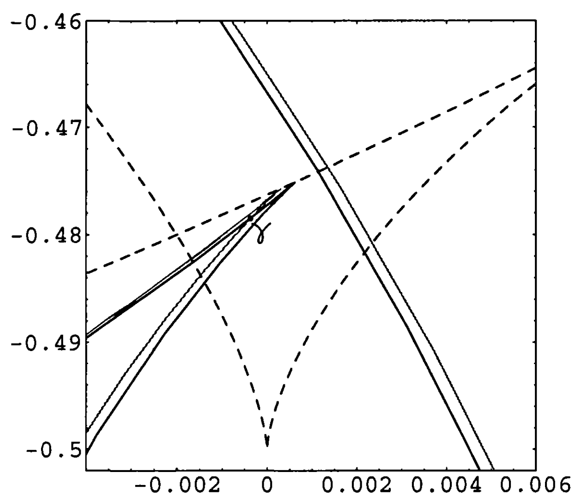

Figure 4.11: Level surfaces passing through $\gamma \in G_1$ (1).

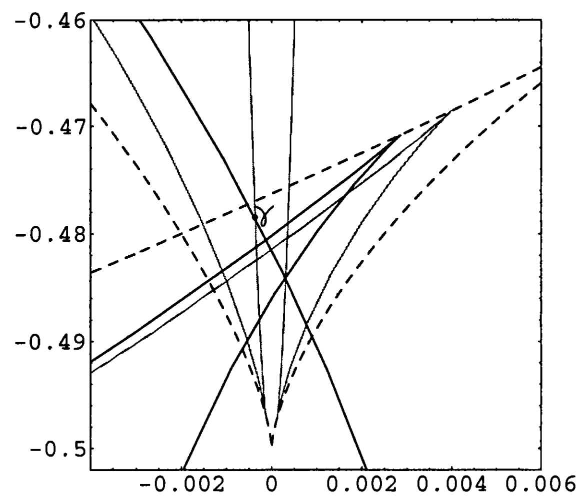

Figure 4.12: Level surfaces passing through $\gamma \in G_1$ (2).

Finally to illustrate case (iii) we choose a point $\gamma \in G_4$. We know that there are four level surfaces passing through γ, three of which correspond to negative $S_i(\gamma, t)$ whilst the remainder corresponds to a positive $S_i(\gamma, t)$. These level surfaces are shown in Figures 4.13 and 4.14. In Figure 4.13 we have plotted the two level surfaces corresponding to

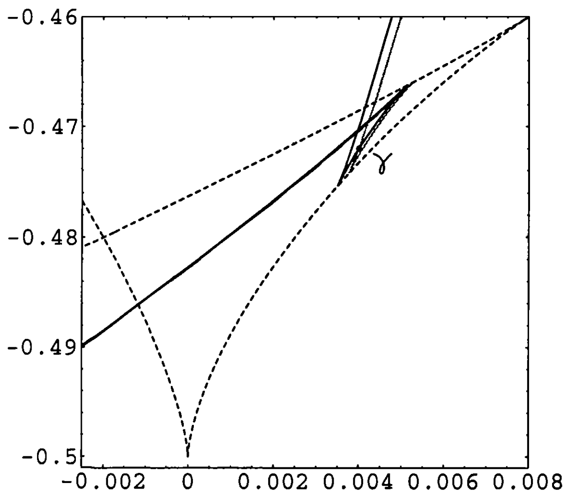

Figure 4.13: Level surfaces passing through $\gamma \in G_4$ (1).

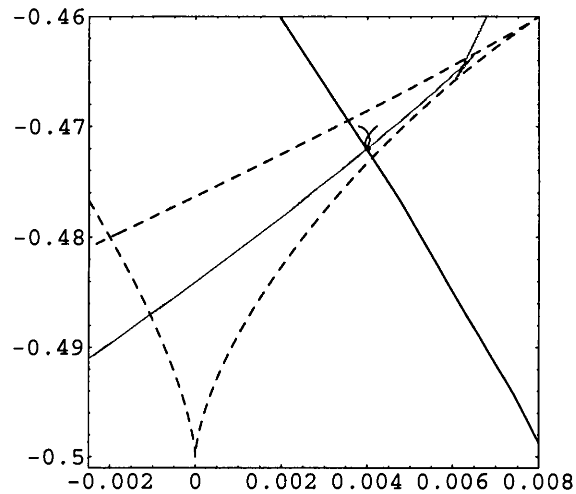

Figure 4.14: Level surfaces passing through $\gamma \in G_4$ (2).

negative $S_i(\gamma, t)$ which have not come from the minimiser $\tilde{\boldsymbol{x}}_0(\gamma, t)$. Clearly as $\gamma \to C_t$ the cusped level surfaces coalesce, but this does not make the caustic cool since the cusped part of the level surface doesn't correspond to the minimiser $\tilde{\boldsymbol{x}}_0(\gamma, t)$. To see what happens to the level surface corresponding to $\tilde{\boldsymbol{x}}_0(\gamma, t)$, we must look to Figure 4.15. Here the level surface corresponding to the minimiser is represented by the light curve and the other represents the positive $S_i(\gamma, t)$. Comparing Figure 4.14 with Figure 4.15 we see that the level surface corresponding to $\tilde{\boldsymbol{x}}_0(\gamma, t)$ continues as γ crosses over C_t passing from G_4 to B_4. Hence we designate one side of this part of the caustic as hot.

Remark 4.4.1. Note that the preceding discussion has not resolved our concerns regarding Case (iii). Although we have shown an example of a point satisfying Case (iii) that is hot we may not conclude that all points of C_t satisfying Case (iii) are hot. We reiterate that the method of analysing the number of negative S_i's has shown that not all of the polynomial swallowtail is cool. However in order to characterise the polynomial swallowtail completely an alternative approach is required.

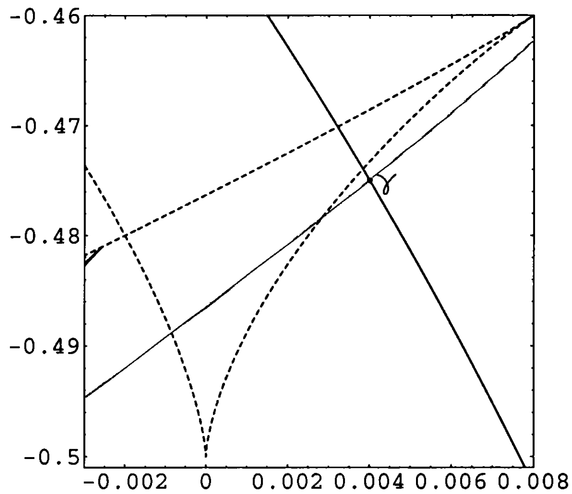

Figure 4.15: Level Surfaces passing through $\gamma \in B_4$.

4.5 A New Approach for Determining Hot and Cool Parts

We prove our main result for the case of one dimensional noise in a fixed general direction. Our main result depends heavily on the following lemma.

Lemma 4.5.1. *If $\gamma = (\xi_\gamma, \eta_\gamma)$ is a fixed point, the assumptions of Lemma 4.2.1 hold and*

$$F(\xi_0) := \frac{(\xi_\gamma - \xi_0)^2}{2t} + \frac{t}{2}\left(\frac{\partial \tilde{S}_0}{\partial \eta_0}(\xi_0, \eta_0(\eta_\gamma, \xi_0))\right)^2 - \frac{\xi_0 \varepsilon}{t}\int_0^t W_u \, \mathrm{d}u + \tilde{S}_0(\xi_0, \eta_0(\eta_\gamma, \xi_0)) \ ,$$

then $S_i(\gamma, t) = F(\xi_0^i(\gamma, t)) + Y_t(\xi_\gamma)$ for $i = 1, 2, \ldots, n$ where $\xi_0^i(\gamma, t)$ are the solutions of $F'(\xi_0) = 0$ and

$$Y_t(\xi_\gamma) := -\xi_\gamma \varepsilon W_t + \frac{\xi_\gamma \varepsilon}{t}\int_0^t W_u \, \mathrm{d}u + \frac{\varepsilon^2}{2t}\left(\int_0^t W_u \, \mathrm{d}u\right)^2 - \frac{\varepsilon^2}{2}\int_0^t W_u^2 \, \mathrm{d}u \ .$$

Proof. Consider a fixed point $\gamma = (x_\gamma, y_\gamma)$ on the image plane. If

$$\Phi_t^{-1}\{\gamma\} = \left\{\boldsymbol{\xi}_0^i(\gamma, t)\right\}_{i=1}^n = \left\{(\xi_0^i(\gamma, t), \eta_0(\eta_\gamma, \xi_0^i(\gamma, t))\right\}_{i=1}^n \ ,$$

then by definition

$$S_i(\gamma, t) = \mathcal{A}(\boldsymbol{\xi}_0^i(\gamma, t), \gamma, t) = \mathcal{A}(\xi_0^i(\gamma, t), \eta_0(\eta_\gamma, \xi_0^i(\gamma, t)), \gamma, t) \ .$$

Omitting variables for brevity we observe that

$$F'(\xi_0) = \frac{\xi_0 - \xi_\gamma}{t} + t\frac{\partial \tilde{S}_0}{\partial \eta_0}\left(\frac{\partial^2 \tilde{S}_0}{\partial \xi_0 \partial \eta_0} + \frac{\partial^2 \tilde{S}_0}{\partial \eta_0^2}\frac{\partial \eta_0}{\partial \xi_0}\right) - \frac{\varepsilon}{t}\int_0^t W_u \, du + \frac{\partial \tilde{S}_0}{\partial \xi_0} + \frac{\partial \tilde{S}_0}{\partial \eta_0}\frac{\partial \eta_0}{\partial \xi_0}$$

$$= \frac{\xi_0}{t} - \frac{\xi_\gamma}{t} - \frac{\varepsilon}{t}\int_0^t W_u \, du + \frac{\partial \tilde{S}_0}{\partial \xi_0} \quad \text{using Equation (4.2.3),}$$
$$= t^{-1}\zeta(\xi_0) \ ,$$

and so from Lemma 4.2.1 the values of $\Phi_t^{-1}\{\gamma\}$ are determined by the solutions of $F'(\xi_0) = 0$. Since $\mathcal{A}(\xi_0, \eta_0(\eta_\gamma, \xi_0), \gamma, t) = F(\xi_0) + Y_t(\xi_\gamma)$ it follows immediately that

$$S_i(\gamma, t) = F(\xi_0^i(\gamma, t)) + Y_t(\xi_\gamma) \ ,$$

where $\xi_0^i(\gamma, t)$ are solutions of $F'(\xi_0) = 0$. □

In light of Lemma 4.5.1 it is evident from Corollary 4.2.4 that as we cross C_t the number of stationary points of $F(\xi_0)$ decreases by a multiple of two. Moreover Lemma 4.2.2 shows that on C_t there will exist point(s) $\xi_0^r(\boldsymbol{\xi}, t)$ which are points of inflection of $F(x_0)$. In effect as we travel from inside to outwith C_t at least one maxima and minima pair merge to form a point of inflection on C_t which disappears as we pass to the outside.

Let γ be a point close to C_t and $\xi_0^M(\gamma, t)$ and $\xi_0^m(\gamma, t)$ be the coalescing maxima and minima respectively. Thus as $\gamma \to C_t$ the level surfaces

$$S_M(\boldsymbol{x}, t) = F(\xi_0^M(\gamma, t)) + Y_t(\xi_\gamma) \ ,$$

and

$$S_m(\boldsymbol{x}, t) = F(\xi_0^m(\gamma, t)) + Y_t(\xi_\gamma) \ ,$$

will coalesce. Moreover since these level surfaces cannot continue over C_t the coalesced level surface must be cusped on the caustic.

Theorem 4.5.2. *Let $\tilde{S}_0(\boldsymbol{\xi}_0) \in C^2$, $\boldsymbol{\xi}_0 = (\xi_0, \eta_0) \in \mathbb{R}^2$ and assume $1 + t\frac{\partial^2 \tilde{S}_0}{\partial \eta_0^2}(\boldsymbol{\xi}_0) \neq 0$ so that $\eta = \eta_0 + t\frac{\partial \tilde{S}_0}{\partial \eta_0}(\boldsymbol{\xi}_0)$ may be solved to obtain $\eta_0(\eta, \xi_0)$. Consider crossing C_t at a non-self intersection point $\gamma = (\xi_\gamma, \eta_\gamma)$ travelling in the direction of decreasing $S_i(\boldsymbol{\xi}, t)$. If*

$$F(\xi_0) := \frac{(\xi_\gamma - \xi_0)^2}{2t} + \frac{t}{2}\left(\frac{\partial \tilde{S}_0}{\partial \eta_0}(\xi_0, \eta_0(\eta_\gamma, \xi_0))\right)^2 - \frac{\xi_0 \varepsilon}{t}\int_0^t W_u \, du + \tilde{S}_0(\xi_0, \eta_0(\eta_\gamma, \xi_0)) \ ,$$

then there will exist a repeated solution $\xi_0^r(\gamma, t)$ of $F'(\xi_0) = 0$. One side of C_t will be cool at γ if and only if

$$F(\xi_0^r(\gamma, t)) \leq \min_{\substack{i=1,2,\ldots,n \\ i \neq r}} F(\xi_0^i(\gamma, t)) \ , \tag{4.5.1}$$

where $\xi_0^i(\gamma, t)$ are the solutions of $F'(\xi_0) = 0$. Moreover the boundary of the cool part of the caustic is given by

$$F(\xi_0^r(\gamma, t)) = \min_{\substack{i=1,2,\ldots,n \\ i \neq r}} F(\xi_0^i(\gamma, t)) \ . \tag{4.5.2}$$

Proof. From Lemma 4.2.2 we know that if $\gamma \in C_t$ then there exists $\xi_0^r(\gamma,t)$ such that $F'(\xi_0^r(\gamma,t)) = F''(\xi_0^r(\gamma,t)) = 0$. From the preceding discussion this point of inflection comes from a maxima and minima pair merging which then disappears off C_t. Thus at γ there will be a coalesced cusped level surface on the caustic. If Equation (4.5.1) is satisfied then the cusped level surface corresponds to the minimising $\xi_0^i(\boldsymbol{\xi},t)$ making C_t cool at γ. When the condition in Equation (4.5.2) is satisfied the value of $F(\xi_0^r(\gamma,t))$ is equal to the value of F at a non-degenerate critical point. Hence we are on the boundary of two regions: one where $F(\xi_0^r(\gamma,t))$ is the minimum stationary value (a cool part of C_t) and the other where a non-degenerate critical point produces the minimum stationary value of F (a hot part of C_t). Thus we are on the boundary of the cool part of C_t. □

Remark 4.5.1. $F(\xi_0)$ will have more than one point of inflection if γ is at a point of self intersection of the caustic. If these occur at $\xi_0^{r_k}(\gamma,t)$ for $k=1,2,\ldots,m$ where $m \le n$ then in this case conditions (4.5.1) becomes

$$\min_{k=1,2,\ldots,m} F(\xi_0^{r_k}(\gamma,t)) \le \min_{\substack{i=1,2,\ldots,n \\ i\neq r_k}} F(\xi_0^i(\gamma,t)) \ .$$

Moreover if the point of self intersection γ is cool then it may be a boundary of the cool part in the following sense. If on one of the branches emanating from γ the minimum of the inflection points splits into a local maximum and minimum at neighbouring points $\gamma+\delta \in C_t$ then these points will be hot. An example of this may be found in our study of the polynomial swallowtail which follows shortly.

Corollary 4.5.3. *$u^0(\boldsymbol{\xi},t)$ is smooth across hot parts of the caustic but switches discontinuously across cool parts.*

Proof. As we cross over C_t the point of inflection disappears. If we are crossing a cool part of C_t this means the minimiser $\xi_0^i(\boldsymbol{\xi},t)$ must disappear and so will switch discontinuously to another one. Thus $u(\boldsymbol{\xi},t)$ will switch discontinuously across cool parts of the caustic. If we are crossing a hot part of the caustic the disappearance of the inflection point has no effect on the minimiser and so $u^0(\boldsymbol{\xi},t)$ is smooth across such parts. □

Corollary 4.5.4. *Under noise parallel to the ξ-axis the hot and cool parts of C_t are the same as in the deterministic case subject to a displacement $\varepsilon\int_0^t W_u\,du$ in the ξ direction. This shows that the hot and cool parts are displaced bodily with the caustic.*

Proof. In order to distinguish between the stochastic and deterministic situation we use superscript ε and 0 respectively. All important in the following is the fact that $\eta_0(\eta_\gamma,\xi_0)$ is a deterministic function.

Writing $\xi^\varepsilon = \Phi_t^\varepsilon(\xi_0)$ and $\xi^0 = \Phi_t^0(\xi_0)$ so that $\xi^\varepsilon = \xi^0 - \varepsilon\int_0^t W_u\,du$ we consider a point $\gamma^0 = (\xi_\gamma^0,\eta_\gamma)$ on the caustic and the corresponding point $\gamma^\varepsilon = (\xi_\gamma^\varepsilon,\eta_\gamma)$ on the random caustic. Clearly

$$\begin{aligned}\frac{\partial^2 F^\varepsilon}{\partial \xi_0^2}(\xi_0) &= \frac{1}{t} + \frac{\partial^2 \tilde{S}_0}{\partial \xi_0^2}(\xi_0,\eta_0(\eta_\gamma,\xi_0)) + \frac{\partial^2 \tilde{S}_0}{\partial\eta_0\partial\xi_0}(\xi_0,\eta_0(\eta_\gamma,\xi_0))\,\frac{\partial\eta_0}{\partial\xi_0}(\eta_\gamma,\xi_0)\\ &= \frac{\partial^2 F^0}{\partial\xi_0^2}(\xi_0)\ ,\end{aligned}$$

but moreover

$$\left.\frac{\partial F^\varepsilon}{\partial \xi_0}(\xi_0)\right|_{\xi_\gamma=\xi_\gamma^\varepsilon} = \left.\frac{\partial F^\varepsilon}{\partial \xi_0}(\xi_0)\right|_{\xi_\gamma=\xi_\gamma^0-\varepsilon\int_0^t W_u\,\mathrm{d}u} = \left.\frac{\partial F^0}{\partial \xi_0}(\xi_0)\right|_{\xi_\gamma=\xi_\gamma^0}.$$

Hence $\xi_0^{i,\varepsilon}(\gamma^\varepsilon,t)=\xi_0^{i,0}(\gamma^0,t)$ for $i=1,2,\dots,n$ and in particular the repeated solutions $\xi_0^{r,\varepsilon}(\gamma^\varepsilon,t)$ and $\xi_0^{r,0}(\gamma^0,t)$ are equal. Thus

$$\begin{aligned} S_i^\varepsilon(\gamma^\varepsilon,t) &= F^\varepsilon(\xi_0^{i,\varepsilon}(\gamma^\varepsilon,t))\big|_{\xi_\gamma=\xi_\gamma^\varepsilon}+Y_t(\xi_\gamma^\varepsilon)\\ &= F^\varepsilon(\xi_0^{i,0}(\gamma^0,t))\big|_{\xi_\gamma=\xi_\gamma^\varepsilon}+Y_t(\xi_\gamma^\varepsilon)\\ &= F^\varepsilon(\xi_0^{i,0}(\gamma^0,t))\big|_{\xi_\gamma=\xi_\gamma^0-\varepsilon\int_0^t W_u\,\mathrm{d}u}+Y_t(\xi_\gamma^\varepsilon)\\ &= F^0(\xi_0^{i,0}(\gamma^0,t))\big|_{\xi_\gamma=\xi_\gamma^0}+\frac{\varepsilon^2}{2t}\left(\int_0^t W_u\,\mathrm{d}u\right)^2+\frac{\varepsilon\xi_\gamma^0}{t}\int_0^t W_u\,\mathrm{d}u+Y_t(\xi_\gamma^\varepsilon)\\ &= S_i^0(\gamma^0,t)+\tilde{Y}_t\,, \end{aligned}$$

where $\tilde{Y}_t := \frac{\varepsilon^2}{2t}\left(\int_0^t W_u\,\mathrm{d}u\right)^2+\frac{\varepsilon\xi_\gamma^0}{t}\int_0^t W_u\,\mathrm{d}u+Y_t$. Thus if $\xi_0^{r,0}(\gamma^0,t)$ minimises $S_i^0(\gamma^0,t)$ then it will also minimise $S_i^\varepsilon(\gamma^\varepsilon,t)$ because $\tilde{Y}_t$ does not depend on $\xi_0^{r,0}(\gamma^0,t)$.

□

Remark 4.5.2. In our original coordinate system the caustic (and hence the hot and cool parts) are displaced by $\varepsilon(\cos\theta,\sin\theta)\int_0^t W_u\,\mathrm{d}u$.

The benefit of Corollary 4.5.4 is that we need only consider the nature of hot and cool parts in the deterministic case and then simply displace everything by $\varepsilon\int_0^t W_u\,\mathrm{d}u$.

4.6 Examples

4.6.1 The Cusp

For the cusp example in the deterministic case we have

$$F(x_0) = -\frac{t}{8}x_0^4+\frac{x_0^2}{2t}(1+ty_\gamma)-\frac{x_0x_\gamma}{t}+\frac{x_\gamma^2}{2t}\,,$$

and

$$F'(x_0) = -\frac{t^2}{2}x_0^3+x_0(1+ty_\gamma)-x_\gamma\,,$$

Since $\gamma=(x_\gamma,y_\gamma)\in C_t$ we know $F'(x_0)=0$ has two solutions: the repeated solution

$$x_0^r(\gamma,t)=\pm\frac{1}{t}\left(\frac{2}{3}(1+ty_\gamma)\right)^{\frac{1}{2}}\,,$$

and

$$x_0^1(\gamma,t) = \mp\frac{2}{t}\left(\frac{2}{3}(1+ty_\gamma)\right)^{\frac{1}{2}},$$

where the sign chosen depends upon the branch of C_t that γ is on. It follows from the shape of $F(x_0)$ or some simple calculations that $F(x_0^r(\gamma,t)) < F(x_0^1(\gamma,t))$, so that the coalescing cusped level surfaces correspond to the minimiser and the whole of one side of the cusp is cool. Hence the level surface

$$\mathcal{S}(x,t) = \frac{(1+ty_\gamma)^2(8ty_\gamma - 1)}{54t^3},$$

is cusped at γ and

$$\mathcal{S}(x,t) = \frac{4(1+ty_\gamma)^2(10+ty_\gamma)}{27t^3},$$

crosses the caustic at γ. This is illustrated in Figures 4.16 and 4.17 which show the pre-level surfaces and level surfaces respectively.

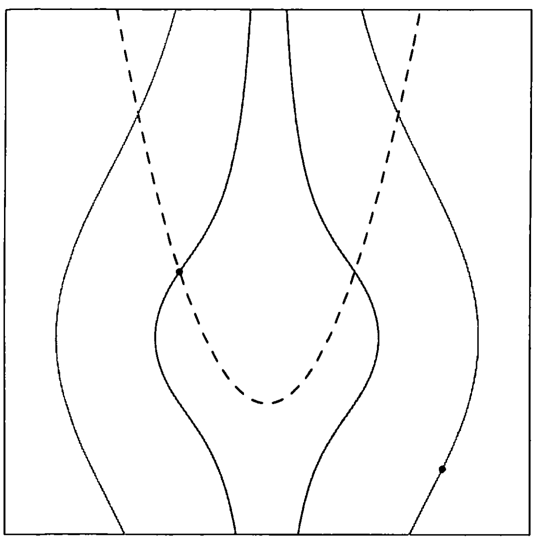

Figure 4.16: Pre-level surfaces.

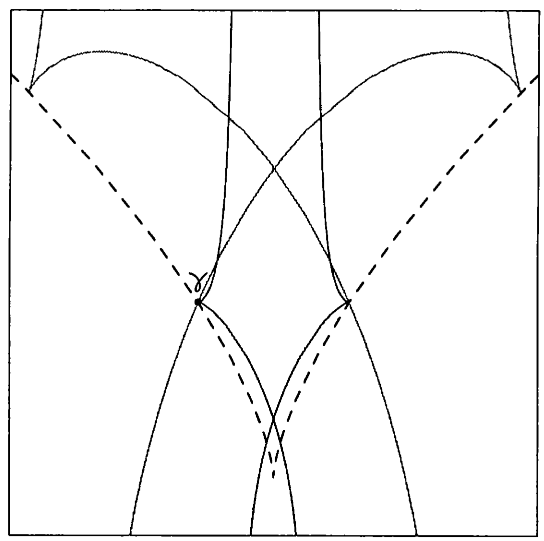

Figure 4.17: Level surfaces at γ

Remark 4.6.1. An immediate consequence of Corollary 4.5.4 is that the whole of one side of the cusp with noise in a fixed general direction is cool.

4.6.2 The Polynomial Swallowtail

For the polynomial swallowtail in the deterministic case we have

$$F(x_0) = \alpha x_0^5 - \frac{t}{2}x_0^4 + \frac{x_0^2}{2t}(1+ty_\gamma) - \frac{x_0 x_\gamma}{t} + \frac{x_\gamma^2}{2t}.$$

Let us consider the two cases studied earlier for $F'(x_0)$.

Case 1 : $y_\gamma < -\frac{1}{2t}$ or $y_\gamma > -\frac{1}{2t} + \frac{t^3}{25\alpha^2}$.

Since $\gamma = (x_\gamma, y_\gamma) \in C_t$ we know $F'(x_0) = 0$ has one only one solution, namely the repeated solution $x_0^r(\gamma, t)$. Thus $F(x_0)$ has only one stationary point which is a point of inflection and so one side of this part of C_t is cool.

Case 2 : $-\frac{1}{2t} \leq y_\gamma \leq -\frac{1}{2t} + \frac{t^3}{25\alpha^2}$.
We once again adopt the labelling scheme for the caustic defined in Figure 4.4. On branch (A), $F'(x_0) = 0$ will have one solution which is repeated and as in Case 1 one side of this part of C_t is cool.

If γ is a point on branch (D) then $F'(x_0) = 0$ will have three solutions $x_0^1(\gamma, t)$, $x_0^r(\gamma, t)$ and $x_0^2(\gamma, t)$ where the middle one is repeated. This implies $F(x_0)$ will have three stationary points occurring from left to right as maximum, inflection and minimum. Hence $F(x_0^r(\gamma, t)) > F(x_0^2(\gamma, t))$ meaning that the coalescing cusped level surfaces do not correspond to the minimiser and so one side of branch (D) is hot.

The situation on branches (B) and (C) is slightly more complicated. If $\gamma \neq (0, -\frac{1}{2t})$ is such a point then $F'(x_0)$ possesses one of the shapes shown in Figure 4.18. The corresponding shapes of $F(x_0)$ are shown in Figure 4.19.

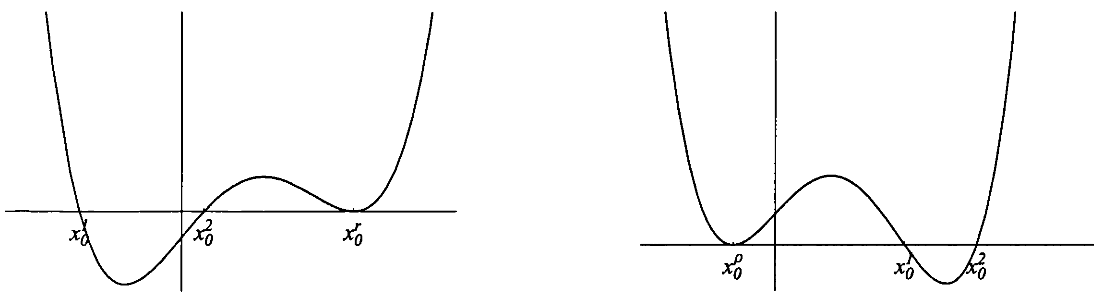

Figure 4.18: Shape of $F'(x_0)$ on branches (B) and (C)

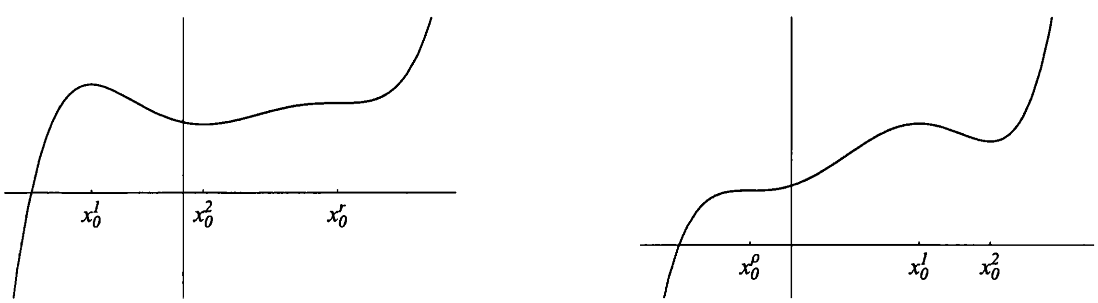

Figure 4.19: Shape of $F(x_0)$ on branches (B) and (C)

Since $F'(0) = -x_\gamma$ it follows that if $x_\gamma > 0$ then $F'(x_0)$ must look like Figure 4.18 left and so $F'(x_0) = 0$ has solutions $x_0^1(\gamma, t)$, $x_0^2(\gamma, t)$ and repeated solution $x_0^r(\gamma, t)$. Thus $F(x_0)$ has three stationary points occurring from left to right as maximum, minimum and point of inflection. Thus $F(x_0^r(\gamma, t)) > F(x_0^2(\gamma, t))$ and so one side of the portion of branch (B) with $x_\gamma > 0$ is hot.

If $x_\gamma \leq 0$ then $F'(0) \geq 0$ and along branch (B) $F'(x_0)$ will look like Figure 4.18 left so that one side of this part of C_t is hot. As we move towards the point of self intersection the global minimum $F'(u) \nearrow 0$ so that at the crossover point $F'(x_0) = 0$ will have two solutions $x_0^\rho(\gamma,t) = u$ and $x_0^r(\gamma,t)$, both of which are repeated. Hence at the point of self intersection $F(x_0)$ will look like Figure 4.20 and so one side of this part of C_t is cool.

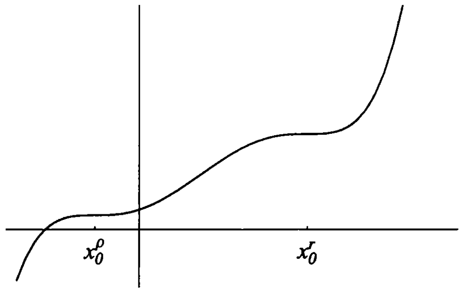

Figure 4.20: Shape of $F(x_0)$ at point of self intersection

Since at the crossover point $x_0^r(\gamma,t) > 0$ then it follows that if we now travel along branch (C) in the direction of decreasing y then $F'(x_0)$ will have the shape shown in Figure 4.18 right. Effectively the repeated solution $x_0^r(\gamma,t)$ splits into the non-repeated solutions $x_0^1(\gamma,t)$ and $x_0^2(\gamma,t)$. Hence $F(x_0)$ will look like Figure 4.19 right where initially $\xi(x_0^\rho(\gamma,t)) < \xi(x_0^2(\gamma,t))$ so that C_t is cool. However by the time we reach the cusp at $(0,-\frac{1}{2t})$, $F(x_0)$ has the shape shown in Figure 4.21 in which the coalescing cusped level surfaces do not correspond to the minimiser so that C_t is hot. Hence there must exist a

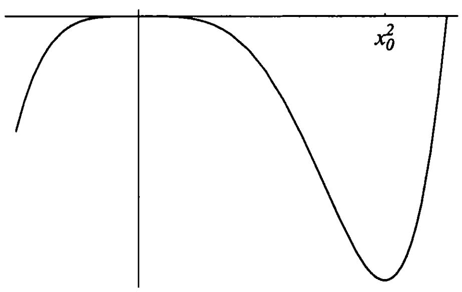

Figure 4.21: Shape of $F(x_0)$ at cusp at $(0,-\frac{1}{2t})$

point λ on branch (C) at which C_t will switch from cool to hot. This is found by solving the four equations

$$\begin{aligned} F(x_0^\rho(\lambda,t)) &= F(x_0^2(\lambda,t)) \ , \\ F'(x_0^2(\lambda,t)) &= 0 \ , \\ F'(x_0^\rho(\lambda,t)) &= 0 \ , \\ F''(x_0^\rho(\lambda,t)) &= 0 \ , \end{aligned}$$

in four unknowns $x_\lambda, y_\lambda, x_0^\rho(\lambda,t)$ and $x_0^2(\lambda,t)$. Solving these yields

$$\lambda = \left(\frac{-t^5(3+8\sqrt{6})}{18000\alpha^3}, -\frac{1}{2t} + \frac{t^3\,(9-\sqrt{6})}{450\alpha^2} \right) ,$$

where $x_0^\rho(\lambda, t) = \frac{t}{10\alpha}\left(1+\sqrt{6}\right)$, $x_0^2(\lambda, t) = \frac{t}{30\alpha}\left(3-2\sqrt{6}\right)$.

The above example provides a complete analysis of the hot and cool parts of the polynomial swallowtail which is summarised in the following theorem.

Theorem 4.6.1. *Let C_t be the polynomial swallowtail caustic curve with initial function $S_0(\boldsymbol{x}_0) = \alpha x_0^5 + x_0^2 y_0$ where $\alpha > 0$. Consider crossing C_t at a point $\gamma = (x_\gamma, y_\gamma)$ travelling in the direction of decreasing S_i. As we cross C_t the number of S_i's will decrease by a multiple of two. Moreover the approached side is cool if*

$$x_\gamma \leq -\frac{t^5}{500\alpha^3},$$

or

$$-\frac{t^5}{500\alpha^3} \leq x_\gamma \leq \frac{-t^5(3+8\sqrt{6})}{18000\alpha^3} \quad \textit{and} \quad -\frac{1}{2t} + \frac{t^3\left(9-\sqrt{6}\right)}{450\alpha^2} \leq y_\gamma \leq -\frac{1}{2t} + \frac{t^3}{50\alpha^2},$$

and hot otherwise.

The results of Theorem 4.6.1 are illustrated in Figure 4.22. Recall that $u^0(\boldsymbol{x}, t)$ will

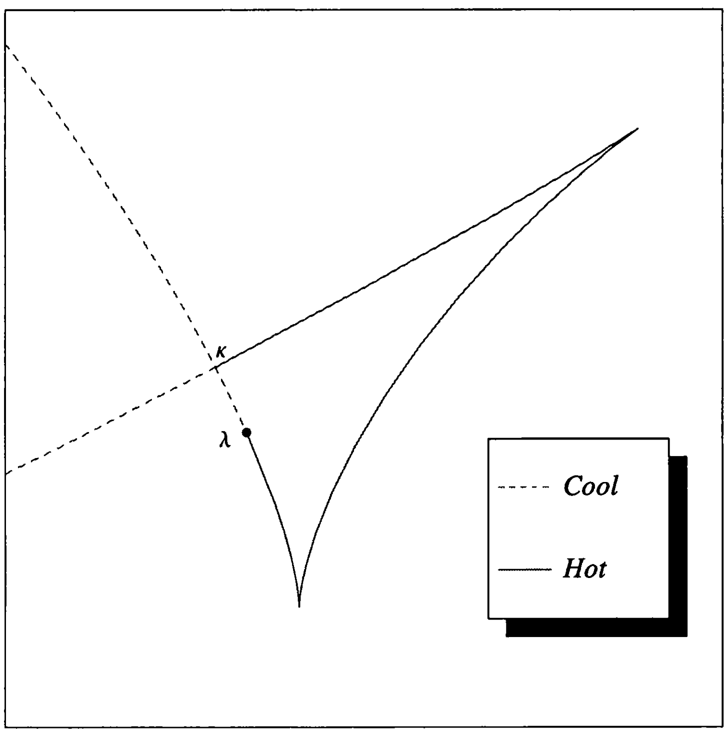

Figure 4.22: Hot and cool parts of the polynomial swallowtail

be discontinuous along the cool parts of the caustic. Thus if κ denotes the point of self intersection then travelling anticlockwise around a circle centred at κ of radius $r \leq \|\kappa - \lambda\|$ we observe that $u^0(\boldsymbol{x}, t)$ will be discontinuous along three crossover points of C_t.

Corollary 4.6.2. *Consider travelling anticlockwise around a circle centred at* $\kappa = \left(-\frac{t^5}{500\alpha^3}, \frac{-1}{2t} + \frac{t^3}{50\alpha^2}\right)$ *with radius* r. *If*

$$r \le \frac{t^3\left(3200\alpha^2 + t^4\left(491 - 176\sqrt{6}\right)\right)^{\frac{1}{2}}}{6000\alpha^3\sqrt{3}} ,$$

then $u^0(\boldsymbol{x}, t)$ *will be discontinuous as it crosses* C_t *at three points. Otherwise* $u^0(\boldsymbol{x}, t)$ *will be discontinuous as it crosses* C_t *at two points.*

Proof. Evaluate $\|\kappa - \lambda\|$ using the explicit expressions for κ and λ. . □

Corollary 4.6.3. *In the case of the stochastic polynomial swallowtail with noise in a general direction the shape is preserved but the point* λ *is now located at*

$$\lambda = \left(-\frac{t^5}{18000\alpha^2}\left(3 + 8\sqrt{6}\right) - \varepsilon\cos\theta\int_0^t W_u\,\mathrm{d}u, -\frac{1}{2t} + \frac{t^3\left(9 - \sqrt{6}\right)}{450\alpha^2} - \varepsilon\sin\theta\int_0^t W_u\,\mathrm{d}u\right) ,$$

and the self intersection point is at

$$\kappa = \left(-\frac{t^5}{500\alpha^2} - \varepsilon\cos\theta\int_0^t W_u\,\mathrm{d}u, -\frac{1}{2t} + \frac{t^3}{50\alpha^2} - \varepsilon\sin\theta\int_0^t W_u\,\mathrm{d}u\right) .$$

4.7 Outline of the n-dimensional free case

Let us briefly consider the n-dimensional free case. Further analysis of this may be found in Section 5.9 of Chapter 5. Here we are interested in the expression

$$u^\mu(\boldsymbol{x}, t) = (2\pi\mu^2 t)^{-\frac{n}{2}} \int_{\mathbb{R}^n} T_0(\boldsymbol{x}_0)\exp\left(-\frac{1}{\mu^2}\mathcal{A}(\boldsymbol{x}_0, \boldsymbol{x}, t)\right)\mathrm{d}\boldsymbol{x}_0 ,$$

where in the free case

$$\mathcal{A}(\boldsymbol{x_0}, \boldsymbol{x}, t) = \frac{|\boldsymbol{x} - \boldsymbol{x_0}|^2}{2t} + S_0(\boldsymbol{x_0}) .$$

If $\boldsymbol{x} = (x^{(1)}, x^{(2)}, \ldots, x^{(n)})$ then we have n equations of the form

$$x^{(i)} = x_0^{(i)} + t\frac{\partial S_0}{\partial x_0^{(i)}}(\boldsymbol{x}_0) , \tag{4.7.1}$$

for $i = 1, 2, \ldots, n$. If $1 + t\frac{\partial^2 S_0}{\partial x_0^{(i)2}}(\boldsymbol{x}_0) \neq 0$ then we may solve the equations (4.7.1) for $i = 2, \ldots, n$ to obtain

$$x_0^{(i)}(\boldsymbol{x}, \{x_0^{(j)}\}_{\substack{j=1,2,\ldots,n \\ j\neq i}}) .$$

Moreover eliminating $x_0^{(i)}$ for $i = 2, \ldots, n$ from the above $n - 1$ equations we obtain $x_0^{(i)}(\boldsymbol{x}, x_0^{(1)})$ for $i = 2, \ldots, n$. Then assuming we may apply Laplace's method $n - 1$ times to the original integral, we obtain

$$u^\mu(\boldsymbol{x},t) \sim \left(2\pi\mu^2 t\right)^{-\frac{1}{2}} \int\limits_{\mathbb{R}} T_0\left(x_0^{(1)}, x_0^{(2)}(\boldsymbol{x}, x_0^{(1)}), \ldots, x_0^{(n)}(\boldsymbol{x}, x_0^{(1)})\right)$$

$$\times \left[\prod_{i=2}^{n} \frac{\partial^2 \tilde{\mathcal{A}}}{\partial x_0^{(i)2}}(x_0^{(1)}, \boldsymbol{x}, t)\right]^{-\frac{1}{2}} \exp\left(-\frac{1}{\mu^2}\tilde{\mathcal{A}}(x_0^{(1)}, \boldsymbol{x}, t)\right) \mathrm{d}x_0^{(1)}$$

as $\mu \sim 0$ where

$$\tilde{\mathcal{A}}(x_0^{(1)}, \boldsymbol{x}, t) = \mathcal{A}(x_0^{(1)}, x_0^{(2)}(\boldsymbol{x}, x_0^{(1)}), \ldots, x_0^{(n)}(\boldsymbol{x}, x_0^{(1)}), \boldsymbol{x}, t)\ .$$

To obtain the caustic equation we must solve

$$\frac{\partial \tilde{\mathcal{A}}}{\partial x_0^{(1)}} = 0 \qquad \text{and} \qquad \frac{\partial^2 \tilde{\mathcal{A}}}{\partial x_0^{(1)2}} = 0\ ,$$

by eliminating $x_0^{(1)}$. Hence if we define

$$F(x_0^{(1)}) = \tilde{\mathcal{A}}(x_0^{(1)}, \boldsymbol{x}, t)\ ,$$

then $\boldsymbol{x} \in C_t$ if and only if there exists $x_0^{(r,1)}(\boldsymbol{x},t)$ such that $F'(x_0^{(r,1)}(\boldsymbol{x},t)) = F''(x_0^{(r,1)}(\boldsymbol{x},t)) = 0$. This is the same condition as in the two dimensional case and so our results there may be extended to the n-dimensional case.

Theorem 4.7.1. *Let* $\boldsymbol{x} = (x^{(1)}, x^{(2)}, \ldots, x^{(n)}) \in \mathbb{R}^n$, $S_0(\boldsymbol{x}_0) \in C^2$ *and assume the equations*

$$x^{(i)} = x_0^{(i)} + t\frac{\partial S_0}{\partial x_0^{(i)}}(\boldsymbol{x}_0)\ ,$$

may be solved to obtain $x_0^{(i)}(\boldsymbol{x}, x_0^{(1)})$ *for* $i = 2, \ldots, n$. *Consider crossing* C_t *at a non self intersection point* $\gamma = (x_\gamma^{(1)}, x_\gamma^{(2)}, \ldots, x_\gamma^{(n)})$ *travelling in the direction of decreasing* $S_i(\boldsymbol{x},t)$. *If*

$$F(x_0^{(1)}) := \frac{\left(x_\gamma^{(1)} - x_0^{(1)}\right)^2}{2t} + \frac{t}{2}\sum_{i=2}^{n}\left(\frac{\partial S_0}{\partial x_0^{(i)}}\left(x_0^{(1)}, x_0^{(2)}(\boldsymbol{x}, x_0^{(1)}), \ldots, x_0^{(n)}(\boldsymbol{x}, x_0^{(1)})\right)\right)^2$$

$$+ S_0\left(x_0^{(1)}, x_0^{(2)}(\boldsymbol{x}, x_0^{(1)}), \ldots, x_0^{(n)}(\boldsymbol{x}, x_0^{(1)})\right)\ ,$$

then there will exist a repeated solution $x_0^{(r,1)}(\gamma,t)$ *of* $F'(x_0^{(1)}) = 0$. *One side of* C_t *will be cool at* γ *if and only if*

$$F(x_0^{(r,1)}(\gamma,t)) \le \min_{\substack{i=1,2,\ldots,k \\ i \ne r}} F(x_0^{(i,1)}(\gamma,t))\ ,$$

where $x_0^{(i,1)}(\gamma,t)$ *are the solutions of* $F'(x_0^{(1)}) = 0$. *Moreover the boundary of the cool part of the caustic is given by*

$$F(x_0^{(r,1)}(\gamma,t)) = \min_{\substack{i=1,2,\ldots,k \\ i \ne r}} F(x_0^{(i,1)}(\gamma,t))\ .$$

4.7.1 The Butterfly

The butterfly is the three dimensional analogue of the cusp singularity and has initial function $S_0(\boldsymbol{x_0}) = x_0^3 y_0 + x_0^2 z_0$. Full details of the butterfly may be found in [41], [14] and [15]. We are only concerned with its hot and cool nature and it may be easily shown that

$$F(x_0) = -\frac{t}{2}x_0^6 - \frac{t}{2}x_0^4 + x_0^3 y_\gamma + \frac{x_0^2}{2t} + x_0^2 z_\gamma - \frac{x_\gamma x_0}{t},$$

so that

$$\begin{aligned} F'(x_0) &= -3tx_0^5 - 2tx_0^3 + 3x_0^2 y_\gamma + x_0\left(\frac{1}{t} + 2z_\gamma\right) - \frac{x_\gamma}{t} , \\ F''(x_0) &= -15tx_0^4 - 6tx_0^2 + 6x_0 y_\gamma + \frac{1}{t} + 2z_\gamma , \\ F'''(x_0) &= -60tx_0^3 - 12tx_0 + 6y_\gamma . \end{aligned}$$

Consider a level surface $y = K$. Observe that $F^{(iv)}(x_0) = 0$ has no real solutions so that $F'''(x_0)$ has no turning points. It may be easily argued that if $\gamma \in C_t$ then $F(x_0)$ has two stationary points: a point of inflection and a maximum. Clearly the value of F at the point of inflection will be less that that at the maximum making the whole of one side of the slice cool. This will be true for all slices making the whole of one side of the butterfly cool.

4.7.2 The Three Dimensional Polynomial Swallowtail

For the polynomial swallowtail in three dimensions the function F is given by

$$F(x_0) = x_0^7 - \frac{t}{2}x_0^6 - \frac{t}{2}x_0^4 + x_0^3 y + x_0^2 z + \frac{x_0^2}{2t} - \frac{x x_0}{t} ,$$

which has derivatives

$$\begin{aligned} F'(x_0) &= 7x_0^6 - 3tx_0^5 - 2tx_0^3 + 3x_0^2 y + 2x_0 z + \frac{x_0}{t} - \frac{x}{t} , \\ F''(x_0) &= 42x_0^5 - 15tx_0^4 + 6tx_0^2 + 6x_0 y + 2z + \frac{1}{t} , \\ F'''(x_0) &= 210x_0^4 - 60tx_0^3 - 12tx_0 + 6y . \end{aligned}$$

Let us consider slices $y = K$. The important observation here is that the number of solutions of $F'''(x_0)|_{y=K} = 0$ determines the number of cusps on C_t. Thus we know that this will have either 0 or 2 solutions depending on the slice being considered.

Slice with zero cusps : Since $F'''(x_0) = 0$ has no real solutions it follows $F''(x_0) = 0$ has one real solutions, say $x_0 = u_1$. Hence $F'(x_0)$ will have a minimum at $x_0 = u_1$. Moreover if $\gamma \in C_t$ then this minimum must be a repeated solution of $F'(x_0) = 0$ so that $F(x_0)$ has only one stationary point, namely a point of inflection. Thus the whole of one side of C_t for such slices is cool.

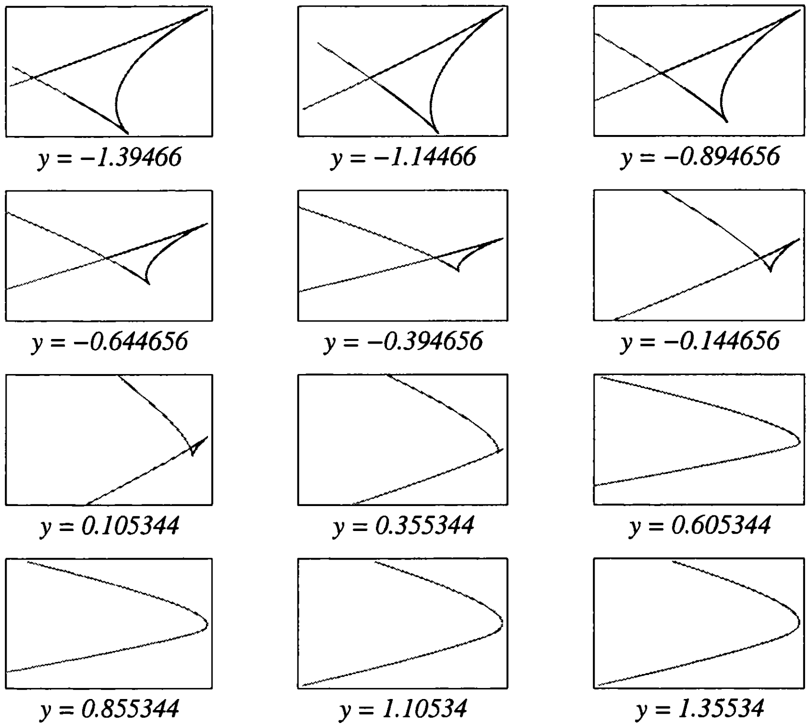

Figure 4.23: Numerical simulation of the hot and cool parts of the three dimensional polynomial swallowtail at $t = 1$.

Slice with two cusps : Adopting the same approach as the two dimensional polynomial swallowtail it may be easily shown that not the whole of the swallowtail is cool. Unfortunately due to the high degree of the polynomials involved we are unable to obtain an explicit expression for the λ curve. However a numerical simulation may be performed, the results of which are shown in Figure 4.23 where the hot parts are represented by the dark parts of the curve.

Chapter 5

Further Applications - Touching Points and Intermittence of Turbulence

---

Until now we have only considered the number of cusps, $\mathcal{N}_C(t)$, on level surfaces of the Hamilton principal function $\mathcal{S}(\boldsymbol{x}, t) = c$ for fixed times $t > 0$. Here we investigate whether varying t brings about changes in $\mathcal{N}_C(t)$, or does it remain constant? Beginning with the deterministic case we consider our usual examples of the cusp and polynomial swallowtail. For the zero level surface ($c \equiv 0$) of the polynomial swallowtail we locate the exact times at which $\mathcal{N}_C(t)$ changes.

We show how the initial function $S_0(\boldsymbol{x}_0)$ may be manipulated in order to build in points of contact between the zero pre-level surface and pre-caustic. This leads to the notion of periodic singularities and the example of the periodic cusp is considered.

Extending this analysis to the stochastic case leads to the concept of *turbulent times*, namely the random times $t(\omega)$ at which $\mathcal{N}_C(t)$ changes. We show how one determines if the turbulence is intermittent by analysing the recurrent nature of a stochastic process. The chapter concludes with a unifying approach which relates our earlier work on hot and cool parts of the caustic to the ideas of turbulence.

5.1 Introduction

We know that if the pre-caustic is given by $y_0 = y_0(x_0, t)$ and the pre-level surface is $p(x_0, y_0, t) = c$ then the pre-curves will meet at solutions x_0 of $F_0(x_0, t) = c$ where $F_0(x_0, t) := p(x_0, y_0(x_0, t), t)$. However these meeting points correspond to the level surface $\mathcal{S}(\boldsymbol{x}, t) = c$ meeting the caustic C_t in generalised cusps. Thus the number of cusped meeting points, $\mathcal{N}_C(t)$, is given by

$$\mathcal{N}_C(t) = \{\# x_0 : F_0(x_0, t) = c\} \ .$$

Recall that if the pre-level surface has no cusps then $\mathcal{N}_C(t)$ will also be the number of cusps on the level surface. Thus far we have only considered $\mathcal{N}_C(t)$ for fixed $t > 0$, but let us now consider the effect of varying $t > 0$. Clearly $\mathcal{N}_C(t)$ will only change when $F_0(x_0, t) = c$ has a repeated root, that is

$$F_0(x_0, t) = c \ , \tag{5.1.1}$$

and

$$\frac{\partial F_0}{\partial x_0}(x_0, t) = 0 \ . \tag{5.1.2}$$

If $\tilde{x}_0(t)$ satisfies Equation (5.1.2) then $\mathcal{N}_C(t)$ will change at solutions $t > 0$ of $F_0(\tilde{x}_0(t), t) = c$. Observe that if $F_0(\tilde{x}_0(t), t) = c$ for all $t > 0$ then this will not constitute a change in $\mathcal{N}_C(t)$.

In the deterministic free case with initial function $S_0(\boldsymbol{x}_0) = f(x_0) + g(x_0)y_0$, Equations (5.1.1) and (5.1.2) yield

$$F_0(x_0, t) = \frac{t}{2}\left\{\left(f' + \frac{g'}{tg''}\left(t^2 g'^2 - tf'' - 1\right)\right)^2 + g^2\right\} + f + \frac{g}{tg''}\left(t^2 g' - tf'' - 1\right) \ , \tag{5.1.3}$$

and

$$\frac{\partial F_0}{\partial x_0}(x_0, t) = \frac{1}{tg''^3}\left(t^2 g'^4 - g'^2(1 + tf'') + gg'' + tf'g'g''\right) \times \left(3t^2 g' g''^2 - tg'' f^{(3)} - t^2 g'^2 g^{(3)} + (1 + tf'')g^{(3)}\right) \ , \tag{5.1.4}$$

where the x_0 variables are omitted for brevity.

5.2 Explicit Examples

Let us consider the behaviour of $\mathcal{N}_C(t)$ as t varies for our archetypal examples of the cusp and polynomial swallowtail.

5.2.1 The Cusp Singularity

For the initial function $S_0(\boldsymbol{x}_0) = \frac{1}{2}x_0^2 y_0$, we set $f \equiv 0$ and take $g(x_0) = \frac{1}{2}x_0^2$ so that Equations (5.1.1) and (5.1.2) reduce to

$$F_0(x_0, t) = \frac{tx_0^4}{8}(4t^2 x_0^2 - 3) \ ,$$

and

$$\frac{\partial F_0}{\partial x_0}(x_0, t) = \frac{3tx_0^3}{2}(2t^2 x_0^2 - 1) \ .$$

Trivially $\frac{\partial F}{\partial x_0} = 0$ has the solutions $x_0 = 0$ and $x_0 = \frac{\pm 1}{t\sqrt{2}}$. We use this fact in the proof of the following proposition.

Proposition 5.2.1. *Consider level surfaces of the Hamilton principal function,* $\mathcal{S}(\boldsymbol{x}, t) = c$*, for the initial function* $S_0(\boldsymbol{x}_0) = \frac{1}{2}x_0^2 y_0$*. If* $c \geq 0$ *then* $\mathcal{N}_C(t)$ *remains constant for all* $t > 0$*, namely* $\mathcal{N}_C(t) = 3$ *for* $c = 0$ *and* $\mathcal{N}_C(t) = 2$ *for* $c > 0$*. If* $c < 0$ *then* $\mathcal{N}_C(t)$ *will change at* $t = \left(\frac{-1}{32c}\right)^{\frac{1}{3}}$ *at which point* $\mathcal{N}_C(t)$ *changes from* 4 *to* 0*. Moreover the cusps disappear at the points*

$$\Phi_{\left(-\frac{1}{32c}\right)^{\frac{1}{3}}}\left(\pm\frac{(32c)^{\frac{1}{3}}}{\sqrt{2}}, y_0\left(\pm\frac{(32c)^{\frac{1}{3}}}{\sqrt{2}}\right)\right).$$

Proof. At $x_0 = \pm\frac{1}{t\sqrt{2}}$ we have $F_0(\pm\frac{1}{t\sqrt{2}}, t) = -\frac{1}{32t^3}$ so that $\mathcal{N}_C(t)$ will change at those $t > 0$ satisfying $t^3 = -\frac{1}{32c}$. This only has a non-negative solution if $c < 0$, in which case $t = \left(-\frac{1}{32c}\right)^{\frac{1}{3}}$.

The only other possibility for changes in $\mathcal{N}_C(t)$ comes from $x_0 = 0$. However $F_0(0, t) = 0$, so that $F_0(0, t) = c$ has no solutions unless $c \equiv 0$, in which case it is true for all $t > 0$ and will not constitute a change in $\mathcal{N}_C(t)$.

Changes in values of $\mathcal{N}_C(t)$ are easily determined from the shape of $F_0(x, t)$ and the fact it is an even function. □

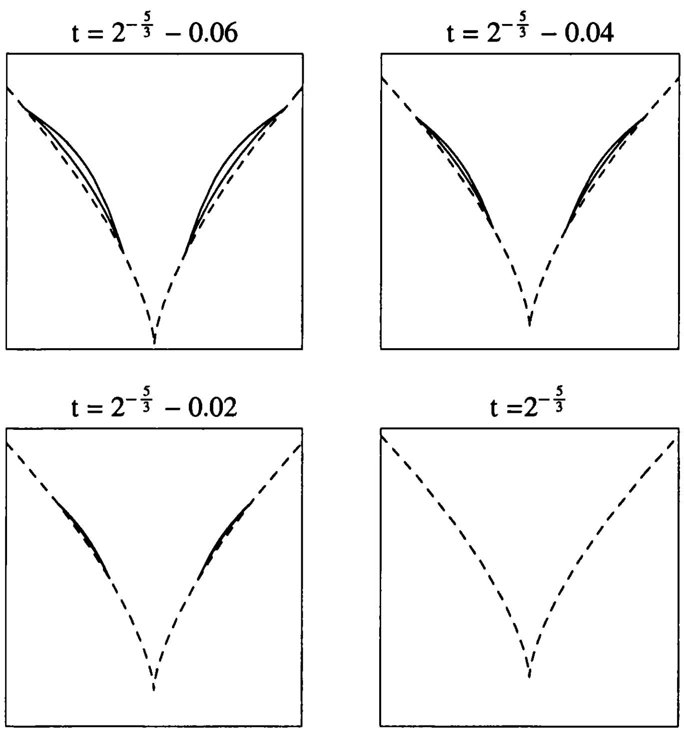

Figure 5.1: Level Surface $c = -1$ and Caustic

In Figure 5.1 we have illustrated Proposition 5.2.1 for $c = -1$. It can be seen that for $t < 2^{-\frac{5}{3}}$ the number of cusped meeting points is four, whilst for $t > 2^{-\frac{5}{3}}$ there are no cusped meeting points. Effectively as $t \searrow 2^{-\frac{5}{3}}$ the lapels on either side reduce to a single point and then disappear.

5.2.2 Polynomial Swallowtail

For the initial function $S_0(\boldsymbol{x_0}) = x_0^5 + x_0^2 y_0$, we set $f(x_0) := x_0^5$ and $g(x_0) := x_0^2$ in Equations (5.1.1) and (5.1.2). This yields

$$F_0(x_0, t) = \frac{225}{2} t x_0^8 - 60 t^2 x_0^7 + 8 t^3 x_0^6 + 6 x_0^5 - \frac{3}{2} t x_0^4 ,$$

and

$$\frac{\partial F_0}{\partial x_0}(x_0, t) = 6 x_0^3 \left(8 t^2 x_0^2 - 30 t x_0^3 - 1\right) (t - 5 x_0) .$$

Clearly $\frac{\partial F}{\partial x_0} = 0$ has the solutions $x_0 = 0$ (3 times) and $x_0 = \frac{t}{5}$. At these points we have

$$F_0(0, t) = 0 \qquad \text{and} \qquad F_0(\tfrac{t}{5}, t) = \frac{1}{31250} t^9 - \frac{3}{6250} t^5 .$$

In addition it appears that we must solve the cubic

$$8 t^2 x_0^2 - 30 t x_0^3 - 1 = 0 ,$$

in x_0, but this may be averted by considering the above as a quadratic in t. This yields the solutions

$$\tilde{t}(x_0) = \frac{15 x_0^2 \pm (8 + 225 x_0^4)^{\frac{1}{2}}}{8 x_0} ,$$

at which we have

$$F_0(x_0, \tilde{t}(x_0)) = \frac{21 x_0^5 \mp x_0^3 (8 + 225 x_0^4)^{\frac{1}{2}}}{16} .$$

Lemma 5.2.2. *Consider level surfaces of the Hamilton principal function, $\mathcal{S}(\boldsymbol{x}, t) = c$, for the initial function $S_0(\boldsymbol{x_0}) = x_0^5 + x_0^2 y_0$. If $c \geq 0$ then there exists $\tilde{t} > 0$ at which $\mathcal{N}_C(t)$ changes.*

Proof. For $x_0 = \frac{t}{5}$ we set $\xi(t) := \frac{1}{31250} t^9 - \frac{3}{6250} t^5 - c$ and observe that $\xi'(t) = 0$ has solutions

$$t = 0 \qquad \text{and} \qquad t = \pm \frac{\sqrt{5}}{3^{\frac{1}{4}}} ,$$

at which

$$\xi(0) = -c \qquad \text{and} \qquad \xi\left(\pm \frac{\sqrt{5}}{3^{\frac{1}{4}}}\right) = \mp \frac{2}{225.3^{\frac{1}{4}} \sqrt{5}} - c .$$

Since $c \geq 0$, clearly $\xi\left(+\frac{\sqrt{5}}{3^{\frac{1}{4}}}\right) < 0$ so that there must exist $\tilde{t}(c) > \frac{\sqrt{5}}{3^{\frac{1}{4}}} > 0$ such that $\xi(\tilde{t}(c)) = 0$. Hence at $\tilde{t}(c)$ the value of $\mathcal{N}_C(t)$ will change. $\square$

Lemma 5.2.3. *Consider level surfaces of the Hamilton principal function, $\mathcal{S}(\boldsymbol{x}, t) = c$, for the initial function $S_0(\boldsymbol{x_0}) = x_0^5 + x_0^2 y_0$. If $c < 0$ then there exists $\tilde{t} > 0$ at which $\mathcal{N}_C(t)$ changes.*

Proof. For $\tilde{t}(x_0) = \frac{15x_0^2-\left(8+225x_0^4\right)^{\frac{1}{2}}}{8x_0}$ we set $\zeta(x_0) := 21x_0^5 + x_0^3\left(8+225x_0^4\right)^{\frac{1}{2}} - 16c$ and observe that $\zeta'(x_0) = 0$ has only one solution $x_0 = 0$. At this point $\zeta(0) = -16c > 0$ so that there must exist $\tilde{x}_0(c) < 0$ such that $\zeta(\tilde{x}_0) = 0$.

Since $15\tilde{x}_0^2 - (8+225\tilde{x}_0^4)^{\frac{1}{2}} < 15\tilde{x}_0^2 - 15\tilde{x}_0^2 = 0$ and $\tilde{x}_0 < 0$ it follows that

$$\tilde{t}(\tilde{x}_0) = \frac{15\tilde{x}_0^2 - (8+225\tilde{x}_0^4)^{\frac{1}{2}}}{8\tilde{x}_0} > 0 \ .$$

Thus at $t = \tilde{t}(\tilde{x}_0)$ the value of $\mathcal{N}_C(t)$ will change. □

Combining Lemmas 5.2.2 and 5.2.3 yields the following proposition.

Proposition 5.2.4. *Consider level surfaces of the Hamilton principal function, $\mathcal{S}(\boldsymbol{x},t) = c$, for the initial function $S_0(\boldsymbol{x}_0) = x_0^5 + x_0^2 y_0$. For any $c \in \mathbb{R}$, there exists $t > 0$ at which $\mathcal{N}_C(t)$ changes.*

For the zero level surface, $c \equiv 0$, we are able to explicitly obtain the times $t > 0$ at which $N_C(t)$ changes. There are only two cases to consider since it follows from the proof of Lemma 5.2.3 that $\tilde{t}(x_0) = \frac{15x_0^2-\left(8+225x_0^4\right)^{\frac{1}{2}}}{8x_0}$ will not yield a positive value of t because $\zeta(x_0) = 0$ only has the solution $\tilde{x}_0 = 0$.

- When $x_0 = \frac{t}{5}$, we have
$$\frac{1}{31250}t^9 - \frac{3}{6250}t^5 = 0 \ ,$$
which has solutions $t = 0$ and $t = 15^{\frac{1}{4}}$.

- For $t = \frac{15x_0^2+\left(8+225x_0^4\right)^{\frac{1}{2}}}{8x_0}$, we have
$$21x_0^5 - x_0^3\left(8+225x_0^4\right)^{\frac{1}{2}} = 0$$
which has solutions $x_0 = 0$ and $x_0 = \pm 3^{-\frac{3}{4}}$. Only $x_0 = 3^{-\frac{3}{4}}$ produces a valid value of t, namely $t = \frac{3^{\frac{5}{4}}}{2}$.

Thus as we vary t, the number of cusps on the zero level surface will change at $t = 15^{\frac{1}{4}}$ and $t = \frac{3^{\frac{5}{4}}}{2}$. Hence for the zero level surface we have the following complete classification of $\mathcal{N}_C(t)$ as t varies.

Range	$0 < t < 15^{\frac{1}{4}}$	$t = 15^{\frac{1}{4}}$	$15^{\frac{1}{4}} < t < \frac{3^{\frac{5}{4}}}{2}$	$t = \frac{3^{\frac{5}{4}}}{2}$	$t > \frac{3^{\frac{5}{4}}}{2}$
$\mathcal{N}_C(t)$	3	4	5	4	3

5.3 Building in Points of Contact

Let us illustrate how the ideas of the previous section lead to a method of building in points of contact and the notion of periodic singularities. We take $S_0(\boldsymbol{x}_0) = f(x_0) + g(x_0)y_0$ throughout.

Proposition 5.3.1. *If $g(\alpha_i) = g'(\alpha_i) = 0$ and $g''(\alpha_i) \neq 0$ for $i = 1, 2, \ldots, n$ then $\mathcal{N}_C(t)$ will change at the times*

$$t_{\alpha_i} = \frac{2\,(c - f(\alpha_i))}{f'(\alpha_i)^2}\,,$$

if $f'(\alpha_i) \neq 0$ and $f(\alpha_i) < c$. Moreover if t_{α_i} is such a time then the change will occur at the point

$$\Phi_{t_{\alpha_i}}\left(\alpha_i, \frac{-1 - t_{\alpha_i} f''(\alpha_i)}{t_{\alpha_i} g''(\alpha_i)}\right) = \left(\alpha_i + t_{\alpha_i} f'(\alpha_i), \frac{-1 - t_{\alpha_i} f''(\alpha_i)}{t_{\alpha_i} g''(\alpha_i)}\right)\,.$$

Proof. If g, g' are zero at α_i and $g''(\alpha_i) \neq 0$ then if follows from Equation (5.1.4), that

$$\left.\frac{\partial F_0}{\partial x_0}\right|_{x_0 = \alpha_i} = 0\,,$$

for $i = 1, 2, \ldots, n$. Thus $\mathcal{N}_C(t)$ will change at solutions $t > 0$ of $F_0(\alpha_i, t) = c$, namely

$$\frac{t}{2} f'(\alpha_i)^2 + f(\alpha_i) = c\,. \tag{5.3.1}$$

Hence if $f'(\alpha_i) \neq 0$ and $f(\alpha_i) < c$ then $N_C(t)$ will change at

$$\tilde{t}_{\alpha_i} = \frac{2(c - f(\alpha_i))}{f'(\alpha_i)^2}\,.$$

□

Corollary 5.3.2. *If f, g, f' and g' are zero at α_i and $g''(\alpha_i) \neq 0$ for $i = 1, 2, \ldots, n$ then the **zero** pre-level surface will **touch** the pre-caustic at the points*

$$\left(\alpha_i, \frac{-1 - t f''(\alpha_i)}{t g''(\alpha_i)}\right)\,, \tag{5.3.2}$$

for all $t > 0$. Hence the zero level surface will meet the caustic in a generalised cusp at

$$\Phi_t\left(\alpha_i, \frac{-1 - t f''(\alpha_i)}{t g''(\alpha_i)}\right) = \left(\alpha_i, \frac{-1 - t f''(\alpha_i)}{t g''(\alpha_i)}\right)\,, \tag{5.3.3}$$

for all $t > 0$.

Proof. From Equation (5.3.1) we see $F_0(\alpha_i, t) = 0$ and $\left.\frac{\partial F_0}{\partial x_0}\right|_{x_0 = \alpha_i} = 0$ for all $t > 0$. Thus for $c \equiv 0$ the pre-curves will touch at the points shown in Equation (5.3.2) for all $t > 0$ and the result follows. □

Remark 5.3.1. Under the assumption that Φ_t is continuous we see that as $t \nearrow \infty$ we obtain generalised cusps at $\Phi_t\left(\alpha_i, -\frac{f''(\alpha_i)}{g''(\alpha_i)}\right)$. Thus for large t the pre-curves will meet at a discrete series of points on the curve $h(x_0) = -\frac{f''(x_0)}{g''(x_0)}$, where we recognise $h(x_0)$ as the time independent part of the pre-caustic

$$y_0(x_0) = \frac{-1}{tg''(x_0)} + \frac{tg'(x_0)^2}{g''(x_0)} \boxed{-\frac{f''(x_0)}{g''(x_0)}} .$$

5.4 Periodic Singularities

5.4.1 A Singularity Periodic in x

The point of Corollary 5.3.2 is that it provides us with a method of building in points of contact by manipulating the initial function.

For instance if we take $f \equiv 0$ then we may build in points of contact at $x_0 = ka$ for $k = 0, 1, 2, \ldots, n$ by taking

$$g(x_0) := \frac{x_0^2}{2} \prod_{k=1}^{n} \left(1 - \frac{x_0^2}{k^2 a^2}\right)^2 .$$

If we let $n \nearrow \infty$ and observe that

$$\sin\left(\frac{\pi x_0}{a}\right) = \frac{\pi x_0}{a} \prod_{k=1}^{\infty} \left(1 - \frac{x_0^2}{k^2 a^2}\right) ,$$

then we see

$$g(x_0) = \frac{a^2}{2\pi^2} \sin^2\left(\frac{\pi x_0}{a}\right) .$$

Thus the initial function

$$S_0(\boldsymbol{x}_0) = \frac{a^2}{2\pi^2} \sin^2\left(\frac{\pi x_0}{a}\right) y_0 , \tag{5.4.1}$$

is periodic in x_0 with period a, $S_0(x_0, y_0) = S_0(x_0 + ka, y_0)$ for $k \in \mathbb{Z}$. Moreover near $\boldsymbol{x}_0 = 0$ we have

$$S_0(x_0, y_0) \sim \frac{1}{2} x_0^2 y_0 .$$

With this in mind we refer to the initial condition in Equation 5.4.1 as a periodic cusp in x. An immediate consequence of Corollary 5.3.2 is the following.

Proposition 5.4.1. *For the the initial function $S_0(\boldsymbol{x}_0) = \frac{a^2}{2\pi^2} \sin^2\left(\frac{\pi x_0}{a}\right) y_0$ the pre-caustic and zero pre-level surface will touch at*

$$(x_0, y_0) = \left(ka, -\frac{1}{t}\right) ,$$

for $k \in \mathbb{Z}$. Moreover the image curves meet in generalised cusps at

$$(x, y) = \left(ka, -\frac{1}{t}\right) ,$$

for $k \in \mathbb{Z}$.

Proof. We simply observe that $g''(x_0) = \cos\left(\frac{2\pi x_0}{a}\right)$, so that $g''(ka) = 1$ which is non-zero. □

Proposition 5.4.2. *For* $S_0(\boldsymbol{x}_0) = \frac{a^2}{2\pi^2}\sin^2\left(\frac{\pi x_0}{a}\right) y_0$ *the pre-caustic is given by*

$$y_0(x_0) = \frac{\sec\left(\frac{2\pi x_0}{a}\right)}{\pi^2 t}\left\{\frac{a^2t^2}{4}\sin^2\left(\frac{2\pi x_0}{a}\right) - \pi^2\right\} , \tag{5.4.2}$$

for $x_0 \neq \frac{(2k+1)a}{4}$ $(k \in \mathbb{Z})$*, whilst the caustic is given by*

$$x(x_0) = x_0 - \frac{a}{16\pi^3}\tan\left(\frac{2\pi x_0}{a}\right)\left\{8\pi^2 - a^2t^2 + a^2t^2\cos\left(\frac{4\pi x_0}{a}\right)\right\} ,$$
$$y(x_0) = \frac{1}{4\pi^2 t}\left\{a^2t^2 - \sec\left(\frac{2\pi x_0}{a}\right)\left(4\pi^2 + a^2t^2\cos\left(\frac{4\pi x_0}{a}\right)\right)\right\} ,$$

for $x_0 \neq \frac{(2k+1)a}{4}$.

Proof. With $\mathcal{A} = \frac{|\boldsymbol{x}-\boldsymbol{x}_0|^2}{2t} + \frac{a^2}{2\pi^2}\sin^2(\frac{\pi x_0}{a})y_0$ the pre-caustic condition $\mathrm{Det}[\mathcal{A}''] = 0$ yields Equation (5.4.2). Moreover Φ_t is determined by $\nabla_{x_0}\mathcal{A} = 0$ which yields

$$\Phi_t \boldsymbol{x}_0 = x_0 + \frac{at}{2\pi}\begin{pmatrix} y_0 \sin\left(\frac{2\pi x_0}{a}\right) \\ \frac{a}{\pi}\sin^2\left(\frac{\pi x_0}{a}\right)\end{pmatrix} ,$$

and applying to Equation (5.4.2) yields the expression for the caustic. □

Proposition 5.4.3. *For* $S_0(\boldsymbol{x}_0) = \frac{a^2}{2\pi^2}\sin^2\left(\frac{\pi x_0}{a}\right) y_0$ *the zero pre-level surface is given by* $\sin^2\left(\frac{\pi x_0}{a}\right) = 0$*, namely* $x_0 = ka$ *for* $k \in \mathbb{Z}$*, and*

$$y_0(x_0) = \begin{cases} -\frac{\sec^2\left(\frac{\pi x_0}{a}\right)}{8\pi t}\left\{4\pi \pm \sqrt{16\pi^2 - 2a^2t^2 + 2a^2t^2\cos\left(\frac{4\pi x_0}{a}\right)}\right\} & x_0 \neq \frac{(2k+1)a}{2} \\ & \text{and } \cos\left(\frac{4\pi x_0}{a}\right) \geq 1 - \frac{8\pi^2}{a^2t^2} , \\ -\frac{a^2 t}{4\pi^2} & x_0 = \frac{(2k+1)a}{2} . \end{cases} \tag{5.4.3}$$

Proof. From the Eikonal equation we obtain

$$\frac{a^2 t}{2\pi^2} y_0^2 \cos^2\left(\frac{\pi x_0}{a}\right)\sin^2\left(\frac{\pi x_0}{a}\right) + \frac{a^4 t}{8\pi^4}\sin^4\left(\frac{\pi x_0}{a}\right) + \frac{a^2}{2\pi^2} y_0 \sin^2\left(\frac{\pi x_0}{a}\right) = 0 ,$$

so that we have $\sin^2\left(\frac{\pi x_0}{a}\right) = 0$ and

$$t y_0^2 \cos^2\left(\frac{\pi x_0}{a}\right) + y_0 + \frac{a^2 t}{4\pi^2}\sin^2\left(\frac{\pi x_0}{a}\right) = 0 .$$

If $x_0 = \frac{(2k+1)a}{2}$ then the above reduces to $y_0 + \frac{a^2t}{4\pi^2} = 0$, so that $y_0\left(\frac{(2k+1)a}{2}\right) = -\frac{a^2t}{4\pi^2}$. Otherwise we have a quadratic in y_0 which may be solved to obtain the remaining expression in Equation (5.4.3). □

Proposition 5.4.4. *For* $S_0(\boldsymbol{x_0}) = \frac{a^2}{2\pi^2}\sin^2\left(\frac{\pi x_0}{a}\right) y_0$ *the zero level surface consists of*

i). $x = ka$ *for* $k \in \mathbb{Z}$,

ii).

$$x(x_0) = x_0 - \frac{a}{8\pi^2}\tan\left(\frac{\pi x_0}{a}\right)\left\{4\pi \pm \sqrt{16\pi^2 - 2a^2t^2 + 2a^2t^2\cos\left(\frac{4\pi x_0}{a}\right)}\right\},$$

$$y(x_0) = \frac{1}{8\pi^2 t}\left\{4a^2t^2\sin^2\left(\frac{\pi x_0}{a}\right) - \pi\left(4\pi \pm \sqrt{16\pi^2 - 2a^2t^2 + 2a^2t^2\cos\left(\frac{4\pi x_0}{a}\right)}\right)\right\},$$

for $x_0 \neq \frac{(2k+1)a}{2}$ *and* $\cos\left(\frac{4\pi x_0}{a}\right) \geq 1 - \frac{8\pi^2}{a^2t^2}$,

iii). $\left(x\left(\frac{(2k+1)a}{2}\right), y\left(\frac{(2k+1)a}{2}\right)\right) = \left(\frac{(2k+1)a}{2}, +\frac{a^2t}{4\pi^2}\right).$

Proof. Simply apply Φ_t to Proposition 5.4.3. □

The pre-curves and image curves for $a = 2$ at time $t = 1$ are shown in Figures 5.2 and 5.3 respectively. As usual the caustic is distinguished by the use of a broken line. We remark that at the touching points $(ka, -\frac{1}{t})$ the common tangent is $y_0'(ka) = 0$.

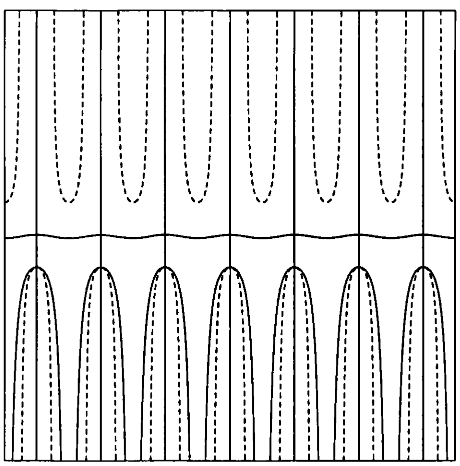

Figure 5.2: Semi-periodic zero pre-level surface and pre-caustic

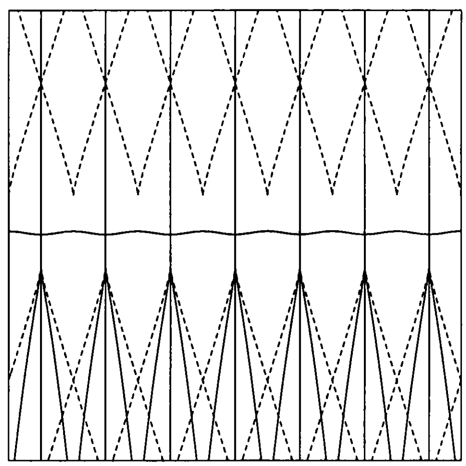

Figure 5.3: Semi-periodic zero level surface and caustic

It may be observed from our figures that touching points of the pre-curves correspond to the zero level surface meeting the caustic in a generalised cusp at a **cusped** part of the caustic. Let us discuss the generic nature of these "cusps within cusps".

Consider a point $\tilde{x}_0$ where the pre-curves touch tangentially and let v_0 be a vector that is parallel to the common tangent. We begin by observing that

$$\frac{\partial \mathcal{A}}{\partial x_0}(\tilde{x}_0 + \varepsilon v_0, x, t) = 0 \iff x = \Phi_t(\tilde{x}_0 + \varepsilon v_0).$$

The first equation here may be expanded to give

$$\frac{\partial \mathcal{A}}{\partial x_0}(\tilde{x}_0, x, t) + \varepsilon v_0.\nabla_{x_0}\frac{\partial \mathcal{A}}{\partial x_0}(\tilde{x}_0, x, t) + \frac{1}{2}\left(\varepsilon v_0.\nabla_{x_0}\right)^2 \frac{\partial \mathcal{A}}{\partial x_0}(\tilde{x}_0, x, t) = 0 ,$$

but at a cusp we know $v_0.\nabla_{x_0}\frac{\partial \mathcal{A}}{\partial x_0}(\tilde{x}_0, x, t) = 0$, so that

$$\frac{\partial \mathcal{A}}{\partial x_0}(\tilde{x}_0, x, t) + \frac{1}{2}\left(\varepsilon v_0.\nabla_{x_0}\right)^2 \frac{\partial \mathcal{A}}{\partial x_0}(\tilde{x}_0, x, t) = 0 .$$

If $x = \tilde{x} + \delta\tilde{x}$ where $\tilde{x} = \Phi_t(\tilde{x}_0)$ and $\delta\tilde{x}$ is of $o(\varepsilon)$ then

$$\tilde{x} + \delta\tilde{x} = \Phi_t(\tilde{x}_0 + \varepsilon v_0) ,$$

or equivalently

$$\frac{\partial \mathcal{A}}{\partial x_0}(\tilde{x}_0 + \varepsilon v_0, \tilde{x} + \delta\tilde{x}, t) = 0 .$$

Expanding this we obtain

$$\frac{\partial \mathcal{A}}{\partial x_0}(\tilde{x}_0, \tilde{x}, t) + \frac{\partial^2 \mathcal{A}}{\partial x \partial x_0}(\tilde{x}_0, \tilde{x}, t)\delta\tilde{x} + \frac{\varepsilon^2}{2}(v_0.\nabla_{x_0})^2\frac{\partial \mathcal{A}}{\partial x_0}(\tilde{x}_0, \tilde{x}, t) = 0 .$$

But $\frac{\partial \mathcal{A}}{\partial x_0}(\tilde{x}_0, \tilde{x}, t) = 0$ since $\tilde{x} = \Phi_t(\tilde{x}_0)$, so that on re-arranging we obtain

$$\delta\tilde{x} = -\frac{\varepsilon^2}{2}\left(\frac{\partial^2 \mathcal{A}}{\partial x \partial x_0}(\tilde{x}_0, \tilde{x}, t)\right)^{-1}(v_0.\nabla_{x_0})^2\frac{\partial \mathcal{A}}{\partial x_0}(\tilde{x}_0, \tilde{x}, t) .$$

Thus it follows that

$$\Phi_t(\tilde{x}_0 \pm \varepsilon v_0) = \Phi_t(\tilde{x}_0) + \varepsilon^2 w(\tilde{x}_0, v_0) + o(\varepsilon^2) ,$$

where

$$w(\tilde{x}_0, v_0) := -\frac{1}{2}\left(\frac{\partial^2 \mathcal{A}}{\partial x \partial x_0}(\tilde{x}_0, \tilde{x}, t)\right)^{-1}(v_0.\nabla_{x_0})^2\frac{\partial \mathcal{A}}{\partial x_0}(\tilde{x}_0, \tilde{x}, t) ,$$

is the cusp axis. Let us see how this works for our periodic cusp example.

Example 5.4.1. If $S_0(\boldsymbol{x}_0) = \frac{a^2}{2\pi^2}\sin^2\left(\frac{\pi x_0}{a}\right) y_0$, we see

$$\frac{\partial \mathcal{A}}{\partial x_0} = \left(\frac{x_0 - x}{t} + \frac{a}{2\pi}\sin\left(\frac{2\pi x_0}{a}\right), \frac{y_0 - y}{t} + \frac{a^2}{2\pi^2}\sin^2\left(\frac{\pi x_0}{a}\right)\right) ,$$

so that

$$\frac{\partial^2 \mathcal{A}}{\partial x \partial x_0} = \begin{pmatrix} -\frac{1}{t} & 0 \\ 0 & -\frac{1}{t} \end{pmatrix} .$$

At our touching points we may take $v_0 = (\pm 1, 0)$ so that $v_0.\nabla = \pm\frac{\partial}{\partial x_0}$ and

$$(v_0.\nabla x_0)^2\frac{\partial \mathcal{A}}{\partial x_0} = \left(-\frac{2\pi}{a}\sin\left(\frac{2\pi x_0}{a}\right), \cos\left(\frac{2\pi x_0}{a}\right)\right) .$$

Thus

$$w(x_0, v_0) = \begin{pmatrix} -\frac{\pi t}{a}\sin\left(\frac{2\pi x_0}{a}\right) \\ \frac{t}{2}\cos\left(\frac{2\pi x_0}{a}\right) \end{pmatrix} ,$$

so that

$$w(ka, v_0) = \begin{pmatrix} 0 \\ \frac{t}{2} \end{pmatrix} .$$

5.4.2 A Singularity Periodic in x and y

Thus far we have only discussed a singularity periodic in x_0. Let us now consider how one may introduce periodicity in the y_0 coordinate.

Lemma 5.4.5. *Consider the initial function $S_0(\boldsymbol{x}_0) = f(x_0) + g(x_0)\gamma(y_0)$. If f, f', g, g' are zero at α_i for $i = 1, 2, \ldots, n$ and $g''(\alpha_i) \neq 0$ then the zero pre-curves will touch at*

$$\left(\alpha_i, \gamma^{-1}\left(\frac{-1 - tf''(\alpha_i)}{tg''(\alpha_i)}\right)\right) , \tag{5.4.4}$$

for $i = 1, 2, \ldots, n$ if γ is invertible.

Proof. The pre-curves meet at solutions x_0 of $F_0(x_0, t) = 0$ where

$$F_0(x_0, t) = \frac{t}{2}\left(f' + g'\gamma(y_0(x_0))\right)^2 + \frac{t}{2} g^2\gamma'(y_0(x_0))^2 + f + g\gamma(y_0(x_0)) ,$$

and $y_0(x_0)$ is the pre-caustic. Now

$$\begin{aligned} \frac{\partial F_0}{\partial x_0}(x_0, t) &= t(f' + g'\gamma(y_0(x_0)))\frac{\partial}{\partial x_0}\left(f' + g'\gamma(y_0(x_0))\right) + tgg'\gamma'(y_0(x_0))^2 \\ &\quad + tg^2\gamma'(y_0(x_0))\gamma''(y_0(x_0))y_0'(x_0) + f' + g'\gamma(y_0(x_0)) + g\gamma'(y_0(x_0))y_0'(x_0) , \end{aligned}$$

so that clearly $F_0(\alpha_i, t) = 0$ and $\left.\frac{\partial F_0}{\partial x_0}\right|_{x_0=\alpha_i} = 0$. Hence the pre-curves will touch at $(\alpha_i, y_0(\alpha_i))$ where $y_0(x_0)$ is the pre-caustic. However in this case the pre-caustic is given by

$$(1 + t(f'' + g''\gamma(y_0))\left(1 + tg\gamma''(y_0)\right) - t^2 g'^2\gamma'(y_0)^2 = 0 ,$$

so that at $x_0 = \alpha_i$

$$\gamma(y_0) = \frac{-1 - tf''(\alpha_i)}{tg''(\alpha_i)} .$$

Hence

$$y_0(\alpha_i) = \gamma^{-1}\left(\frac{-1 - tf''(\alpha_i)}{tg''(\alpha_i)}\right) .$$

□

Corollary 5.4.6. *If $S_0(\boldsymbol{x}_0) = f(x_0) + g(x_0)\gamma(y_0)$ where γ is a periodic function with period b and f, g, f', g' are zero at α_i for $i = 1, 2, \ldots, n$ whilst $g''(\alpha_i) \neq 0$ then the pre-curves will touch at*

$$(x_0, y_0) = \left(\alpha_i, \gamma^{-1}\left(\frac{-1 - tf''(\alpha_i)}{tg''(\alpha_i)}\right) + lb\right) ,$$

for $l \in \mathbb{Z}$ and $i = 1, 2, \ldots, n$.

In order to obtain a periodic cusp singularity we set $\gamma(\cdot) := \frac{b}{2\pi}\sin\left(\frac{2\pi}{b}\,\cdot\right)$, where $b > 0$, so that γ has period b and $\gamma(y) \sim y$ for $y \sim 0$. Clearly if we take $f \equiv 0$ and $g(x_0) := \frac{a^2}{2\pi^2}\sin^2\left(\frac{\pi x_0}{a}\right)$ then f, g, f' and g' are zero at $x_0 = ka$ ($k \in \mathbb{Z}$) and $g''(ka) = 1$. Moreover

$$\begin{aligned}\gamma^{-1}\left(\frac{-1 - tf''(ka)}{tg''(ka)}\right) &= \gamma^{-1}\left(-\frac{1}{t}\right) \\ &= \frac{b}{2\pi}\arcsin\left(-\frac{2\pi}{bt}\right),\end{aligned}$$

which exists if $b \geq \frac{2\pi}{t}$. Since the conditions of Corollary 5.4.6 are satisfied we obtain the following proposition.

Proposition 5.4.7. *Consider the initial function* $S_0(\boldsymbol{x}_0) = \frac{a^2 b}{4\pi^3}\sin^2\left(\frac{\pi x_0}{a}\right)\sin\left(\frac{2\pi y_0}{b}\right)$. *If* $b \geq \frac{2\pi}{t}$ *then the pre-curves will touch at*

$$(x_0, y_0) = \left(ka, \frac{b}{2\pi}\arcsin\left(-\frac{2\pi}{bt}\right) + lb\right),$$

for $k, l \in \mathbb{Z}$.

In Figures 5.4 and 5.5 we have shown the pre-curves and image curves respectively where $a = 3$, $b = 4$ and $t = 2$ so that $b \geq \frac{2\pi}{t}$.

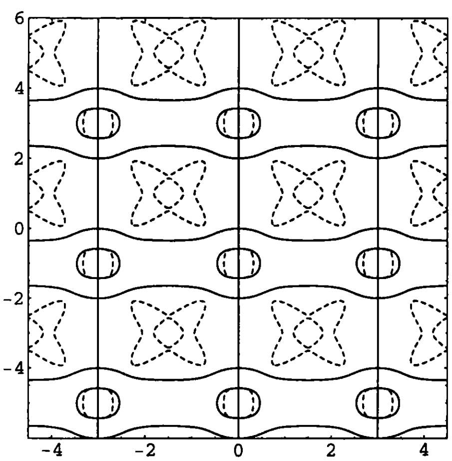

Figure 5.4: Periodic zero pre-level surface and pre-caustic

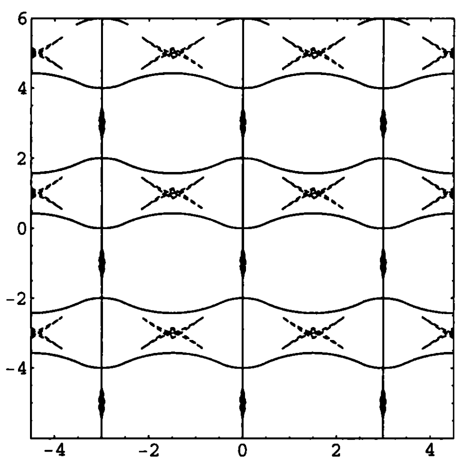

Figure 5.5: Periodic zero level surface and caustic

We shall not pursue the notion of periodic singularities any further, but suffice to say many examples may be easily created. Moreover, it may be possible to use this setup for investigating Burgers equation on a sphere.

5.5 Turbulent Times

Let us now return to the stochastic case where we consider a random force parallel to the x-axis which is white noise in time. Namely we take $k(\boldsymbol{x}, t) = x$ and consider the stochastic heat equation

$$\partial u(\boldsymbol{x},t) = \frac{1}{2}\mu^2\Delta u(\boldsymbol{x},t)dt + \frac{\varepsilon}{\mu^2}xu(\boldsymbol{x},t)\circ \partial W_t \ .$$

Denoting the level surface and caustic by H_t and C_t respectively, we define turbulent times as follows.

Definition 5.5.1. *Turbulent times are those random times $t(\omega)$ such that the pre-level surface $\Phi_t^{-1}H_t$ and the pre-caustic $\Phi_t^{-1}C_t$ touch at a set of points $\{a_1, a_2, \ldots, a_n\}$.*

Clearly as time evolves the number of cusps $\mathcal{N}_C(t)$ will change at these turbulent times. Evidently if $\mathcal{N}_C(t)$ is given by the number of solutions x_0 of $F_\varepsilon(x_0,t) = c$, then the turbulent times $t(\omega)$ must satisfy

$$F_\varepsilon(x_0,t) = c \ ,$$

and

$$\frac{\partial F_\varepsilon}{\partial x_0}(x_0,t) = 0 \ .$$

Thus in the stochastic case the turbulent times $t(\omega)$ will be the zeros of the stochastic process

$$Y_t(\omega) := F_\varepsilon(\tilde{x}_0(t,\omega),t,\omega) - c \ ,$$

where

$$\left.\frac{\partial F_\varepsilon}{\partial x_0}\right|_{x_0=\tilde{x}_0(t,\omega)} = 0 \ .$$

For an initial function of the form $S_0(\boldsymbol{x_0}) = f(x_0) + g(x_0)y_0$ we know from Chapter 3 that the function F_ε determining the number of cusped meeting points is given by

$$\begin{aligned} F_\varepsilon(x_0,t) = \frac{t}{2}\left\{\left(f' + \frac{g'}{tg''}\left(t^2g'^2 - tf'' - 1\right)\right)^2 + g^2\right\} + f + \frac{g}{tg''}\left(t^2g'^2 - tf'' - 1\right) \\ - \frac{\varepsilon^2}{2}\int_0^t W_u^2\,\mathrm{d}u - \left(x_0 - \varepsilon\int_0^t W_u\,\mathrm{d}u + tf' + \frac{g'}{g''}\left(t^2g'^2 - tf'' - 1\right)\right)\varepsilon W_t \ , \quad (5.5.1) \end{aligned}$$

where we have suppressed the x_0 variable for brevity. Differentiating with respect to x_0 and simplifying yields

$$\begin{aligned} \frac{\partial F_\varepsilon}{\partial x_0} = \frac{1}{tg''^2}\left\{g'^2\left(t^2g'^2 - tf'' - 1\right) + g''\left(g + tg'\left(f' - \varepsilon W_t\right)\right)\right\} \\ \times \left\{tg''\left(3tg'g'' - f^{(3)}\right) - g^{(3)}\left(t^2g'^2 - tf'' - 1\right)\right\} \ . \quad (5.5.2) \end{aligned}$$

Proposition 5.5.1. *Consider an initial condition of the form $S_0(\boldsymbol{x_0}) = f(x_0) + g(x_0)y_0$ where f, g, f' and g' are zero at $x_0 = \alpha_i$ and $g''(\alpha_i) \neq 0$ for $i = 1, 2, \ldots, n$. Then the zeros of the stochastic process*

$$Y_t(\omega) = -\alpha_i\varepsilon W_t + \varepsilon^2 W_t\int_0^t W_u\,\mathrm{d}u - \frac{\varepsilon^2}{2}\int_0^t W_u^2\,\mathrm{d}u - c \ ,$$

will be turbulent times. Moreover, the turbulence at $\Phi_t\left(\alpha_i, \frac{-1-tf''(\alpha_i)}{tg''(\alpha_i)}\right)$ is intermittent.

Proof. This follows immediately from Equations (5.5.1) and (5.5.2) by observing

$$\left.\frac{\partial F_\varepsilon}{\partial x_0}\right|_{x_0=\alpha_i} = 0 ,$$

so that $\mathcal{N}_C(t)$ changes at the solutions $t(\omega) > 0$ of $Y_t(\omega) = 0$ where $Y_t(\omega) := F_\varepsilon(\alpha_i, t) - c$. The intermittency will be discussed in Sections 5.6 and 5.7. □

Remark 5.5.1.

i). There is no analogue of this proposition in the deterministic case since the solutions $x_0 = \alpha_i$ do not provide us with times $t > 0$ at which $\mathcal{N}_C(t)$ changes. Recall that in the deterministic case the expression $F_0(\alpha_i, t) = c$ will either be true for all time (if $c \equiv 0$) or false for all time (if $c \not\equiv 0$). Hence no change in $\mathcal{N}_C(t)$ occurs.

ii). In general there will be other turbulent times in addition to those which are zeros of the stochastic process $Y_t(\omega)$. These are not necessarily intermittent.

Observe that if we set $g(x_0) := x_0^2$ then Equations (5.5.1) and (5.5.2) reduce to

$$F_\varepsilon(x_0, t) = 8t^3x_0^6 - \left(4t^2 f'' + \frac{3t}{2}\right) x_0^4 + 4t^2 (f' - \varepsilon W_t) x_0^3 + \frac{f''}{2} (1 + tf'') x_0^2$$
$$- (f' - t\varepsilon W_t f'' + tf'f'') x_0 + f + \frac{1}{2} tf'^2 - t\varepsilon W_t f' + \varepsilon^2 W_t \int_0^t W_u \, du - \frac{\varepsilon^2}{2} \int_0^t W_u^2 \, du ,$$

and

$$\frac{\partial F_\varepsilon}{\partial x_0} = \frac{1}{2} x_0 \left(x_0 \left(8t^2x_0^2 - 1\right) + 2t (f' - x_0 f'' - \varepsilon W_t)\right) \left(12tx_0 - f^{(3)}\right) . \tag{5.5.3}$$

In light of Remark 5.5.1 (ii) and the fact that Equation (5.5.3) admits such a convenient factorisation we are able to state and prove the following proposition for initial functions of the form $S_0(\boldsymbol{x}_0) = x_0^n + x_0^2 y_0$ where $n \geq 5$.

Proposition 5.5.2. *Consider an initial condition of the form* $S_0(\boldsymbol{x}_0) = x_0^n + x_0^2 y_0$ *where* $n \geq 5$. *The turbulent times are given by the zeros of the stochastic processes*

i). $Y_t(\omega)$

ii). $\xi_t(\omega) := F_\varepsilon \left(\left(\frac{12t}{n(n-1)(n-2)} \right)^{\frac{1}{n-4}}, t \right) - c ,$

iii). $\zeta_t(\omega) := F_\varepsilon(\tilde{x}_0^i(t, \omega), t) - c$, *where* $\tilde{x}_0^i(t, \omega)$ *are the real solutions of*

$$2tn(n-2)x_0^{n-1} - 8t^2x_0^3 + x_0 + 2t\varepsilon W_t = 0 .$$

Proof. Clearly the conditions of Proposition 5.5.1 hold so that the positive zeros of $Y_t(\omega)$ are turbulent times. Moreover

$$\frac{\partial F_\varepsilon}{\partial x_0} = \frac{1}{2} x_0^2 \left(x_0(8t^2x_0^2 - 1) + 2t \left(nx_0^{n-1}(2 - n) - \varepsilon W_t\right)\right) \left(12t - n(n-1)(n-2)x_0^{n-4}\right) ,$$

so that the zeros of $\frac{\partial F_\varepsilon}{\partial x_0} = 0$ are given by $x_0 = 0$, $x_0 = \left(\frac{12t}{n(n-1)(n-2)}\right)^{\frac{1}{n-4}}$ and the real solutions of

$$2tn(n-2)x_0^{n-1} - 8t^2x_0^3 + x_0 + 2t\varepsilon W_t = 0 \ .$$

The required result then follows. □

5.6 Perfect Sets

In this section we discuss the notion of perfect sets and the relationship with the set of turbulent times. We begin with some necessary background work concerning the Strong Markov Property and the *reflection principle* for Brownian motion.

5.6.1 The Reflection Principle

Theorem 5.6.1 (Strong Markov Property). *Let $(W_t)_{t\geq 0}$ be a Wiener process on the probability space $(\Omega, \mathcal{F}, \mathbb{P})$ with filtration $\{\mathcal{F}_t\}$, and let τ be a finite-valued $\mathcal{F}_t$ stopping time. Then the process*

$$W_t^* = W_{\tau+t} - W_\tau \ , \qquad t \geq 0,$$

is a Wiener process independent of $\mathcal{F}_\tau$.

Proof. See [44]. □

We define the processes

$$M(t) := \max\{W_s : 0 \leq s \leq t\} \ ,$$

and

$$m(t) := \min\{W_s : 0 \leq s \leq t\} \ .$$

If the path W_s is replaced by $-W_s$ then the maximum and minimum are interchanged and negated. But $-W_s$ is again a Wiener process so that

$$M(t) \stackrel{\text{Dist}}{=} -m(t) \ . \tag{5.6.1}$$

In addition we define the *hitting time* of a by

$$H_a := \inf\{t > 0 : W_t = a\} \ .$$

Let us now state the so-called *reflection principle* for Brownian motion.

Proposition 5.6.2 (Reflection Principle). *For fixed $a \in \mathbb{R}$, the process*

$$\tilde{W}_t := \begin{cases} W_t & t < H_a \\ 2a - W_t & t \geq H_a \end{cases} ,$$

is a Wiener process. The process $\tilde{W}_t$ is illustrated in Figure 5.6.

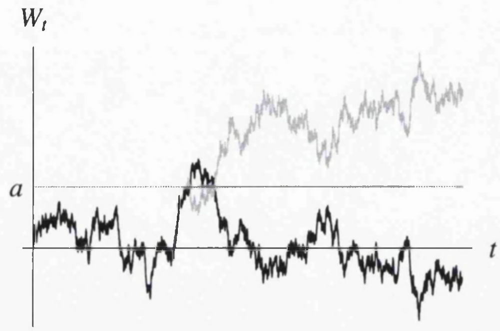

Figure 5.6: Sample path and its reflection

Proof. Following [44] we consider the processes $Y_t := W_t$ $(0 \leq t \leq H_a)$ and $Z_t := W_{t+H_a} - a$. By the Strong Markov Property, Z_t is a Wiener process independent of Y_t. Thus $-Z_t$ is a Wiener process independent of Y and so $(Y_t, Z_t) \overset{\text{Dist}}{=} (Y_t, -Z_t)$.

The map

$$\phi : (Y, Z) \to \left(Y_t \mathcal{X}_{\{t \leq H_a\}} + (a + Z_{t-H_a})\mathcal{X}_{\{t > H_a\}}\right)_{t \geq 0} ,$$

produces a continuous process, which will therefore have the same law as $\phi(Y, -Z)$. But $\phi(Y, Z) = W_t$ and $\phi(Y, -Z) = \tilde{W}_t$. □

Corollary 5.6.3.

$$\mathbb{P}[H_a \leq t] = \mathbb{P}[M_t \geq a] = 2\mathbb{P}[W_t \geq a] = 2 - 2\Phi(at^{-\frac{1}{2}}) , \tag{5.6.2}$$

where $\Phi(\cdot)$ is the $N(0,1)$ distribution function.

Proof. We first observe that for $y \geq 0$

$$\begin{aligned}\mathbb{P}[M_t \geq a, W_t \leq a - y] &= \mathbb{P}[M_t \geq a, \tilde{W}_t \leq a - y] \\ &= \mathbb{P}[W_t \geq a + y] .\end{aligned}$$

Thus

$$\begin{aligned}\mathbb{P}[H_a \leq t] &= \mathbb{P}[M_t \geq a] \\ &= \mathbb{P}[M_t \geq a, W_t \leq a] + \mathbb{P}[M_t \geq a, W_t \geq a] \\ &= \mathbb{P}[W_t \geq a] + \mathbb{P}[W_t \geq a] = 2 - 2\Phi(at^{-\frac{1}{2}}) .\end{aligned}$$

□

5.6.2 Level Sets of the Wiener Process

Definition 5.6.1. A closed set X is called *perfect* if every point of X is an *accumulation point* of X. Equivalent characterisations are:

i). X is closed and contains no isolated points,

ii). X is closed and dense in itself.

We are interested in the properties of the zero level set of the Wiener process,

$$\mathcal{Z}_0 := \{t \geq 0 : W_t = 0\} .$$

In particular we wish to show that the set $\mathcal{Z}_0$ is perfect. It follows immediately from the continuity of the path W_t that $\mathcal{Z}_0$ will be closed. Moreover with probability one $\mathcal{Z}_0$ has Lebesgue measure zero. This follows from Fubini's theorem,

$$\begin{aligned} \mathbb{E}\left[\mu(\mathcal{Z}_0)\right] &= \mathbb{E}\left[\int_0^\infty \mathcal{X}_{\{W_t=0\}}\,\mathrm{d}t\right] \\ &= \int_0^\infty \mathbb{E}\left[\mathcal{X}_{\{W_t=0\}}\right]\,\mathrm{d}t \\ &= \int_0^\infty \mathbb{P}\left[W_t = 0\right]\,\mathrm{d}t = 0 , \end{aligned}$$

where $\mu(\mathcal{Z}_0)$ is the Lebesgue measure of $\mathcal{Z}_0$.

Lemma 5.6.4. *With probability one, W_t has infinitely many zeros in every time interval $(0, \epsilon)$, where $\epsilon > 0$.*

Proof. From Equation (5.6.2), $\mathbb{P}[M_\epsilon > 0] = 1$ so that $\mathbb{P}[m_\epsilon < 0] = 1$, by Equation (5.6.1). Since W_t is continuous it follows from the intermediate value theorem that W_t will have at least one zero on $(0, \epsilon]$ almost surely. Thus for each $k \in \mathbb{N}$ there exists at least one zero in $(0, \frac{1}{k})$ almost surely. But now we can find a zero $t_1 \in (0, 1)$, then by choosing k large enough so that $\frac{1}{k} < t_1$ we can find a zero $t_2 \in (0, \frac{1}{k})$, and so on. Thus with probability one we can find an infinite sequence $\{t_n\}$ of zeros converging to zero. □

We now state and prove the main result concerning $\mathcal{Z}_0$. Variations of the following argument may be found in [27], [32] and [20].

Proposition 5.6.5. *With probability one, the set $\mathcal{Z}_0$ is a perfect set.*

Proof. We already know $\mathcal{Z}_0$ is closed so it remains to show that for every $t \in \mathcal{Z}_0$ there is a sequence of distinct elements $t_n \in \mathcal{Z}_0$ such that $\lim_{n\to\infty} t_n = t$.

Consider $q \in \mathbb{Q}^+$ and define

$$H_0^q := \inf\{t \geq q : W_t = 0\} .$$

Since $W_q \neq 0$ almost surely, then H_0^q is well defined and $H_0^q > q$ almost surely. By the Strong Markov Property and Lemma 5.6.4, $W[H_0^q + t] - W[H_0^q]$ will have infinitely many zeros in the time interval $(0, \epsilon)$. But $W[H_0^q] = 0$ and $\mathbb{Q}^+$ is countable so that W_t will have infinitely many zeros in every interval $(H_0^q, H_0^q + \epsilon)$ where $q \in \mathbb{Q}+$ and $\epsilon > 0$.

To conclude we let t be any zero of the path. If there exists an increasing sequence t_n of zeros such that $t_n \nearrow t$ then we are done. If not then there will exist an interval $(t - \epsilon, t)$ which is free of zeros for some $\epsilon > 0$. But now there exists a rational $q \in (t - \epsilon, t)$ so that $H_0^q = t$. Hence by the preceding discussion there exists a decreasing sequence of zeros $\{t_n\}$ such that $t_n \searrow t$. □

An immediate consequence of the above and the strong Markov property is the following corollary.

Corollary 5.6.6. *For each c, the set*

$$\mathcal{Z}_c := \{t \geq 0 : W_t = c\} \ ,$$

is almost surely a perfect set.

5.6.3 Turbulent Times and Perfect Sets

Let us assume for the moment that the Wiener process is one of the stochastic processes whose zeros determine the turbulent times. Then it follows from Proposition 5.6.5 that the set of turbulent times will contain a perfect set. Of course we are more interested in the set of zeros of the stochastic process

$$Y_t = -\varepsilon\alpha_i W_t + \varepsilon^2 W_t \int_0^t W_u \, \mathrm{d}u - \frac{\varepsilon^2}{2}\int_0^t W_u^2 \, \mathrm{d}u - c \ ,$$

where α_i and c are time independent constants. It may be shown that Y_t is a continuous semi-martingale. This follows by applying the product rule,

$$\mathrm{d}\left[W_t \int_0^t W_u \, \mathrm{d}u\right] = \mathrm{d}W_t \int_0^t W_u \, \mathrm{d}u + W_t^2 \, \mathrm{d}t \ ,$$

so that

$$Y_t = -\varepsilon\alpha_i W_t + \varepsilon^2 \int_0^t \left(\int_0^u W_s \, \mathrm{d}s\right) \mathrm{d}W_u + \frac{\varepsilon^2}{2}\int_0^t W_u^2 \, \mathrm{d}u - c \, .$$

In Section VI.(1.26) of [40], Revuz and Yor show that the set $\mathcal{Z}_0(\omega) = \{t : M_t(\omega) = 0\}$, where M_t is a continuous $\mathcal{F}_t$-martingale with $M_0 = 0$, is a perfect set. It is possible that this result may be extended to cover the case of a continuous semi-martingale. However for our notion of turbulent behaviour the following argument will suffice.

We use the law of the iterated logarithm, namely

$$\limsup_{t \searrow s} \frac{W_t - W_s}{h(t-s)} = 1 \quad \text{a.s.},$$

and

$$\liminf_{t \searrow s} \frac{W_t - W_s}{h(t-s)} = -1 \quad \text{a.s.},$$

where $h(s) := \left(2s \log\log\left(\frac{1}{s}\right)\right)^{\frac{1}{2}}$. Now

$$\begin{aligned} Y_t - Y_s &= -\varepsilon\alpha_i(W_t - W_s) + \varepsilon^2 W_t \int_0^t W_u \, \mathrm{d}u - \varepsilon^2 W_s \int_0^s W_u \, \mathrm{d}u - \frac{\varepsilon^2}{2}\int_s^t W_u^2 \, \mathrm{d}u \\ &= -\varepsilon\alpha_i(W_t - W_s) + \varepsilon^2(W_t - W_s)\int_0^t W_u \, \mathrm{d}u + \varepsilon^2 W_s \int_s^t W_u \, \mathrm{d}u - \frac{\varepsilon^2}{2}\int_s^t W_u^2 \, \mathrm{d}u \, . \end{aligned}$$

Hence by the law of the iterated logarithm and continuity it follows that with probability one there will exist a sequence $\{t_k\}_{k=1,2,\dots}$ such that

$$\lim_{t_k \searrow s} \frac{Y_{t_k} - Y_s}{h(t_k - s)} = \left(-\varepsilon\alpha_i + \varepsilon^2 \int_0^s W_u \, du \right) .$$

Similarly with probability one there exists a sequence $\{s_k\}_{k=1,2,\dots}$ such that

$$\lim_{s_k \searrow s} \frac{Y_{t_k} - Y_s}{h(t_k - s)} = - \left(-\varepsilon\alpha_i + \varepsilon^2 \int_0^s W_u \, du \right) .$$

But with probability one, $-\varepsilon\alpha_i + \varepsilon^2 \int_0^s W_u \, du \neq 0$ for $\varepsilon \neq 0$, so that $\limsup \frac{Y_t - Y_s}{h(t-s)}$ and $\liminf \frac{Y_t - Y_s}{h(t-s)}$ are non-zero and have opposite signs. Hence if we choose s such that $Y_s = 0$ (we know there will exist such an s by the work in Section 5.7) then there will be infinitely many changes of sign in a neighbourhood of s. This illustrates the turbulent nature of the process.

Remark 5.6.1. Since we have used the law of the iterated logarithm there will be a set of measure zero of times at which it will fail. Thus we are unable to claim that the set $\{t : Y_t = 0\}$ is perfect, but our result is sufficient to prove the turbulent nature.

5.7 Intermittence of Turbulence

The work in this section is based upon ideas by David Williams concerning Strassen's law of the iterated logarithm. We begin by stating Strassen's result and providing a (brief) sketch proof. Full details may be found on pages 49–68 of [20] or in the original account [49] by Strassen.

Definition 5.7.1. A subset H of $C[0,1]$ is *compact* if and only if every sequence in H has a convergent subsequence whose limit is in H. H is said to be *relatively compact* if each subsequence converges to a limit not necessarily in H.

Definition 5.7.2. Let K be the set of absolutely continuous functions f on $[0,1]$ with $f(0) = 0$ and $\int_0^1 f'(u) \, du \leq 1$. We refer to such functions as **Strassen functions**.

Remark 5.7.1. It may be shown, see [20], that the set K is compact.

Theorem 5.7.1 (Strassen's Law of the Iterated Logarithm). *Define*

$$Z_n(t) := (2n \log\log n)^{-\frac{1}{2}} W_{nt}(\omega) ,$$

for $0 \leq t \leq 1$ *where* W_t *is the Wiener process on the probability triple* $(\Omega, \mathcal{F}, \mathbb{P})$. *For* $n \geq 3$, Z_n *may be viewed as a measurable map from* $(\Omega, \mathcal{F})$ *to* $(C[0,1], \mathcal{B}[0,1])$, *where* $\mathcal{B}[0,1]$ *is the Borel* σ*-field in* $C[0,1]$, *and for almost all* ω *the indexed subset*

$$\{Z_n(\cdot, \omega) : n = 3, 4, \dots\} ,$$

of $C[0,1]$ *is relatively compact with limit set* K.

Proof. The proof is divided into three parts:

Part (1) (Show Z_n approaches K)
Define a system $Z_{n,m}(\cdot,\omega) \in C[0,1]$ by the requirements

- $Z_{n,m}\left(\frac{i}{m},\omega\right) = Z_n\left(\frac{i}{m},\omega\right)$ for $i = 0,1,\dots,m$,
- $Z_{n,m}(\cdot,\omega)$ is linear on $\left[\frac{i-1}{m},\frac{i}{m}\right]$ for $i = 1,2,\dots,m$.

Let $a > 1, b > 1$ and make the following set definitions.

i). $G_1(a,b,m)$ is the set of $\omega \in \Omega$ for which there exists a $J_1(a,b,m,\omega) < \infty$ such that $j \geq J_1$ implies $a^{-1}Z_{b^j,m}(\cdot,\omega) \in K$.

ii). $G_2(\epsilon,b,m)$ is the set of $\omega \in \Omega$ for which there exists a $J_2(\epsilon,b,m,\omega) < \infty$ such that $j \geq J_2$ implies $\|Z_{b^j,m}(\cdot,\omega) - Z_{b^j}(\cdot,\omega)\| \leq \epsilon$.

iii). $G_3(\delta,b)$ is the set of $\omega \in \Omega$ for which there exists a $J_3(\delta,b,\omega) < \infty$ such that $j \geq J_3$ implies $b^{j-1} \leq n < b^j$ implies $\|Z_n(\cdot,\omega) - b(n,j)Z_{b^j}(\cdot,\omega)\| \leq \delta$ where $\delta > 0$, $b > 1$ and $b(n,j) = (n\log\log n)^{-\frac{1}{2}}(b^j\log\log b^j)^{\frac{1}{2}}$.

iv). $G_4(\eta)$ is the set of $\omega \in \Omega$ for which there exists an $N = N(\eta,\omega) < \infty$ such that $n \geq N$ implies $d(Z_n(\cdot,\omega),K) < \eta$.

Essentially it may be shown that $G_i \in \mathfrak{F}$ and $\mathbb{P}(G_i) = 1$ for $i = 1,\dots,4$. Hence if $G_5 := \bigcap_{n=1}^{\infty} G_4\left(\frac{1}{n}\right)$ then $G_5 \in \mathfrak{F}$ and $\mathbb{P}(G_5) = 1$. But G_5 is the set of $\omega \in \Omega$ such that $\lim_{n\to\infty} d(Z_n(\cdot,\omega),K) = 0$, thus

$$\mathbb{P}\left[\lim_{n\to\infty} d(Z_n(\cdot,\omega),K) = 0\right] = 1 \; . \tag{5.7.1}$$

Part (2) (Show Z_n approaches a countable dense subset of K)
For $m = 1,2,\dots$, let C_m be the set of $f \in C[0,1]$ such that:

- $f(0) = 0$
- $f(\frac{i}{m})$ is rational for $i = 1,\dots,m$,
- f is linear on $[\frac{i-1}{m},\frac{i}{m}]$ for $i = 1,\dots,n$,
- $\int_0^1 f'(u)^2\,du < 1$.

If $C = \bigcup_{m=1}^{\infty} C_m$ then C is a countable subset of K. Moreover it may be shown that C is dense in K. Take $\epsilon > 0$ and $f \in C$ and let $A(f,\epsilon)$ be the set of $\omega \in \Omega$ such that

$$\|Z_n(\cdot,\omega) - f\| < \epsilon \; ,$$

for infinitely many n. It may be shown that $A(f,\epsilon) \in \mathfrak{F}$ and $\mathbb{P}[A(f,\epsilon)] = 1$. Thus if we now define

$$\mathcal{A} := \bigcap \left\{A(f,\tfrac{1}{n}) : f \in C \text{ and } n = 1,2,\dots\right\} \; ,$$

then $\mathcal{A} \in \mathcal{F}$ and $\mathbb{P}[\mathcal{A}] = 1$. But $\mathcal{A}$ is the set of $\omega \in \Omega$ such that

$$\liminf_{n\to\infty} \|Z_n(\cdot,\omega) - f\| = 0 \ ,$$

for all $f \in C$. Thus

$$\mathbb{P}\left[\liminf_{n\to\infty} \|Z_n(\cdot,\omega) - f\| = 0\right] = 1 \ , \tag{5.7.2}$$

for all $f \in C$, which is a countable dense subset of K.

Part (3) (Conclusion) Consider the space $C[0,1]^\infty$ of sequences $\phi = (\phi_0, \phi_1, \dots)$ of elements of $C[0,1]$. Let H be a compact subset of $C[0,1]$ and H^* be the set of $\phi \in C[0,1]^\infty$ such that the indexed subset $(\phi_n : n = 0, 1, \dots)$ of $C[0,1]$ is relatively compact, with limit set H. Define

$$A := \{\phi : \phi \in C[0,1]^\infty \text{ and } \limsup_{n\to\infty} d(\phi_n, H) = 0 \text{ and } \liminf_{n\to\infty} d(\phi_n, g) = 0 \text{ for all } g \in H_0\} \ ,$$

where H_0 is a countable dense subset of H. It may be shown that

$$H^* = A \ . \tag{5.7.3}$$

The desired result follows for Equations (5.7.1), (5.7.2) and (5.7.3). □

Theorem 5.7.2. *Consider the stochastic process*

$$Y_t(\omega) := -\alpha_i \varepsilon W_t + \varepsilon^2 W_t \int_0^t W_u \,\mathrm{d}u - \frac{\varepsilon^2}{2} \int_0^t W_u^2 \,\mathrm{d}u - c \ ,$$

where $W_t(\omega)$ is a Wiener process starting at zero, c is a real constant and α_i are time independent. Then there exists a sequence (t_n) of times with $t_n \nearrow \infty$ such that $Y_{t_n} = 0$ for every n almost surely.

Proof. We begin by finding a sequence of times tending to infinity at which $Y_t \geq 0$. Define $f(r) := r$ for $0 \leq r \leq 1$ so that clearly f is absolutely continuous, $f(0) = 0$ and $\int_0^1 f'(u)^2 \,\mathrm{d}u \leq 1$. Thus $f(r)$ is a Strassen function.

Hence by Strassen's Law of the Iterated Logarithm we know that after throwing away a null set of paths, we can path-wise find a sequence t_n such that if

$$h(t) := (2t \ln\ln t)^{\frac{1}{2}} \ ,$$

then

$$h(t_n)^{-1} W_{rt_n} \to f(r) \ ,$$

uniformly over r in $[0,1]$.

We show that for each ω with $t_n = t_n(\omega)$ we have $h(t_n)^{-2} t_n^{-1} Y_{t_n} \to \frac{\varepsilon^2}{3}$. Let us consider each of the terms that comprise the stochastic process $Y_t(\omega)$.

i).

$$\alpha_i h(t_n)^{-2} t_n^{-1} W_{t_n} \to 0 \ .$$

ii).

$$h(t_n)^{-2}t_n^{-1}W_{t_n}\int_0^{t_n} W_u\,\mathrm{d}u = h(t_n)^{-1}W_{t_n}\int_0^1 h(t_n)^{-1}W_{rt_n}\,\mathrm{d}r$$
$$\to f(1)\int_0^1 f(r)\,\mathrm{d}r = \frac{1}{2}\,.$$

iii).

$$-\frac{1}{2}h(t_n)^{-2}t_n^{-1}\int_0^{t_n} W_u^2\,\mathrm{d}u = -\frac{1}{2}\int_0^1 \left(h(t_n)^{-1}W_{rt_n}\right)^2\mathrm{d}r$$
$$\to -\frac{1}{2}\int_0^1 f(r)^2\,\mathrm{d}r = -\frac{1}{6}\,.$$

Combining the above we see that for each ω with $t_n = t_n(\omega)$ we have

$$h(t_n)^{-2}t_n^{-1}Y_{t_n} \to \varepsilon^2\left(\frac{1}{2}-\frac{1}{6}\right) = \frac{\varepsilon^2}{3}\,.$$

To conclude we must find a sequence of times tending to infinity at which $Y_t \leq 0$. If $c > 0$ then we simply choose times when $W_t = 0$. For $c \leq 0$ we must choose a Strassen function such that

$$h(t_n)^{-2}t_n^{-1}W_{t_n}\int_0^{t_n} W_s\,\mathrm{d}s \to f(1)\int_0^1 f(r)\,\mathrm{d}r < 0\,.$$

Taking

$$f(r) = \begin{cases} r & \text{for } 0 \leq r \leq \frac{1}{3}\,, \\ \frac{2}{3} - r & \text{for } \frac{1}{3} \leq r \leq 1\,, \end{cases}$$

it may be easily shown that $f \in K$ and $f(1)\int_0^1 f(u)\,\mathrm{d}u = -\frac{1}{54} < 0$. □

Remark 5.7.2. The recurrent nature of the process Y_t coupled with the fact that there will be infinitely many changes of sign in a neighbourhood of s where $Y_s = 0$ produces the intermittency of turbulence mentioned in Proposition 5.5.1. Essentially we witness the occurrence of bouts of turbulence.

5.8 Explicit Examples

5.8.1 The Cusp Singularity

Consider $S_0(\boldsymbol{x}_0) = \frac{1}{2}x_0^2 y_0$ so that setting $f \equiv 0$ and $g(x_0) := \frac{1}{2}x_0^2$ in Equations (5.5.1) and (5.5.2) yields

$$F_\varepsilon(x_0,t) = \frac{t^3}{2}x_0^6 - \frac{3}{8}tx_0^4 - t^2x_0^3\varepsilon W_t + \varepsilon^2 W_t\int_0^t W_u\,\mathrm{d}u - \frac{\varepsilon^2}{2}\int_0^t W_u^2\,\mathrm{d}u\,,$$

and

$$\frac{\partial F_\varepsilon}{\partial x_0}(x_0,t) = \frac{3}{2}tx_0^2\left(2t^2x_0^3 - x_0 - 2t\varepsilon W_t\right) \ .$$

Hence the turbulent times are given by the solutions of

$$\varepsilon^2 W_t \int_0^t W_u \,\mathrm{d}u - \frac{\varepsilon^2}{2}\int_0^t W_u^2 \,\mathrm{d}u - c = 0 \tag{5.8.1}$$

and

$$\xi_t(\omega) = 0 \ ,$$

where $\xi_t(\omega) := F_\varepsilon(\tilde{x}_0^i(t,\omega),t) - c$, $\tilde{x}_0^i(t,\omega)$ being the real solutions of the cubic

$$2t^2x_0^3 - x_0 - 2t\varepsilon W_t = 0 \ . \tag{5.8.2}$$

It follows from Equation (5.8.1) and Theorem 5.7.2 with $\alpha_i = 0$ that the turbulence at $\Phi_{t(\omega)}(0, -\frac{1}{t(\omega)})$ is intermittent and recurrent.

In order to analyse the remaining turbulent times we must solve the cubic in Equation (5.8.2). Adopting the method outlined in [38] we consider the reduced cubic

$$ax_0^3 - 3a\delta^2 x_0 + y_N = 0 \ , \tag{5.8.3}$$

where in our case $a = 2t^2$, $3a\delta^2 = 1$ and $y_N = -2t\varepsilon W_t$. Hence $\delta^2 = \frac{1}{6t^2}$. Using the identity

$$(p+q)^3 - 3pq(p+q) - (p^3+q^3) \equiv 0 \ ,$$

we see that $x_0 = p + q$ is a solution where

$$pq = \delta^2 \qquad \text{and} \qquad p^3 + q^3 = -\frac{y_N}{a} \ . \tag{5.8.4}$$

Solving the above equations yields a quadratic in p^3 which may be solved to obtain

$$p^3 = \frac{1}{36t^3}\left(18t^2\varepsilon W_t \pm \sqrt{324t^4\varepsilon^2 W_t^2 - 6}\right) \ .$$

There are two cases we need to consider:

Case 1: $\varepsilon^2 W_t^2 > \frac{1}{54t^4}$. Here the cubic has one real solution given by

$$\begin{aligned} x_0 &= p + \delta^2 p^{-1} \\ &= \frac{6^{\frac{1}{3}} + \left(18t^2\varepsilon W_t + \sqrt{324t^4\varepsilon^2 W_t^2 - 6}\right)^{\frac{2}{3}}}{6^{\frac{2}{3}}t\left(18t^2\varepsilon W_t + \sqrt{324t^4\varepsilon^2 W_t^2 - 6}\right)^{\frac{1}{3}}} \ . \end{aligned}$$

For large t it is evident that $x_0 \sim 0$ so that

$$F_\varepsilon(x_0(\omega,t),t) \sim \varepsilon^2 W_t \int_0^t W_u \,\mathrm{d}u - \frac{\varepsilon^2}{2}\int_0^t W_u^2 \,\mathrm{d}u \ .$$

Hence as before we expect the turbulence will be recurrent.

Case 2: $\varepsilon^2 W_t^2 < \frac{1}{54t^4}$. In this case the cubic will have three real solutions. These are found by substituting $x_0 = 2\delta\cos\theta$ in Equation (5.8.3), giving

$$2a\delta^3\left(4\cos^3\theta - 3\cos\theta\right) + y_N = 0 \ .$$

Hence

$$\cos 3\theta = -\frac{y_N}{2a\delta^3} = 3\sqrt{6}t^2\varepsilon W_t \ ,$$

so that

$$\theta = \frac{1}{3}\arccos\left(3\sqrt{6}t^2\varepsilon W_t\right) \ .$$

Thus the solutions of the cubic are given by

$$\begin{aligned} x_0 &= 2\delta\cos\left(\theta + \frac{2k\pi}{3}\right) \\ &= \frac{1}{t}\sqrt{\frac{2}{3}}\cos\left[\frac{1}{3}\arccos\left(3\sqrt{6}t^2\varepsilon W_t\right) + \frac{2k\pi}{3}\right] \ , \end{aligned}$$

for $k = 0, 1, 2$. Hence $x_0 \sim 0$ for large t and we arrive at the same stochastic process as in Case 1.

5.8.2 Polynomial Swallowtail

Let us now consider the polynomial swallowtail initial condition $S_0(\boldsymbol{x_0}) = x_0^5 + x_0^2 y_0$. Setting $f(x_0) := x_0^5$ and $g(x_0) := x_0^2$ in Equations (5.5.1) and (5.5.2) yields

$$\begin{aligned} F_\varepsilon(x_0, t) = \frac{225}{2}tx_0^8 - 60t^2x_0^7 + 8t^3x_0^6 + 6x_0^5 + \left(15\varepsilon t W_t - \frac{3t}{2}\right)x_0^4 - 4\varepsilon t^2 W_t x_0^3 \\ + \varepsilon^2 W_t \int_0^t W_u \,\mathrm{d}u - \frac{\varepsilon^2}{2}\int_0^t W_u^2 \,\mathrm{d}u \ , \end{aligned}$$

and

$$\frac{\partial F_\varepsilon}{\partial x_0} = 6x_0^2\left(-30tx_0^4 + 8t^2x_0^3 - x_0 - 2t\varepsilon W_t\right)(t - 5x_0) \ .$$

The solutions of $\frac{\partial F_\varepsilon}{\partial x_0} = 0$ are $x_0 = 0$, $x_0 = \frac{t}{5}$ and the solutions $\tilde{x}_0^i(\omega, t)$ of the quartic

$$30tx_0^4 - 8t^2x_0^3 + x_0 + 2t\varepsilon W_t = 0 \ . \tag{5.8.5}$$

Thus the turbulent times are given by the solutions of

$$\varepsilon^2 W_t \int_0^t W_u \,\mathrm{d}u - \frac{\varepsilon^2}{2}\int_0^t W_u^2 \,\mathrm{d}u - c = 0 \ , \tag{5.8.6}$$

$$\frac{1}{31250}t^9 - \left(\frac{\varepsilon W_t}{125} + \frac{3}{6250}\right)t^5 + \varepsilon^2 W_t \int_0^t W_u \,\mathrm{d}u - \frac{\varepsilon^2}{2}\int_0^t W_u^2 \,\mathrm{d}u - c = 0 \ , \tag{5.8.7}$$

and

$$F_\varepsilon(\tilde{x}_0^i(\omega, t), t) = c \ . \tag{5.8.8}$$

The process in Equation (5.8.6) is recurrent by Theorem 5.7.2. For the process in Equation (5.8.7) it follows from the large time behaviour of W_t that for large t the process is dominated by the t^9 term. Hence the process will not be recurrent.

Turning our attention to the quartic in Equation (5.8.5) we remark that solving it explicitly yields an extremely complicated expression. Instead we opt to analyse the equation numerically as illustrated in the table below.

t	Solutions		
10^{14}	-0.0000195743	2.66667×10^{13}	$9.78717 \times 10^{-6} \pm 0.0000169519i$
10^{15}	-9.0856×10^{-6}	2.66667×10^{14}	$4.5428 \times 10^{-6} \pm 7.86836 \times 10^{-6}i$
10^{16}	-4.21716×10^{-6}	2.66667×10^{15}	$2.10858 \times 10^{-6} \pm 3.65217 \times 10^{-6}i$
10^{17}	-1.95743×10^{-6}	2.66667×10^{16}	$0 \pm 1.69519 \times 10^{-6}i$
10^{18}	0	2.66667×10^{17}	0

We expect three of the solutions to tend to zero whilst the other tends to infinity. Hence for large t we expect the equation to behave like $8x_0^3 = 0$. This has solution $x_0 = 0$ (3 times) so that for large t, $F_\varepsilon(\tilde{x}_0^i(\omega,t),t) - c$ behaves like the recurrent process $\varepsilon^2 W_t \int_0^t W_u \, du - \frac{\varepsilon^2}{2}\int_0^t W_u^2 \, du - c$.

In summary the stochastic processes in Equations (5.8.6) and (5.8.8) will be recurrent, but the process in Equation (5.8.7) will not.

5.9 A Unifying Approach

In this section we aim to expound upon the ideas of Chapter 4. We will discuss how the method employed in Chapter 4 to analyse hot and cool parts of the caustic may be extended to study intermittence of turbulence.

Let $\boldsymbol{x} = (x^1, x^2, \ldots, x^n)$ and $\boldsymbol{x}_0 = (x_0^1, x_0^2, \ldots, x_0^n)$. We know that

$$\boldsymbol{x} = \Phi_t \boldsymbol{x}_0 \iff \nabla_{\boldsymbol{x}_0} \mathcal{A}(\boldsymbol{x}_0, \boldsymbol{x}, t) = 0 \ .$$

Assume that $\frac{\partial^2 \mathcal{A}}{(\partial x_0^i)^2} \neq 0$ for $i = 2, 3, \ldots, n$, so that

$$\frac{\partial \mathcal{A}}{\partial x_0^n}(x_0^1, x_0^2, \ldots, x_0^n, \boldsymbol{x}, t) = 0 \iff x_0^n = x_0^n(\boldsymbol{x}, x_0^1, x_0^2, \ldots, x_0^{n-1}, t) \ .$$

Using the shorthand notation $x_0^n(\ ) = x_0^n(\boldsymbol{x}, x_0^1, x_0^2, \ldots, x_0^{n-1}, t)$ we see

$$\frac{\partial \mathcal{A}}{\partial x_0^{n-1}}\left(x_0^1, x_0^2, \ldots, x_0^{n-1}, x_0^n(\ ), t\right) = 0 \iff x_0^{n-1} = x_0^{n-1}(\boldsymbol{x}, x_0^1, \ldots, x_0^{n-2}, t) \ ,$$
$$\frac{\partial \mathcal{A}}{\partial x_0^{n-2}}\left(x_0^1, x_0^2, \ldots, x_0^{n-1}(\ ), x_0^n((\ )), t\right) = 0 \iff x_0^{n-2} = x_0^{n-2}(\boldsymbol{x}, x_0^1, \ldots, x_0^{n-3}, t) \ ,$$

which eventually leads to

$$\frac{\partial \mathcal{A}}{\partial x_0^2}\left(x_0^1, x_0^2, x_0^3(\ ), x_0^4((\ )), \ldots, x_0^n(((\cdots))), t\right) = 0 \iff x_0^2 = x_0^2(\boldsymbol{x}, x_0^1, t) \ .$$

Using back substitution we have

$$\begin{aligned}
x_0^2 &= x_0^2(\boldsymbol{x}, x_0^1, t) = x_0^2(\,)\ , \\
x_0^3 &= x_0^3(\boldsymbol{x}, x_0^1, x_0^2, t) = x_0^3(\boldsymbol{x}, x_0^1, x_0^2(\,), t)) = x_0^3((\,))\ , \\
x_0^4 &= x_0^4(\boldsymbol{x}, x_0^1, x_0^2, x_0^3, t) = x_0^4(\boldsymbol{x}, x_0^1, x_0^2(\,), x_0^3((\,))) = x_0^4(((\,)))\ , \\
&\vdots \\
x_0^n &= x_0^n\left(\boldsymbol{x}, x_0^1, x_0^2(\,), x_0^3((\,)), \ldots, x_0^{n-1}(((\cdots)))\right)\ .
\end{aligned}$$

Thus substituting these $n-1$ expressions into $\mathcal{A}(\boldsymbol{x}_0, \boldsymbol{x}, t)$ we define the function

$$f(x_0^1, \boldsymbol{x}, t) := \mathcal{A}\left(x_0^1, x_0^2(\,), x_0^3((\,)), \ldots, x_0^{n-1}(((\cdots))), \boldsymbol{x}, t\right),$$

where we recall that f was the function we defined and studied in Chapter 4.

By the method of stationary phase and repeated integration we have

$$\begin{aligned}
&\int_{\mathbb{R}} \cdots \int_{\mathbb{R}} T_0(\boldsymbol{x}_0) \exp\left\{-\frac{i}{\mu^2}\mathcal{A}(\boldsymbol{x}_0, \boldsymbol{x}, t)\right\} \mathrm{d}x_0^n\, \mathrm{d}x_0^{n-1} \ldots \mathrm{d}x_0^1 \\
&\sim \left(2\pi\mu^2\right)^{\frac{1}{2}} e^{\pm\frac{i\pi}{4}} \int_{\mathbb{R}} \cdots \int_{\mathbb{R}} T_0(x_0^1, x_0^2, \ldots, x_0^n(\,)) \left(\frac{\partial^2 \mathcal{A}}{(\partial x_0^n)^2}(x_0^1, x_0^2, \ldots, x_0^n(\,), \boldsymbol{x}, t)\right)^{-\frac{1}{2}} \\
&\qquad \times \exp\left\{-\frac{i}{\mu^2}\mathcal{A}\left(x_0^1, x_0^2, \ldots, x_0^n(\,), \boldsymbol{x}, t\right)\right\} \mathrm{d}x_0^{n-1} \ldots \mathrm{d}x_0^1 \\
&\sim \left(2\pi\mu^2\right)^{\frac{2}{2}} e^{\pm\frac{i\pi}{4}} e^{\pm\frac{i\pi}{4}} \int_{\mathbb{R}} \cdots \int_{\mathbb{R}} T_0(x_0^1, \ldots, x_0^{n-1}(\,), x_0^n((\,))) \\
&\qquad \times \left(\frac{\partial^2 \mathcal{A}}{(\partial x_0^n)^2}(x_0^1, \ldots, x_0^{n-1}(\,), x_0^n((\,)), \boldsymbol{x}, t)\right)^{-\frac{1}{2}} \\
&\qquad \times \left(\frac{\partial^2 \mathcal{A}}{(\partial x_0^{n-1})^2}(x_0^1, \ldots, x_0^{n-1}(\,), x_0^n((\,)), \boldsymbol{x}, t)\right)^{-\frac{1}{2}} \\
&\qquad \times \exp\left\{-\frac{i}{\mu^2}\mathcal{A}\left(x_0^1, \ldots, x_0^{n-1}(\,), x_0^n((\,)), \boldsymbol{x}, t\right)\right\} \mathrm{d}x_0^{n-2} \ldots \mathrm{d}x_0^1 \\
&\sim \left(2\pi\mu^2\right)^{\frac{n-1}{2}} e^{\sum_{k=1}^{n-1}\nu_k\frac{i\pi}{4}} \int_{\mathbb{R}} \tilde{T}_0(x_0^1, \boldsymbol{x}, t) \left(\prod_{i=2}^{n} \frac{\partial^2 \mathcal{A}}{(\partial x_0^i)^2}(x_0^1, x_0^2(\,), \ldots, x_0^n(((\cdots))), \boldsymbol{x}, t)\right)^{-\frac{1}{2}} \\
&\qquad \times \exp\left\{-\frac{i}{\mu^2} f(x_0^1, \boldsymbol{x}, t)\right\} \mathrm{d}x_0^1\ ,
\end{aligned}$$

where $\tilde{T}_0(x_0^1, \boldsymbol{x}, t) = T_0\left(x_0^1, x_0^2(), x_0^3((\,)), \ldots, x_0^n(((\cdots)))\right)$ and $\nu_k = \pm 1$.

If x_0^1 is a degenerate critical point then it follows that the caustic is given by

$$\begin{aligned}
\mathrm{Det}\left(\frac{\partial^2 \mathcal{A}}{\partial \boldsymbol{x}_0^2}(\boldsymbol{x}_0, \boldsymbol{x}, t)\right)\Bigg|_{\boldsymbol{x}=\Phi_t \boldsymbol{x}_0} &= \prod_{i=1}^{n} \frac{\partial^2 \mathcal{A}}{(\partial x_0^i)^2}\left(x_0^1, x_0^2(\,), \ldots, x_0^n(((\cdots)))\right) \\
&= 0\ ,
\end{aligned}$$

where the first term in the product is $f''(x_0^1, \boldsymbol{x}, t)$.

Let us now return to the two dimensional setting where $\boldsymbol{x} = (x, y) \in \mathbb{R}^2$ and $\boldsymbol{x}_0 = (x_0, y_0) \in \mathbb{R}^2$. Recalling our work in Chapter 4 on the function $f(x_0^1, \boldsymbol{x}, t)$, we see that for fixed $t > 0$ the number of cusps is given by

$$\mathcal{N}_C(t) = \left\{ \# x_0 : f(x_0, \boldsymbol{x}, t) = c \ , \ \frac{\partial f}{\partial x_0}(x_0, \boldsymbol{x}, t) = 0 \ , \ \frac{\partial^2 f}{\partial x_0^2}(x_0, \boldsymbol{x}, t) = 0 \right\} \ .$$

We have three equations in three unknowns x_0, x, y which may be solved to obtain the common points of the pre-curves $x_0(t)$. Using $f(x_0, \boldsymbol{x}, t) = c$ and $\frac{\partial f}{\partial x_0}(x_0, \boldsymbol{x}, t) = 0$ we obtain $\boldsymbol{x} = \boldsymbol{x}(x_0, t)$ so that

$$\mathcal{N}_C(t) = \left\{ \# x_0(t) : \left. \frac{\partial^2 f}{\partial x_0^2}(x_0, \boldsymbol{x}, t) \right|_{\boldsymbol{x} = \boldsymbol{x}(x_0, t)} = c \right\} \ . \tag{5.9.1}$$

It is helpful to think of the equations $f = c$, $f' = 0$ and $f'' = 0$ as being intrinsically linked with the level surface, flow mapping and caustic respectively.

If we now allow $t > 0$ to vary then $\mathcal{N}_C(t)$ will change when

$$\frac{d}{dx_0} \left[\left. \frac{\partial^2 f}{\partial x_0^2}(x_0, \boldsymbol{x}, t) \right|_{\boldsymbol{x} = \boldsymbol{x}(x_0, t)} \right] = 0 \ ,$$

that is

$$\left[\frac{\partial^3 f}{\partial x_0^3}(x_0, \boldsymbol{x}, t) + \left(\frac{\mathrm{d}\boldsymbol{x}}{\mathrm{d}x_0} . \nabla_{\boldsymbol{x}} \right) \frac{\partial^2 f}{\partial x_0^2} \right]_{\boldsymbol{x} = \boldsymbol{x}(x_0, t)} = 0 \ . \tag{5.9.2}$$

Hence the turbulent times are given by those $t(\omega)$ satisfying Equations (5.9.1) and (5.9.2). Namely if $x_0 = x_0(t)$ satisfy Equation (5.9.1) then the turbulent times are given by the solutions of

$$\left[\frac{\partial^3 f}{\partial x_0^3}(x_0, \boldsymbol{x}, t) + \left(\frac{\mathrm{d}\boldsymbol{x}}{\mathrm{d}x_0} . \nabla_{\boldsymbol{x}} \right) \frac{\partial^2 f}{\partial x_0^2} \right]_{\substack{\boldsymbol{x} = \boldsymbol{x}(x_0, t) \\ x_0 = x_0(t)}} = 0 \ .$$

We remark that the *true* turbulent times are those random times $t(\omega)$ at which the number of cusps on cool parts of the caustic changes. Of course for the cusp singularity all turbulent times are *true* turbulent times because the whole of the cusp is cool. For the polynomial swallowtail we are only interested in the number of cusps changing on the λ-shaped part of the caustic. Denoting the set of turbulent times by Turb t, it follows that the *true* turbulent times will be given by

$$t(\omega) \in \text{Turb } t \cap \{ t : \boldsymbol{x}(x_0(t), t) \in \text{Cool}(C_t) \} \ .$$

Chapter 6

Harmonic Oscillator Potential

In this chapter we no longer restrict ourselves to the case of a zero potential. Instead we consider the harmonic oscillator potential $V(\boldsymbol{x}) = \frac{1}{2}\boldsymbol{x}^T\Omega^2\boldsymbol{x}$ where Ω^2 is a real symmetric positive definite matrix. Considering both the deterministic and stochastic situations we obtain the Mehler heat kernel and corresponding stochastic Mehler heat kernel for noise potential $k(x,t) = x$. These are employed to obtain explicit expressions for the caustic and level surface under the harmonic oscillator potential. Our usual examples of the cusp and polynomial swallowtail are studied in some detail.

The chapter concludes with a discussion of hot and cool parts of the caustic and turbulent times. Several of our results from Chapters 4 and 5 are extended to include the case of the harmonic oscillator potential.

6.1 Harmonic Oscillator Potential

6.1.1 Introduction

In this chapter we study the Burgers equation

$$\frac{\partial v^\mu}{\partial t}(\boldsymbol{x},t) + (v^\mu \cdot \nabla)v^\mu = \frac{\mu^2}{2}\Delta v^\mu - \frac{1}{2}\nabla(\boldsymbol{x}^T\Omega^2\boldsymbol{x}) - \varepsilon\dot{W}_t\ ,$$

with initial velocity $v^\mu(\boldsymbol{x},0) = \nabla S_0(\boldsymbol{x})$, representing a fluid whose particles are subject to the force $(-\frac{1}{2}\nabla(\boldsymbol{x}^T\Omega^2\boldsymbol{x}) - \varepsilon\dot{W}_t)$. The corresponding Stratonovich type stochastic heat equation is

$$\frac{\partial u^\mu}{\partial t}(\boldsymbol{x},t) = \frac{\mu^2}{2}\Delta u^\mu + \frac{1}{2\mu^2}(\boldsymbol{x}^T\Omega^2\boldsymbol{x})u^\mu + \frac{\varepsilon}{\mu^2}xu^\mu \circ \dot{W}_t\ ,$$

with $u^\mu(\boldsymbol{x},0) = \exp\left(-\frac{1}{\mu^2}S_0(\boldsymbol{x})\right)$. We initially consider the deterministic case $\varepsilon \equiv 0$.

Consider the time dependent Schrödinger equation

$$i\hbar\frac{\partial}{\partial t}\psi_t(x) = \left(-\frac{\hbar^2}{2}\Delta + V(x)\right)\psi_t(x)\ ,$$

which on dividing through by $\hbar$ and re-labelling as μ^2 becomes

$$i\frac{\partial}{\partial t}\psi_t(x) = \left(-\frac{\mu^2}{2}\Delta + \frac{1}{\mu^2}V(x)\right)\psi_t(x) . \tag{6.1.1}$$

More on Schrödinger's equation and other aspects of quantum mechanics may be found in [34]. We are simply interested in the well known fact that for harmonic oscillator potential $V(x) = \frac{1}{2}\omega^2 x^2$, the Schrödinger equation has Green's function

$$G_t(x, x_0) = \sqrt{\frac{\omega}{2\pi i\mu^2\sin(\omega t)}}\exp\left(\frac{i\omega}{2\mu^2}\frac{(x^2+x_0^2)\cos(\omega t) - 2xx_0}{\sin(\omega t)}\right) , \tag{6.1.2}$$

for all positive $t \neq \frac{k\pi}{\omega}$.

It is possible, see for example [10], to reduce several types of partial differential equation to the heat equation. In particular, applying the transformations $t \mapsto it$ and $\omega \mapsto i\omega$ in Equation (6.1.1), namely setting $\tau = it$ and $\tilde{\omega} = i\omega$, yields

$$\begin{aligned}
\frac{\partial}{\partial\tau}\psi(x,t(\tau)) &= \left.\frac{\partial}{\partial t}\psi(x,t)\right|_{t=t(\tau)}\frac{\partial t}{\partial\tau} \\
&= -i\left.\frac{\partial}{\partial t}\psi(x,t)\right|_{t=t(\tau)} \\
&= \left(\frac{\mu^2}{2}\Delta + \frac{1}{2}\tilde{\omega}^2x^2\right)\psi(x,t(\tau)) .
\end{aligned}$$

Setting $u(x,\tau) = \psi(x,t(\tau))$ and re-labelling τ as t and $\tilde{\omega}$ as ω yields the heat equation with harmonic oscillator potential

$$\frac{\partial u}{\partial t}(x,t) = \left(\frac{\mu^2}{2}\Delta + \frac{1}{2}\omega^2x^2\right)u(x,t) .$$

Hence the Green's function for the heat equation with harmonic oscillator potential is found by setting $t = -it$ and $\omega = -i\omega$ in Equation (6.1.2). This gives the *Mehler heat kernel*

$$G_t(x, x_0) = \sqrt{\frac{\omega}{2\pi\mu^2\sin(\omega t)}}\exp\left(-\frac{\omega}{2\mu^2}\frac{(x^2+x_0^2)\cos(\omega t) - 2xx_0}{\sin(\omega t)}\right) . \tag{6.1.3}$$

Thus the heat equation for the harmonic oscillator potential with initial condition $u(x,0) = \exp\left(-\frac{1}{\mu^2}S_0(x)\right)$ has solution

$$\begin{aligned}
u(x,t) &= \int_{\mathbb{R}} G_t(x,x_0)\exp\left(-\frac{1}{\mu^2}S_0(x_0)\right)\,\mathrm{d}x_0 \\
&= \sqrt{\frac{\omega}{2\pi\mu^2\sin(\omega t)}}\int_{\mathbb{R}}\exp\left(-\frac{1}{\mu^2}\mathcal{A}(x_0,x,t)\right)\,\mathrm{d}x_0 ,
\end{aligned}$$

where the phase function $\mathcal{A}(x_0,x,t)$ is given by

$$\mathcal{A}(x_0,x,t) = \frac{\omega}{2}\frac{(x^2+x_0^2)\cos(\omega t) - 2xx_0}{\sin(\omega t)} + S_0(x_0) .$$

Remark 6.1.1. In practice one would obtain the Mehler heat kernel in Equation (6.1.3) directly by the method described in [4]. However, since we intend discussing the stochastic case, we have chosen a method analogous to the one we shall use in the stochastic setting.

6.1.2 Caustics and Level Surfaces

If we define the real $n \times n$ diagonal matrix Ω by

$$(\Omega)_{ij} = \begin{cases} \omega_i & \text{if } i = j, \\ 0 & \text{otherwise,} \end{cases}$$

then for a column vector $\boldsymbol{x}$ the phase function $\mathcal{A}(\boldsymbol{x}_0, \boldsymbol{x}, t)$ may be written as

$$\mathcal{A}(\boldsymbol{x}_0, \boldsymbol{x}, t) = \frac{1}{2}\boldsymbol{x}^T \Omega \cot(\Omega t)\boldsymbol{x} + \frac{1}{2}\boldsymbol{x_0}^T \Omega \cot(\Omega t)\boldsymbol{x_0} - \boldsymbol{x}^T \Omega \left[\sin(\Omega t)\right]^{-1} \boldsymbol{x_0} + S_0(\boldsymbol{x_0}) \ . \quad (6.1.4)$$

Hence the flow mapping Φ_t defined by $\nabla_{\boldsymbol{x}_0}\mathcal{A}(\boldsymbol{x}_0, \boldsymbol{x}, t) = 0$ is given by

$$\boldsymbol{x} = \cos(\Omega t)\boldsymbol{x_0} + \Omega^{-1} \sin(\Omega t) \nabla S_0(\boldsymbol{x_0}) \ . \quad (6.1.5)$$

Proposition 6.1.1. *For the deterministic case with harmonic oscillator potential the (pre-)caustic is given by*

$$\operatorname{Det}\left[\Omega \cot(\Omega t) + S_0''(\boldsymbol{x}_0)\right] = 0 \ ,$$

evaluated at $\boldsymbol{x}_0 = \Phi_t^{-1}\boldsymbol{x}$.

Proof. This follows immediately by inserting Equation (6.1.4) in the pre-caustic condition $\operatorname{Det}[\mathcal{A}''] = 0$. □

Proposition 6.1.2. *For the deterministic case with harmonic oscillator potential the (pre-)level surface is given by*

$$-\frac{1}{4}\boldsymbol{x}_0^T \Omega \sin(2\Omega t)\boldsymbol{x}_0 - \boldsymbol{x}_0^T \sin^2(\Omega t) \nabla S_0(\boldsymbol{x}_0) + \frac{1}{4}\nabla S_0^T \Omega^{-1} \sin(2\Omega t) \nabla S_0(\boldsymbol{x}_0) + S_0(\boldsymbol{x}_0) = c \ , \quad (6.1.6)$$

evaluated at $\boldsymbol{x}_0 = \Phi_t^{-1}\boldsymbol{x}$.

Proof. The pre-level surface is determined by $\mathcal{A}(\boldsymbol{x}_0, \boldsymbol{x}, t) = c$ and $\nabla_{\boldsymbol{x}_0}\mathcal{A}(\boldsymbol{x}_0, \boldsymbol{x}, t) = 0$. Inserting Equation (6.1.5) into (6.1.4) and observing that all matrices are real diagonal, we see that the pre-level surface is given by

$$\frac{1}{2}\boldsymbol{x_0}^T \Omega \cot(\Omega t)(\cos^2(\Omega t) - I)\boldsymbol{x_0} + \boldsymbol{x_0}^T (\cos^2(\Omega t) - I) \nabla S_0 \\ + \frac{1}{2}(\nabla S_0)^T \Omega^{-1} \cos(\Omega t) \sin(\Omega t) \nabla S_0 + S_0(\boldsymbol{x_0}) = c \ .$$

Using the identities $\cos^2(\Omega t) - I = -\sin^2(\Omega t)$ and $\cos(\Omega t)\sin(\Omega t) = \frac{1}{2}\sin(2\Omega t))$ we obtain

$$-\frac{1}{4}\boldsymbol{x_0}^T \Omega \sin(2\Omega t)\boldsymbol{x_0} - \boldsymbol{x_0}^T \sin^2(\Omega t) \nabla S_0 + \frac{1}{4}\nabla S_0^T \Omega^{-1} \sin(2\Omega t) \nabla S_0 + S_0(\boldsymbol{x_0}) = c \ .$$

□

6.2 Explicit Examples

If we take $S_0(\boldsymbol{x}_0) = f(x_0) + g(x_0)y_0$ in Proposition 6.1.1 then we see that the pre-caustic is determined by

$$\omega_2 \cot(\omega_2 t)\left(\omega_1 \cot(\omega_1 t) + f''(x_0) + y_0 g''(x_0)\right) - g'(x_0)^2 = 0 .$$

If $g''(x_0) \neq 0$ and $t \neq \frac{(2k+1)\pi}{2\omega_2}$ then this may be solved to give the pre-caustic as

$$y_0(x_0) = \frac{1}{g''(x_0)}\left(\frac{g'(x_0)^2}{\omega_2}\tan\omega_2 t - f''(x_0) - \omega_1 \cot\omega_1 t\right) . \tag{6.2.1}$$

Similarly, it follows from Proposition 6.1.2 that the pre-level surface is determined by

$$\begin{aligned} &-\frac{x_0^2}{4}\omega_1 \sin(2\omega_1 t) - \frac{y_0^2}{4}\omega_2 \sin(2\omega_2 t) - x_0 \sin^2(\omega_1 t)(f' + g'y_0) - y_0 \sin^2(\omega_2 t) g \\ &\qquad + \frac{1}{4\omega_1}\sin(2\omega_1 t)(f' + g'y_0)^2 + \frac{1}{4\omega_2}\sin(2\omega_2 t) g^2 + f + g y_0 = c , \end{aligned} \tag{6.2.2}$$

where the x_0 variables have been omitted for brevity.

Remark 6.2.1. If $t = \frac{(2k+1)\pi}{2\omega_2}$ then the pre-caustic condition reduces to $g'(x_0) = 0$ so that the caustic is given by

$$\begin{aligned} x(x_0) &= \left[\cos(\omega_1 t)x_0 + \omega_1^{-1}\sin(\omega_1 t) f'(x_0)\right]_{x_0=(g')^{-1}(0)} , \\ y(x_0) &= \left[\omega_2^{-1}(-1)^k g(x_0)\right]_{x_0=(g')^{-1}(0)} . \end{aligned}$$

6.2.1 The Cusp Singularity

Here we set $f \equiv 0$ and $g(x_0) := \frac{1}{2}x_0^2$. Then $g'(x_0) = x_0$ and $g''(x_0) = 1$ so that the pre-caustic

$$y_0(x_0) = \frac{x_0^2}{\omega_2}\tan(\omega_2 t) - \omega_1 \cot(\omega_1 t) .$$

for $t \neq \frac{(2k+1)\pi}{2\omega_2}$. The flow mapping is

$$\boldsymbol{x} = \Phi_t \boldsymbol{x}_0 = \cos(\Omega t)\begin{pmatrix} x_0 \\ y_0 \end{pmatrix} + \Omega^{-1}\sin(\Omega t)\begin{pmatrix} x_0 y_0 \\ \frac{x_0^2}{2} \end{pmatrix} ,$$

so that the caustic is

$$\begin{aligned} x(x_0) &= \frac{1}{\omega_1\omega_2} x_0^3 \tan(\omega_2 t)\sin(\omega_1 t) , \\ y(x_0) &= \frac{3}{2\omega_2}\sin(\omega_2 t)x_0^2 - \omega_1 \cot(\omega_1 t)\cos(\omega_2 t) . \end{aligned}$$

Observe that the vertical orientation of the pre-caustic is determined by $\operatorname{sgn}(\omega_2^{-1}\tan(\omega_2 t))$. Namely, in quadrants 1 and 3 the pre-caustic will have its usual orientation but in quadrants 2 and 4 it will be upside down. Similarly, in the deterministic case the vertical orientation of the cusp is determined by $\operatorname{sgn}(\omega_2^{-1}\sin(\omega_2 t))$ so that in quadrants 1 and 2 the cusp has its usual orientation but in quadrants 3 and 4 it is upside down.

Remark 6.2.2. If $t = \frac{(2k+1)\pi}{2\omega_2}$ then the pre-caustic is given by the line $x_0 = 0$ so that the caustic is $(x, y) = (0, 0)$.

To obtain the pre-level surface we use Proposition 6.1.2. This gives

$$-\frac{1}{4}\omega_1 \sin(2\omega_1 t)x_0^2 - \frac{1}{4}\omega_2 \sin(2\omega_2 t)y_0^2 - \sin^2(\omega_1 t)x_0^2 y_0 - \frac{1}{2}\sin^2(\omega_2 t)x_0^2 y_0 \\ + \frac{1}{4\omega_1}\sin(2\omega_1 t)x_0^2 y_0^2 + \frac{1}{16\omega_2}\sin(2\omega_2 t)x_0^4 + \frac{1}{2}x_0^2 y_0 = c ,$$

which is a quadratic in y_0. Solving this quadratic yields

$$y_0(x_0) = \frac{2\omega_1 x_0^2 \sin^2(\omega_1 t) - \omega_1 x_0^2 \cos^2(\omega_2 t) \pm \omega_1 \sqrt{\mathcal{D}_t}}{x_0^2 \sin(2\omega_1 t) - \omega_1\omega_2 \sin(2\omega_2 t)} ,$$

for $\mathcal{D}_t \geq 0$ where

$$\mathcal{D}_t := \frac{1}{4}\Big\{x_0^4 \left(1 - 2\cos(2\omega_1 t) - \cos(2\omega_2 t)\right)^2 + \frac{1}{\omega_1\omega_2}\left(x_0^2 \sin(2\omega_1 t) - \omega_1\omega_2 \sin(2\omega_2 t)\right) \\ \times \left(4x_0^2 \sin(2\omega_1 t)\omega_1\omega_2 + 16c\omega_2 - x_0^4 \sin(2\omega_2 t)\right)\Big\} .$$

In order to obtain the level surface we apply the flow mapping which gives

$$x(x_0) = \frac{x_0^3 \sin(\omega_1 t)(1 - \cos^2(\omega_2 t)) - x_0\omega_1\omega_2 \cos(\omega_1 t)\sin(2\omega_2 t) \pm x_0 \sin(\omega_1 t)\sqrt{\mathcal{D}_t}}{x_0^2 \sin(2\omega_1 t) - \omega_1\omega_2 \sin(2\omega_2 t)} ,$$

$$y(x_0) = \frac{\frac{1}{2\omega_2}x_0^4 \sin(\omega_2 t)\sin(2\omega_1 t) + x_0^2\omega_1 \cos(\omega_2 t)(2\sin^2(\omega_1 t) - 1) \pm \omega_1 \cos(\omega_2 t)\sqrt{\mathcal{D}_t}}{x_0^2 \sin(2\omega_1 t) - \omega_1\omega_2 \sin(2\omega_2 t)} ,$$

for $\mathcal{D}_t \geq 0$.

Figures 6.1 and 6.2 show the pre-curves and image curves, respectively, of the cusp singularity with $\omega_1 = \frac{4}{5}$ and $\omega_2 = \frac{3}{2}$. As usual the caustic is identified by the use of a broken line and we have varied t from 0.1 to 3.6 in steps of size 0.1.

6.2.2 The Polynomial Swallowtail

Here we take $f(x_0) := x_0^5$ and $g(x_0) := x_0^2$. Inserting into Proposition 6.1.1 we see that for $t \neq \frac{(2k+1)\pi}{2\omega_2}$ the pre-caustic is given by

$$y_0(x_0) = \frac{2x_0^2}{\omega_2}\tan(\omega_2 t) - 10x_0^3 - \frac{\omega_1}{2}\cot(\omega_1 t) .$$

The flow in this case is given by

$$\boldsymbol{x} = \Phi_t \boldsymbol{x}_0 = \cos(\Omega t)\begin{pmatrix} x_0 \\ y_0 \end{pmatrix} + \Omega^{-1}\sin(\Omega t)\begin{pmatrix} 5x_0^4 + 2x_0 y_0 \\ x_0^2 \end{pmatrix} ,$$

so that the caustic is

$$x(x_0) = -\frac{15}{\omega_1}x_0^4 \sin(\omega_1 t) + \frac{4x_0^3}{\omega_1\omega_2}\sin(\omega_1 t)\tan(\omega_2 t) ,$$

$$y(x_0) = \frac{3x_0^2}{\omega_2}\sin(\omega_2 t) - 10x_0^3 \cos(\omega_2 t) - \frac{\omega_1}{2}\cot(\omega_1 t)\cos(\omega_2 t) .$$

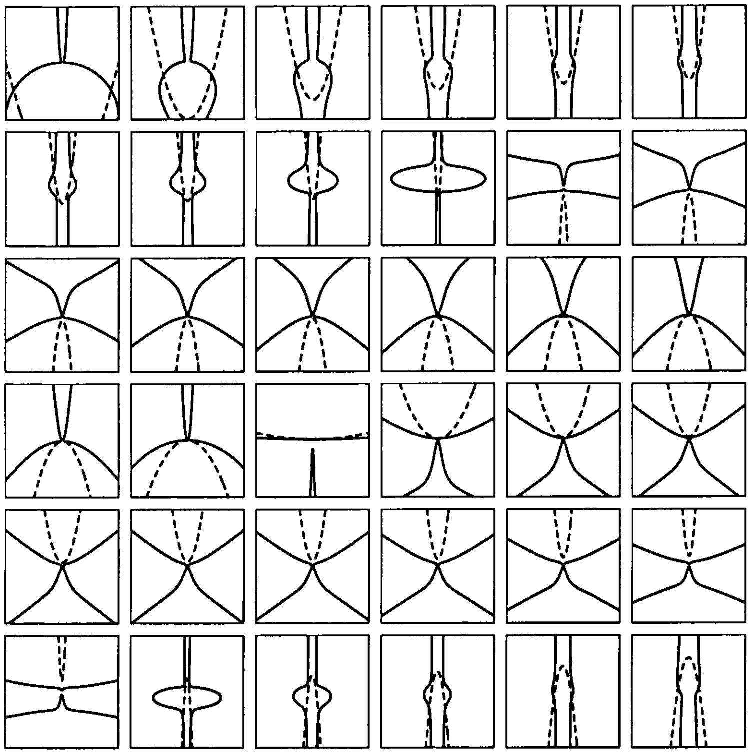

Figure 6.1: Pre-Curves with $\omega_1 = \frac{4}{5}$ and $\omega_2 = \frac{3}{2}$ for the cusp singularity

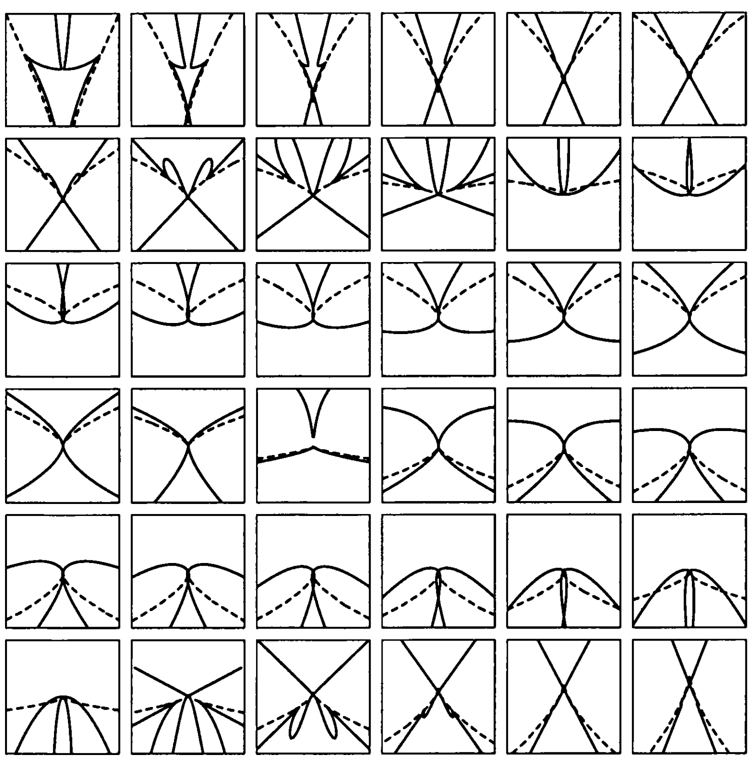

Figure 6.2: Image-Curves with $\omega_1 = \frac{4}{5}$ and $\omega_2 = \frac{3}{2}$ for the cusp singularity

Remark 6.2.3. Observe that the horizontal orientation of the polynomial swallowtail is controlled by $\operatorname{sgn}(\omega_1^{-1}\sin(\omega_1 t))$.

From Proposition 6.1.2 we see that the pre-level surface is determined by the quadratic

$$y_0^2\left(-\frac{1}{4}\omega_2\sin(2\omega_2 t)+\frac{x_0^2}{\omega_1}\sin(2\omega_1 t)\right)$$
$$+\,y_0\left(-2x_0^2\sin^2(\omega_1 t)-x_0^2\sin^2(\omega_2 t)+\frac{5}{\omega_1}x_0^5\sin(2\omega_1 t)+x_0^2\right)$$
$$+\left(-\frac{x_0^2}{4}\omega_1\sin(2\omega_1 t)-5x_0^5\sin^2(\omega_1 t)+\frac{25}{4\omega_1}x_0^8\sin(2\omega_1 t)+\frac{1}{4\omega_2}x_0^4\sin(2\omega_2 t)+x_0^5-c\right)=0\,.$$

Solving we obtain

$$y_0(x_0)=\frac{4\omega_1 x_0^2\sin^2(\omega_1 t)-10x_0^5\sin(2\omega_1 t)-2\omega_1 x_0^2\cos^2(\omega_2 t)\pm\omega_1\sqrt{\mathcal{D}_t}}{4x_0^2\sin(2\omega_1 t)-\omega_1\omega_2\sin(2\omega_2 t)}\,,$$

for $\mathcal{D}_t\geq 0$, where

$$\begin{aligned}\mathcal{D}_t=&\frac{25x_0^8\omega_2}{\omega_1}\sin(2\omega_1 t)\sin(2\omega_2 t)+\frac{4x_0^7}{\omega_1}\sin(2\omega_1 t)(1+5\cos(2\omega_2 t))\\&-\frac{4x_0^6}{\omega_1\omega_2}\sin(2\omega_1 t)\sin(2\omega_2 t)+2x_0^5\omega_2(5\cos(2\omega_1 t)-3)\sin(2\omega_2 t)\\&+2x_0^4\left(3-2\cos(2\omega_1 t)+\cos(2t(\omega_1-\omega_2))-\cos(2\omega_2 t)+\cos(2t(\omega_1+\omega_2))\right)\\&+\frac{x_0^2}{\omega_1}\sin(2\omega_1 t)\left(16c-\sin(2\omega_2 t)\omega_1^2\omega_2\right)-4c\omega_2\sin(2\omega_2 t)\,.\end{aligned}$$

Thus applying Φ_t we obtain the level surface,

$$\begin{aligned}x(x_0)=&\left(4x_0^2\sin(2\omega_1 t)-\omega_1\omega_2\sin(2\omega_2 t)\right)^{-1}\Big\{-5x_0^4\omega_2\sin(\omega_1 t)\sin(2\omega_2 t)\\&+4x_0^3\sin(\omega_1 t)(2-\cos^2(\omega_2 t))-x_0\omega_1\omega_2\sin(2\omega_2 t)\cos(\omega_1 t)\pm 2x_0\sin(\omega_1 t)\sqrt{\mathcal{D}_t}\Big\}\,,\end{aligned}$$

$$\begin{aligned}y(x_0)=&\left(4x_0^2\sin(2\omega_1 t)-\omega_1\omega_2\sin(2\omega_2 t)\right)^{-1}\Big\{-10x_0^5\sin(2\omega_1 t)\cos(\omega_2 t)\\&+\frac{4x_0^4}{\omega_2}\sin(2\omega_1 t)\sin(\omega_2 t)-2x_0^2\omega_1\cos(\omega_2 t)\cos(2\omega_1 t)\pm\omega_1\cos(\omega_2 t)\sqrt{\mathcal{D}_t}\Big\}\,,\end{aligned}$$

for $\mathcal{D}_t\geq 0$.

Figures 6.3 and 6.4 show the pre-curves and image curves, respectively, of the polynomial swallowtail with $\omega_1=\frac{4}{5}$ and $\omega_2=\frac{3}{2}$. As usual the caustic is identified by the use of a broken line and we have taken t from 0.1 to 3.6 in steps of size 0.1.

Remark 6.2.4. Proposition 6.1.1 and 6.1.2 may of course be used to find explicit formulae for the butterfly and three dimensional polynomial swallowtail with harmonic oscillator potential. Due to the fact that the argument is identical to the two dimensional case we have chosen to omit the derivation and result.

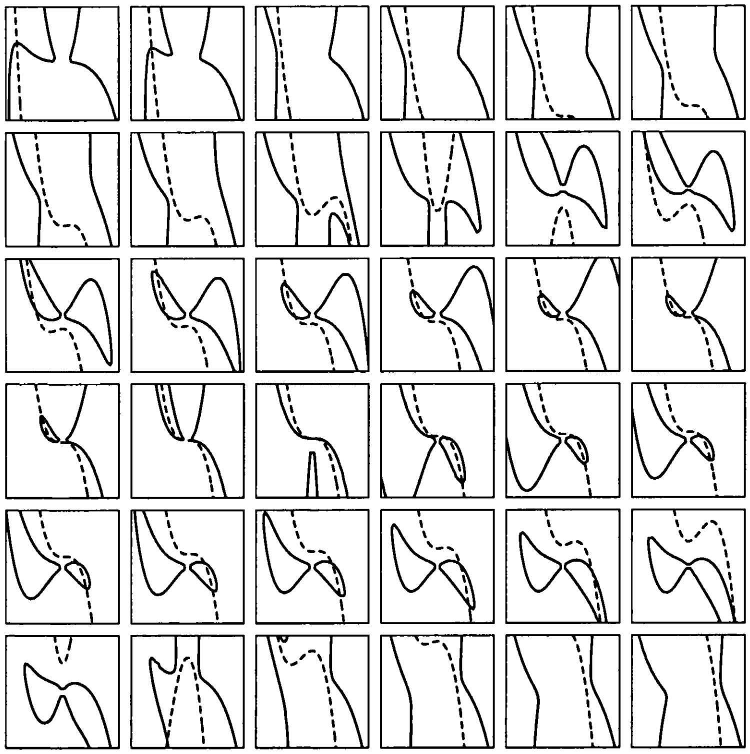

Figure 6.3: Pre-Curves with $\omega_1 = \frac{4}{5}$ and $\omega_2 = \frac{3}{2}$ for the polynomial swallowtail

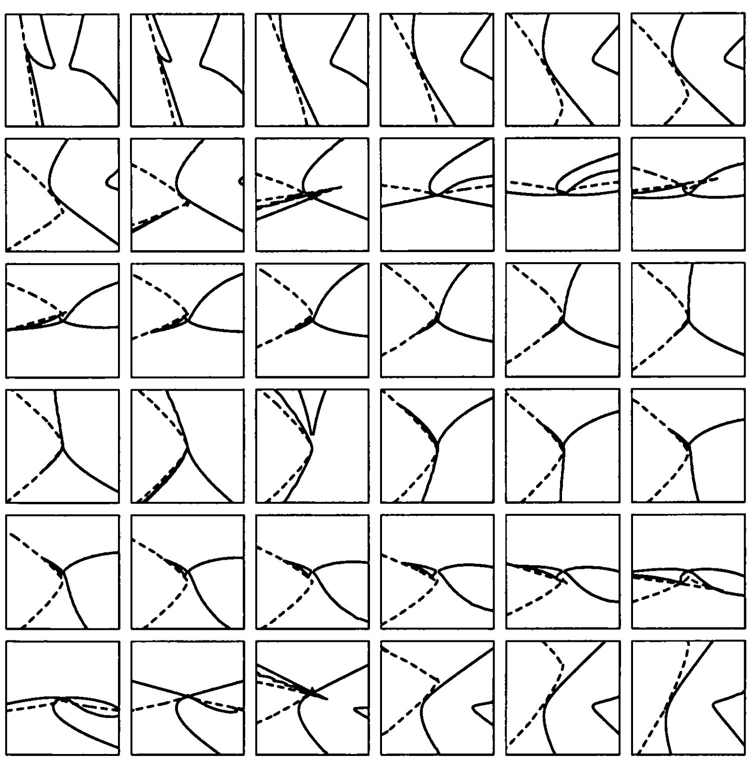

Figure 6.4: Image-Curves with $\omega_1 = \frac{4}{5}$ and $\omega_2 = \frac{3}{2}$ for the polynomial swallowtail

6.3 Harmonic Oscillator Potential with Noise

6.3.1 Stochastic Mehler Heat Kernel

In this section we begin with the stochastic Schrödinger equation for harmonic oscillator potential, namely

$$i\hbar \, \mathrm{d}\psi_t(x) = \left(-\frac{\hbar^2}{2}\Delta + \frac{1}{2}\omega^2 x^2\right)\psi_t(x)\,\mathrm{d}t - \varepsilon k(x,t)\psi_t(x)\circ\partial W_t \,, \tag{6.3.1}$$

where W_t is a one dimensional Wiener process and $\circ$ indicates the Stratonovich stochastic differential. Dividing through by $\hbar$ and relabelling as μ^2 yields

$$i\,\mathrm{d}\psi_t(x) = \left(-\frac{\mu^2}{2}\Delta + \frac{1}{2\mu^2}\omega^2 x^2\right)\psi_t(x)\,\mathrm{d}t - \frac{\varepsilon}{\mu^2}k(x,t)\psi_t(x)\circ\partial W_t \,.$$

We use the following well known fact: if the noise W_t in some stochastic Stratonovich equation is approximated by means of smooth functions

$$W_t \approx \int_0^t q(s)\,\mathrm{d}s \,, \tag{6.3.2}$$

then the solutions of the corresponding deterministic equations will tend to the solution of the given stochastic equation. Considering W_t to be of the form in Equation (6.3.2) we have

$$i\,\mathrm{d}\psi_t(x) = \left(-\frac{\mu^2}{2}\Delta + \frac{1}{2\mu^2}\omega^2 x^2\right)\psi_t(x)\,\mathrm{d}t - \frac{\varepsilon}{\mu^2}k(x,t)\psi_t(x)q(t)\,\mathrm{d}t \,.$$

Applying the transformations $t \mapsto it$ and $\omega \mapsto i\omega$, namely setting $\tau = it$ and $\tilde{\omega} = i\omega$ yields

$$i\,\mathrm{d}\psi(x,t(\tau)) = i\left(\frac{\mu^2}{2}\Delta + \frac{1}{2\mu^2}\tilde{\omega}^2 x^2\right)\psi(x,t(\tau))\,\mathrm{d}\tau + i\frac{\varepsilon}{\mu^2}k(x,t(\tau))\psi(x,t(\tau))q(t(\tau))\,\mathrm{d}\tau \,.$$

Setting $u(x,\tau) := \psi(x,t(\tau))$ and $\tilde{k}(x,\tau) := k(x,t(\tau))$ gives

$$\mathrm{d}u(x,\tau) = \left(\frac{\mu^2}{2}\Delta + \frac{1}{2\mu^2}\tilde{\omega}^2 x^2\right)u(x,\tau)\,\mathrm{d}t + \frac{\varepsilon}{\mu^2}\tilde{k}(x,\tau)u(x,\tau)q(t(\tau))\,\mathrm{d}\tau \,,$$

which on re-labelling τ as t and $\tilde{\omega}$ as ω will tend to the stochastic heat equation

$$\mathrm{d}u(x,t) = \left(\frac{\mu^2}{2}\Delta + \frac{1}{2\mu^2}\omega^2 x^2\right)u(x,t)\,\mathrm{d}t + \frac{\varepsilon}{\mu^2}\tilde{k}(x,t)u(x,t)\circ\partial W_t \,.$$

We remark that if $k(x,t) = k(x)$, namely k is time independent, then we have $k = \tilde{k}$. In particular this will be true for the position operator case, $(ku)(x) = xu(x)$, which we now consider.

Proposition 6.3.1. *The Stratonovich type stochastic heat equation with harmonic oscillator potential,*

$$\mathrm{d}u(x,t) = \left(\frac{\mu^2}{2}\Delta + \frac{1}{2\mu^2}\omega^2 x^2\right) u(x,t)\,\mathrm{d}t + \frac{\varepsilon}{\mu^2} x u(x,t) \circ \partial W_t \ ,$$

with initial condition $u(x,0) = F(x) \in C_0^\infty(\mathbb{R})$ *has a solution*

$$u(x,t) = \int_{\mathbb{R}} G_t(x,x_0) F(x_0)\,\mathrm{d}x_0 \ ,$$

where the ***stochastic Mehler heat kernel*** $G_t(x,x_0)$ *is given by*

$$\begin{aligned} G_t(x,x_0) := & \sqrt{\frac{\omega}{2\pi\mu^2 \sin(\omega t)}} \exp\left\{-\frac{\omega}{2\mu^2}\frac{(x^2+x_0^2)\cos(\omega t) - 2xx_0}{\sin(\omega t)}\right\} \\ & \times \exp\left\{\frac{\varepsilon}{\mu^2}\int_0^t \frac{x\sin(\omega r) - x_0 \sin(\omega(r-t))}{\sin(\omega t)} \circ \partial W_r\right\} \\ & \times \exp\left\{-\frac{\varepsilon^2}{\mu^2}\int_0^t \left[\int_0^r \frac{\sin(\omega s)\sin(\omega(r-t))}{\omega \sin(\omega t)} \circ \partial W_s\right] \circ \partial W_r\right\} \ , \end{aligned} \tag{6.3.3}$$

for all positive $t \neq \frac{k\pi}{\omega}$ *where* $k \in \mathbb{Z}$.

Proof. It is known, see [52] and [42], that the Schrödinger equation

$$i\,\mathrm{d}\psi_t(x) = \left(-\frac{\mu^2}{2}\Delta + \frac{1}{2\mu^2}\omega^2 x^2\right)\psi_t(x) - \frac{\varepsilon}{\mu^2} x\psi_t(x) \circ \partial W_t \ ,$$

has stochastic Mehler kernel

$$\begin{aligned} G_t(x,x_0) = & \sqrt{\frac{\omega}{2\pi i\mu^2 \sin(\omega t)}} \exp\left(\frac{i\omega}{2\mu^2}\frac{(x^2+x_0^2)\cos(\omega t) - 2xx_0}{\sin(\omega t)}\right) \\ & \times \exp\left\{\frac{\varepsilon i}{\mu^2}\int_0^t \frac{x\sin(\omega r) - x_0 \sin(\omega(r-t))}{\sin(\omega t)} \circ \partial W_r\right\} \\ & \times \exp\left\{\frac{\varepsilon^2 i}{\mu^2}\int_0^t \left[\int_0^r \frac{\sin(\omega s)\sin(\omega(r-\omega t))}{\omega \sin(\omega t)} \circ \partial W_s\right] \circ \partial W_r\right\} \ , \end{aligned}$$

for all positive $t \neq \frac{k\pi}{\omega}$. To obtain the stochastic Mehler heat kernel we must set $\tau = it$ and $\tilde{\omega} = i\omega$, which gives

$$\begin{aligned} G(x,x_0) = & \sqrt{\frac{\tilde{\omega}}{2\pi\mu^2 \sin(\tilde{\omega}\tau)}} \exp\left\{-\frac{\tilde{\omega}}{2\mu^2}\frac{(x^2+x_0^2)\cos(\tilde{\omega}\tau) - 2xx_0}{\sin(\tilde{\omega}\tau)}\right\} \\ & \times \exp\left\{\frac{\varepsilon i}{\mu^2}(-i)\int_0^\tau \frac{-x\sin(\tilde{\omega}\tilde{r}) + x_0 \sin(\tilde{\omega}(\tilde{r}-\tau))}{-\sin(\tilde{\omega}\tau)} \circ \partial W_{\tilde{r}}\right\} \\ & \times \exp\left\{\frac{\varepsilon^2 i}{\mu^2}(-i)^2\int_0^\tau \left[\int_0^{\tilde{r}} \frac{(-\sin(\tilde{\omega}\tilde{s}))\,(-\sin(\tilde{\omega}(\tilde{r}-\tau)))}{i\tilde{\omega}\sin(\tilde{\omega}\tau)} \circ \partial W_{\tilde{s}}\right] \circ \partial W_{\tilde{r}}\right\} \ . \end{aligned}$$

Re-labelling τ as t and dropping the tildes yields the desired result. □

Remark 6.3.1. Observe that if we allow $\omega \searrow 0$ in Equation (6.3.3) then by virtue of small angles we obtain

$$\begin{aligned} G_t &= \sqrt{\frac{1}{2\pi t\mu^2}} \exp\Bigg\{ -\frac{(x-x_0)^2}{2t\mu^2} + \frac{\varepsilon}{\mu^2}\int_0^t \frac{xr - x_0(r-t)}{t} \circ \partial W_r \\ &\qquad - \frac{\varepsilon^2}{\mu^2}\int_0^t \left[\int_0^r \frac{s(r-t)}{t} \circ \partial W_s\right] \circ \partial W_r \Bigg\} \\ &= \sqrt{\frac{1}{2\pi t\mu^2}} \exp\Bigg\{ \frac{(x-x_0)^2}{2t\mu^2} + \frac{\varepsilon x}{\mu^2} W_t - \frac{\varepsilon}{t\mu^2}(x-x_0)\int_0^t W_u \, \mathrm{d}u \\ &\qquad + \frac{\varepsilon^2}{\mu^2}\int_0^t \int_0^r s\left(1 - \frac{r}{t}\right) \circ \partial W_s \circ \partial W_r \ , \end{aligned}$$

which agrees with the stochastic heat kernel considered in Chapter 3.

6.3.2 Caustics and Level Surfaces with Noise

Continuing with the nomenclature adopted in the deterministic case we see, that for $\boldsymbol{x} \in \mathbb{R}^n$, the action may be written as

$$\begin{aligned} \mathcal{A}(\boldsymbol{x}_0, \boldsymbol{x}, t) &= \frac{1}{2}\boldsymbol{x}^T \Omega \cot(\Omega t)\boldsymbol{x} + \frac{1}{2}\boldsymbol{x}_0^T \Omega \cot(\Omega t)\boldsymbol{x}_0 - \boldsymbol{x}^T \Omega \left[\sin(\Omega t)\right]^{-1} \boldsymbol{x}_0 \\ &\quad - \varepsilon \int_0^t \frac{x \sin(\omega_1 r) - x_0 \sin(\omega_1 (r-t))}{\sin(\omega_1 t)} \circ \partial W_r \\ &\quad + \varepsilon^2 \int_0^t \left[\int_0^r \frac{\sin(\omega_1 s)\sin(\omega_1(r-t))}{\omega_1 \sin(\omega_1 t)} \circ \partial W_s\right] \circ \partial W_r + S_0(\boldsymbol{x}_0) \ , \end{aligned} \tag{6.3.4}$$

so that the flow mapping Φ_t defined by $\nabla_{\boldsymbol{x}_0}\mathcal{A}(\boldsymbol{x}_0, \boldsymbol{x}, t) = 0$ is given by

$$\boldsymbol{x} = \Phi_t \boldsymbol{x}_0 = \cos(\Omega t)\boldsymbol{x}_0 + \Omega^{-1}\sin(\Omega t)\nabla S_0 + \varepsilon \Omega^{-1} \begin{pmatrix} \int_0^t \sin(\omega_1(r-t)) \circ \partial W_r \\ 0 \\ \vdots \\ 0 \end{pmatrix} . \tag{6.3.5}$$

Remark 6.3.2. Note that if $\Phi_t^0(\boldsymbol{x}_0)$ denotes the flow mapping in the deterministic setting then

$$\Phi_t^\varepsilon(\boldsymbol{x}_0) = \Phi_t^0(\boldsymbol{x}_0) + \varepsilon \int_0^t \Omega^{-1}\sin(\Omega(r-t)) \circ \partial \widetilde{W}_r \ ,$$

where

$$\widetilde{W}_t(\omega) = \begin{pmatrix} W^{(1)}(t,\omega) \\ 0 \\ \vdots \\ 0 \end{pmatrix} .$$

It follows from the action expression in Equation (6.3.4) that the pre-caustic $\Phi_t^{-1}C_t$ is still determined by

$$\operatorname{Det}\left[\Omega\cos(\Omega t)+S_0''(\boldsymbol{x}_0)\right]=0\ .$$

Since the pre-caustic is purely deterministic, it is clear from the preceding remark that noise does not affect the shape of the caustic. It merely displaces C_t by the random amount $\varepsilon\int_0^t\Omega^{-1}\sin(\Omega(r-t))\circ\partial\widetilde{W}_r$.

Proposition 6.3.2. *Let $\boldsymbol{x}\in\mathbb{R}^n$ and consider the Stratonovich type stochastic heat equation with harmonic oscillator potential $V(\boldsymbol{x})=\frac{1}{2}\boldsymbol{x}^T\Omega\boldsymbol{x}$,*

$$\partial u(\boldsymbol{x},t)=\left(\frac{\mu^2}{2}\Delta+\frac{1}{2\mu^2}\boldsymbol{x}^T\Omega\boldsymbol{x}\right)u(\boldsymbol{x},t)+\frac{\varepsilon}{\mu^2}xu(\boldsymbol{x},t)\circ\partial W_t\ ,$$

where $u(\boldsymbol{x},0)=\exp\left(-\frac{S_0(\boldsymbol{x})}{\mu^2}\right)$. The (pre-)level surface of the Hamilton principal function, $\mathcal{S}(\boldsymbol{x},t)=c$, is given by

$$\begin{aligned}
&-\frac{1}{4}\boldsymbol{x}_0^T\Omega\sin(2\Omega t)\boldsymbol{x}_0-\boldsymbol{x}_0^T\sin^2(\Omega t)\nabla S_0(\boldsymbol{x}_0)+\frac{1}{4}\nabla S_0(\boldsymbol{x}_0)^T\Omega^{-1}\sin(2\Omega t)\nabla S_0(\boldsymbol{x}_0)\\
&+\varepsilon\left(x_0\cot(\omega_1 t)+\frac{1}{\omega_1}\frac{\partial S_0}{\partial x_0}\right)\left(\cos(\omega_1 t)\int_0^t\sin(\omega_1(r-t))\circ\partial W_r-\int_0^t\sin(\omega_1 r)\circ\partial W_r\right)\\
&+\frac{\varepsilon^2\cot(\omega_1 t)}{2\omega_1}\left(\int_0^t\sin(\omega_1(r-t))\circ\partial W_r\right)^2-\varepsilon^2\int_0^t\left(\int_r^t\frac{\sin(\omega_1 s)\sin(\omega_1(r-t))}{\omega_1\sin(\omega_1 t)}\circ\partial W_s\right)\circ\partial W_r\\
&\qquad\qquad+S_0(\boldsymbol{x}_0)=c\ ,
\end{aligned}$$

evaluated at $\boldsymbol{x}_0=\Phi_t^{-1}\boldsymbol{x}$.

Proof. The pre-level surface is obtained by evaluating $\mathcal{A}(\boldsymbol{x}_0,\boldsymbol{x},t)=c$ at $\boldsymbol{x}=\Phi_t\boldsymbol{x}_0$. This amounts to inserting Equation (6.3.5) in Equation (6.3.4), giving

$$\begin{aligned}
&\frac{1}{2}\left(\boldsymbol{x_0}^T\cos(\Omega t)+\nabla S_0^T\Omega^{-1}\sin(\Omega t)+\varepsilon\left(\int_0^t\sin(\Omega(r-t))\circ\partial\widetilde{W}_r\right)^T\Omega^{-1}\right)\Omega\cot(\Omega t)\\
&\times\left(\cos(\Omega t)\boldsymbol{x}_0+\Omega^{-1}\sin(\Omega t)\nabla S_0+\varepsilon\Omega^{-1}\int_0^t\sin(\Omega(r-t))\circ\partial\widetilde{W}_r\right)+\frac{1}{2}\boldsymbol{x}_0^T\Omega\cot(\Omega t)\boldsymbol{x}_0\\
&-\left(\boldsymbol{x}_0^T\cos(\Omega t)+\nabla S_0^T\Omega^{-1}\sin(\Omega t)+\varepsilon\left(\int_0^t\sin(\Omega(r-t))\circ\partial\widetilde{W}_r\right)^T\Omega^{-1}\right)\Omega\left[\sin(\Omega t)\right]^{-1}\boldsymbol{x}_0\\
&\quad-\varepsilon\left(\boldsymbol{x}_0^T\cos(\Omega t)+\nabla S_0^T\Omega^{-1}\sin(\Omega t)+\varepsilon\left(\int_0^t\sin(\Omega(r-t))\circ\partial\widetilde{W}_r\right)^T\Omega^{-1}\right)\\
&\quad\times\left[\sin(\Omega t)\right]^{-1}\int_0^t\sin(\Omega r)\circ\partial\widetilde{W}_r+\varepsilon\boldsymbol{x}_0^T\left[\sin(\Omega t)\right]^{-1}\int_0^t\sin(\Omega(r-t))\circ\partial\widetilde{W}_r\\
&\quad+\varepsilon^2\int_0^t\left(\int_0^r\sin(\Omega s)\sin(\Omega(r-t))\circ\partial\widetilde{W}_s\right)^T\Omega^{-1}\left[\sin(\Omega t)\right]^{-1}\circ\partial\widetilde{W}_r+S_0(\boldsymbol{x_0})=c\ ,
\end{aligned}$$

which after expansion becomes

$$
\begin{aligned}
&\frac{1}{2}\boldsymbol{x}_0^T\Omega\cot(\Omega t)(\cos^2(\Omega t)-I)\boldsymbol{x}_0+\boldsymbol{x}_0^T(\cos^2(\Omega t)-I)\nabla S_0+\frac{1}{2}\nabla S_0^T\Omega^{-1}\sin(\Omega t)\cos(\Omega t)\nabla S_0\\
&+\varepsilon\left(x_0\cot(\omega_1 t)+\frac{1}{\omega_1}\frac{\partial S_0}{\partial x_0}\right)\left(\cos(\omega_1 t)\int_0^t\sin(\omega_1(r-t))\circ\partial W_r-\int_0^t\sin(\omega_1 r)\circ\partial W_r\right)\\
&\qquad+\frac{\varepsilon^2\cot(\omega_1 t)}{2\omega_1}\left(\int_0^t\sin(\omega_1(r-t))\circ\partial W_r\right)^2\\
&\qquad-\frac{\varepsilon^2}{\omega_1\sin(\omega_1 t)}\int_0^t\sin(\omega_1(r-t))\circ\partial W_r\int_0^t\sin(\omega_1 r)\circ\partial W_r\\
&\qquad+\frac{\varepsilon^2}{\omega_1\sin(\omega_1 t)}\int_0^t\left(\int_0^r\sin(\omega_1 s)\sin(\omega_1(r-t))\circ\partial W_s\right)\circ\partial W_r+S_0(\boldsymbol{x}_0)=c\,.
\end{aligned}
$$

Using the identities $\cos^2(\Omega t)-I\equiv-\sin^2(\Omega t)$, $\cos(\Omega t)\sin(\Omega t)\equiv\frac{1}{2}\sin(2\Omega t)$ and observing that

$$
\begin{aligned}
&\int_0^t\left(\int_0^t\sin(\omega_1 s)\sin(\omega_1(r-t))\right)\circ\partial W_r-\int_0^t\left(\int_0^r\sin(\omega_1 s)\sin(\omega_1(r-t))\right)\circ\partial W_r\\
&\qquad=\int_0^t\left(\int_r^t\sin(\omega_1 s)\sin(\omega_1(r-t))\right)\circ\partial W_r\,,
\end{aligned}
$$

yields the required result. □

6.3.3 An Aside on Itô Forms of the Heat Kernel

Lemma 6.3.3. *The stochastic Mehler heat kernel in Itô form is given by*

$$
\begin{aligned}
G_t(x,x_0):=&\sqrt{\frac{\omega}{2\pi\mu^2\sin(\omega t)}}\exp\left\{-\frac{\omega}{2\mu^2}\frac{(x^2+x_0^2)\cos(\omega t)-2xx_0}{\sin(\omega t)}\right\}\\
&\times\exp\left\{\frac{\varepsilon}{\mu^2}\int_0^t\frac{x\sin(\omega r)-x_0\sin(\omega(r-t))}{\sin(\omega t)}\,\mathrm{d}W_r\right\}\\
&\times\exp\left\{\frac{\varepsilon^2}{\mu^2}\left(\frac{1}{2}\int_0^t W_r^2\,\mathrm{d}r-\omega\int_0^t\int_0^r\frac{W_rW_s\cos(\omega(r-t))\cos(\omega s)}{\sin(\omega t)}\,\mathrm{d}s\,\mathrm{d}r\right)\right\}\,, \quad (6.3.6)
\end{aligned}
$$

for all positive $t\neq\frac{k\pi}{\omega}$ where $k\in\mathbb{Z}$.

Proof. If

$$
X_t:=-\int_0^t\left[\int_0^r\frac{\sin(\omega s)\sin(\omega(r-t))}{\omega\sin(\omega t)}\circ\partial W_s\right]\circ\partial W_r\,,
$$

and

$$
Y_t:=\frac{1}{2}\int_0^t W_r^2\,\mathrm{d}r-\omega\int_0^t\int_0^r\frac{W_rW_s\cos(\omega(r-t))\cos(\omega s)}{\sin(\omega t)}\,\mathrm{d}s\,\mathrm{d}r\,,
$$

then we need only show that $X_t=Y_t$ almost surely.

Using integration by parts we see

$$\begin{aligned}
X_t &= \int_0^t W_r \partial_r \left\{ \int_0^r \frac{\sin(\omega s)\sin(\omega(r-t))}{\omega \sin(\omega t)} \circ \partial W_s \right\} \\
&= \int_0^t W_r \left\{ \frac{\cos(\omega(r-t))}{\sin(\omega t)} \, \mathrm{d}r \int_0^r \sin(\omega s)\, \mathrm{d}W_s + \frac{\sin(\omega r)\sin(\omega(r-t))}{\omega\sin(\omega t)} \circ \partial W_r \right\} \\
&= \int_0^t \frac{W_r \cos(\omega(r-t))}{\sin(\omega t)} \left\{ W_r \sin(\omega r) - \int_0^r W_s \cos(\omega s)\omega \, \mathrm{d}s \right\} \mathrm{d}r \\
&\qquad + \int_0^t \frac{\sin(\omega r)\sin(\omega(r-t))}{\omega \sin(\omega t)} \circ \partial \left(\frac{W_r^2}{2} \right) \\
&= \int_0^t \frac{W_r^2 \sin(\omega r)\cos(\omega(r-t))}{\sin(\omega t)} \, \mathrm{d}r - \omega \int_0^t \int_0^r \frac{W_r W_s \cos(\omega(r-t))\cos(\omega s)}{\sin(\omega t)} \, \mathrm{d}s \, \mathrm{d}r \\
&\qquad - \int_0^r \frac{W_r^2}{2\omega\sin(\omega t)} \partial_r \left\{ \sin(\omega r)\sin(\omega(r-t)) \right\} \\
&= \frac{1}{2} \int_0^t \frac{W_r^2 \sin(\omega r - \omega r + \omega t)}{\sin(\omega t)} \, \mathrm{d}r - \omega \int_0^t \int_0^r \frac{W_r W_s \cos(\omega(r-t))\cos(\omega s)}{\sin(\omega t)} \, \mathrm{d}s \, \mathrm{d}r \\
&= Y_t \ .
\end{aligned}$$

□

Corollary 6.3.4. *The (pre-)level surface of the Hamilton principal function, $\mathcal{S}(\boldsymbol{x}, t) = c$, is given by*

$$\begin{aligned}
&- \frac{1}{4} \boldsymbol{x}_0^T \Omega \sin(2\Omega t) \boldsymbol{x}_0 - \boldsymbol{x}_0^T \sin^2(\Omega t) \nabla S_0(\boldsymbol{x}_0) + \frac{1}{4} \nabla S_0(\boldsymbol{x}_0)^T \Omega^{-1} \sin(2\Omega t) \nabla S_0(\boldsymbol{x}_0) \\
&\quad + \varepsilon \left(x_0 \cot(\omega_1 t) + \frac{1}{\omega_1} \frac{\partial S_0}{\partial x_0} \right) \left(\cos(\omega_1 t) \int_0^t \sin(\omega_1 (r-t)) \, \mathrm{d}W_r - \int_0^t \sin(\omega_1 r) \, \mathrm{d}W_r \right) \\
&+ \frac{\varepsilon^2 \cot(\omega_1 t)}{2\omega_1} \left(\int_0^t \sin(\omega_1(r-t)) \, \mathrm{d}W_r \right)^2 - \varepsilon^2 \omega_1 \int_0^t \int_r^t \frac{W_r W_s \cos(\omega_1(r-t))\cos(\omega_1 s)}{\sin(\omega_1 t)} \, \mathrm{d}s \, \mathrm{d}r \\
&\qquad - \frac{\varepsilon^2}{2} \int_0^t W_r^2 \, \mathrm{d}r + \varepsilon^2 W_t \int_0^t W_r \cos(\omega_1(r-t)) \, \mathrm{d}r + S_0(\boldsymbol{x}_0) = c \ ,
\end{aligned}$$

evaluated at $\boldsymbol{x}_0 = \Phi_t^{-1} \boldsymbol{x}$.

Proof. This follows from Proposition 6.3.2, Lemma 6.3.3 and the fact that

$$\begin{aligned}
&\int_0^t \left(\int_0^t \frac{\sin(\omega s)\sin(\omega(r-t))}{\omega\sin(\omega t)} \circ \partial W_s \right) \circ \partial W_r \\
&\quad = \frac{1}{\omega \sin(\omega t)} \left(\int_0^t \sin(\omega(r-t)) \circ \partial W_r \right) \left(\int_0^t \sin(\omega r) \circ \partial W_r \right) \\
&\quad = -W_t \int_0^t W_r \cos(\omega(r-t)) \, \mathrm{d}r + \omega \int_0^t \int_0^t \frac{W_r W_s \cos(\omega(r-t))\cos(\omega s)}{\sin(\omega t)} \, \mathrm{d}s \, \mathrm{d}r \ .
\end{aligned}$$

□

Remark 6.3.3. Observe that if we allow $\omega \searrow 0$ in Corollary 6.3.4 then we obtain

$$\frac{t}{2}|\nabla S_0|^2 - \varepsilon\left(x_0 + t\frac{\partial S_0}{\partial x_0}\right)W_t + \frac{\varepsilon^2}{2t}\left(\int_0^t (r-t)\,\mathrm{d}W_r\right)^2 - \frac{\varepsilon^2}{t}\left\{\left(\int_0^t W_r\,\mathrm{d}r\right)^2 - \int_0^t\int_0^r W_r W_s\,\mathrm{d}s\,\mathrm{d}r\right\} - \frac{\varepsilon^2}{2}\int_0^t W_r^2\,\mathrm{d}r + \varepsilon^2 W_t\int_0^t W_r\,\mathrm{d}r + S_0 = c\,. \quad (6.3.7)$$

Using the facts that

$$\left(\int_0^t W_s\,\mathrm{d}s\right)^2 = 2\int_0^t\int_0^r W_r W_s\,\mathrm{d}s\,\mathrm{d}r\,,$$

and

$$\int_0^t (r-t)\,\mathrm{d}W_r = -\int_0^t W_r\,\mathrm{d}r\,,$$

we see that the expression in Equation (6.3.7) coincides with that obtained in Chapter 3 for the stochastic free case.

6.4 Explicit Examples

Let us consider the initial function $S_0(\boldsymbol{x}_0) = f(x_0) + g(x_0)y_0$. We know that for $t \neq \frac{(2k+1)\pi}{2\omega_2}$ and $g''(x_0) \neq 0$ the pre-caustic is given by

$$y_0(x_0) = \frac{1}{\omega_2 g''(x_0)}\left\{\tan(\omega_2 t)g'(x_0)^2 - \cot(\omega_1 t)\omega_1\omega_2 - \omega_2 f''(x_0)\right\}\,.$$

The flow mapping is now

$$\boldsymbol{x} = \Phi_t\boldsymbol{x}_0 = \cos(\Omega t)\boldsymbol{x}_0 + \Omega^{-1}\sin(\Omega t)\begin{pmatrix} f'(x_0) + g'(x_0)y_0 \\ g(x_0)\end{pmatrix} + \varepsilon\Omega^{-1}\begin{pmatrix}\int_0^t \sin(\omega_1(r-t))\circ\partial W_r \\ 0\end{pmatrix}\,,$$

so that the caustic is given by

$$x(x_0) = \frac{1}{\omega_1\omega_2 g''}\Big\{\sin(\omega_1 t)\tan(\omega_2 t)g'^3 - \omega_2\sin(\omega_1 t)g'f'' + \omega_2\sin(\omega_1 t)f'g'' - \omega_1\omega_2\cos(\omega_1 t)(g' - x_0 g'')\Big\} + \frac{\varepsilon}{\omega_1}\int_0^t \sin(\omega_1(r-t))\circ\partial W_r\,,$$

$$y(x_0) = \frac{1}{\omega_2 g''}\left\{\sin(\omega_2 t)g'^2 - \cos(\omega_2 t)\cot(\omega_1 t)\omega_1\omega_2 - \cos(\omega_2 t)\omega_2 f'' + gg''\sin(\omega_2 t)\right\}\,,$$

where the x_0 variables are omitted for brevity. In order to obtain the pre-level surface we must use $S_0(\boldsymbol{x}_0) = f(x_0) + g(x_0)y_0$ in Proposition 6.3.2, which yields

$$\begin{aligned}
&-\frac{1}{4}x_0^2\omega_1\sin(2\omega_1 t) - \frac{1}{4}y_0^2\omega_2\sin(2\omega_2 t) - x_0\sin^2(\omega_1 t)(f' + g'y_0) \\
&\qquad - y_0\sin^2(\omega_2 t)g + \frac{1}{4\omega_1}\sin(2\omega_1 t)(f' + g'y_0)^2 + \frac{1}{4\omega_2}\sin(2\omega_2 t)g^2 \\
&+\varepsilon\left(x_0\cot(\omega_1 t) + \frac{1}{\omega_1}(f' + g'y_0)\right)\left(\cos(\omega_1 t)\int_0^t \sin(\omega_1(r-t))\circ\partial W_r - \int_0^t \sin(\omega_1 r)\circ\partial W_r\right) \\
&\qquad + \frac{\varepsilon^2\cot(\omega_1 t)}{2\omega_1}\left(\int_0^t \sin(\omega_1(r-t))\circ\partial W_r\right)^2 \\
&\qquad - \varepsilon^2\int_0^t\left(\int_r^t \frac{\sin(\omega_1 s)\sin(\omega_1(r-t))}{\omega_1\sin(\omega_1 t)}\circ\partial W_s\right)\circ\partial W_r + f + gy_0 = c\,. \qquad (6.4.1)
\end{aligned}$$

It may easily be observed that Equation (6.4.1) is a quadratic in y_0 which may be solved to obtain the pre-level surface as $y_0(x_0, t)$. The formula for the level surface is then obtained by applying the flow mapping so that $(x(x_0), y(x_0)) = \Phi_t(x_0, y_0(x_0, t))$. The explicit formulae are omitted here for the sake of brevity.

In Figures 6.5 and 6.6 we have illustrated the pre-curves and image curves for the cusp example. As usual the caustic is identified by the use of a broken line and for the purposes of our example we have taken $\omega_1 = \frac{4}{5}$, $\omega_2 = \frac{3}{2}$, $\varepsilon = \frac{1}{10}$ and $c = -2^{-4}$. The random terms have been generated by means of a numerical simulation similar to that outlined in Appendix A.

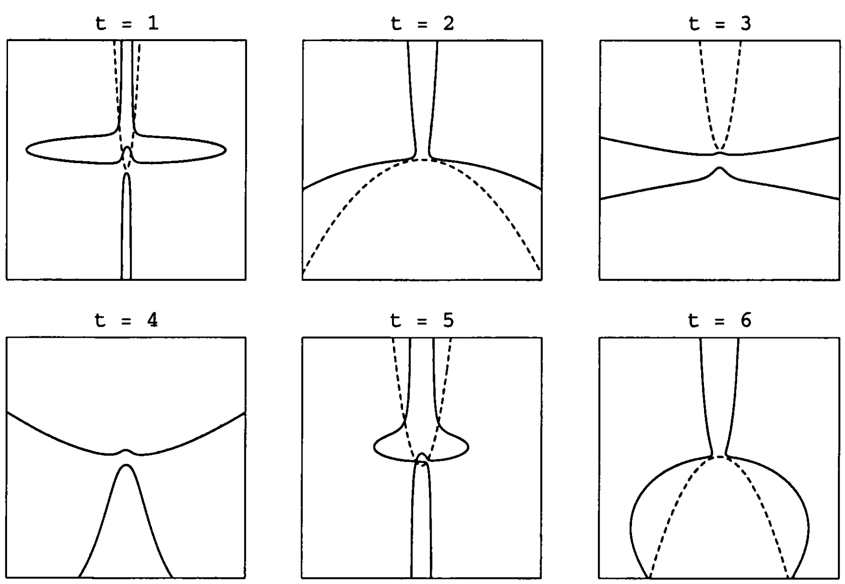

Figure 6.5: Pre-Curves for the stochastic cusp with harmonic oscillator potential

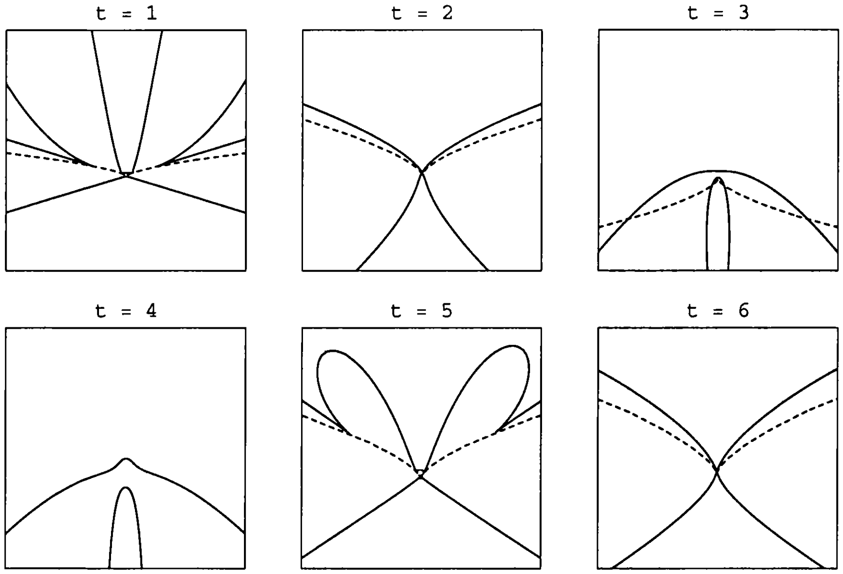

Figure 6.6: Image-Curves for the stochastic cusp with harmonic oscillator potential

6.5 Hot and Cool Parts of the Caustic with Harmonic Oscillator Potential

Recall that in the stochastic harmonic oscillator case we have

$$\begin{aligned}\Phi_t^\varepsilon(\boldsymbol{x}_0) &= \cos(\Omega t)\boldsymbol{x}_0 + \Omega^{-1}\sin(\Omega t)\nabla S_0(\boldsymbol{x}_0) + \varepsilon\int_0^t \Omega^{-1}\sin(\Omega(r-t))\circ\partial\widetilde{W}_r \\ &= \Phi_t^0(\boldsymbol{x}_0) + \varepsilon\int_0^t \Omega^{-1}\sin(\Omega(r-t))\circ\partial\widetilde{W}_r\ .\end{aligned} \tag{6.5.1}$$

Observe that if $\cos(\omega_2 t) + \omega_2^{-1}\sin(\omega_2 t)\frac{\partial S_0}{\partial y_0} \neq 0$, then the y coordinate in Equation (6.5.1) may be solved to obtain the purely deterministic expression $y_0 = y_0(y, x_0, \omega_2)$. Moreover, the values of $(\Phi_t^\varepsilon)^{-1}\{\boldsymbol{x}\}$ are obtained from the solutions $x_0^i(\boldsymbol{x}, t)$ of $\zeta(x_0) = 0$, where

$$\zeta(x_0) := \cos(\omega_1 t)x_0 + \frac{\sin(\omega_1 t)}{\omega_1}\frac{\partial S_0}{\partial x_0}(x_0, y_0(y, x_0, \omega_2)) + \frac{\varepsilon}{\omega_1}\int_0^t \sin(\omega_1(r-t))\circ\partial W_r\ .$$

Adopting the same approach as used in Chapter 4 for the free case, we obtain the following analogue of our earlier theorem concerning hot and cool parts of the caustic.

Theorem 6.5.1. *Take $S_0(\boldsymbol{x}_0)$ to be a smooth function of $\boldsymbol{x}_0 = (x_0, y_0) \in \mathbb{R}^2$, $t \neq \frac{k\pi}{\omega_i}$ for $k \in \mathbb{Z}$ and assume $\cos(\omega_2 t) + \omega_2^{-1}\sin(\omega_2 t)\frac{\partial^2 S_0}{\partial y_0^2} \neq 0$, so that $y = \cos(\omega_2 t)y_0 + \omega_2^{-1}\sin(\omega_2 t)\frac{\partial S_0}{\partial y_0}$ may be solved to obtain $y_0 = y_0(y, x_0, \omega_2)$. Consider crossing C_t at the point $\gamma = (x_\gamma, y_\gamma)$ travelling in the direction of decreasing $S_i(\boldsymbol{x}, t)$. If*

$$\begin{aligned}F(x_0) := \frac{\omega_1}{2}\frac{x_0^2\cos(\omega_1 t) - 2x_\gamma x_0}{\sin(\omega_1 t)} + \frac{\omega_2}{2}\frac{y_0(y_\gamma, x_0, \omega_2)^2\cos(\omega_2 t) - 2y_\gamma y_0(y_\gamma, x_0, \omega_2)}{\sin(\omega_2 t)} \\ + \varepsilon x_0\int_0^t \frac{\sin(\omega_1(r-t))}{\sin(\omega_1 t)}\circ\partial W_r + S_0(x_0, y_0(y_\gamma, x_0, \omega_2))\ ,\end{aligned} \tag{6.5.2}$$

then there will exist a repeated solution $x_0^r(\gamma,t)$ *of* $F'(x_0)=0$. *One side of* C_t *will be* ***cool*** *at* γ *if and only if*

$$F(x_0^r(\gamma,t)) \le \min_{\substack{i=1,2,\ldots,n \\ i\neq r}} F(x_0^i(\gamma,t)) ,$$

where $x_0^i(\gamma,t)$ *are the solutions of* $F'(x_0)=0$. *Moreover the* ***boundary*** *of the cool part is given by*

$$F(x_0^r(\gamma,t)) = \min_{\substack{i=1,2,\ldots,n \\ i\neq r}} F(x_0^i(\gamma,t)) .$$

Remark 6.5.1. It may easily be shown that $F'(x_0) = \frac{\omega_1}{\sin(\omega_1 t)}\zeta(x_0)$. Moreover, since $\frac{\omega_1}{\sin(\omega_1 t)} \neq 0$ it follows that $F'(x_0)=0$ has the same solutions as $\zeta(x_0)=0$.

Observe that since $F''(x_0)=0$ is deterministic it may be shown, by the same method employed in the free case, that the nature of the hot and cool parts in unchanged by the introduction of noise parallel to the x-axis. They are simply displaced bodily with the caustic by the random amount $Y_t = \varepsilon\int_0^t \Omega^{-1}\sin(\Omega(r-t))\circ\partial\widetilde{W}_r$. Hence for $k(x,t)=x$ we need only consider the hot and cool nature of the deterministic caustic.

6.5.1 Example: The Cusp

Earlier we saw that the cusp caustic is determined by

$$\begin{aligned} x(x_0) &= \frac{x_0^3}{\omega_1\omega_2}\sin(\omega_1 t)\tan(\omega_2 t) , \\ y(x_0) &= \frac{3x_0^2}{2\omega_2}\sin(\omega_2 t) - \omega_1\cot(\omega_1 t)\cos(\omega_2 t) , \end{aligned}$$

where we observe that the vertical orientation of the caustic is determined by sgn $\left(\frac{\sin(\omega_2 t)}{\omega_2}\right)$. Thus the caustic, C_t, will have the usual orientation in quadrants 1 and 2, but will be "upside down" in quadrants 3 and 4.

For the cusp example, the condition $\cos(\omega_2 t) + \frac{\sin(\omega_2 t)}{\omega_2}\frac{\partial^2 S_0}{\partial y_0^2} \neq 0$ reduces to $\cos(\omega_2 t)\neq 0$, that is $t \neq \frac{(2k+1)\pi}{2\omega_2}$. Assuming this is true we may solve

$$y = y_0\cos(\omega_2 t) + \frac{x_0^2}{2\omega_2}\sin(\omega_2 t) ,$$

to obtain

$$y_0(y,x_0,\omega_2) = y\sec(\omega_2 t) - \frac{x_0^2}{2\omega_2}\tan(\omega_2 t) .$$

Substituting into Equation (6.5.2) with $\varepsilon\equiv 0$ and omitting terms not containing x_0, since these do not affect the shape of $F(x_0)$, yields

$$F(x_0) = -\frac{x_0^4}{8\omega_2}\tan(\omega_2 t) + \frac{x_0^2}{2}\left(\omega_1\cot(\omega_1 t) + y_\gamma\sec(\omega_2 t)\right) - x_0 x_\gamma\omega_1\,\mathrm{cosec}(\omega_1 t) .$$

The first two derivatives of this function are given by

$$F'(x_0) = -\frac{x_0^3}{2\omega_2}\tan(\omega_2 t) + x_0\left(\omega_1\cot(\omega_1 t) + y_\gamma\sec(\omega_2 t)\right) - x_\gamma\omega_1\operatorname{cosec}(\omega_1 t) ,$$

and

$$F''(x_0) = -\frac{3x_0^2}{2\omega_2}\tan(\omega_2 t) + \omega_1\cot(\omega_1 t) + y_\gamma\sec(\omega_2 t) .$$

Solving $F''(x_0) = 0$ yields

$$x_0^r = \pm\left(\frac{2\omega_2}{3}\cot(\omega_2 t)\left(\omega_1\cot(\omega_1 t) + y_\gamma\sec(\omega_2 t)\right)\right)^{\frac{1}{2}} ,$$

both of which must be real since $\gamma \in C_t$. Now $F'(x_0)$ is a cubic with two zeros: a non-repeated zero and a repeated zero at x_0^r. Hence $F(x_0)$ will possess two stationary points, one of which will be a maxima or minima and the other a point of inflection.

i). If $\frac{1}{\omega_2}\tan(\omega_2 t) > 0$ then $\lim_{x\to\pm\infty} F(x_0) = -\infty$, so that $F(x_0)$ has a maximum and a point of inflection. Due to the shape of $F(x_0)$ the value at x_0^r will be less than the maximum so that the whole of one side of C_t is cool.

ii). If $\frac{1}{\omega_2}\tan(\omega_2 t) < 0$ then $\lim_{x\to\pm\infty} F(x_0) = +\infty$, so that $F(x_0)$ has a minimum and a point of inflection. Due to the shape of $F(x_0)$ the value at x_0^r will be greater than the minimum so that the whole of one side of C_t is hot.

Proposition 6.5.2. *The hot and cool nature of the cusp caustic is determined by the vertical orientation of the pre-caustic. Namely, when the pre-caustic has its usual orientation (quadrants 1 or 3) the whole of one side of C_t will be cool, but when the pre-caustic is upside down (quadrants 2 or 4) the whole of one side of C_t will be hot.*

Remark 6.5.2. It follows that there exist hot and cool versions of the cusp with usual orientation and the upside down cusp.

6.5.2 Example: The Polynomial Swallowtail

In this case the function $F(x_0)$ is given by

$$F(x_0) = x_0^5 - \frac{x_0^5}{2\omega_2}\tan(\omega_2 t) + x_0^2\left(\frac{\omega_1}{2}\cot(\omega_1 t) + y_\gamma\sec(\omega_2 t)\right) - x_0 x_\gamma\omega_1\operatorname{cosec}(\omega_1 t) ,$$

so that

$$F'(x_0) = 5x_0^4 - \frac{2x_0^3}{\omega_2}\tan(\omega_2 t) + x_0\left(\omega_1\cot(\omega_1 t) + 2y_\gamma\sec(\omega_2 t)\right) - x_\gamma\omega_1\operatorname{cosec}(\omega_1 t) ,$$

$$F''(x_0) = 20x_0^3 - \frac{6x_0^2}{\omega_2}\tan(\omega_2 t) + \omega_1\cot(\omega_1 t) + 2y_\gamma\sec(\omega_2 t) ,$$

$$F'''(x_0) = 60x_0^2 - \frac{12x_0}{\omega_2}\tan(\omega_2 t) .$$

Clearly $F'''(x_0) = 0$ has solutions $x_0 = 0$ and $x_0 = \frac{\tan(\omega_2 t)}{5\omega_2}$, so that by Section 6.2.2 the cusps are located at

$$\left(0, -\frac{\omega_1}{2}\cot(\omega_1 t)\cos(\omega_2 t)\right) ,$$

and

$$\left(\frac{\sin(\omega_1 t)\tan^4(\omega_2 t)}{125\omega_1\omega_2^4}, -\frac{1}{2}\omega_1\cot(\omega_1 t)\cos(\omega_2 t) + \frac{\sin(\omega_2 t)\tan^2(\omega_2 t)}{25\omega_2^3}\right) .$$

In order to determine the hot and cool parts of the polynomial swallowtail we must perform an analysis of the function $F(x_0)$ similar to that conducted in Chapter 4. This yields the following Proposition.

Proposition 6.5.3. *If* $\frac{\tan(\omega_2 t)}{\omega_2} > 0$ *then the hot and cool parts of the caustic are as shown in Figure 6.7 where*

$$\lambda = \left(-\frac{(3+8\sqrt{6})\sin(\omega_1 t)\tan^4(\omega_2 t)}{18000\omega_1\omega_2^4}, -\frac{\cos(\omega_2 t)(225\cot(\omega_1 t)\omega_1\omega_2^3 - (9-\sqrt{6})\tan^3(\omega_2 t)}{450\omega_2^3}\right) . \tag{6.5.3}$$

However if $\frac{\tan(\omega_2 t)}{\omega_2} < 0$ *then the hot and cool parts of the caustic are as shown in Figure 6.8 where*

$$\lambda = \left(\frac{(-3+8\sqrt{6})\sin(\omega_1 t)\tan^4(\omega_2 t)}{18000\omega_1\omega_2^4}, -\frac{\cos(\omega_2 t)(225\cot(\omega_1 t)\omega_1\omega_2^3 - (9+\sqrt{6})\tan^3(\omega_2 t)}{450\omega_2^3}\right) . \tag{6.5.4}$$

In both cases the point κ *is given by*

$$\kappa = \left(-\frac{\sin(\omega_1 t)\tan^4(\omega_2 t)}{500\omega_1\omega_2^4}, -\frac{\omega_1}{2}\cot(\omega_1 t)\cos(\omega_2 t) + \frac{\sin(\omega_2 t)\tan(\omega_2 t)^2}{50\omega_2^3}\right) .$$

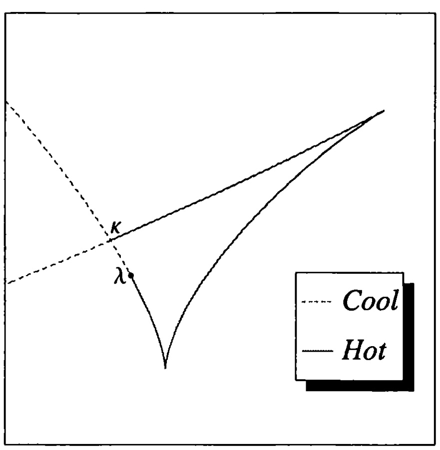

Figure 6.7: Hot and cool parts of the polynomial swallowtail for $\omega_2^{-1}\tan(\omega_2 t) > 0$.

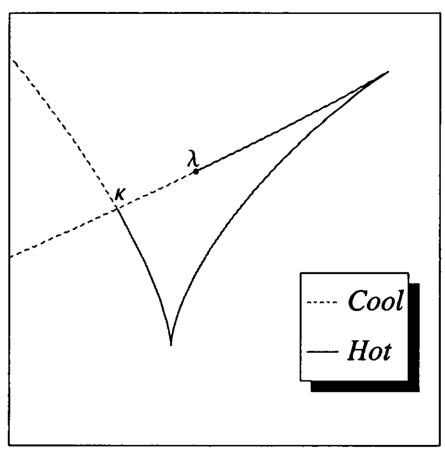

Figure 6.8: Hot and cool parts of the polynomial swallowtail for $\omega_2^{-1}\tan(\omega_2 t) < 0$.

Proof (sketch). If $\gamma \in C_t$ is a point vertically above the highest cusp or below the lowest then $F'''(x_0) = 0$ has only one real solution, which will be the single (repeated) solution of $F'(x_0) = 0$. Hence $F(x_0)$ has only one stationary point, which is a point of inflection, thus all such points γ are cool.

If $\gamma \in C_t$ is a point vertically between the cusps then $F'(x_0)$ has three stationary points occurring from left to right as minimum, maximum and minimum. We adopt the labelling scheme defined in Figure 4.4 and assume for simplicity that $\omega_1^{-1}\sin(\omega_1 t) > 0$ so that the polynomial swallowtail has the usual horizontal orientation.

As in the free case, branches (A) and (D) are easily shown to be cool and hot, respectively. For branches (B) and (C) there are two cases to consider.

Case 1: $\frac{\tan(\omega_2 t)}{\omega_2} > 0$

In this case $F'(x_0)$ will look like one of the graphs in Figure 6.9. If $x_\gamma > 0$ then $F'(0) =$

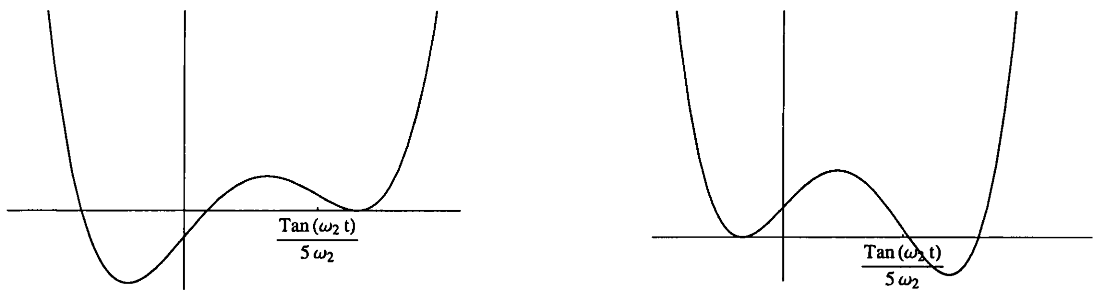

Figure 6.9: Shape of $F'(x_0)$ on branches (B) and (C) for case 1

$-x_\gamma \omega_1 \operatorname{cosec}(\omega_1 t) < 0$ so that $F'(x_0)$ must have the shape in Figure 6.9 left. Thus $F(x_0)$ will have three stationary points occurring from left to right as maximum, minimum and inflection. But the value at the point of inflection will be greater than the local minimum so that for $x_\gamma > 0$ branch (B) is hot. Arguing, as in Chapter 4, it may be shown that as we travel anticlockwise around branch (B) and then (C) the caustic remains hot until we reach the λ point given by Equation (6.5.3).

Case 2: $\frac{\tan(\omega_2 t)}{\omega_2} < 0$

In this case $F'(x_0)$ will look like one of the graphs in Figure 6.10. If $x_\gamma > 0$ then $F'(0) < 0$

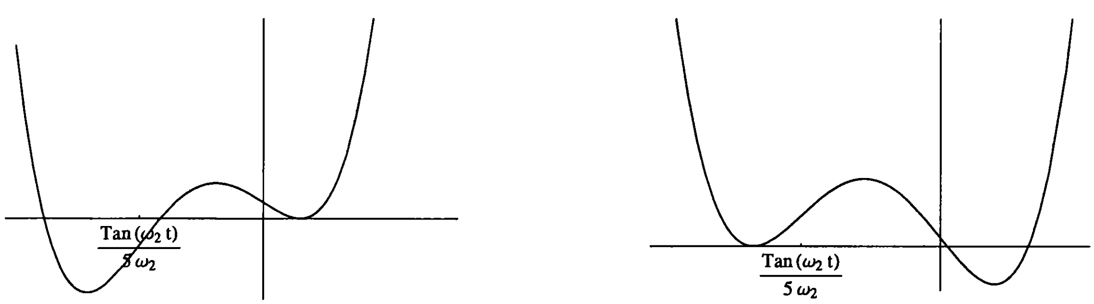

Figure 6.10: Shape of $F'(x_0)$ on branches (B) and (C) for case 2

so that $F'(x_0)$ must have the shape in Figure 6.10 right. Thus on branch (B), $F'(x_0)$

has the shape in Figure 6.10 right whilst on branch (C) it will have the shape in Figure 6.10 left. Clearly branch (C) will be hot since $F(x_0)$ will have three stationary points occurring from left to right as maximum, minimum and inflection. Moreover as we travel clockwise along (B), away from the point of self intersection, the caustic will be initially cool until we reach the λ point given by Equation (6.5.4). □

Remark 6.5.3. As with the cusp example it is changes in the sign of $\omega_2^{-1}\tan(\omega_2 t)$ that alters the hot and cool nature of the caustic.

6.6 Turbulent Times and the Harmonic Oscillator

Let us consider the initial function $S_0(\boldsymbol{x_0}) = f(x_0) + g(x_0)y_0$. We know that the pre-caustic is given by

$$y_0(x_0,t) = \frac{1}{g''(x_0)}\left\{\frac{g'(x_0)^2}{\omega_2}\tan(\omega_2 t) - f''(x_0) - \omega_1\cot(\omega_1 t)\right\},$$

whilst the pre-level surface is given by $p(x_0,y_0,t) = c$ where $p(x_0,y_0,t)$ is the left hand side of Equation (6.4.1).

The pre-curves will meet at solutions $x_0(t)$ of $F_\varepsilon(x_0,t) = c$ where we define $F_\varepsilon(x_0,t) := p(x_0,y_0(x_0,t),t)$. Recall that in order to obtain the turbulent times we must find those $t > 0$ satisfying $F_\varepsilon(x_0,t) = c$ and $\frac{\partial F_\varepsilon}{\partial x_0}(x_0,t) = 0$.

Using our expression for $p(x_0,y_0(x_0,t),t)$ it may be shown that

$$\begin{aligned}\frac{\partial F_\varepsilon}{\partial x_0} &= -\frac{1}{2}x_0\omega_1\sin(2\omega_1 t) - \frac{1}{2}y_0(x_0,t)y_0'(x_0,t)\omega_2\sin(2\omega_2 t) - \sin^2(\omega_1 t)(f' + g'y_0(x_0,t)) \\ &\quad - x_0\sin^2(\omega_1 t)(f'' + g''y_0(x_0,t) + g'y_0'(x_0,t)) - y_0'(x_0,t)g\sin^2(\omega_2 t) \\ &- y_0(x_0,t)\sin^2(\omega_2 t)g' + \frac{1}{2\omega_1}\sin(2\omega_1 t)\left(f' + g'y_0(x_0,t)\right)\left(f'' + g''y_0(x_0,t) + g'y_0'(x_0,t)\right) \\ &\quad + \frac{gg'}{2\omega_2}\sin(2\omega_2 t) + \varepsilon\left(\cot(\omega_1 t) + \frac{1}{\omega_1}(f'' + g''y_0(x_0,t) + g'y_0'(x_0,t)\right) \\ &\qquad \times\left(\cos(\omega_1 t)\int_0^t \sin(\omega_1(r-t))\circ\partial W_r - \int_0^t \sin(\omega_1 t)\circ\partial W_r\right) \\ &\qquad\qquad + f' + g'y_0(x_0,t) + gy_0'(x_0,t)\,. \end{aligned} \tag{6.6.1}$$

Proposition 6.6.1. *Consider the initial condition* $S_0(\boldsymbol{x_0}) = f(x_0) + g(x_0)y_0$ *where* f, g, f', g', f''' *and* g''' *are zero at* $x_0 = \alpha_i$ *and* $g''(\alpha_i) \neq 0$ *for* $i = 1, 2, \ldots n$. *Then* *the zeros $t(\omega)$ of the stochastic process*

$$\begin{aligned}
Y_t := & -\frac{1}{4}\alpha_i^2\omega_1 \sin(2\omega_1 t) - \frac{1}{4}\omega_2 \frac{\sin(2\omega_2 t)}{g''(\alpha_i)} \left(f''(\alpha_i) + \omega_1 \cot(\omega_1 t)\right)^2 \\
& + \varepsilon\alpha_i \cot(\omega_1 t)\left(\cos(\omega_1 t)\int_0^t \sin(\omega_1(r-t)) \circ \partial W_r - \int_0^t \sin(\omega_1 r) \circ \partial W_r\right) \\
& + \frac{\varepsilon^2}{2\omega_1}\cot(\omega_1 t)\left(\int_0^t \sin(\omega_1(r-t)) \circ \partial W_r\right)^2 \\
& - \frac{\varepsilon^2}{\omega_1 \sin(\omega_1 t)}\int_0^t \left(\int_r^t \sin(\omega_1 s)\sin(\omega_1(r-t)) \circ \partial W_s\right) \circ \partial W_r - c\ , \qquad (6.6.2)
\end{aligned}$$

will be turbulent times. Moreover, if $t(\omega)$ are the solutions of $Y_t = 0$, then the turbulence occurs at the points

$$\Phi_{t(\omega)}\left(\alpha_i, \frac{-1}{g''(\alpha_i)}\left(f''(\alpha_i) + \omega_1 \cot(\omega_1 t)\right)\right)\ .$$

Proof. It may be easily shown that $y_0'(\alpha_i) = 0$ so that

$$\begin{aligned}
\left.\frac{\partial F_\varepsilon}{\partial x_0}\right|_{x_0=\alpha_i} = & -\frac{1}{2}\alpha_i\omega_1 \sin(2\omega_1 t) - \alpha_i \sin^2(\omega_1 t)\left(f''(\alpha_I) + g''(\alpha_i) y_0(\alpha_i)\right)) \\
& + \varepsilon\left(\cot(\omega_1 t) + \frac{1}{\omega_1}(f''(\alpha_i) + g'' y_0(\alpha_i)\right) \\
& \times \left(\cos(\omega_1 t)\int_0^t \sin(\omega_1(r-t)) \circ \partial W_r - \int_0^t \sin(\omega_1 t) \circ \partial W_r\right)\ .
\end{aligned}$$

Moreover, we observe

$$y_0(\alpha_i) = \frac{-1}{g''(\alpha_i)}\left(f''(\alpha_i) + \omega_1 \cot(\omega_1 t)\right)\ ,$$

so that $\left.\frac{\partial F_\varepsilon}{\partial x_0}\right|_{x_0=\alpha_i} = 0$. Hence the turbulent times are given by solutions of $Y_t(\omega) := F_\varepsilon(\alpha_i, t) - c$, which on evaluation yields the expression in Equation (6.6.2). □

Proposition 6.6.2. *There exists an increasing sequence $\{t_i\}$ with $t_i \nearrow \infty$ such that $Y_{t_i}(\omega) = 0$ almost surely.*

Proof. Observe that the stochastic process $Y_t(\omega)$ may be written as

$$\begin{aligned}
Y_t(\omega) = & -\frac{\omega_2}{4g''(\alpha_i)}\sin(2\omega_2 t)\operatorname{cosec}^2(\omega_1 t)\left\{\sin(\omega_1 t) f''(\alpha_i) + \omega_1 \cos(\omega_1 t)\right\}^2 \\
& + \varepsilon \operatorname{cosec}(\omega_1 t) R_t(\omega) - \frac{1}{4}\alpha_i^2\omega_1 \sin(2\omega_1 t) - c\ ,
\end{aligned}$$

where

$$R(\omega) := \alpha_i \left(\cos^2(\omega_1 t) \int_0^t \sin(\omega_1(r-t)) \circ \partial W_r - \cos(\omega_1 t) \int_0^t \sin(\omega_1 r) \circ \partial W_r \right)$$
$$+ \frac{\varepsilon}{2\omega_1} \cos(\omega_1 t) \left(\int_0^t \sin(\omega_1(r-t)) \circ \partial W_r \right)$$
$$- \frac{\varepsilon}{\omega_1} \int_0^t \int_r^t \sin(\omega_1 s) \sin(\omega_1(r-t)) \circ \partial W_s \circ \partial W_r \ ,$$

is a stochastic process well defined for all t.

As $t \to \frac{k\pi}{\omega_1}$ we have $\operatorname{cosec}^2(\omega_1 t) \to \infty$. Let $\{t_k\}$ denote an increasing sequence at which $\operatorname{cosec}^2(\omega_1 t_k) = \infty$, then $\lim_{t\to t_k} Y_t = -\infty$ if $\frac{\sin(2\omega_2 t_k)}{g''(\alpha_i)} > 0$ but $\lim_{t\to t_k} Y_t = +\infty$ if $\frac{\sin(2\omega_2 t_k)}{g''(\alpha_i)} < 0$. However, we can find an infinite increasing subsequence $\{t_{k_j}\}$ such that Y_t is continuous on $(t_{k_j}, t_{k_{j+1}})$ and

$$\operatorname{sgn}\left(\sin(2\omega_2 t_{k_j}\right) = -\operatorname{sgn}\left(\sin(2\omega_2 t_{k_{j+1}}\right) \ ,$$

so that $\lim_{t\to t_{k_j}} Y_t$ successively switches between plus and minus infinity.

Hence, by continuity and the intermediate value theorem, there will exist an increasing sequence $\{t_j\}$ with $t_j \nearrow \infty$ at which $Y_{t_j} = 0$ almost surely. □

Remark 6.6.1.

i). The above argument fails if

$$\operatorname{sgn}\left(\sin\left(\frac{2\omega_2 k\pi}{\omega_1}\right)\right) \ ,$$

is the same for all $k \in \mathbb{Z}^+$. This will only be the case if $\frac{2\omega_2\pi}{\omega_1} = 2n\pi$, namely $\omega_2 = n\omega_1$, for some $n \in \mathbb{Z}$. Hence in Proposition 6.6.2 we must assume $\omega_2 \neq n\omega_1$ for all $n \in \mathbb{Z}$.

ii). There is no need to use Strassen's law of the iterated logarithm in this situation.

Appendix A

Simulating Brownian Motion

We have written the following module in *Mathematica* in order to simulate a random walk approximating Brownian Motion. This is used to calculate the random quantities we require.

```
Brownian1[T_, a_, Optional[s_, PlotStyle -> RGBColor[0, 0, 0]]] :=

    Module[{k, S, t, X, n, d},

    S[0] = 0; t[0] = 0; d = Sqrt[a]; n = Floor[T/a];

    Do[k = Random[Integer]; If[k == 1, X = d, X = -d];

        S[i] = S[i - 1] + X; t[i] = t[i - 1] + a, {i, n}];

    W1[r] := S[Floor[r/a]];

    W2[r] := Sum[S[i - 1](t[i] - t[i - 1]), {i, Floor[r/a]}];

    W3[r] := Sum[S[i - 1]^2(t[i] - t[i - 1]), {i, Floor[r/a]}];

    ListPlot[Table[{t[i], S[i]}, {i, 0, n}], PlotJoined -> True, s]]
```

In the above module the user selects the time (T) that the process will run for and the time step size (a) to be used. This produces a sample path and calculates the following quantities

$$\begin{aligned} \texttt{W1[t]} &\approx W(t)\ , \\ \texttt{W2[t]} &\approx \int_0^t W(u)\,\mathrm{d}u\ , \\ \texttt{W3[t]} &\approx \int_0^t W(u)^2\,\mathrm{d}u\ . \end{aligned}$$

Finally the command `ListPlot` produces a picture of the sample path. Information on the *Mathematica* commands used in the above module may be found in [56]

Appendix B

Mathematica Module for Calculating the Number of Negative Roots

Firstly we define the functions $F'(x_0)$ and $S_i(\boldsymbol{x}, t)$ using the letters `h` and `S` respectively as follows:

```
h[X_, Y_, t_, a_] := 5 a t x^4 - 2 t^2 x^3 + x(1 + 2tY)
 - X

S[X_, Y_, x_, y_, a_] := (X - x)^2/(2 t)+ (Y - y)^2/(2t) + a x^5 +
x^2 y
```

The module used to determine the number of negative $S_i(\boldsymbol{x}, t)$'s is shown below.

```
NegS[X_, Y_, t_, a_] := Module[{negvals, r, valsofS},

r = Cases[x /. NSolve[F[X, Y, t, a] == 0, x], _Real];

valsofS = Table[S[X, Y, r[[i]], Y - t r[[i]]^2, t, a], {i,
Length[r]}]; negvals = Count[Select[valsofS, #1 < 0 &], _];

Print[r];

Print[valsofS];

StringJoin["Number of solutions = ", ToString[Length[r]], ",
Number of negative S's = ", ToString[negvals]]]
```

The real solutions of the equation $F'(x_0) = 0$ are assigned to the variable `r`. $S_i(\boldsymbol{x}, t)$ is evaluated at each of these solutions and the results are assigned to the variable `valsofS`. Using the `Count` command the number of negative S_i's are counted and this is assigned to the variable `negvals`. The remaining commands simply print the real solutions of

$F'(x_0) = 0$, the corresponding values of S_i and the number of negative S_i's. An example of the module in practice with $t = \alpha = 1$ is shown below.

```
in[1]:=  NegS[-0.5, 0.483, 1, 1]

         {-0.447542, -0.305457}

         {0.0601047, 0.0569773}

out[1]=  "Number of solutions = 2, Number of negative S's = 0"
```

Appendix C

Behaviour of $u^{\mu}(x,t)$ when there's no minimiser

We are interested in the behaviour of an integral of the form

$$I(x,t) = \int T_0(x_0) \exp\left\{-\mu^{-2}\mathcal{A}(x_0,x,t)\right\}\, \mathrm{d}x_0 \ .$$

In the case when the equation $\nabla_{x_0}\mathcal{A}(x_0,x,t) = 0$ has solutions $x_0 = x_0(x,t) \in \mathbb{R}$ and there is a unique minimiser $\tilde{x}_0 = \tilde{x}_0(x,t)$ this leads to the behaviour

$$I(x,t) \sim \left(2\pi\mu^2\right)^{\frac{1}{2}} T_0(\tilde{x}_0(x,t))\left[\mathcal{A}''(\tilde{x}_0(x,t),x,t)\right]^{-\frac{1}{2}} \exp\left\{-\mu^{-2}\mathcal{A}(\tilde{x}_0(x,t),x,t)\right\} \ .$$

Now let us assume that for all $x \in S$ there does not exist a minimiser $x_0(x,t)$. Namely for all $x \in S$,

$$\nabla_{x_0}\mathcal{A}(x_0,x,t) \neq 0 \ ,$$

for any $x_0 \in \mathbb{R}$. What can we say about the behaviour of $u^{\mu}(x,t)$ in this case? Turning our attention to $I(x,t)$ we observe

$$\begin{aligned} I(x,t) &= \int T_0(x_0) \exp\left\{-\mu^{-2}\mathcal{A}(x_0,x,t)\right\} \left(-\mu^{-2}\frac{d\mathcal{A}}{dx_0}\right)\left(-\mu^{-2}\frac{d\mathcal{A}}{dx_0}\right)^{-1} \mathrm{d}x_0 \\ &= \int T_0(x_0)\frac{d}{dx_0} \exp\left\{-\mu^{-2}\mathcal{A}(x_0,x,t)\right\} \left(-\mu^{-2}\frac{d\mathcal{A}}{dx_0}\right)^{-1} \mathrm{d}x_0 \\ &= \mu^2 \int \exp\left\{-\mu^{-2}\mathcal{A}(x_0,x,t)\right\}\frac{d}{dx_0}\left\{T_0(x_0)\left(\frac{d\mathcal{A}}{dx_0}\right)^{-1}\right\} \mathrm{d}x_0 \ , \end{aligned}$$

by integration by parts. Applying the same method again yields

$$\begin{aligned} I(x,t) &= \mu^2 \int \frac{d}{dx_0} \exp\left\{-\mu^{-2}\mathcal{A}(x_0,x,t)\right\}\left(-\mu^{-2}\frac{d\mathcal{A}}{dx_0}\right)^{-1} \frac{d}{dx_0}\left\{T_0(x_0)\left(\frac{d\mathcal{A}}{dx_0}\right)^{-1}\right\} \mathrm{d}x_0 \\ &= \mu^4 \int \exp\left\{-\mu^{-2}\mathcal{A}(x_0,x,t)\right\}\frac{d}{dx_0}\left\{\left(\frac{d\mathcal{A}}{dx_0}\right)^{-1}\frac{d}{dx_0}\left(T_0(x_0)\left(\frac{d\mathcal{A}}{dx_0}\right)^{-1}\right)\right\} \mathrm{d}x_0 \ . \end{aligned}$$

Thus if this process is repeated N times then we observe that $I(x,t) \sim o(\mu^{2N})$ as $\mu \sim 0$.

List of Figures

Bibliography

[1] V. I. Arnold. *Singularity Theory.* Cambridge University Press, 1981.

[2] V.I. Arnold. *Mathematical Methods of Classical Mechanics.* Addison–Wesley, second edition, 1989.

[3] V.I. Arnold. *Singularities of Caustics and Wave Fronts*, volume 62 of *Mathematics and Its Applications (Soviet Series).* Kluwer Academic Publishers, 1990.

[4] N. Berline, E. Getzler, and M. Vergne. *Heat Kernel and Dirac Operators*, volume 298 of *Grundlehren der mathematischen Wissenschaften.* Springer-Verlag, 1992.

[5] J. Bertoin. Structure of shocks in Burgers turbulence with stable noise initial data. *Commun. Math. Phys.*, pages 729–741, 1999.

[6] A. T. Bharucha-Reid and M. Sambandham. *Random Polynomials.* Academic Press, 1986.

[7] N. G. De Bruign. *Asymptotic Methods in Analysis*, volume 4 of *Bibliotheca Mathematica.* North-Holland Publishing Co., 1958.

[8] Z. Brzeźniak and T. Zastawniak. *Basic Stochastic Processes.* Springer, 1999.

[9] J. M. Burgers. The nonlinear diffusion equation, 1974.

[10] J. R. Cannon. *The One-Dimensional Heat Equation.* Encyclopedia of Mathematics and its Applications. Addison–Wesley Publishing Company, 1984.

[11] J. L. Casti. *Five Golden Rules : Great Theories of 20th-Century Mathematics – and Why They Matter.* Wiley, 1996.

[12] T. Chan, D. S. Dean, K. M. Jansons, and L. C. G. Rogers. On polymer conformations in elongational flows. *Commun. Math. Phys.*, 160(2):239–258, 1994.

[13] A. J. Chorin and J. E. Marsden. *A Mathematical Introduction to Fluid Mechanics.* Springer-Verlag, second edition, 1990.

[14] I. M. Davies, A. Truman, and H. Z. Zhao. Stochastic heat and Burgers equations and their singularities - geometrical and analytical properties (the fish and the butterfly, and why.). MRR preprint, 2001. http://www.ma.utexas.edu/mp_arc-bin/mpa?yn=01-45.

[15] I. M. Davies, A. Truman, and H. Z. Zhao. Stochastic heat and Burgers equations and their singularities I - geometrical properties. *J. Math. Phys.*, 43:3293–3328, 2002.

[16] D. S. Dean and K. M. Jansons. Excursions for polymers in elongational flows. preprint, 1994.

[17] A. Edelman and E. Kostlan. How many zeros of a random polynomial are real? *Bull. American Math. Soc.*, 32(1):1–37, 1995.

[18] K. D. Elworthy, A. Truman, and H. Z. Zhao. Stochastic elementary formulae on caustics I: One dimensional linear heat equations. MRRS preprint, 2002.

[19] M. V. Fedoriuk. The stationary phase method and pseudodifferential operators. *Uspeki Mat. Nauk*, 26:67–112, 1971.

[20] D. Freedman. *Brownian Motion and Diffusion.* Holden-Day, Inc., 1971.

[21] M. I. Freidlin and A. D. Wentzell. *Random Perturbations of Dynamical Systems.* Springer, second edition, 1998.

[22] H. Goldstein. *Classical Mechanics.* Addison–Wesley, 1950.

[23] A. Grigis and J. Sjöstrand. *Microlocal Analysis for Differential Operators (An Introduction)*, volume 196 of *London Mathematical Society Lecture Note Series.* Cambridge University Press, 1994.

[24] J. M. Harrison. *Brownian Motion and Stochastic Flow Systems.* Wiley, 1985.

[25] H. Hilton. *Plane Algebraic Curves.* Oxford University Press, 1920.

[26] E. Hopf. The partial differential equation $u_t + uu_x = \mu u_{xx}$. *Comm. Pure Appl. Math*, 3:201–230, 1950.

[27] K. Itô and H. McKean. *Diffusion Processes and their Sample Paths.* Springer-Verlag, 1965.

[28] M. Kac. On the average number of real roots of a random algebraic equation (II). *Proceedings of the London Mathematical Society*, 50(2).

[29] M. Kac. On the average number of real roots of a random algebraic equation. *Bull. American Math. Soc.*, 49:314–320, 1943.

[30] M. Kac. On the distribution of values of trigonometric sums with linearly independent frequencies. *American J. of Math.*, 65(4):609–615, 1943.

[31] M. Kac. *Probability and Related Topics in Physical Sciences.* Interscience Publishers, Inc., 1959.

[32] I. Karatzas and S. E. Shreve. *Brownian Motion and Stochastic Calculus.* Springer, second edition, 1991.

[33] Kloeden, P. E. and Platen, E. *Numerical Solution of Stochastic Differential Equations*, volume 23 of *Applications of Mathematics.* Springer-Verlag, 1992.

[34] R. L. Liboff. *Introductory Quantum Mechanics.* Addison Wesley, 1980.

[35] V. P. Maslov and M. V. Fedoriuk. *Semi-Classical Approximation in Quantum Mechanics*, volume 7 of *Mathematical Physics and Applied Mathematics.* D. Reidel Publishing Company, 1981.

[36] H. P. McKean, Jr. *Stochastic Integrals*, volume 5 of *Probability and Mathematical Statistics.* Academic Press, 1969.

[37] J. Milnor. *Morse Theory*, volume 51 of *Annals of Mathematics Studies.* Princeton University Press, 1963.

[38] R. W. D. Nickalls. A new approach to solving the cubic: Cardan's solution revealed. *The Mathematical Gazette*, 77:354–359, 1993.

[39] B. Øksendal. *Stochastic Differential Equations : an introduction with applications.* Springer, fifth edition, 1998.

[40] D. Revuz and M. Yor. *Continuous Martingales and Brownian Motion*, volume 293 of *Grundlehren der mathematischen Wissenschaften.* Springer-Verlag, 1980.

[41] B. Reynolds. *Some Exact Singularities of Burgers and Heat Equations.* PhD thesis, University of Wales, Swansea, 2002.

[42] L. A. Rincón. *Topics on Stochastic Schrödinger Equations and Estimates for the Derivative of Diffusion Semigroups.* PhD thesis, University of Wales, Swansea, 1999.

[43] L. C. G. Rogers and D. Williams. *Diffusions, Markov processes and martingales*, volume 2. John Wiley and Sons, 1987.

[44] L. C. G. Rogers and D. Williams. *Diffusions, Markov processes and martingales*, volume 1. Cambridge University Press, second edition, 2000.

[45] P. Saunders. *An Introduction to Catastrophe Theory.* Cambridge University Press, 1980.

[46] S. F. Shandarin and Ya. B. Zeldovich. The large-scale structure of the universe: Turbulence, intermittency, structures in a self-gravitating medium. *Reviews of Modern Physics*, 61:185–274, 1989.

[47] M. R. Spiegel. *Theory and Problems of Theoretical Mechanics with an introduction to Lagrange's Equations and Hamiltonian Theory.* Schaum's Outline Series. McGraw Hill, 1967.

[48] I. Stewart and T. Poston. *Catastrophe Theory.* Pitman, 1978.

[49] V. Strassen. An invariance principle for the law of the iterated logarithm. *Z. Wahrscheinlichkeitstheorie*, 3:211–226, 1964.

[50] A. Truman. Notes on the lagrangian formulation of mechanics and analytical dynamics. Mathematics Department, University of Wales Swansea.

[51] A. Truman and D. Williams. Excursions and Itô calculus in Nelson's stochastic mechanics. In *Recent Developments in Quantum Mechanics.* Kluwer Academic Publishers, 1991.

[52] A. Truman and T. Zastawniak. Stochastic pde's of Schrödinger type and stochastic mehler kernels - a path integral approach. *Progress in Probability*, 45, 1999.

[53] A. Truman and H. Z. Zhao. On stochastic diffusion equations and stochastic Burgers' equations. *J. Math. Phys.*, 37:283–307, 1996.

[54] A. Truman and H. Z. Zhao. Stochastic Burgers' equations and their semi classical expansions. *Comm. Math. Phys.*, 194:231–248, 1998.

[55] D. H. Wilson. *Hydrodynamics.* Edward Arnold, second edition, 1959.

[56] S. Wolfram. *The Mathematica Book.* Cambridge University Press, fourth edition, 2000.